Canadian
Journal of Chemistry

Editor: LÉO MARION

REFERENCES—CANADIAN JOURNAL OF CHEMISTRY

This is to announce a change from the present system of citing references. Beginning in January 1958, references will be numbered and listed in the order of first citation in the text, not in alphabetical order by authors' names. Authors are requested to follow the new system in all manuscripts submitted henceforth.

SEPARATION, MOLECULAR WEIGHT, AND INTERACTIONS OF HORSE GLOBIN COMPONENTS[1]

ARNE HAUG[2] AND DAVID B. SMITH

ABSTRACT

Horse globin had been shown previously to dissociate into four subunits by suitable adjustment of pH and ionic strength. Two components have been separated electrophoretically. One of these separated components associates readily as pH and ionic strength are varied. The second component shows little tendency to associate with itself. The behavior of unfractionated globin indicates that interactions occur between these two components.

INTRODUCTION

The behavior of horse hemoglobin and globin in solutions of low pH has recently been investigated by Reichmann and Colvin (19). In a 0.05 M NaCl solution at pH 2, light scattering gave a weight average molecular weight (M_w) of 21,000–23,000, and osmotic pressure measurements a number average molecular weight (M_n) of 16,000±1,000. From this and other evidence these authors concluded that horse globin splits into four units of approximately equal molecular weight, 16,000, under the chosen conditions. Under the same conditions, electrophoresis of globin gave two distinct peaks, thus showing that at least two electrophoretically different components exist.

The present work describes the separation of these two components and supplies some information about the interactions that take place between them in acid solution.

MATERIALS AND METHODS

Preparation and Fractionation

Twice-recrystallized horse oxyhemoglobin was prepared from freshly drawn citrated blood by the method of Heidelberger (9). Ultracentrifugal and electrophoretic analysis of 0.25% solutions in 0.05 M phosphate, pH 6.8, always showed single peaks.

Globin was prepared according to Jope, Jope, and O'Brien (12) by pouring an approximately 5% solution of oxyhemoglobin in water into acetone containing 0.15 M HCl at −15°. The precipitate was filtered, washed with acid acetone and acetone, and dissolved in water at 0°. Three more cycles of precipitation and washing as above preceded freezing and lyophilization of the final solution. The product was stored at 4° and no changes in properties have been noted after storage up to a year.

The two electrophoretic components existing at pH 1.8–2.0 were separated using Kekwick's modification (14) of the standard Tiselius cell in the Klett electrophoresis apparatus. To permit maximum separation of these two components having only small

mobility differences (19) the apparatus was run for 18 hours, the boundaries being kept in the Kekwick cell by compensation (11). The addition of two standard Tiselius center sections below the Kekwick section permitted long runs without allowing the δ boundary to reach the bottom. Separations were made under the following preparative conditions:

1. Ionic strength 0.05 (*a*) in H_3PO_4–NaH_2PO_4 buffer and (*b*) in HCl–NaCl. The samples were isolated by freeze-drying after dialysis against 0.01 N HCl.

2. (*a*) and (*b*). Ionic strength as in 1(*a*) and (*b*) and in phosphate and chloride buffers respectively, but without subsequent dialysis and freeze-drying.

3. Ionic strength 0.1 (*a*) in phosphate and (*b*) in chloride buffers. Isolated by freeze-drying after prior dialysis against 0.01 N HCl.

4. (*a*) and (*b*). Differ from conditions 3(*a*) and (*b*) in that no dialysis and freeze-drying was done.

The separation did not appear to be affected by the nature of the buffer salts. About 10 mg. per run of the faster moving component could be obtained from the ascending limb. Because of boundary spreading, especially at the lower ionic strength, yields of the slower component from the descending limb were less.

Light Scattering

Light scattering measurements were carried out in a B.S. Light-scattering Photometer (3). Two cells were used: a cylindrical cell with 3.5 cm. diameter (25), and a small cell with 1.3×1.3 cm. cross-section (7). Narrow slits were used for both cells. The calibration of the apparatus is described by Brice, Halwer, and Speiser (3). The value of the refractive index increment of globin was taken as 0.200 ml./g., $\lambda = 436$ mμ (19), and the same value was assumed for the globin components. The constant K in the light scattering equation (6), $Kc/R_{90} = 1/M_w + Bc$, therefore, has the value 6.46×10^{-7}. R_{90} is the reduced intensity of the light scattered at 90°, c, the concentration, and B, the second virial coefficient.

Dust-free water was prepared by distillation. Solvent was cleaned by filtration through an ultrafine sintered glass filter. Solutions were clarified by centrifugation at approximately 80,000 g for 90 minutes in a Spinco preparative ultracentrifuge, followed by filtration through the ultrafine sintered glass filter.

Solutions were prepared by dissolving the protein in the chosen buffer and then dialyzing against large amounts of the same solvent. Subsequent dialysis against other buffers were made, where necessary, to change the pH or ionic strength. In some light scattering experiments, pH was changed by adding acid or alkali directly into the solution in the light scattering cell. In all cases, the pH was measured with a Beckman pH meter calibrated with commercial standards.

In experiments with globin, approximately 0.5% solutions were clarified and the concentration was determined by means of a Brice-Speiser differential refractometer (2). Solvent scattering was determined first, and then successive amounts of stock solution were added followed by magnetic stirring.

For the separated globin components, centrifuged solution was filtered directly into the small square cell. The solution was diluted by filtering solvent into the cell. If necessary the diluted solution was filtered again. After each filtration, the concentration was determined by absorption measurements at 280 mμ in a Beckman spectrophotometer, calibrated against the differential refractometer.

Sedimentation

A Spinco analytical ultracentrifuge was used for sedimentation studies. The optical

system was equipped with a diagonal wire. Molecular weights were obtained from the schlieren pattern at the meniscus end before the disappearance of the plateau region following Klainer and Kegeles' modification (16) of the method of Archibald (1). The second moment of the relevant section of the pattern was evaluated using an Amsler mechanical integrator as described by Smith, Wood, and Charlwood (20). The shape of the pattern is favorable for mechanical integration by this type of instrument (10). Concentrations were determined refractometrically.

The partial specific volume ($\bar{V}$) of globin at pH 1.9 in 0.05 N HCl, NaCl was determined by the magnetic float method of MacInnes (17) using the apparatus and procedures of Charlwood (4). Concentrations of the stock globin solutions were determined by drying samples at 105°. Samples of the solvent against which the stock solution had been dialyzed were dried similarly. Two separate determinations involving stock solutions, 1.75_4 and $1.93_0\%$ respectively, were made. The densities of three concentrations in the range 0.2–0.5% were measured in each case.

Osmotic Pressures

Osmotic pressures were determined in osmometers of the type described by Donnan and Rose (5), the volume of solution necessary being reduced by a plastic insert in the sac (18). Membranes were made according to Mallette (18), omitting addition of ethylene glycol to the collodion. Equilibrium could be reached in less than 20 hours and the pressure remained unchanged for more than 12 hours thereafter.

Electrophoresis

Electrophoretic analysis was conducted in a Perkin Elmer Model 38 apparatus.

RESULTS AND DISCUSSION

Partial Specific Volume of Horse Globin

Two separate determinations of $\bar{V}$ gave the values 0.754_6 and 0.754_2, each consistent to less than $\pm 0.1\%$. Previous pycnometric determinations of $\bar{V}$ of horse hemoglobin have given the values 0.749 (23), 0.754 (24), and 0.749 (22).

Molecular Weight and Interactions of Globin

Preliminary light scattering experiments showed that Kc/R_{90} plotted against concentration gave straight, horizontal lines in the pH region 2.0–3.4 (Fig. 1) with the molecular weight increasing as the pH was raised. The scattering of these solutions did not change over a 20-hour period. At pH 3.75, the second virial coefficient had a positive value and the scattering increased with time (Fig. 1).

If the reactions between the globin subunits could be regarded as a simple monomer–dimer equilibrium with a monomer molecular weight of 16,000, a plot of $1/M_w$ against concentration would give distinctly curved lines in the region of concentrations and molecular weights covered by these experiments (21). No evidence of such an equilibrium was found.

Taking the second virial coefficient as zero in the pH region 2.0–3.5, Kc/R_{90} is equal to $1/M_w$. Fig. 2 shows the weight average molecular weight of whole (unfractionated) globin as a function of pH. Curve A is obtained by adding alkali to a solution originally at pH 2.1, curve B by adding acid to a solution originally at pH 3.4.

In Table I are the results of a series of experiments (i, ii, iii) where the pH was changed, except as indicated, by dialysis. Statistical procedures show that the differences between groups (i) and (ii), including the starting point of curve A (Fig. 2) and the end point of
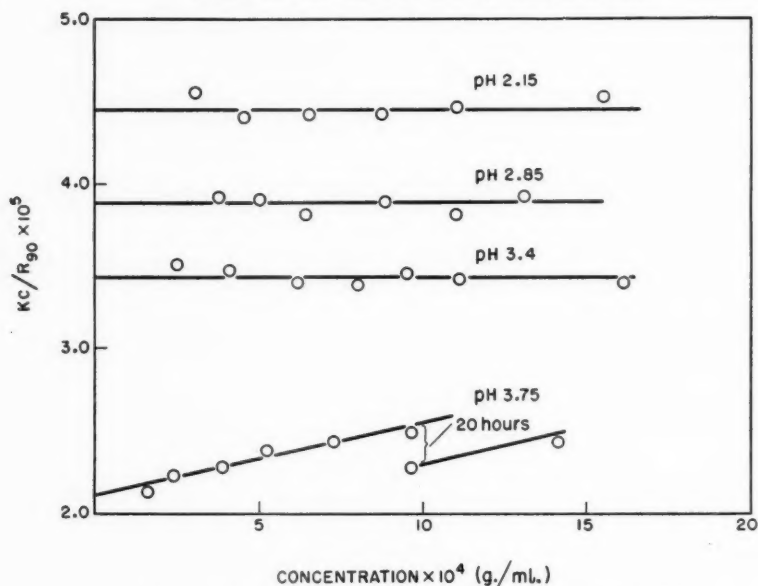
FIG. 1. Light scattering data for globin in 0.05 M NaCl solution.

TABLE I

EFFECT OF CHANGES IN pH AND IONIC STRENGTH ON MOLECULAR WEIGHT OF GLOBIN

Original solvent		M_w in original solvent	Solvent after dialysis		M_w after dialysis
pH	Ionic str.		pH	Ionic str.	
2.1	0.05	22,400	—	—	— ⎫
2.1	0.05	21,400	—	—	— ⎬ i
3.4	0.05	—	2.1	0.05	24,700 ⎫
3.7	0.05	—	2.1	0.05	24,000 ⎬ ii
4.1	0.05	—	2.1	0.05	25,300 ⎭
2.1	0.05	—	3.3	0.05	30,000 ⎫ iii
3.3	0.05	29,500	—	—	— ⎭
1.8	0.10	30,300	—	—	—
1.8	0.10	27,900	1.8	0.05	29,200
2.0	0.10	27,500	2.0	0.05	29,100
2.0	0.20	49,300	2.0	0.05	33,800
2.0	0.20	—	2.0	0.05	35,200
3.3	0.10	29,400	—	—	—
3.3	0.20	78,000	3.3	0.05	50,000

curve B, are highly significant. The association that takes place when the pH is increased is, therefore, partly irreversible. There was no significant difference between solution brought down from pH 3.4 and pH 4.1, which indicates that the association that takes place at higher pH is reversible, as has been noted by Reichmann and Colvin (19).

At ionic strengths 0.1 and 0.2 in acidified NaCl solutions, second virial coefficients were zero or slightly negative. Molecular weights at these ionic strengths are also given in Table I together with the molecular weights observed after dialysis against 0.05 M
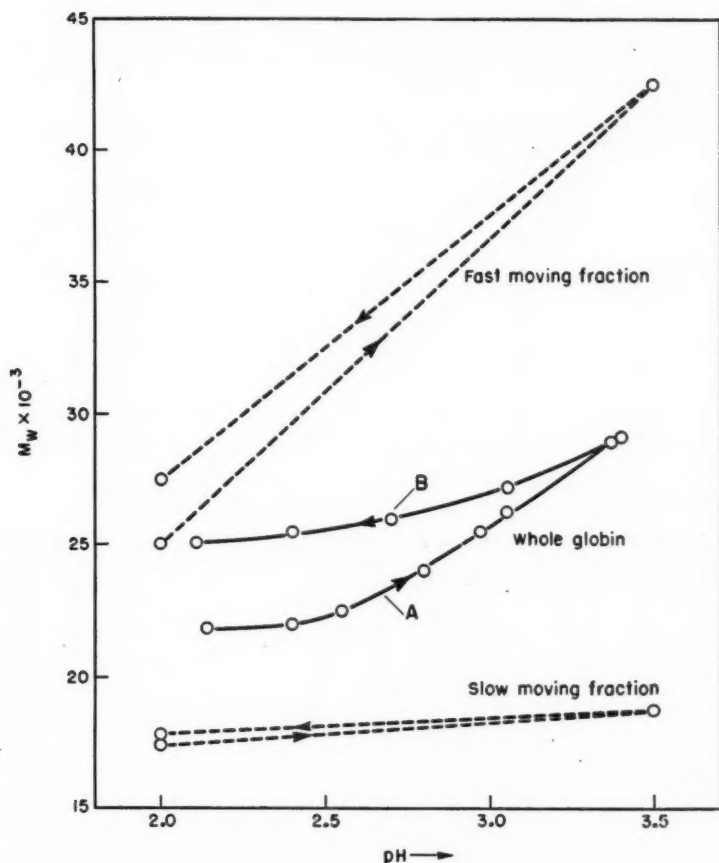
FIG. 2. Weight average molecular weights of globin and globin fractions as a function of pH.

NaCl. At pH 2.0 the association taking place when the ionic strength is increased to 0.1 M NaCl is completely irreversible. At pH 3.3 the molecular weight was the same in 0.1 and 0.05 M NaCl. The association that occurred when the ionic strength was further increased to 0.2 M NaCl was partly reversible both at pH 2.0 and 3.3.

Sedimentation experiments using Archibald's method confirmed that aggregation occurs as the ionic strength is increased. Weight average molecular weights in phosphate buffer, pH 2.0, at ionic strengths 0.05 and 0.1 are given in Table II. The absence of disturbing charge effects at pH 2.0 and ionic strength 0.05 was indicated by a measurement on lysozyme. A value of 14,700 was obtained for the molecular weight in agreement with other findings (20). Reichmann and Colvin (19) found the sedimentation rate of ribonuclease unaffected in a similar low ionic strength and pH medium.

Sedimentation velocity experiments on 0.5% solutions in NaCl, HCl at pH 1.9 reveal a partial aggregation at ionic strength 0.05 (Fig. 3 A) and an extensive aggregation at ionic strength 0.1 (Fig. 3 B). Sedimentation rates ($S_{20,w}$) measured on the maximum ordinates were 1.00 and 1.45 Svedbergs respectively.

TABLE II

MOLECULAR WEIGHTS FROM SEDIMENTATION AND OSMOTIC PRESSURE

Material	Preparation conditions*	Molecular wt. method	Solvent		M_w	M_n
			pH	Ionic str.		
Globin	—	Sed.	2.0	0.05 phos.	21,200	
Globin	—	Sed.	2.0	0.10 phos.	29,600	
Globin	—	O.P.	2.0	0.05 Cl⁻		15,000–16,000
Globin	—	O.P.	3.4	0.05 Cl⁻		17,000–18,000
Faster comp.	2(a)	Sed.	1.9	0.05 phos.	19,400	
Faster comp.	1(a)	Sed.	1.9	0.05 phos.	27,500	
Faster comp.	3(a)	Sed.	1.8	0.05 phos.	31,600	
Faster comp.	3(a)	Sed.	3.1	0.05 phos.	41,800	
Faster comp.	3(a)	Sed.	5.5	0.05 acetate	101,000	
Faster comp.	2(b)	O.P.	2.0	0.05 Cl⁻		17,000

*See text.

Osmotic pressure data for globin in 0.05 M NaCl solution at pH 2.0 and 3.4 are given in Fig. 4 and Table II. The number average molecular weight of globin at these values of pH was found to be 15,000–16,000 and 17,000–18,000 respectively.
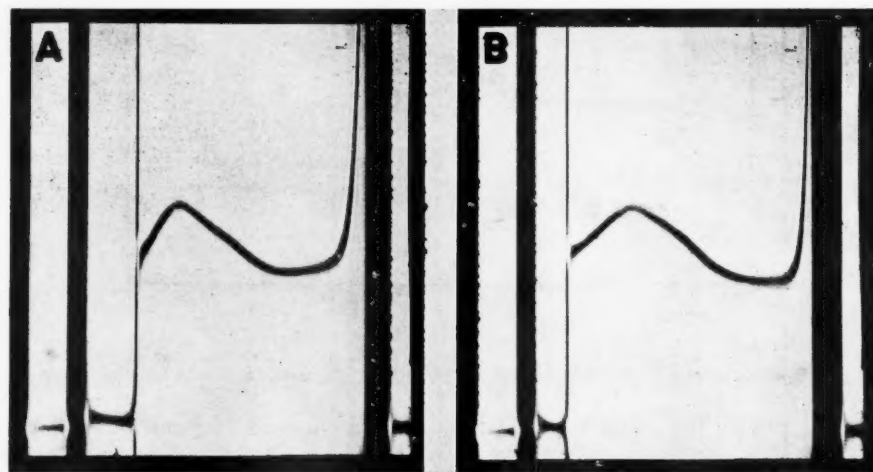
FIG. 3. Sedimentation patterns of globin 0.5% in NaCl, HCl, pH 1.9: A, ionic strength 0.05; B, ionic strength 0.10; 126 minutes at 59,780 r.p.m.

The difference between the number and weight average molecular weights at ionic strength 0.05, pH 1.9 and 2.0, and the indication of heavier material in Fig. 3 A show that there is not complete dissociation to subunits of 16,000 molecular weight under these conditions but suggest that this would be the limiting case.

Molecular Weight and Interactions of Globin Fractions

The effects of pH and ionic strength on the faster moving fraction were investigated by light scattering and the average results are shown in Table III.

The initial molecular weight of the freeze-dried preparation (condition 1(a)) was significantly higher than that of the unisolated sample (condition 2(b)) indicating that the
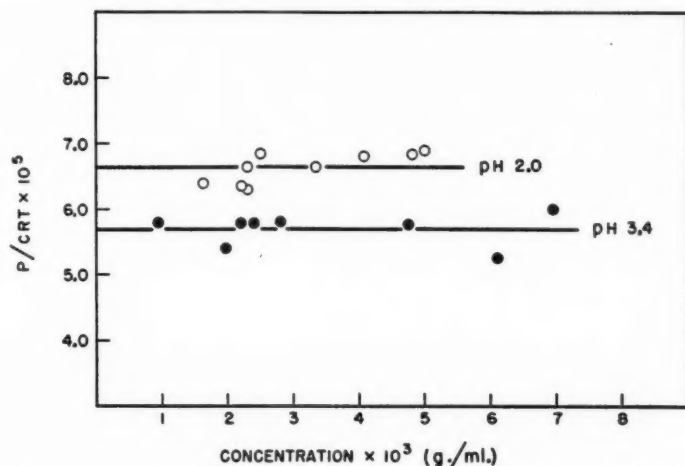
FIG. 4. Osmotic pressure data for globin in 0.05 M NaCl solution at pH 2.0 and 3.4.

TABLE III

MOLECULAR WEIGHTS OF GLOBIN COMPONENTS BY LIGHT SCATTERING IN 0.05 M NaCl, pH INITIALLY 2.0,
RAISED TO 3.5, AND RETURNED TO 2.0

Material	Preparative conditions*	No. of preparations	pH 2.0	→	pH 3.5	→	pH 2.0
Faster comp.	1(a)	4	33,000		45,500		31,000
Faster comp.	2(b)	2	25,000		42,500		27,500
Faster comp.	4(b)	1	33,000		40,000		31,500
Slower comp.	1(b)	2	17,500		18,700		17,700

*See text.

dialysis and lyophilization procedures produced an irreversible association. The degree of association of the freeze-dried sample was comparable with that produced by 0.1 M NACl without lyophilization (condition 4(b)). At pH 3.5, all three preparations of the faster moving fraction showed about the same degree of association. With material prepared under conditions 1(a) and 4(b) the association taking place between pH 2.0 and 3.5 was completely reversible. The difference between the initial and final molecular weights of the sample isolated by condition 2 is small (Figs. 2 and 5) and may indicate partial irreversibility.

Molecular weights obtained from sedimentation showed a similar pattern, Table II. The faster moving fraction isolated at low ionic strength and not freeze-dried (preparation condition 2(a)) had a lower molecular weight than material separated under similar conditions but dialyzed and freeze-dried (condition 1(a)). When prepared at ionic strength 0.1 and freeze-dried (condition 3(a)), the faster component had a molecular weight of 31,000 even in a lower ionic strength medium and further aggregation occurred at higher pH's.

Osmotic pressure measurements on a sample of the faster component (prepared in 0.05 M NaCl, pH 2.0, and not freeze-dried) gave a value of approximately 17,000.

Light scattering experiments with freeze-dried samples only were carried out with

the slower fraction. Results are shown in Figs. 2 and 6 and Table III. The slower fraction had a considerably lower molecular weight than the faster, and there was only a slight difference in its molecular weights at pH 2.0 and 3.5. The low molecular weight and lack of tendency to aggregate indicate that no irreversible association occurs during freeze-drying.
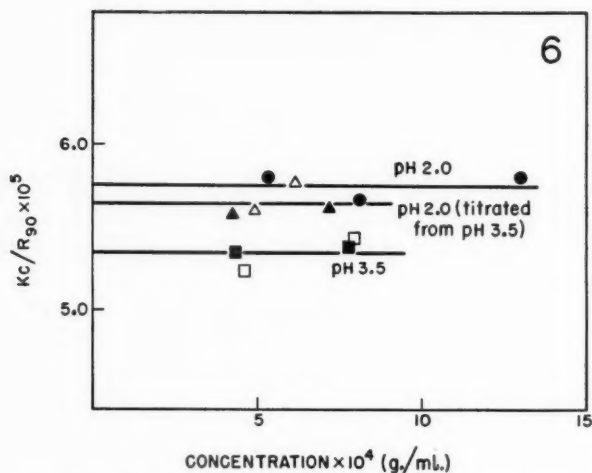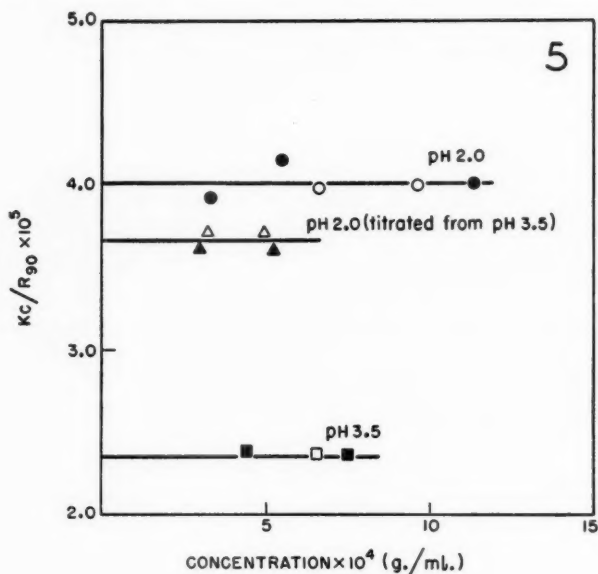
FIG. 5. Light scattering data for the faster moving fraction prepared without freeze-drying (preparative condition 2(b), in 0.05 M NaCl solution.

FIG. 6. Light scattering data for the slower moving fraction (preparative condition 1(b)) in 0.05 M NaCl solution.

Electrophoretic Examination of Globin and Fractions

The aggregation that occurs at pH 2.0 and below as the ionic strength is increased is not reflected by changes in the electrophoretic pattern. Two components only show at ionic strengths 0.035, 0.05, 0.075, and 0.1.

The ascending electrophoretic patterns of globin in 0.05 *M* NaCl solution at pH 2.0, 3.5, and 2.0 after dialysis from pH 3.5 are shown in Fig. 7 A, B, and C. The two main peaks shown by globin below pH 2.0 appear in Fig. 7 A (together with the beginning of the pattern complexity that develops above pH 2.0 (19)). Comparison of Fig. 7 A and C shows the irreversibility of the association reactions in globin. The isolated fractions
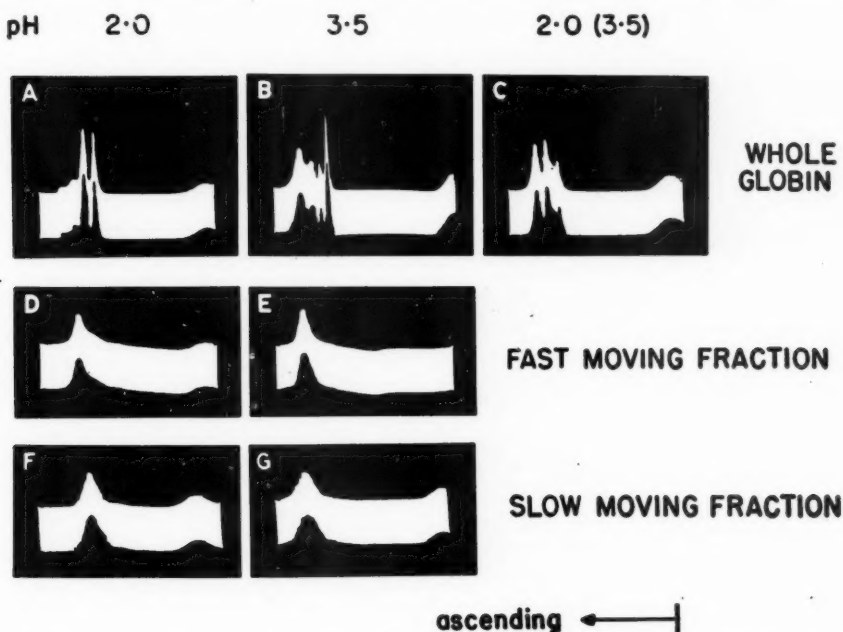
FIG. 7. Electrophoretic patterns (ascending) of globin and globin fractions in 0.05 *M* NaCl: A, globin, pH 2.0; B, after dialysis of A to pH 3.5; C, after dialysis of B to pH 2.0; D, faster component, pH 2.0; E, after dialysis of D to pH 3.5; F, slower component, pH 2.0; G, after dialysis of F to pH 3.5.

show only one peak each at both pH's (Fig. 7 D–G), while unfractionated globin gives rise to a complex pattern (Fig. 7 C) at the higher pH value (Fig. 7 B). These results indicate that association products are formed between globin components when the pH's of globin solutions are raised above 2.0 and that the aggregates of the faster component do not differ electrokinetically from the monomer.

CONCLUSION

Reichmann and Colvin (19) have summarized the evidence indicating that horse globin splits, at low pH and ionic strength, into four subunits, all of molecular weight about 16,000. At pH values below 2 and an ionic strength of 0.05, the splitting is nearly complete. Under these conditions, the electrophoretic pattern shows two components. Samples of each of these components have now been obtained and investigated separately.

The faster moving component had a M_w of about 25,000 at low ionic strength and pH and associated readily as the pH was raised. This association due to pH change was nearly reversible. The slower moving component had a M_w of about 17,000 and showed little tendency to associate. Unfractionated globin aggregated to a lesser extent than the faster component as the pH was raised but this aggregation was much less reversible, which points towards interaction between the two components. Extra peaks appearing in the electrophoretic pattern of unfractionated globin above pH 2 are probably due to aggregates of the faster component with itself and with the slower component but not due to aggregation of the slower component only. The aggregation that occurs at pH 2.0 and below when the ionic strength is increased presumably involves only the faster component.

The ready aggregation of these highly positively charged globin subunits may be due to interactions between non-polar parts of the molecules (13). That these may be particularly important in globin is suggested by interfacial tension studies of Haurowitz *et al.* (8) which were interpreted in terms of unusual numbers or unusually favorably distributed non-polar groupings on the exterior of the globin molecule. Attractive forces (15) arising as carboxyl groups are ionized (above pH 2) may bring these non-polar regions into suitable orientation and once in contact they would not necessarily dissociate as the pH is lowered. Configurational changes, too, may possibly be involved.

ACKNOWLEDGMENTS

REFERENCES

1. ARCHIBALD, W. J. J. Phys. & Colloid Chem. **51**, 1204 (1947).
2. BRICE, B. A. and HALWER, M. J. Opt. Soc. Amer. **41**, 1033 (1951).
3. BRICE, B. A., HALWER, M., and SPEISER, R. J. Opt. Soc. Amer. **40**, 768 (1950).
4. CHARLWOOD, P. A. J. Am. Chem. Soc. **79**, 776 (1957)
5. DONNAN, F. G. and ROSE, R. C. Can. J. Research, B, **28**, 105 (1950).
6. DOTY, P. and EDSALL, J. T. Advances in Protein Chem. **6**, 35 (1951).
7. DOTY, P. and MYERS, G. E. Discussions Faraday Soc. **13**, 51 (1953).
8. HAUROWITZ, F., BOUCHER, P., and DICKS, M. Federation Proc. **12**, 215 (1953).
9. HEIDELBERGER, M. J. Biol. Chem. **53**, 31 (1922).
10. JENSEN (DJURTOFT), R. J. Polymer Sci. **12**, 401 (1954).
11. JOHNSON, P. and SHOOTER, E. M. Science, **109**, 39 (1949).
12. JOPE, E. M., JOPE, H. M., and O'BRIEN, J. R. P. Nature, **164**, 622 (1949).
13. KAUZMANN, W. J. Cellular Comp. Physiol. **47** (Suppl. 1), 113 (1956).
14. KEKWICK, R. A., LYTTLETON, J. W., BREWER, E., and DEBLOW, E. S. Biochem. J. **49**, 233 (1951).
15. KIRKWOOD, J. G. *In* The mechanism of enzyme action. *Edited by* McElroy, W. D. and Glass, B. Johns Hopkins Press, Baltimore, Md. 1954.
16. KLAINER, S. M. and KEGELES, G. J. Phys. Chem. **59**, 952 (1955).
17. MacINNES, D. A., DAYHOFF, M. O., and RAY, B. R. Rev. Sci. Instr. **22**, 642 (1951).
18. MALLETTE, M. F. Arch. Biochem. and Biophys. **48**, 315 (1954).
19. REICHMANN, M. E. and COLVIN, J. R. Can. J. Chem. **34**, 411 (1956).
20. SMITH, D. B., WOOD, G. C., and CHARLWOOD, P. A. Can. J. Chem. **34**, 364 (1956).
21. STEINER, R. F. Arch. Biochem. and Biophys. **34**, 333 (1952).
22. STEINHARDT, J. J. Biol. Chem. **123**, 543 (1938).
23. SVEDBERG, T. and FAHRAEUS, R. J. Am. Chem. Soc. **48**, 430 (1926).
24. SVEDBERG, T. and NICHOLS, J. B. J. Am. Chem. Soc. **49**, 2920 (1927).
25. WITNAUER, L. P. and SCHERR, H. J. Rev. Sci. Instr. **23**, 99 (1952).

A SYNTHESIS OF
5,6-DIDEOXY-D-XYLOHEXOSE(5-DEOXY-5-C-METHYL-D-XYLOSE)[1]

J. K. N. Jones and J. L. Thompson[2]

ABSTRACT

A synthesis of 5,6-dideoxy-D-xylohexose (I) from D-glucose is described. The action of sodium iodide in acetone on some toluene-p-sulphonyl esters of sugar derivatives is detailed.

INTRODUCTION

A synthesis by enzymes of 5,6-dideoxy-D-threo-2-hexulose (5-deoxy-5-C-methyl-D-threo-2-pentulose) from propionaldehyde, hexose diphosphate, and aldolase has been described (4). This sugar was characterized as the phenylosazone of 5,6-dideoxy-D-xylohexose (5-deoxy-5-C-methyl-D-xylose) (I) which was prepared from D-glucose by McSweeny and Wiggins (7) and from D-fructose by Gorin, Hough, and Jones (4).

As a result of an investigation of the reaction of toluene-p-sulphonyl and methane-sulphonyl esters of secondary alcohols with sodium iodide an additional method of preparation of the dideoxy sugar (I) was attained. While this work was in progress another method of synthesis was described by English and Levy (2).

It was observed that the 5,6-di-O-toluene-p-sulphonyl (tosyl), 3,5,6-tri-O-methane-sulphonyl (mesyl) (11), and 3,5,6-tri-O-toluene-p-sulphonyl esters (8) of 1,2-O-isopropylidene-D-glucofuranose when heated with sodium iodide liberated iodine with the formation of unsaturated compounds. The first of these compounds gave 5,6-dideoxy-1,2-O-isopropylidene-D-xylohexosene-5 (II) which on catalytic reduction furnished the 1,2-O-isopropylidene derivative of the cyclic form of (I). 5,6-Dideoxy-1,2-O-isopropylidene-3-O-methanesulphonyl-D-xylohexosene-5 was identified as the product produced from the second substance. The tri-O-tosyl compound gave a sirupy unsaturated O-tosyl ester which was not further investigated.

Toluene-p-sulphonyl groups can be removed by reductive hydrolysis with sodium amalgam with comparative ease but the methanesulphonyl grouping could not be removed in this fashion. However, it was possible to remove this ester grouping by heating the methanesulphonate with sodium hydroxide solution.
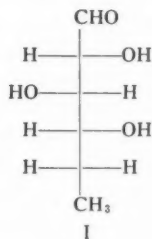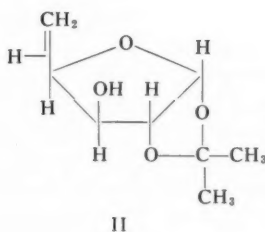
The elimination of toluene-p-sulphonyl groups situated on vicinal primary and secondary alcoholic groups by heating the esters with sodium iodide solution with the resultant formation of a substituted ethylene has been observed previously in the hexitol series

(12). This type of reaction however has been little studied in the hexose series (cf. Bell, Friedmann, and Williamson (1); and Vischer and Reichstein (13)).

Reduction of the unsaturated sugar derivative either catalytically or with boiling ethanol and a Raney nickel catalyst gave a derivative of the dideoxy sugar (I). On acidic hydrolysis the reducing sugar was obtained as a sirup; it was converted to the crystalline phenylosazone. This was observed to have a variable melting point which was dependent upon the solvent used to recrystallize it. This may account for the different melting point obtained for the osazone by Lehninger and Sice (6).

The action of Finkelstein's reagent (3) (sodium iodide in acetone) on 2,3-O-isopropylidene-1,4,5-tri-O-toluene-p-sulphonyl-β-D-fructose, methyl 2,3,4-tri-O-toluene-p-sulphonyl-β-L-arabinoside, methyl 2,3,4-tri-O-toluene-p-sulphonyl-α-D-riboside, and methyl 2,3,4-tri-O-toluene-p-sulphonyl-β-D-xyloside was also studied. It was found that if the temperature was sufficiently high (ca. 130° C.) all of the above compounds liberated iodine. The products were complex mixtures from which it was not found possible to isolate crystalline derivatives, perhaps because of further decomposition of the products formed. All these tosyl esters were relatively stable to hot solutions of sodium hydroxide, sodium acetate in wet acetic acid, sodium acetate in acetic anhydride, and hydrochloric acid.

EXPERIMENTAL

Solutions were evaporated under reduced pressure. Optical rotations were measured in water at 20° C. ±2° (unless otherwise stated). Sugars were separated chromatographically and were detected with the silver nitrate – sodium hydroxide spray.

Synthesis of 5,6-Dideoxy-1,2-O-isopropylidene-D-xylohexosene-5

1,2-O-Isopropylidene-5,6-di-O-toluene-p-sulphonyl-D-glucose (1.3 g., m.p. 150–155° C.) was heated in a sealed tube at 90° C. for 70 minutes with acetone (5 ml.) and sodium iodide (4.8 g.). The tube was cooled, opened, and the contents were poured into ether. The dark brown ethereal solution which contained free iodine was shaken once with an aqueous solution of sodium thiosulphate and sodium bicarbonate and then washed with water. It was dried over calcium sulphate and evaporated to give a clear, colorless sirup (0.51 g.).

Hydrogenation of 5,6-Dideoxy-1,2-O-isopropylidene-D-xylohexosene-5

The sirup mentioned above (507 mg.) was dissolved in ethanol (25 ml.) and shaken (15 minutes) in a hydrogenation apparatus at room temperature and at slightly greater than atmospheric pressure in the presence of Adams' platinic oxide catalyst (51 mg.). Hydrogen (43 cc.) was absorbed, mostly in the first 5 minutes. The catalyst was removed by filtration and the filtrate was concentrated. The residual sirup could not be induced to crystallize and a sodium fusion revealed that it contained traces of sulphur compounds. Accordingly it was further treated with sodium amalgam in order to remove them. The sirup was dissolved in a mixture of water (4 ml.) and methanol (10 ml.). Sodium amalgam (4%, 5.6 g.) was added and the mixture was stirred overnight. Water and chloroform were added to the reaction mixture and the solutions were separated from mercury. The chloroform layer was separated from the aqueous layer which was again extracted with chloroform. The combined chloroform extracts were dried (anhydrous sodium carbonate), filtered, and the filtrate evaporated to a sirup which crystallized. The product, 5,6-dideoxy-1,2,-O-isopropylidene-D-xylohexose, was recrystallized from light petroleum, b.p. 60–80° C. It was further purified by subliming it under vacuum.

Yield: 177 mg., m.p. 77–78° C., $[\alpha]_D^{22} = -22° \pm 1°$ (c, 4.45 in chloroform). Anal. Calc. for $C_9H_{16}O_4$: C, 57.4; H, 8.6%. Found: C, 57.2; H, 8.5%.

5,6-Dideoxy-D-xylohexose Phenylosazone

5,6-Dideoxy-1,2-O-*iso*propylidene-D-*xylo*hexose (65 mg.) was heated with N/10 sulphuric acid for 1 hour at 100° C. The solution was neutralized with barium carbonate, filtered, and evaporated to dryness to give the sirupy aldose which had $[\alpha]_D$ +2° (c, 3.5 in MeOH) and moved at 2.1 times the speed of rhamnose in n-butanol–pyridine–water (3:1:1, v/v). This aldose was dissolved in a mixture of acetic acid (0.5 ml.), water (2 ml.), and phenylhydrazine (0.14 ml.) and the solution was heated at 100° C. for 10 minutes. The osazone which formed was dark yellow and melted at 171.5° C. It was recrystallized twice from methanol–water, m.p. 172.5° C., yield 12 mg. The X-ray powder photograph of the osazone was indistinguishable from that of 5,6-dideoxy-D-*threo*-2-hexulose phenylosazone. The above preparation was repeated except that the osazone was allowed to form at room temperature and was recrystallized from ethanol–water. The product was bright yellow, had m.p. 142–143° C. and $[\alpha]_D$ +14° C. $\pm$6° (c, 0.43 in pyridine:ethanol, 3.2). Anal. Calc. for $C_{18}H_{22}O_2N_4$: C, 66.2; H, 6.8; N, 17.2%. Found: C, 66.2; H, 6.7; N, 17.0%.

The osazone, m.p. 142–143° C., was changed to the form with m.p. 169–170° C. by equilibration in pyridine–ethanol (3:2) and crystallization by addition of water.

5,6-Dideoxy-1,2-O-isopropylidene-3-O-methanesulphonyl-D-xylohexosene-5

1,2-O-*Iso*propylidene-3,5,6-tri-O-methanesulphonyl-D-glucose, m.p. 163° C. (10 g.) (11), was heated for a short time at 100° C. with sodium iodide (26 g., fourfold excess) and acetone (100 ml.). The dark brown reaction mixture was poured into chloroform and the mixture was stirred with water containing a little sodium bicarbonate and 10 g. of sodium thiosulphate pentahydrate (the theoretical quantity required was 11 g.) to remove iodine. The pale yellow solution was not further decolorized when a few crystals of sodium thiosulphate were added to it. The chloroform layer was separated, washed twice with water, dried (anhydrous sodium carbonate), and evaporated. The crude product (6.06 g., 87%) remained as a crystalline mass, m.p. 78–81° C. It was recrystallized from aqueous ethanol and then had m.p. 81° C. Anal. Calc. for $C_{10}H_{16}O_6S$: C, 45.5; H, 6.1; S, 12.1%. Found: C, 45.6; H, 6.65; S, 12.3%.

Attempted Removal of the 3-O-Methanesulphonyl Group with Sodium Amalgam

A portion (3.68 g.) of the crude product above was dissolved in methanol (50 ml.), and sodium amalgam (27 g., 4%) and water (2 ml.) were added. The mixture was stirred at room temperature overnight. Water was added, the mercury was separated, and the aqueous solution was extracted with chloroform. The chloroform extracts were dried (anhydrous sodium carbonate), filtered, and the solvent was removed to give unchanged 5,6-dideoxy-1,2-O-*iso*propylidene-3-O-methanesulphonyl-D-*xylo*hexosene-5. Yield: 3.22 g.

The recrystallized sample had m.p. 81° C., $[\alpha]_D$ −9° (c, 3.1 in acetone), −36° (c, 1.49 in CHCl₃). The mixed m.p. with an authentic specimen of 1,2-O-*iso*propylidene-5,6-dideoxy-D-*xylo*hexose, m.p. 77–78° C., was greatly depressed. Anal. Calc. for $C_{10}H_{16}O_6S$: C, 45.5; H, 6.1; S, 12.1%. Found: C, 45.6; H, 6.1; S, 12.0%.

Formation of 5,6-Dideoxy-1,2-isopropylidene-3-O-methanesulphonyl-D-xylohexose (I)

In an attempt to remove the methanesulphonyl group 1,2-O-*iso*propylidene-3-O-methanesulphonyl-5,6-dideoxy-D-*xylo*hexosene-5 (0.46 g.) was dissolved in ethanol (50 ml.) and shaken in a hydrogenation apparatus at slightly greater than atmospheric pressure in the presence of Raney nickel catalyst (3 g.). Most of the gas which was

absorbed was taken up in the first 4 hours. After 24 hours the catalyst was removed by filtration through "Celite", which was thoroughly washed with ethanol, and the combined filtrates were evaporated to a sirup, which soon crystallized. The product was recrystallized from ethanol–water. Yield: 300 mg.; m.p. 93° C., $[\alpha]_D^{23°}$ $-23°$ (c, 2.4 in $CHCl_3$). Anal. Calc. for $C_9H_{16}O_4$: C, 57.4; H, 8.6%. Calc. for the 3-O-methanesulphonyl ester derivative, $C_{10}H_{18}O_6S$: C, 45.1; H, 6.8; S, 12.0%. Found: C, 45.1; H, 6.6; S, 12.2%.

In a second experiment the D-xylohexosene-5 derivative (2 g.) was boiled under reflux in ethanol (100 ml.) with the addition of Raney nickel (1 g.). After 60 hours the cooled solution, which contained acetaldehyde, was filtered and evaporated to a sirup (1.9 g.), which crystallized. The product was recrystallized from aqueous ethanol and had m.p. 93° C., not depressed on admixture with an authentic specimen of the 1,2-O-isopropylidene 3-O-mesyl derivative of I.

Removal of the Methanesulphonoxy Group by Hydrolysis with Alkali

The product of hydrogenation (1 g.) was dissolved in methanol (15 ml.), and water (4 ml.) and sodium hydroxide (1 g.) were added. The solution was boiled under reflux for about 7 hours. Magnesium sulphate was added to lower the pH. The mixture was filtered and the residue was washed with ethanol. The combined filtrates were evaporated to dryness and the residue was extracted with chloroform. The chloroform extracts were filtered and the filtrate concentrated. Yield: 600 mg., 78% of recrystallized product which showed no depression on admixture with an authentic specimen of 1,2-O-isopropylidene-5,6-dideoxy-D-xylohexose, 77–78° C.

Formation of 5,6-Dideoxy-1,2-O-isopropylidene-3-O-methanesulphonyl-D-xylohexose (II)

5,6-Dideoxy-1,2-O-isopropylidene-D-xylohexose (45 mg.) was dissolved in dry pyridine (1 ml.) and methanesulphonyl chloride (5 drops) was added. The solution was allowed to stand overnight. A further portion of methanesulphonyl chloride (3 drops) was added and the mixture was allowed to stand 4 hours longer. A little water was then added to destroy excess methanesulphonyl chloride. After the mixture had cooled a further 10 ml. of water was added and the mixture was evaporated until crystals appeared (m.p. 86–87° C.). The crystals were collected and recrystallized from methanol. The product had m.p. 90–91° C. not depressed on admixture with an authentic specimen 90–91° C. Yield: 21 mg.

2,3-O-Isopropylidene-1,4,5-tri-O-toluene-p-sulphonyl-D-fructose

Sirupy 2,3-O-isopropylidene-D-fructopyranose (2.16 g.) (9) was dissolved in pyridine (10 ml.) and the solution was warmed at 42° C. for 30 hours with toluene-p-sulphonyl chloride (11 g.). The reaction mixture was poured into an excess of aqueous sodium bicarbonate. The gummy precipitate solidified on stirring and was collected. It was recrystallized from ethanol, m.p. 130° C., $[\alpha]_D^{21}$ 22°±3° (c, 0.64 in EtOH). Yield: 5.3 g., 76%. Calc. for $C_{30}H_{34}O_{12}S_3$: C, 52.8%; H, 5.0%; S, 14.1%. Found: C, 52.6%; H, 5.0%; S, 13.8%.

Methyl 2,3,4-Tri-O-toluene-p-sulphonyl-β-L-arabinoside

Methyl-β-L-arabinopyranoside (1.55 g.) (10) and toluene-p-sulphonyl chloride (10 g.) were dissolved in pyridine (15 ml.) and kept at 45° for 18 hours. The solution was cooled in ice-water while water was added to destroy the excess toluene-p-sulphonyl chloride, and the mixture was then poured into aqueous sodium bicarbonate. The product precipitated as an oil. The oil was then taken up in chloroform, washed with water, and dried over "Drierite". The sirupy product thus obtained after filtration and removal

of the solvent was crystallized from methanol. Yield: 2.66 g., 45%, m.p. of a recrystallized sample, 116–117° C., $[\alpha]_D^{23}$ 99.5° C.±1° (c, 1.97 in CHCl₃). Calc. for $C_{27}H_{30}O_{11}S_3$: C, 51.7%; H, 4.8%; S, 15.3%. Found: C, 51.9%; H, 4.9%; S, 15.3%.

Methyl 2,3,4-Tri-O-toluene-p-sulphonyl-D-ribopyranoside

Sirupy methyl-D-ribopyranoside (3 g.) obtained by the method known to give the pyranose form (5) was kept at 40° for 18 hours in pyridine (70 ml.) in which was dissolved an excess of toluene-p-sulphonyl chloride (30 g.). The product was isolated as described above. The substance was twice recrystallized from methanol to give 5.8 g. of silky needles (50%), m.p. 129–130° C., $[\alpha]_D^{23}$ 31° (c, 2.86 in chloroform). Calc. for $C_{27}H_{30}O_{11}S_3$: C, 51.7%; H, 4.8%; S, 15.3%. Found: C, 51.7%; H, 4.8%; S, 15.3%.

Methyl 2,3,4-Tri-O-toluene-p-sulphonyl-β-D-xyloside

Methyl-β-D-xylopyranoside (3 g.) was dissolved in pyridine (70 ml.) which contained toluene-p-sulphonyl chloride (30 g.). The solution was allowed to stand overnight at 40° C. The product was isolated in the usual way. Yield 61% of a product with m.p. 140–141° C. and $[\alpha]_D^{23}$ −36° C.±2° (c, 0.94 in CHCl₃) after recrystallization from aqueous methanol. Calc. for $C_{27}H_{30}O_{11}S_3$: C, 51.7%; H, 4.8%; S, 15.3%. Found: C, 51.8%; H, 4.9%; S, 15.7%.

Action of Sodium Iodide in Acetone on the Above-described Tosyl Esters

Each of the above-described pentose derivatives and the fructose derivative (1 g.) when heated in acetone solution (20 ml.) with sodium iodide (1 g.) in a sealed tube at 120° C. yielded dark brown solutions which contained free iodine. No crystalline product other than unchanged starting material was isolated from the reaction mixtures.

When each of the pentoside tri-O-toluene-p-sulphonate derivatives (1 g.) was dissolved (a) in acetic acid (10 ml.) in which was dissolved sodium acetate (3 g.) and water (1 ml.) or (b) in acetic anhydride (10 ml.) and sodium acetate (3 g.) no exchange of tosyl groups for acetoxy groups was detected even after the solutions had been heated for 48 hours under reflux.

Action of Concentrated Hydrochloric Acid on 2,3,4-Tri-O-toluene-p-sulphonyl Methyl-β-D-Xyloside

This compound (0.2 g.) dissolved in concentrated hydrochloric acid (5 ml.) on warming the solution. After removal of the acid in the steam bath the original compound was recovered unchanged in 90% yield.

REFERENCES

1. BELL, D. J., FRIEDMANN, E., and WILLIAMSON, S. J. Chem. Soc. 252 (1937).
2. ENGLISH, J., Jr. and LEVY, M. F. J. Am. Chem. Soc. 78, 2846 (1956).
3. FINKELSTEIN, F. Ber. 43, 1528 (1910).
4. GORIN, P. A. J., HOUGH, L., and JONES, J. K. N. J. Chem. Soc. 3843 (1955).
5. JACKSON, E. L. and HUDSON, C. S. J. Am. Chem. Soc. 63, 1229 (1941).
6. LEHNINGER, A. L. and SICE, J. J. Am. Chem. Soc. 77, 5343 (1955).
7. McSWEENY, G. P. and WIGGINS, L. F. Nature, 168, 874 (1951).
8. OHLE, H. and DICKHAUSER, E. Ber. 58, 2593 (1925).
9. OHLE, H. and KOLLER, I. Ber. 57, 1566 (1924).
10. OLDHAM, M. A. and HONEYMAN, J. J. Chem. Soc. 986 (1946).
11. SHYLUK, W. P., HONEYMAN, J., and TIMELL, T. E. Can. J. Chem. 33, 1202 (1955).
12. TIPSON, R. S. and CRETCHER, L. H. J. Org. Chem. 8, 95 (1943).
13. VISCHER, R. and REICHSTEIN, T. Helv. Chim. Acta, 27, 1338 (1944).

THE DIVERGENT BEHAVIOR OF THE HYDROXIDES OF LITHIUM, SODIUM, AND OF POTASSIUM, RUBIDIUM, AND CESIUM IN THE XANTHATION OF CELLULOSE AND STARCH[1]

E. G. Adamek[2] and C. B. Purves

ABSTRACT

When a suspension of cellulose, or a solution of starch, in 17.8% aqueous sodium hydroxide was shaken with a large excess of carbon disulphide, a sodium xanthate of degree of substitution (D.S.) about 0.4 was obtained. The replacement of the sodium hydroxide by 17.8% potassium hydroxide resulted in a product of D.S. about 1.3. Plots were made of the D.S. of cellulose xanthate resulting from the use of various concentrations of the hydroxides of lithium, sodium, potassium, rubidium, and cesium; the plots for the last three hydroxides were similar, and differed sharply in form from those of the first two.

Potassium cellulose or starch xanthate of D.S. about unity was freely soluble in water as well as in aqueous alkalies and the solutions "ripened". When immersed in methyl iodide, the dry salts yielded the corresponding S-methyl xanthates without change in the D.S. These S-methyl xanthates were white substances insoluble in water but dissolved or dispersed by carbon disulphide. They could be acetylated with sulphuric acid as catalyst and without change in the S-methyl xanthate D.S. The acetylated cellulose derivative was freely dispersed by chloroform or trichloroethylene.

INTRODUCTION

Viscose is ordinarily prepared in the rayon and cellophane industries by the "press weight ratio" method, in which excess 18% or 20% alkali is squeezed from a cellulose – caustic soda mixture before carbon disulphide is added to the solid alkali cellulose. The "press weight ratio" is the weight of the alkali cellulose to that of the original cellulose, and in practice may vary between 2.5 and 4. Although the details of this process have been intensively studied for over 60 years and are summarized in standard textbooks like that by Ott and Spurlin (15), only a very few papers describe the effects of replacing the sodium hydroxide by the hydroxide of another alkali metal. The omission of the pressing operation results in a xanthation by the "slurry" method, which is much less economic because of the relatively larger amounts of carbon disulphide and alkali required. With the exception of a research by Bartunek (1), xanthations of cellulose by the "slurry" method have employed only sodium hydroxide among the alkali metal bases, and the same remark is true of the similar xanthation of starch by Ost, Westhoff, and Gessner (14). Their work in 1911 is the only systematic study of the xanthation of starch found in the literature, although Wolffenstein and Oeser (22) have used sodium starch xanthate solutions to precipitate the corresponding salts of various heavy metals. Lieser and Hackl (11) describe a crude copper starch xanthate of degree of substitution (D.S.) about 0.5 obtained in the same way. Crude preparations of the sodium salt have also been patented as adhesives for wood veneers (19), and as textile sizes (4). Only two patents (3) describe the preparation, by a modified "press weight ratio" method, of crude sodium and potassium starch xanthate, for use as aids in mineral flotation. It thus seems desirable to increase knowledge of the xanthation of cellulose and starch by the "slurry" method in the presence of alkali metal bases other than sodium hydroxide, and the present article describes experiments with this object in view.

Ost, Westhoff, and Gessner (14) showed that a good viscose resulted when a solution

of starch in 2 to 3 molar equivalents of 5 to 20% aqueous sodium hydroxide was shaken for several hours at room temperature with a large excess of carbon disulphide. Addition of the viscose to a large excess of alcohol caused the precipitation of sodium starch xanthate as a dough, which was purified by three or four washings with 70% or 75% aqueous alcohol before being dried by solvent-exchange. Products whose sulphur content suggested a sodium xanthate substitution of 0.4 to 0.9 contained about twice as much sodium as expected, and presumably had not been adequately purified. The correct 2:1 ratio of sulphur to sodium atoms was found in some samples of D.S. 0.3 to 0.5. The present experiments were on similar lines, but the inclusion of a little acetic acid in the methanol used for washing the crude products eliminated the excess base, and the sulphur–sodium ratio was correct on the occasions when it was checked.

As Ost and his co-workers (14) noted, the gelatinous particles of sodium starch xanthate were difficult to separate from aqueous alcohol either by filtration or on the centrifuge. This separation was nevertheless retained in the present work, because the physical properties of the sodium xanthates were not improved by using sodium chloride or ammonium chloride instead of alcohol as the precipitating agent. The use of these salts yielded products with the same low D.S. (Table I, experiments 1 and 2). Recent results with cellulose xanthate (21) showed that methyl iodide converted the sodium salt easily and quantitatively to the much more stable and more readily purified S-methyl ester,

$$R—O—CS.SNa \xrightarrow{CH_3I} R—O—CS.SCH_3,$$

and this procedure was preferred in the present work. Experiment 3 established the fact that the conversion to S-methyl ester occasioned no significant change in the D.S. of the starch xanthate. The observation was then made that the replacement of the sodium hydroxide used in the xanthation by an equimolecular concentration of potassium hydroxide more than doubled the D.S. obtained (Experiments 4 and 5).

Experiment 6 showed that the maximum D.S. resulted when xanthations at 5° were carried on for about 24 hours, and these conditions were adopted in the subsequent

TABLE I

XANTHATIONS OF STARCH[a]

Expt.	Alkali	%	Reaction, hours	Isolated as	S, %	D.S.
			Temperature 23°			
1	NaOH	15	2	Salt[b]	6.93	0.20
2	NaOH	15	2	Salt[c]	6.89	0.20
3	NaOH	10	48	Salt	10.8	0.33
				Ester[d]	11.1	0.33
4	NaOH	15	2.5	Ester	10.5	0.31
5	KOH	21	2.5	Ester	21.4	0.78
			Temperature 5°			
6	KOH	21	12	Ester	22.1	0.81
			24	Ester	24.6	0.95
			48	Ester	23.7	0.90
7	NaOH	17.8	24	Ester	12.4	0.38
8	KOH	17.8	24	Ester	30.8	1.38
9	KOH	21	24	Ester	24.6	0.95

[a]Samples, 2.5 g., shaken with 30 ml. of the alkali and 15 ml. of carbon disulphide. Isolated as salt or as S-methyl xanthate ester.

[b]By precipitation with saturated aqueous sodium chloride.

[c]By precipitation with saturated aqueous ammonium chloride.

[d]Sulphated ash, 1.6%.

work. The last three experiments, made under carefully standardized conditions, confirmed the fact that sodium hydroxide was greatly inferior to potassium hydroxide of the same percentage concentration in promoting the xanthation of starch by the "slurry" method, and that the optimum concentration of potassium hydroxide was less than 21%. These white, amorphous starch potassium xanthates were non-gelatinous solids which could be readily isolated on a filter or centrifuge and which dissolved readily in water to yield clear, viscous solutions. The white, powdery S-methyl xanthates were insoluble in all liquids tried, but samples of D.S. about unity were so swollen by carbon disulphide that a superficial inspection suggested that they had gone into solution. One sample of the S-methyl xanthate was recovered unchanged in D.S. after storage in a stoppered bottle for 7 months, and also another sample after having been kept highly swollen in dry pyridine near 23° for 2 weeks. Although fairly stable to dilute acids, the S-methyl xanthates were readily decomposed by dilute alkali.

The superiority of potassium hydroxide to sodium hydroxide in the xanthation of starch led to similar experiments on the xanthation of cellulose with the hydroxides of all the alkali metals. In these experiments the ratio of carbon disulphide to cellulose to volume of alkali, and the reaction time and temperature, were kept constant, and only the kind and concentration of the alkali were varied (Table II and Fig. 1). When the

TABLE II

EFFECT OF ALKALI ON EFFICIENCY OF XANTHATION[a]

Alkali[b]		S-Methyl-xanthate	
%	N	S, %	D.S.
Lithium hydroxide			
2.4	1.0	2.55	0.07
6.0	2.5	7.6	0.22
12.0	5.0	10.5	0.31
Sodium hydroxide			
4.0	1.0	5.3	0.15
10.0	2.5	10.8	0.32
17.8	4.5	13.8	0.44
Potassium hydroxide			
6.0	1.1	6.4	0.18
10.0	1.8	12.6	0.39
12.0	2.1	20.8	0.75
14.0	2.5	26.3	1.06
17.8	3.2	28.0	1.17[c]
25.0	4.5	25.8	1.03
50.0	8.9	20.4	0.73
Rubidium hydroxide			
10.3	1.0	8.96	0.26
19.3	1.9	19.7	0.69
25.6	2.5	27.8	1.16
32.8	3.2	30.1	1.32
42.8	4.2	28.9	1.24
Cesium hydroxide			
15.0	1.0	10.5	0.31
27.0	1.8	19.8	0.69
39.2	2.6	28.4	1.20
46.5	3.1	29.9	1.31
64.8	4.3	29.5	1.28

[a] Alaska pine pulp (viscose grade), 2.5 g. in all cases.
[b] Volume 30 ml.; mixture shaken with 15 ml. of carbon disulphide for 24 hours at 5°.
[c] Mean of independent experiments yielding D.S. 1.12 and 1.23.

D.S. of the S-methyl esters was plotted against the normalities of the alkalies, it was clear that the maximum D.S. of about 0.45, attainable in 4.5 N (18%) sodium hydroxide, could also be attained by using 1.8 N (10%) potassium hydroxide, or still lower normalities of rubidium and cesium hydroxides. The hydroxides of potassium, rubidium, and cesium, as opposed to those of sodium and lithium, became much more efficient xanthating agents as their normalities increased, and their efficiencies passed through maxima near 3.2 N. The same conclusions followed when D.S. was plotted against the percentage concentration or the molecular weight of the alkali. The latter plot showed that in 1 N solution the efficiencies of the hydroxides increased linearly and gradually from lithium to cesium, but that the sharp discontinuity between the first two and the last three was well established in 2.5 N solutions.
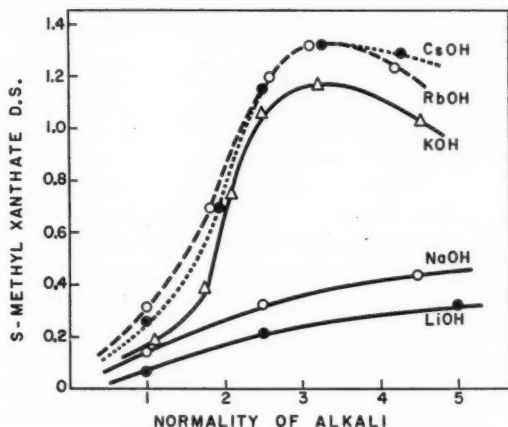
FIG. 1. Effect of various alkali hydroxides and a constant excess of carbon disulphide on degree of substitution of resulting cellulose xanthate. See Table II.

Although the results summarized in Table III were obtained at different times and were not quite comparable, they served to demonstrate that the use of potassium hydroxide of suitable concentration made it possible to prepare cellulose xanthates of D.S. near unity at room temperature as well as at 5°, a xanthating period of 6 hours being near the optimum (Expt. 1). At −10°, however, rotation of the xanthating slurry on a ball mill for 24 hours gave rather low substitution, and at least 72 hours was necessary. Three different dissolving pulps, cotton linters, and a pulp made from milkweed, another seed hair, all gave similar results. A sample of potassium cellulose xanthate of D.S. 0.52 (not shown in Table III) was also twice re-xanthated with 17.8% potassium hydroxide for 24 hours at 5°, a portion being converted on each occasion to the S-methyl ester for analysis. The D.S. increased to 1.23 and 1.41, but a third re-xanthation with 12% alkali caused only a slight further increase to D.S. 1.46. Another series of re-xanthations was carried out with samples of cellulose xanthate-S-methyl ester of D.S. 1.12 and 1.03, which had the advantage of being readily dispersed in carbon disulphide. Re-xanthation with 17.8% or 25% potassium hydroxide for 24 hours at 5° produced only a slight increase, but a D.S. of 1.41 was reached with a saturated (66%) solution. Carbon disulphide and powdered potassium hydroxide reduced the D.S. from 1.12 to 0.94.

The difficulty in promoting a still higher substitution, unless with a quaternary

TABLE III

XANTHATION AT DIFFERENT TEMPERATURES AND WITH DIFFERENT CELLULOSES

		Potassium hydroxide[b]			S-Methyl xanthate	
Expt.	Cellulose[a]	%	Hours	Temp.	S, %	D.S.
1	Pulp A	17.8	2	23°	22.8	0.85
			6	23°	24.9	0.97
			10	23°	20.6	0.74
2	Pulp A	14	24	−10°	13.1	0.41
			48[c]	−10°	19.2	0.67
			72	−10°	24.1	0.93
3	Pulp A	25	24	5°	25.8	1.03
4	Pulp B	25	24	5°	23.3	0.88
5	Pulp C	25	24	5°	22.6	0.84
6	Cotton linters	21	24	5°	26.4	1.06
7	Cellulose	21	24	5°	25.8	1.03

[a]*Pulps A, B, C, were Alaska pine (viscose grade), B.C. wood fiber (textile yarn sulphite), and Natchez wood pulp (Tenacel) respectively. The linters were acetate grade and were dewaxed; our colleague Mr. F. W. Barth isolated the cellulose from common milkweed (Asclepias syriaca L.) by the chlorine process.*

[b]*Volume 30 ml. for a 2.5 g. sample, and 15 ml. of carbon disulphide.*

[c]*Some product isolated as potassium salt, and re-xanthated in the same way for 24 hours.*

ammonium base (12, 13) or with sodium in liquid ammonia (17, 18), was not inconsistent with the suggestion that the presence of the xanthate ion in either the second or third position of the anhydroglucose unit of cellulose hindered the substitution of a second ion in the other position (20). If so, the maximum D.S. to be expected in an ionic substitution was 2 and not 3. By combining alkali cellulose with a great excess of carbon disulphide, Lieser (10) attained a D.S. of about 1.7 estimated as the dixanthogenate, and Fink, Stahn, and Matthes (5) used N,N'-diethylchloroacetamide to precipitate a xanthate derivative of the same high D.S. from a viscose. The decrease in substitution caused by precipitation with methanol was avoided in the latter case.

Finely divided cellulose-S-methyl xanthate with D.S. 1.06 swelled noticeably in pyridine and in dimethyl sulphoxide, CH_3SOCH_3, at room temperature, and carbon disulphide gave an almost water-clear dispersion, only a few swollen fibers remaining visible. The xanthate ester was insoluble in the other common organic liquids. When acetylated with an acetic acid – acetic anhydride – sulphuric acid mixture, however, the S-methyl ester readily yielded a white, fibrous acetate readily soluble in trichloroethylene and in chloroform. This acetate retained the original S-methyl xanthate D. S., 1.06, almost completely, and the total D.S. approximated to trisubstitution.

Potassium, rubidium, and cesium cellulose xanthates of D.S. about 1 dissolved in water to give nearly neutral, clear yellow solutions. These three salts were readily precipitated from solutions in the corresponding alkali by the addition of methanol, and the precipitates differed from those of the sodium and lithium salts (of lower D.S.) in being easy to wash and to recover on a filter. The "ripening" behavior of a potassium cellulose xanthate of D.S. 1.23 was briefly studied by noting the time of discharge through a standard funnel of a 2.0% aqueous solution, and of one of 2.3% concentration made up in 9.1% (1.6 N) potassium hydroxide (Table IV). Both solutions were clear and highly viscous, that in water having a lighter yellow color than that in the alkali. Although the viscosities were measured in arbitrary units, they were sufficient to show that the "ripening" plots differed greatly not only in rate but also in direction (Fig. 2). Heuser and Schuster (6) made a similar observation for a technical sodium cellulose xanthate of D.S. 0.5 or less.

TABLE IV

CHANGE WITH TIME IN VISCOSITY OF A POTASSIUM CELLÚLOSE XANTHATE[a]

In potassium hydroxide (9.1%)		In water (pH 9)	
Hours	Seconds[b]	Hours	Seconds[b]
0	16	0	70
2	14	6	90
12	8	12	120
26	6	26	490
58	4	58	Gel
74	3	74	Ppt.
111	3		
134	2.5		
158	2		
194	2.5		
218	Gel		

[a]D.S. 1.23; 2.3% solution in alkali and 2% in water. Measurements at room temperature and concentrations based on cellulose content.
[b]Time of discharge through standard funnel.

In 1926 Heuser and Schuster (6) prepared viscoses from each of the five alkali hydroxides, pressing the alkali cellulose to a weight ratio of 3 and limiting the carbon disulphide to 44% by weight of the cellulose. Bartunek (2) in 1955 used a similar method in a further study of the hydroxides of lithium, sodium, and potassium. In both articles the main objective was an attempt to correlate the efficiency of the alkali in the viscose process with its electrical conductivity or ability to swell cellulose, and the D.S. of the xanthates produced apparently did not exceed 0.75 ("γ-number", 75). None of the potassium, rubidium, or cesium xanthates were completely soluble in any concentration of the corresponding alkali, although some dissolved completely in a suitable concentration of sodium or lithium hydroxide. These results were not necessarily inconsistent with those now reported, because pressing a 14% potassium hydroxide – Alaska pine pulp slurry to a ratio of 3.5 before adding the customary large amount of carbon disulphide reduced the D.S. of the resulting cellulose xanthate-S-methyl ester from 1.06 to 0.52. In
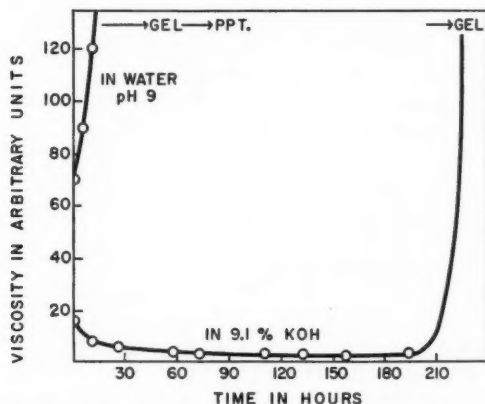
FIG. 2. Ripening of 2–2.3% solutions of potassium cellulose xanthate (D.S. ∼1) in water and in potassium hydroxide at room temperature. See Table IV.

a second experiment, the combined effect of pressing and of limiting the carbon disulphide to 40% of the cellulose was to reduce the D.S. from 1.17 to 0.38. Omission of pressing but limitation of the carbon disulphide to the above percentage resulted in D.S. 0.41. From a graph given by Lauer and Pauer (8) the pressing of a sodium hydroxide cellulose to ratios of 10 and 3, followed by addition of 100% of carbon disulphide, yielded xanthates of D.S. about 0.3 and 0.2, respectively. Kuriyama and Shiratsuchi (7) obtained similar results. The effect of pressing the present potassium hydroxide – cellulose appeared to have been much greater.

The present results, however, were in disagreement with those of Bartunek (1), who shook 1 g. samples of cotton linters for 6 hours at 20° with 20 ml. of carbon disulphide (a large excess) and 100 ml. of sodium or potassium hydroxide of various concentrations. The most favorable concentration of potassium hydroxide in this "slurry" method was 25%, but only 60% of the cellulose yielded a soluble xanthate, the remaining xanthate being soluble in 8.5% sodium hydroxide. It was probable that the D.S. of the potassium cellulose xanthate attained in these experiments was low, although no analytical data were quoted.

EXPERIMENTAL

Materials and Analytical Methods

Most of the xanthations of cellulose were carried out with Alaska pine wood pulp (Viscose Grade), those of starch with a defatted, purified sample from wheat kindly supplied by Dr. K. M. Gaver, of Ogilvie Flour Mills Limited, Montreal, Que. The hydroxides of rubidium and cesium were prepared by slowly adding a boiling aqueous solution of the corresponding sulphate to a boiling aqueous solution containing the calculated amount of barium hydroxide. Nitrogen gas was bubbled continuously through the latter solution as a protection against atmospheric carbon dioxide. After the removal of barium sulphate by filtration, the clear filtrate was evaporated in nitrogen under diminished pressure until the titration of an aliquot with 0.1 N acid showed that the desired concentration of rubidium or cesium hydroxide had been attained.

Sulphur was determined as sulphate ion after oxidizing about 0.2 g. samples of the xanthate with 0.2 g. of potassium perchlorate and 4 g. of sodium peroxide in a Parr semimicro bomb (16). The method proved to be closely reproducible. If x was the xanthate substitution in a sodium cellulose (or starch) xanthate, then $S\% = 6400x/(162.1+98x)$; the equation for other salts required an appropriate change in the denominator, which assumed the value $162.1+90x$ for the S-methyl xanthates. Ash contents were determined by heating small samples moistened with a few drops of concentrated sulphuric acid to constant weight in a muffle furnace at 600°.

Xanthation

(a) "Slurry" Method

A 2.5 g. sample of air-dry starch or shredded cellulose, 30 ml. of the aqueous alkali, and 15 ml. of carbon disulphide were shaken mechanically for 24 hours in a stoppered, wide-necked bottle kept in a room at 5°. These conditions were usually constant while the concentration and nature of the alkali were varied.

At the end of the xanthation, the product was vigorously stirred with not more than an equal volume of water until a homogeneous mixture resulted. The highly viscous, orange mass was then dropped in small portions into 10 to 20 volumes of ice-cold methanol, which was very vigorously stirred in order to precipitate the xanthate salt in a fairly uniform particle size. The suspension was filtered through sintered glass of coarse porosity,

or was centrifuged when the precipitate was gelatinous, and the residue was washed three times with small volumes of ice-cold methanol containing a little glacial acetic acid. After another wash with ether, the product was thoroughly ground in a mortar and the washings with methanol and ether were repeated. Part of the material was dried *in vacuo* over phosphorus pentoxide, and part was transformed into the much more stable S-methyl xanthate (see below). Found for a typical starch potassium xanthate: sulphated ash, 27.8; S, 20.4%. Calc. for 0.32 potassium and 0.64 sulphur atoms per anhydroglucose unit: K_2SO_4, 27.8; S, 20.4%. All the potassium could therefore be attributed to xanthate salt—OCSSK.

(b) "Press" Method

The technical procedure was modified to make it conform more closely to the "slurry" method just described. The cellulose was steeped in aqueous alkali of the kind and concentration desired for 24 hours at 5°. After being pressed to the desired weight ratio, the alkali cellulose was not "aged" but was straightway shredded by hand and shaken in a closely stoppered bottle for 24 hours at 5° with the desired amount of carbon disulphide. Isolation of the product was as described in (a).

Preparation of S-Methyl Xanthates (Ref. 21)

The alkali xanthate of cellulose or starch, still wet with ether, was transferred into a flask containing an approximately equal weight of freshly distilled methyl iodide diluted with 3 volumes of ether. The flask was well shaken, stoppered, and left in a dark place at room temperature for not less than 2 days. After that time the S-methyl xanthate was recovered on a filter, was washed with methanol and then with water containing a few drops of acetic acid. When the washings were free of alkali iodide, the product was solvent-exchanged through methanol into ether and was dried to constant weight *in vacuo* over phosphorus pentoxide at room temperature. The yield was practically quantitative. Found: ash, 0.45%.

Stability of Starch-S-methyl Xanthate

(a) A sample of the starch-S-methyl xanthate of D.S. 1.38 (S, 30.8%) described in Table I, Expt. 8, was kept in a stoppered bottle near 23° for 7 months. The sample was then washed with methanol, with water containing a few drops of acetic acid, again with methanol, and finally with ether. After being dried *in vacuo* over phosphorus pentoxide, the product had S, 30.7% (D.S. almost unchanged at 1.37).

(b) The starch-S-methyl xanthate of Expt. 6, Table I, and D.S. 0.95 (S, 24.6%) was stirred for an hour in dry pyridine. After the resulting very viscous, slightly turbid gel had been kept at room temperature for 14 days, part was precipitated into a large excess of water near 0°, and another part into a large excess of ethanol near 0°. Precipitation into methanol yielded a slimy product that was difficult to isolate. The two precipitates were washed and dried as described in (a). Found for the precipitate from water: S, 23.8; for the precipitate from methanol: S, 24.5%. The corresponding D.S. values of 0.91 and 0.95 showed that the former precipitation had caused a slight decrease, but not the precipitation in methanol.

Acetylated Starch-S-methyl Xanthate

Ten grams of the S-methyl xanthate, D.S. 1.02, was mixed in a stoppered flask with 38 ml. of cold glacial acetic acid, 38 ml. of acetic anhydride, and 1.5 ml. of concentrated sulphuric acid. The mixture was still heterogeneous after being kept for 70 hours at room temperature, but no odor originating in the decomposition of the xanthate ester

group was observed. After the mixture had been poured with vigorous stirring into 2 liters of ice and water, and the suspension had been kept near 5° for 24 hours, the product was separated on a sintered glass filter from the water-clear filtrate. The precipitate was washed on the filter with water until no trace of sulphate ion could be detected in the effluent, was then washed repeatedly in methanol and finally with ether. Drying was *in vacuo* at room temperature over phosphorus pentoxide. Found: S, 19.3; acetyl, 23.5, 23.9%. Calc. for starch substituted to D.S. 0.98 with S-methyl xanthate and to D.S. 1.80 with acetyl groups: S, 19.3; acetyl, 23.7%. Acetyl groups were determined by oxidizing the sample with chromic acid and recovering acetic acid by distillation (9).

The total substitution was thus 2.78 instead of the theoretical 3.00, and acetylation caused a decrease of about 0.04 in the D.S. of the xanthate groups. This acetylated starch-S-methyl xanthate was a snow-white powder only slightly swollen in acetone, carbon tetrachloride, or carbon disulphide, but highly swollen in chloroform or trichloroethylene. Reacetylation in pyridine – acetic anhydride increased the acetyl D.S. from 1.80 to 1.90, and decreased that of the S-methyl xanthate groups from 0.98 to 0.90, the total substitution remaining almost unchanged. This product had a slight brown color.

Acetylated Cellulose-S-methyl Xanthate (cf. Ref. 21)

Cellulose-S-methyl xanthate of D.S. 1.06 was acetylated exactly as described for the starch derivative, but after 50 hours at room temperature the mixture was a clear, slightly green dope containing only traces of suspended material. No evidence of the decomposition of the xanthate ester group was noted. The pure white product was isolated as already described. Found: S, 18.6; acetyl (9), 26.7%. Calc. for cellulose substituted with 0.99 S-methyl xanthate and 2.11 acetyl groups: S, 18.6; acetyl, 26.7%. In this case the D.S. of the S-methyl xanthate group decreased by 0.07 units, but the analyses were obviously inaccurate because the total apparent substitution was 3.1 instead of 3.0.

The acetylated cellulose-S-methyl xanthate, unlike the corresponding starch derivative, gave water-clear, viscid solutions in chloroform and trichloroethylene, and swelled in acetone, carbon tetrachloride, and carbon disulphide.

REFERENCES

1. BARTUNEK, R.   Das Papier, **6**, 356 (1952).
2. BARTUNEK, R.   Das Papier, **9**, 254 (1955).
3. BROWN, E. H.   Canadian Patent Nos. 499,304, 499,305 (Jan. 19, 1954).
4. ELSSNER, R.   U.S. Patent No. 2,000,887 (1935); Chem. Abstr. **29**, 4175 (1935).
5. FINK, H., STAHN, R., and MATTHES, A.   Z. angew. Chem. **47**, 602 (1934).
6. HEUSER, E. and SCHUSTER, M.   Cellulosechemie, **7**, 17 (1926).
7. KURIYAMA, S. and SHIRATSUCHI, E.   J. Chem. Soc. Japan, Ind. Chem. Sect. **54**, 62 (1951); Chem. Abstr. **47**, 1384 (1953).
8. LAUER, K. and PAUER, O.   Kolloid-Z. **119**, 151 (1950).
9. LEMIEUX, R. U. and PURVES, C. B.   Can. J. Research, B, **25**, 485 (1947).
10. LIESER, T.   Ann. **528**, 276 (1937).
11. LIESER, T. and HACKL, A.   Ann. **511**, 128 (1934).
12. LIESER, T., JAKS, R., and GLITSCHER, E. A.   Ann. **548**, 212 (1941).
13. LIESER, T. and LECKZYCK, E.   Ann. **522**, 56 (1936).
14. OST, H., WESTHOFF, F., and GESSNER, L.   Ann. **382**, 340 (1911).
15. OTT, E. and SPURLIN, H. M.   Cellulose and cellulose derivatives. 2nd ed. Interscience Publishers, Inc., New York, N.Y. 1954. Part II, Chap. IXF *by* E. Kline, p. 959 *et seq.*
16. PARR INSTRUMENT COMPANY, Moline, Illinois, Manual 121 (1950).
17. SCHERER, P. C., Jr., GOTSCH, L. P. *et al.* Virginia Polytech. Inst. Eng. Expt. Sta. Series Bull. No. 39, 3 (1939); Chem. Abstr. **34**, 229 (1940).
18. SHINO, K., ANDO, T., and FUSE, A.   Science Repts. Research Insts. Tôhoku Univ. Ser. A, **7**, 229 (1955); Chem. Abstr. **49**, 16426 (1955).
19. STERN, E.   U.S. Patent No. 1,412,020 (1922); Chem. Abstr. **16**, 2014 (1922).
20. SWAN, E. P. and PURVES, C. B.   Unpublished results.
21. VINCENT, D. L., SANYAL, A. K., FALCONER, E. L., and PURVES, C. B.   Unpublished results.
22. WOLFFENSTEIN, R. and OESER, E.   Kunstseide, **7**, 27 (1925); Chem. Zentr. [7] **2**, 366 (1925).

THE INFRARED AND RAMAN SPECTRA OF
$HC(CD_3)_3$ AND $DC(CD_3)_3$[1]

J. K. WILMSHURST[2] AND H. J. BERNSTEIN

ABSTRACT

The Raman spectra of liquid $(CD_3)_3CH$ and $(CD_3)_3CD$ were obtained photoelectrically together with depolarization ratios, and the infrared spectra of the corresponding gases were obtained from 3 to 35 μ. A vibrational assignment consistent with depolarization ratios and band contours has been made for the molecules on the basis of C_{3v} symmetry. The spectra have been correlated with the spectra of $(CH_3)_3CH$ and $(CH_3)_3CD$ and modified assignments for two modes have been given for these molecules. Tentative assignments have been made for the 'inactive' A_2 modes (which are 'active' if the molecule has symmetry C_3) to explain some of the observed frequencies around 1000 cm.$^{-1}$ which could not be satisfactorily assigned as summation or difference tones.

INTRODUCTION

Though the vibrational spectrum of isobutane has been the subject of numerous investigations (6) some ambiguities in the vibrational assignment still remain. Sheppard and Simpson (6) suggest that further experimental work is required to decide upon the frequency assignment of the deformation modes and the asymmetrical skeletal stretching mode. Recently Evans and Bernstein (3) have studied the vibrational spectrum of isobutane and isobutane-d_1 but the assignment of the asymmetrical stretching mode was not established.

In order to clarify the situation with regard to this molecule the Raman spectra of liquid $HC(CD_3)_3$ and $DC(CD_3)_3$ have been obtained together with depolarization ratios, and the infrared spectra of their vapors have also been obtained. Complete vibrational assignments have been made for the two molecules and an unambiguous assignment of the asymmetrical skeletal stretching mode made. This requires interchanging ν_{16} and ν_{18} in the assignment of Evans and Bernstein (3). Further the earlier Pitzer and Kilpatrick (4) assignment of the a_1 methyl rocking mode, which was altered by Evans and Bernstein (3) for consistency with the product ratio for $HC(CH_3)_3$ and $DC(CH_3)_3$, was altered again to be consistent with the product ratio of all the deuterium substituted isobutanes.

EXPERIMENTAL

The two deuterated isobutanes studied in the present investigation were obtained in cylinders from Merck and Co., Montreal, Canada.

The Raman spectra of the liquids were obtained photoelectrically at $-40°$ C. in a cold cell described by Evans and Bernstein (2) with a White grating Raman spectrometer (7). Depolarization ratios were measured by the method of Edsall and Wilson (1) and corrected for convergence error by the method of Rank and Kagarise (5). The spectra are shown in Fig. 1.

The infrared spectra were obtained with a Perkin Elmer model 112 double pass spectrometer equipped with LiF, NaCl, KBr, and CsBr optics. The spectra of $HC(C_3D)_3$ and $DC(CD_3)_3$, shown in Figs. 2 and 3 respectively, were obtained using a 10 cm. sample cell with the gas at the pressure indicated.

The observed infrared and Raman data for $HC(CD_3)_3$ and $DC(CD_3)_3$ are given in Tables II and III respectively.
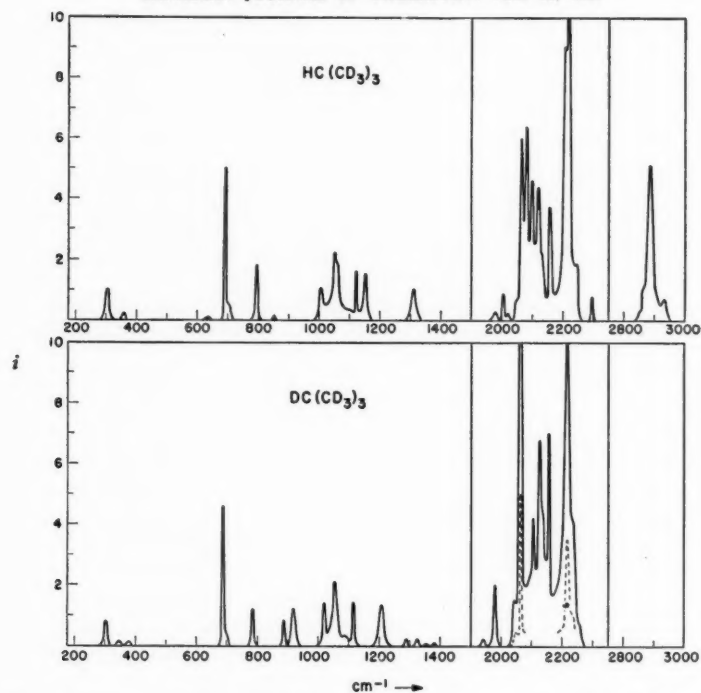
FIG. 1. The Raman spectra of HC(CD₃)₃ and DC(CD₃)₃. Intensity scale of dotted line, one-third that of heavy line.
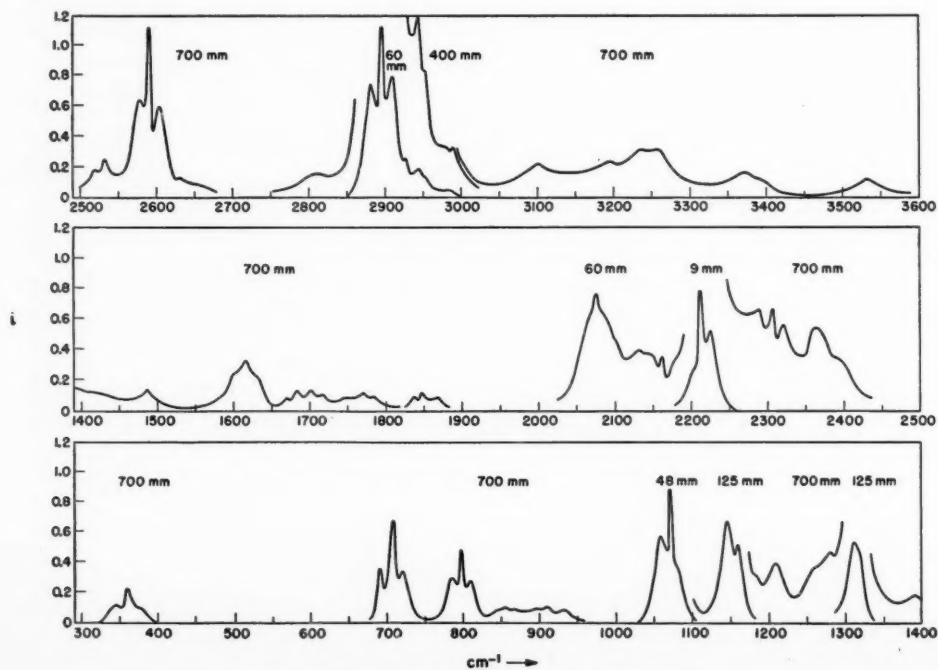
FIG. 2. The infrared spectrum of gaseous HC(CD₃)₃.
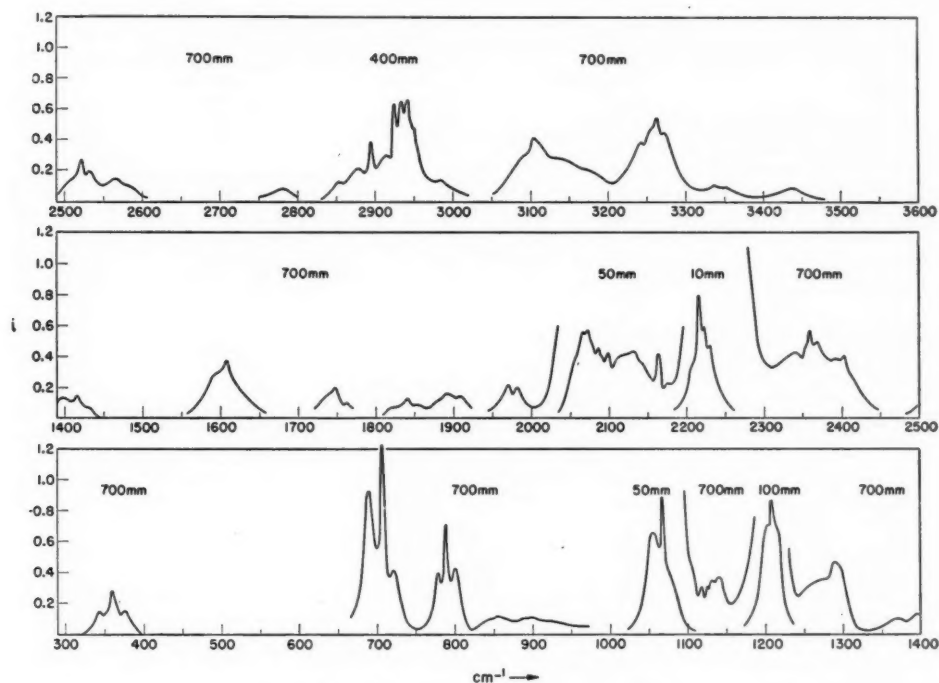
FIG. 3. The infrared spectrum of gaseous $DC(CD_3)_3$.

DISCUSSION

Isobutane and its deuterium substituted derivatives can be considered for the purposes of a vibrational assignment to have the point group symmetry C_{3v} for which the 36 fundamental vibrations divide into symmetry species as $8A_1 + 4A_2 + 12E$. The A_1 and E modes are active in both the infrared and Raman spectrum while the A_2 modes are inactive in both spectra. The type A_1 modes give rise to polarized bands in the Raman spectrum, and parallel type bands with PR separation* of about 27 cm.$^{-1}$ in the infrared spectrum. The type E modes give rise to depolarized bands in the Raman spectrum and perpendicular type bands with a weak Q branch (in the absence of Coriolis coupling) in the infrared spectrum.

In Table I the modes of vibration of isobutane have been classified according to the approximate description of internal and external modes of the CH_3 group and also in terms of other groups in the molecule. For convenience the numbering of the vibrations

*The PR doublet separation was calculated from the formula of Gerhard and Dennison, Phys. Rev. **43**, 197 (1933). The moments of inertia, in g. cm.^{2}, of the isotopic isobutanes (calculated assuming $r_{CH} = 1.09$, $r_{CC} = 1.54$ and all angles tetrahedral) are:

	$HC(CH_3)_3$	$DC(CH_3)_3$	$HC(CD_3)_3$	$DC(CD_3)_3$
$I_A = I_B$	103.7×10^{-40}	107.4×10^{-40}	135.3×10^{-40}	140.1×10^{-40}
I_C	183.9×10^{-40}	183.9×10^{-40}	241.0×10^{-40}	241.0×10^{-40}

TABLE I

THE FUNDAMENTAL VIBRATIONS OF ISOBUTANE (C_{3v})

Species	No.		CH$_3$ external	CH$_3$ internal
a_1	ν_1			ν_{CH} unsym.
	ν_2			ν_{CH} sym.
	ν_3	ν_{CH}		
	ν_4			δ_{CH_3} unsym.
	ν_5			δ_{CH_3} sym.
	ν_6		δ_{CCH_3}	
	ν_7	ν_{CC}		
	ν_8	δ_{CCC}		
e	ν_9			ν_{CH} unsym.
	ν_{10}			ν_{CH} unsym.
	ν_{11}			ν_{CH} sym.
	ν_{12}			δ_{CH_3} unsym.
	ν_{13}			δ_{CH_3} unsym.
	ν_{14}			δ_{CH_3} sym.
	ν_{15}	δ_{CH}		
	ν_{16}		δ_{CCH_3}	
	ν_{17}		δ_{CCH_3}	
	ν_{18}	ν_{CC}		
	ν_{19}	δ_{CCC}		
	ν_{20}		Torsion	
a_2	ν_{21}			ν_{CH} unsym.
	ν_{22}		δ_{CCH_3}	
	ν_{23}			δ_{CH_3} unsym.
	ν_{24}		Torsion	

is the same as that given by Evans and Bernstein (3). The spectra are best discussed under their respective symmetry types.

The A_1 Vibrations

The parallel type infrared bands at 2212 and 2076 cm.$^{-1}$ in HC(CD$_3$)$_3$ and at 2216 and 2073 cm.$^{-1}$ in DC(CD$_3$)$_3$ are assigned as ν_1 and ν_2 respectively. ν_3 is assigned to the parallel type infrared band and strong polarized Raman band at 2887 cm.$^{-1}$ in HC(CD$_3$)$_3$ and to the strong polarized Raman band at 2063 cm.$^{-1}$ in DC(CD$_3$)$_3$. The polarized Raman bands at 1122 cm.$^{-1}$ in HC(CD$_3$)$_3$ and at 1117 cm.$^{-1}$ in DC(CD$_3$)$_3$ are assigned to the methyl bending mode ν_4, while the parallel type infrared bands at 1071 cm.$^{-1}$ in HC(CD$_3$)$_3$ and 1067 cm.$^{-1}$ in DC(CD$_3$)$_3$ are assigned to the other methyl bending mode ν_5. The polarized Raman bands and parallel type infrared bands at 692 and 360 cm.$^{-1}$ in HC(CD$_3$)$_3$ and at 687 and 359 cm.$^{-1}$ in DC(CD$_3$)$_3$ are assigned to ν_7 and ν_8 respectively. The remaining a_1 mode, ν_6, can be assigned with considerable certainty to the parallel type infrared bands at 798 cm.$^{-1}$ in HC(CD$_3$)$_3$ and 789 cm.$^{-1}$ in DC(CD$_3$)$_3$. The A_1 fundamentals are given in Table IV and their Teller Redlich product ratio in Table V.

The present assignment of the A_1 species for HC(CD$_3$)$_3$ agrees with that of Evans and Bernstein (3) for HC(CH$_3$)$_3$ except for the methyl rocking mode, ν_6, which has shifted from their value at 1184 cm.$^{-1}$ in HC(CH$_3$)$_3$ to 798 cm.$^{-1}$ in HC(CD$_3$)$_3$ (an isotopic shift greater than $\sqrt{2}$). Application of the Teller Redlich product rule to HC(CH$_3$)$_3$ and HC(CD$_3$)$_3$, using the assignment of Evans and Bernstein for HC(CH$_3$)$_3$, gives a product ratio of 6.35 very much greater than the theoretical value of 5.26. The Teller Redlich product rule for HC(CD$_3$)$_3$/HC(CH$_3$)$_3$ predicts a value for ν_6 in HC(CH$_3$)$_3$ around 980 cm.$^{-1}$. Consequently we now assign ν_6 in HC(CH$_3$)$_3$ to the Raman band at 966 cm.$^{-1}$ coincident with $\nu_{17}(e)$, while the corresponding band in DC(CH$_3$)$_3$ is taken at 944 cm.$^{-1}$ coincident with $\nu_{15}(e)$. These assignments are consistent with the Teller Redlich product rule for all the isotopic isobutanes (Table V).

TABLE II
The infrared and Raman spectrum of $HC(CD_3)_3$

Infrared (vapor)				Raman (liquid)			Assignment (assuming point group symmetry C_{3v})
cm.$^{-1}$	Int.*	PR separation	Type	cm.$^{-1}$	Relative intensity	Depolarization ratio	
				306	(1)	dp	$\nu_{19}(e)$
345 360 ~378	w	33	(‖)	359	(0)	p	$\nu_3(a_1)$
				636	(0)	?	$\nu_{18}(e)$
— 691	m		(‖)	692	(5)	0.24	$\nu_7(a_1)$
708 720	m		(⊥)	~705	(0)	dp	$\nu_{17}(e)$
786 798 809	m	23	(‖)	797	(2)	0.75	$\nu_6(a_1)$
~846 857 867	w	21	(‖)	852	(0)	p	$\nu_{23}(a_2)$†
898 910 934	w	36	(‖)?				$\nu_{16}+\nu_{19} = 942(A_1)$
				1006	(1)	0.80	$\nu_{22}(a_2)$†
				1052	(2)	dp	$\nu_{14}(e)$
1058 1071 1082	s	24	(‖)	~1064	(2)	dp?	$\nu_5(a_1)$
				~1102	(0)	?	$\nu_{12}(e), \nu_{13}(e)$
				1122	(2)	0.10	$\nu_4(a_1)$
1146 1160	s		(⊥)	1152	(2)	dp	$\nu_{11}(e)$
~1181	w						$\nu_6+\nu_7-\nu_{19} = 1183(E)$
1209	w						$\nu_3+\nu_{23} = 1217$ cm.$^{-1}(A_2)$†
~1259 1281	w		(⊥)?				$\nu_2-\nu_6 = 1284(A_1)$?
1312 1319	s		(⊥)	1312	(1)	dp	$\nu_{15}(e)$
1391	w						$\nu_7+\nu_{16} = 1397(E)$
~1419	w						$\nu_5+\nu_8 = 1431(A_1)$
1486	w						$\nu_6+\nu_7 = 1490(A_1)$
~1600 1616 1632	m	32	(‖)				$\nu_{15}+\nu_{19} = 1621(A_1)$
1670 1683	w		(⊥)				$\nu_8+\nu_{15} = 1675(E)$
1702 1717	w		(⊥)				$\nu_{16}+\nu_{22} = 1711(E)$
1747	w						$\nu_5+\nu_7 = 1763(A_1)$
1770 1784	w		(⊥)				$\nu_5+\nu_{16} = 1776(E)$
1836 1847 1868	w	32	(‖)				$\begin{cases}\nu_{16}+\nu_{18} = 1861(A_1)\\ \nu_5+\nu_6 = 1869(A_1)\end{cases}$
				1981	(0)	?	$\nu_4+\nu_{22} = 1974(A_2)$†
				2005	(1)	p	$2\nu_{22} = 2012(A_1)$
				2020	(0)	?	$\nu_{15}+\nu_{16} = 2020(A_1)$
				2050	(1)	p	$\nu_{14}+\nu_{22} = 2058(E)$?
				2066	(6)	0.20	$\nu_5+\nu_{22} = 2077(A_2)$†
~2066 2076 ~2089	s	23	(‖)	2082	(6)	0.20	$\nu_2(a_1)$
~2101	s			2100	(5)	0.20	$2\times\nu_{14} = 2104(A_1)$
~2122	s			2121	(4)	0.20	$\nu_4+\nu_{22} = 2128(A_2)$†
2131	s			2131	(2)	p	$2\nu_5 = 2142(A_1)$

TABLE II—*concluded*

THE INFRARED AND RAMAN SPECTRUM OF $HC(CD_3)_3$

Infrared (vapor)				Raman (liquid)			Assignment (assuming point group symmetry C_{3v})
cm.$^{-1}$	Int.*	PR separation	Type	cm.$^{-1}$	Relative intensity	Depolarization ratio	
$\sim$2145 ⎫ 2162 ⎬ $\sim$2179 ⎭	s	34	($\parallel$)	2158	(4)	0.25	$\nu_{12}+\nu_{14} = 2154(A_1)$
				2208	(9)	dp	$\nu_4+\nu_{12} = 2224(E)$
$\sim$2204 ⎫ 2212 ⎬ 2225 ⎭	vs	21	($\parallel$)				$\nu_1(a_1)$
				2219	(10)	dp	$\nu_9(e)$, $\nu_{10}(e)$, $\nu_{11}(e)$, $\nu_{21}(a_2)$
				2247	(2)	0.65	$2\times\nu_4 = 2244(A_1)$
2291 ⎫ 2308 ⎬ 2321 ⎭	m	30	($\parallel$)	2298	(1)	0.15	$2\times\nu_{18} = 2312(A_1)$
2364 ⎫ 2392 ⎭	m		($\perp$)				$\nu_5+\nu_{15} = 2386(E)$
2519 ⎫ 2532 ⎬ — ⎭	w		($\parallel$)?				$\nu_3-\nu_8 = 2536(A_1)$
2578 ⎫ 2590 ⎬ 2603 ⎭	m	25	($\parallel$)				$2\times\nu_{15} = 2630(A_1)$
— ⎫ 2631 ⎬ $\sim$2650 ⎭	w		($\parallel$)?				$\nu_7+\nu_{15}+\nu_{17} = 2643(A_1)$
2812	w						$\nu_1+2\nu_{19} = 2824(A_1)$
				2855	(0)	?	$\nu_9+\nu_{17} = 2855(A_1)$
				2867	(0)	0.40	$\nu_2+\nu_6 = 2874(A_1)$
2882 ⎫ 2896 ⎬ 2910 ⎭	s	28	($\parallel$)	2887	(5)	0.35	$\nu_3(a_1)$
				2909	(0)	?	$\nu_1+\nu_7 = 2904(A_1)$
2927	m			2932	(1)	0.25	$\nu_2+\nu_{23} = 2928(A_2)$†
2944 ⎫ $\sim$2952 ⎭	m		($\perp$)				$\nu_9+2\nu_8 = 2939(E)$
$\sim$2978 ⎫ 2990 ⎭	w		($\perp$)?				$\nu_6+\nu_9 = 3017(E)$
3102	w						$\nu_2+\nu_{14} = 3128(E)$
3195	w						$\nu_2+\nu_4 = 3198(A_1)$
3236 ⎫ 3258 ⎭	w		($\perp$)				$\nu_1+\nu_{14} = 3264(E)$
3373 ⎫ 3392 ⎭	w		($\perp$)				$\nu_2+\nu_{15} = 3391(E)$
3532	w						$\nu_9+\nu_{15} = 3534(A_1)$

*w, m, s, and v = weak, medium, strong, and very, respectively.
†This band is type A, and therefore active, if the molecule has the lower symmetry C_3.

The E Vibrations

The strong depolarized Raman band at 2219 cm.$^{-1}$ in $DC(CD_3)_3$ is assigned to the fundamentals ν_9, ν_{10}, and ν_{11}. In $HC(CD_3)_3$ this band is split into two depolarized components at 2219 and 2208 cm.$^{-1}$, but since ν_9, ν_{10}, and ν_{11} appear to be accidentally degenerate in the other three isotopic isobutanes the stronger component at 2219 cm.$^{-1}$ is assigned as ν_9, ν_{10}, ν_{11}, and the weaker component as $\nu_4+\nu_{11} = 2224$ cm.$^{-1}(E)$. ν_{12} and ν_{13} were assumed to be coincident in the light molecules and assuming that they remain coincident in the heavy molecules they are assigned here to the depolarized Raman bands at 1102 cm.$^{-1}$ in $HC(CD_3)_3$ and 1087 cm.$^{-1}$ in $DC(CD_3)_3$. The symmetrical methyl bending mode ν_{14} is assigned to the depolarized Raman band at 1052 cm.$^{-1}$ in $HC(CD_3)_3$ (1056

TABLE III

THE INFRARED AND RAMAN SPECTRUM OF $DC(CD_3)_3$

	Infrared (vapor)				Raman (liquid)		Assignment (assuming point group symmetry C_{3v})
cm.$^{-1}$	Int.*	PR separation	Type	cm.$^{-1}$	Relative intensity	Depolarization ratio	
				304	(1)	dp	$\nu_{19}(e)$
343							
359	w	33	(∥)	345	(0)	?	$\nu_8(a_1)$
376				379	(0)	?	$\nu_7 - \nu_{19} = 383(E)$
—			(∥)				
690	m			687	(5)	0.24	$\nu_7(a_1)$
708	m		(⊥)	~702	(0)	dp	$\nu_{16}(e)$
721							
779							
789	m	21	(∥)	786	(1)	0.62	$\nu_6(a_1)$
800							
840							
857	w	26	(∥)				$\nu_{23}(a_2)$†
866							
889	w		(⊥)?	887	(1)	0.5	?
900							
~920	w			918	(1)	dp	$\nu_{15}(e)$
				1020	(1)	0.55	$\nu_{22}(a_2)$†
				1056	(2)	dp	$\nu_{14}(e)$
1056							
1068	s	~21	(∥)				$\nu_5(a_1)$
~1077							
				~1087	(0)	dp?	$\nu_{12}(e)$
~1106							
1118	w	20	(∥)	1117	(1)	0.32	$\nu_4(a_1)$
1126							
1131	w		(⊥)?				$\nu_{19} + \nu_{23} = 1161(E)$
1140							
1202							
1208	s		(⊥)?	1209	(1)	dp	$\nu_{18}(e)$
~1216							
~1262	w		(⊥)				$\nu_8 + \nu_{15} = 1277(E)$
~1272							
1290	m		(⊥)	1290	(0)	?	$\nu_{16} + 2\nu_{19} = 1317(E)$
1296				1326	(0)	?	$\nu_7 + \nu_{17} = 1339(E)$
				1357	(0)	?	$\nu_{14} + \nu_{19} = 1360(A_1)$
1370	w			1381	(0)	?	$\nu_7 + \nu_{16} = 1389(E)$
1396							
1415	w	~36	(∥)				$\nu_5 + \nu_8 = 1427(A_1)$
~1432							
~1592	w		(⊥)				$\nu_7 + \nu_{15} = 1605(E)$
1608							
~1735							
1748	w	28	(∥)?				$\nu_5 + \nu_7 = 1755(A_1)$
1763							
~1822							
1840	w	~22	(∥)				$\nu_5 + \nu_6 = 1857(A_1)$
1854							
1880							
1893	w	~29	(∥)				$\nu_{16} + \nu_{18} = 1910(A_1)$
1909							
				1943	(0)	?	$\nu_4 + \nu_{23} = 1974(A_2)$†
1970	w		(⊥)				$\nu_5 + \nu_{15} = 1986(E)$
1981				1981	(2)	0.30	$\nu_{12} + \nu_{15} = 2005(A_1)$
				2045	(1)	0.35	$2 \times \nu_{22} = 2040(A_1)$

TABLE III—*concluded*

THE INFRARED AND RAMAN SPECTRUM OF DC(CD$_3$)$_3$

Infrared (vapor)				Raman (liquid)			Assignment (assuming point group symmetry C_{3v})
cm.$^{-1}$	Int.*	PR separation	Type	cm.$^{-1}$	Relative intensity	Depolarization ratio	
~2058 2067 2078	s		(∥)	2063	(15)	0.27	ν_3
— 2073 2086	s		(∥)				ν_2
~2090 2099 2113	s	~23	(∥)	2107	(4)	0.40	$2\times\nu_{14} = 2112(A_1)$
~2120 2132 ~2142	s	~22	(∥)	2127	(7)	0.26	$\nu_4+\nu_{22} = 2137(A_2)$†
				~2141	(4)	0.34	$2\times\nu_5 = 2136(A_1)$
— 2164 2175	s		(∥)	2158	(7)	0.40	$\nu_{12}+\nu_{14} = 2143(A_1)$
~2206 2216 —	vs		(∥)				ν_1
— 2223 2230	s		(⊥)	2217	(10)	dp	$\nu_9,\ \nu_{10},\ \nu_{11},\ \nu_{21}$
				~2238	(4)	0.50	$2\times\nu_4 = 2234(A_1)$
				~2259	(1)	?	$\nu_{14}+\nu_{18} = 2264(A_1)$
2341 ~2354	m		(⊥)?				$\nu_3+\nu_{19} = 2367(E)$
2358 2367	m		(⊥)?				$\nu_2+\nu_{19} = 2377(E)$
2392 2403 ~2411	w	~19	(∥)?				$2\times\nu_{18} = 2416(A_1)$
2508 2522 2531	w	23	(∥)				$\nu_9+\nu_{19} = 2521(A_1)$
2566 ~2582	w		(⊥)				$\nu_8+\nu_9 = 2576(E)$
2781	w						$\nu_2+\nu_{16} = 2787(E)$
2853	w						$\nu_9+\nu_{17} = 2869(A_1)$
2878 2894 2915	m	37	(∥)				$\nu_3[HC(CD_3)_3]$
2925 —	m		(∥)				$\nu_2+\nu_{23} = 2930(A_2)$†
2934 2943	m		(⊥)				$\nu_9+2\nu_8 = 2935(E)$
2940 2950	m		(⊥)?				$\nu_9+\nu_{16} = 2939(A_1)$?
~2946 2954	m		(⊥)?				$\nu_3+\nu_{15} = 2981(E)$
2984	w						$\nu_2+\nu_{15} = 2991(E)$
3093 3104	w		(⊥)				$\nu_3+\nu_{14} = 3119(E)$
~3111	w						$\nu_2+\nu_{14} = 3129(E)$
~3142	w						$\nu_9+\nu_{15} = 3135(A_1)$
~3172	w						$\nu_2+\nu_4 = 3190(A_1)$
3243 3256	w		(⊥)				$\nu_1+\nu_{14} = 3272(E)$
3263 3272	w		(⊥)				$\nu_2+\nu_{18} = 3281(E)$
3337 ~3350	w		(⊥)				$\nu_4+\nu_9 = 3334(E)$
3437	w						$\nu_1+\nu_{18} = 3424(E)$

*w, m, s, and v = weak, medium, strong, and very, respectively.

†*This band is type A and therefore active, if the molecule has the lower symmetry C_3.*

TABLE IV

FUNDAMENTAL FREQUENCIES OF THE DEUTERIUM SUBSTITUTED ISOBUTANES

	Frequency	$HC(CH_3)_3$*	$DC(CH_3)_3$*	$HC(CD_3)_3$	$DC(CD_3)_3$
a_1	ν_1	2920	2920	2212	2216
	ν_2	2907	2903	2076	2073
	ν_3	2869	2146	2887	2063
	ν_4	1477	1477	1122	1117
	ν_5	1394	1394	1071	1068
	ν_6	966†	944†	798	789
	ν_7	795	796	692	687
	ν_8	433	426	360	359
e	ν_9	2958	2956	2219	2217
	ν_{10}	(2958)	(2956)	(2219)	(2217)
	ν_{11}	(2958)	(2956)	(2219)	(2217)
	ν_{12}	1450	1450	~1102	~1087
	ν_{13}	(1450)	(1450)	(~1102)	(~1087)
	ν_{14}	1370	1370	1052	1056
	ν_{15}	1330	950	1315	918
	ν_{16}	918†	812†	705	702
	ν_{17}	(966)	1065	636	~652‡
	ν_{18}	1172†	1233†	1156	1208
	ν_{19}	367	370	306	304
	ν_{20}	—	—	—	—
a_2	ν_{21}	(2958)†	(2956)†	(2219)	(2217)
	ν_{22}	(1450)†	(1450)†	1006	1020
	ν_{23}	1184†	1166†	852	857
	ν_{24}	—	—	—	—

*Assignment is that of Evans and Bernstein (2) unless otherwise indicated.
†Present assignment.
‡Estimated from product rule.

TABLE V

TELLER REDLICH PRODUCT RATIOS FOR THE DEUTERIUM SUBSTITUTED ISOBUTANES

		$HC(CH_3)_3/DC(CH_3)_3$	$HC(CD_3)_3/DC(CD_3)_3$	$HC(CH_3)_3/HC(CD_3)_3$
a_1	$\tau_{calc.}$	1.402	1.403	5.263
	$\tau_{obs.}$	1.390	1.441	5.180
e	$\tau_{calc.}$	1.377	1.384	13.169*
	$\tau_{obs.}$	1.354	[1.384]	13.011
a_2	$\tau_{calc.}$	1.000	1.000	2.506*
	$\tau_{obs.}$	1.015	0.981	2.670

*Torsional mode factorized out. Ratio of the torsional frequencies is 1.394.

cm.$^{-1}$ in $DC(CD_3)_3$), the frequency being close to and slightly less than that of the corresponding mode $\nu_5(a_1)$ analogous to the assignment in the light molecules. The CH bending mode ν_{15} is assigned to the perpendicular type infrared band at 1315 cm.$^{-1}$ in $HC(CD_3)_3$ and to the depolarized Raman band at 918 cm.$^{-1}$ in $DC(CD_3)_3$. Of the two methyl rocking modes ν_{16} and ν_{17} one, ν_{16} say, can certainly be assigned to the depolarized Raman band at 705 cm.$^{-1}$ in $HC(CD_3)_3$ and 702 cm.$^{-1}$ in $DC(CD_3)_3$ while the other can be associated with the weak Raman band at 636 cm.$^{-1}$ in $HC(CD_3)_3$. No band was observed around 630 cm.$^{-1}$ in $DC(CD_3)_3$ but application of the Teller Redlich product rule to $HC(CD_3)_3$ and $DC(CD_3)_3$ predicts a frequency around 652 cm.$^{-1}$ for ν_{17}. This could easily be overlapped by the strong grating 'ghost'† at ~660 cm.$^{-1}$ present in the Raman spectrum of $DC(CD_3)_3$. ν_{19} is assigned to the depolarized Raman bands at 306 and 304 cm.$^{-1}$ in $HC(CD_3)_3$ and $DC(CD_3)_3$ respectively.

†When the sample is not of the highest optical purity or too little sample is available to fill the Raman tube, the light scattering is high and the grating spectrometer has a ghost of medium intensity ~660 cm.$^{-1}$.

It now remains only to assign ν_{18}, the asymmetrical skeletal stretching mode. Very strong perpendicular type infrared bands are observed at 1156 cm.$^{-1}$ in HC(CD$_3$)$_3$ and 1208 cm.$^{-1}$ in DC(CD$_3$)$_3$ and, since all the remaining E type fundamentals have been satisfactorily assigned, these frequencies must be associated with ν_{18}. The anomalous increase in the frequency of this mode on deuteration can be explained plausibly by considering interaction between ν_{15} and ν_{18} in HC(CD$_3$)$_3$, which lowers ν_{18} from an unperturbed value around 1210 cm.$^{-1}$ (say) to 1156 cm.$^{-1}$ and raises ν_{15} by the same amount to 1315 cm.$^{-1}$. On deuteration the CH bending mode ν_{15} shifts considerably, thereby removing the cause of the interaction, and ν_{18} appears at its unperturbed position at 1208 cm.$^{-1}$. The fundamentals are given in Table IV and the Teller Redlich product ratio in Table V.

A comparison of the type E fundamentals for HC(CD$_3$)$_3$ and DC(CD$_3$)$_3$ with the corresponding fundamentals assigned by Evans and Bernstein for HC(CH$_3$)$_3$ and DC(CH$_3$)$_3$ is consistent for all the vibrations except ν_{16} and ν_{18}, which they place at 1169 cm.$^{-1}$ and 917 cm.$^{-1}$ respectively. The asymmetrical skeletal stretching mode, ν_{18}, should not change appreciably on deuterium substitution and can now be assigned unambiguously to the strong perpendicular type infrared bands at 1172 cm.$^{-1}$ in HC(CH$_3$)$_3$ and 1233 cm.$^{-1}$ in DC(CD$_3$)$_3$ in agreement with the corresponding assignments of 1156 cm.$^{-1}$ in HC(CD$_3$)$_3$ and 1208 cm.$^{-1}$ in DC(CD$_3$)$_3$. The increase in the frequency of this mode in DC(CH$_3$)$_3$ from that in HC(CH$_3$)$_3$ is analogous to the increase in the frequency of this mode in DC(CD$_3$)$_3$ from that in HC(CD$_3$)$_3$ and can be explained in the same manner by interaction with ν_{15} (see above). ν_{16} is now associated with the perpendicular type bands at 918 cm.$^{-1}$ in HC(CH$_3$)$_3$ and 812 cm.$^{-1}$ in DC(CH$_3$)$_3$ to give consistency with the Teller Redlich product rule for all the deuterium substituted molecules. The present assignment for ν_{16} and ν_{18} in HC(CH$_3$)$_3$ and DC(CH$_3$)$_3$ differs from that of Evans and Bernstein only by an interchange of the two frequencies. Further, their explanation of the anomalous frequency shifts in passing from HC(CH$_3$)$_3$ to DC(CH$_3$)$_3$ involving interaction between ν_{15}, ν_{16}, and ν_{17} has not been modified. In DC(CD$_3$)$_3$ ν_{16} and ν_{17} have both been lowered considerably, removing the cause of the interaction with ν_{15} observed in DC(CH$_3$)$_3$, and accordingly the correlation between HC(CD$_3$)$_3$ and DC(CD$_3$)$_3$ for these frequencies is quite straightforward. This provides some indirect support for the proposed interactions between ν_{15}, ν_{16}, and ν_{17} in DC(CH$_3$)$_3$. The type E fundamentals are given in Table IV for all the isotopic molecules and the Teller Redlich product ratios are given in Table V.

The A_2 Vibrations

In the preceding discussion we assumed the molecule to have the high symmetry C_{3v} for which the fundamentals divide into symmetry species as $8A_1 + 4A_2 + 12E$, the type A_1 and E modes being active and the type A_2 modes inactive in both spectra. However, it is improbable that the molecule has this high symmetry and almost certainly the methyl groups will be staggered, giving the lower point group symmetry C_3 for the molecule. In this case the fundamentals divide into symmetry species as $12A + 12E$, all modes being both infrared and Raman active. In particular the type A_2 modes of the C_{3v} symmetry model become type A modes in the lower symmetry model and are therefore capable of giving rise to polarized Raman bands and parallel type infrared bands. The other modes remain A or E as in the C_{3v} model. With this in mind it is now possible to assign some of the bands in the spectra of the isotopic isobutanes which could not be explained satisfactorily on the basis of the C_{3v} model and the present assignment. Thus, in HC(CH$_3$)$_3$ the Raman band at 1184 cm.$^{-1}$ may be assigned to the methyl

rocking mode, ν_{22}, while in $DC(CH_3)_3$ the polarized Raman band at 1166 cm.$^{-1}$ may be taken as ν_{22}. In $HC(CD_3)_3$ ν_{22} is assigned to the polarized Raman band, parallel type infrared band, at 852 cm.$^{-1}$ while in $DC(CD_3)_3$ it is assigned to the parallel type infrared band at 857 cm.$^{-1}$. In the lighter molecules ν_{21} and ν_{23} would undoubtedly be overlapped but can be assigned coincident with the analogous modes ν_9 and ν_{12} respectively. In the heavier molecules ν_{21} would again be overlapped but can be assigned coincident with ν_9, while ν_{23} is assigned to the polarized Raman bands at 1006 cm.$^{-1}$ in $HC(CD_3)_3$ and 1020 cm.$^{-1}$ in $DC(CD_3)_3$. Strictly the Teller Redlich product rule should be applied to the isobutanes on the basis of C_3 symmetry for which only two factors corresponding to the type A and type E modes would be obtained. However, to a good approximation, we can consider the type A modes of the C_3 model to factorize into type A_1 and A_2 modes of the C_{3v} model, in which case the Teller Redlich product rule can be applied to each species separately. The application of the product rule to the type A_2 frequencies (Table V) gives reasonable agreement between observed and calculated ratios.

The present assignment will not alter materially the results of the thermodynamic functions calculated by Pitzer and Kilpatrick (4) since only one fundamental frequency has been seriously changed from 1098 cm.$^{-1}$ in their assignment to 966 cm.$^{-1}$ here. Their band at 1098 cm.$^{-1}$ was not observed by Evans and Bernstein (3) but can be assigned (3) as ν_3 excited by λ 4047.

REFERENCES

1. EDSALL, J. T. and WILSON, E. B., Jr.   J. Chem. Phys. **6**, 124 (1938).
2. EVANS, J. C. and BERNSTEIN, H. J.   Can. J. Chem. **33**, 1792 (1955).
3. EVANS, J. C. and BERNSTEIN, H. J.   Can. J. Chem. **34**, 1037 (1956).
4. PITZER, K. and KILPATRICK, J.   Chem. Revs. **39**, 439 (1946).
5. RANK, D. H. and KAGARISE, R.   J. Opt. Soc. Amer. **40**, 89 (1950).
6. SHEPPARD, N. and SIMPSON, D. M.   Quart. Revs. (London), **7**, 19 (1953).
7. WHITE, J. U., ALPERT, N. L., and DE BELL, A. G.   J. Opt. Soc. Amer. **45**, 154 (1955).

YIELDS IN U^{235} THERMAL NEUTRON FISSION[1]

A. P. Baerg and Rosalie M. Bartholomew

ABSTRACT

Quantitative ion exchange and 4π counting techniques have been used to measure the yields of four nuclides not previously determined by mass spectrometric analysis. Values of 6.57, 6.30, 4.74, and 5.71% were obtained respectively for Ba^{139}, La^{141}, Sr^{89}, and Sr^{91} relative to a value of 6.32% for the yield of Ba^{140}. A precision better than 1.3% was achieved in the measurements.

INTRODUCTION

The earliest techniques used to investigate the yields of various fission product masses were based on radiochemistry. These methods are considered reliable to 10–20% (15) though the accuracy in some cases may be considerably better. On the other hand, yields obtained by mass spectrometry are believed to have a precision of 1–2% among isotopes of a given element (10, 15). Until recently absolute mass spectrometric yields were obtained by normalization to radiochemical yields. Hence these absolute values were only as accurate as the latter.

Most of the published radiochemical yields have been obtained by the use of end-window Geiger counters to measure the absolute disintegration rates of the fission-produced nuclides. The corrections associated with this method of counting (i.e. self-absorption, back scattering, etc.) are considered the major source of the inaccuracies. Other errors arise from inaccuracies in half-lives, decay schemes, analyses of complex decay curves, and chemical stoichiometry.

These errors are not present in mass spectrometric yield measurements since the mass analyses are made upon the stable end products, after essentially complete decay of all the radioactive nuclides in the mass chains. By using isotope dilution techniques, mass spectrometry has now been adapted to the determination of absolute fission yields (10, 15), and values obtained in this way are believed reliable to 3–5%.

Among the fission-produced mass chains there are, however, several which cannot be determined by mass spectrometric techniques. These include chains which decay to stable or long-lived members which are mono-isotopic. Others are not amenable to mass analysis because the stable end product is an isotope of preponderant abundance in the natural element. This leads to large errors in the isotope dilution techniques and from contamination by natural sources of the element. Mass chains of these types which have significant fission yields are masses 89, 99, 103, 105, 139, and 141.* The fission yields of these can better be obtained by radiochemical methods.

The purpose of this work was to measure radiochemically the yields of Sr^{89}, Sr^{91}, Ba^{139}, and La^{141} relative to that of Ba^{140}, with a reliability comparable with that achieved in mass spectrometry. The yield of Sr^{91} was included because it could be conveniently measured and because a reliable value would be useful in the normalization of relative mass spectrometric yields in this mass region. The mass chains studied and decay mechanisms (7, 9) are given below. The nuclides isolated are shown underlined.
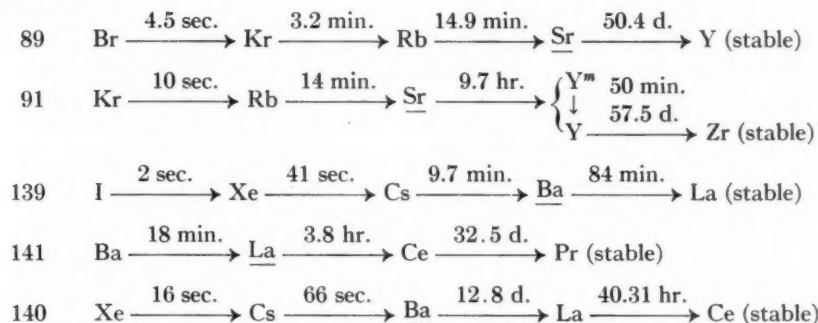
It appears that new techniques in mass spectrometry may now permit analysis for such longer-lived nuclides as 50-day Sr^{89}, 40-day Ru^{103}, and 32-day Ce^{141}.

Mass No.

$$89 \quad Br \xrightarrow{\text{4.5 sec.}} Kr \xrightarrow{\text{3.2 min.}} Rb \xrightarrow{\text{14.9 min.}} \underline{Sr} \xrightarrow{\text{50.4 d.}} Y \text{ (stable)}$$

$$91 \quad Kr \xrightarrow{\text{10 sec.}} Rb \xrightarrow{\text{14 min.}} \underline{Sr} \xrightarrow{\text{9.7 hr.}} \begin{cases} Y^m \quad 50 \text{ min.} \\ \downarrow \quad\quad 57.5 \text{ d.} \\ Y \xrightarrow{} Zr \text{ (stable)} \end{cases}$$

$$139 \quad I \xrightarrow{\text{2 sec.}} Xe \xrightarrow{\text{41 sec.}} Cs \xrightarrow{\text{9.7 min.}} \underline{Ba} \xrightarrow{\text{84 min.}} La \text{ (stable)}$$

$$141 \quad Ba \xrightarrow{\text{18 min.}} \underline{La} \xrightarrow{\text{3.8 hr.}} Ce \xrightarrow{\text{32.5 d.}} Pr \text{ (stable)}$$

$$140 \quad Xe \xrightarrow{\text{16 sec.}} Cs \xrightarrow{\text{66 sec.}} \underline{Ba} \xrightarrow{\text{12.8 d.}} La \xrightarrow{\text{40.31 hr.}} Ce \text{ (stable)}$$

EXPERIMENTAL

The nuclides studied were separated from other fission products and from each other using ion exchange methods. A preliminary anion exchange separation using hydrochloric acid eluant isolated the alkali metals, alkaline earths, and rare earths from the uranium and most of the other fission products (8). Subsequent elution from a cation exchange resin, using ammonium α-hydroxy-isobutyrate (1, 14) separated the strontium, barium, and lanthanum from each other and from the alkali metals, and other fission product elements. These methods permitted quantitative recoveries using microgram amounts of carrier only. The minimal mass of carrier, added to prevent losses on the walls of containers, was advantageous in the preparation of sources for 4π counting. This counting technique was used throughout for the determination of absolute disintegration rates.

Samples of 10 to 50 mg. of uranium oxide (UO_2), sealed in quartz, were irradiated for periods of 0.5 to 2 hours in the Chalk River N.R.X. reactor. About 30 minutes after the irradiation, the sample was crushed in a solution 8 N in hydrochloric acid, 2 N in nitric acid, and containing 100 μg. each of rubidium, cesium, strontium, lanthanum, and barium carriers. The resultant solution was evaporated to dryness to remove most of the nitrate ion. The residue was taken up quantitatively in 8 N hydrochloric acid and passed through a small Dowex-1 anion exchange column.* Most of the anions and the uranium are adsorbed on the resin (8). The effluent (about 5 ml: including column washings) containing the alkali metals, rare earths, and alkaline earths was evaporated to dryness to remove the bulk of hydrochloric acid in preparation for the cation exchange separation.

Dowex-50W resin with 12% cross linkage and particles graded to a settling rate of 0.3 to 0.5 cm. per minute in water was used to separate the cations. The column was 3 cm. long and 0.31 cm. in diameter, maintained at a temperature of 87° C. The effluent residue from the anion column was taken up in a minimum of 0.5 N hydrochloric acid and transferred quantitatively to the top of the Dowex-50W resin column which was initially in the hydrogen form. The elution was then begun using 0.4 M ammonium α-hydroxy-isobutyrate at a pH of 4.2 and a flow rate of 0.17 ml. per minute.† This eluant provided for rapid elution of the alkali metals and the heavier rare earths while permitting adequate separation of cerium from lanthanum without significant movement

---

*Dowex-1 resin with 4% cross linkage as particles with a settling rate of 3–9 cm. per minute in water was packed as a column 4 cm. long and 6 mm. in diameter.

†Elution was not started until 2.5 hours after the end of the irradiation to allow time for the 18-minute Ba^{141} and 19-minute La^{143} to decay.

of strontium and barium from the top of the column. The sequence of elution is shown schematically in Fig. 1. Throughout the elutions a collimated Geiger probe with a recorder was used to monitor the effluent drops. This avoided incomplete separations arising from peak shifts caused by slight changes in concentration or pH of the eluant.

In the interest of speed and to reduce volumes the concentration of the eluant was increased to 1.2 M following the elution of cerium. In this way the lanthanum was eluted in approximately one column volume of effluent. The eluant was then again
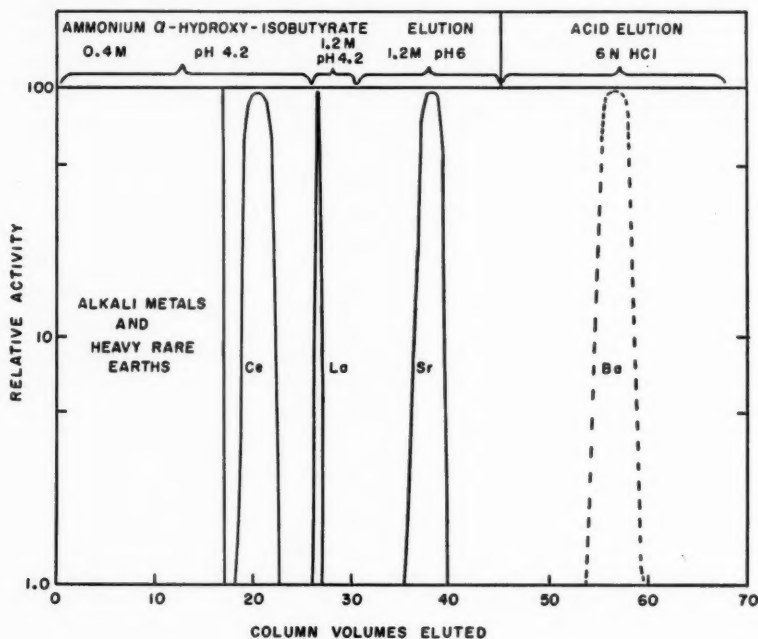

FIG. 1. Schematic of cation exchange separation.

changed to 1.2 M at a pH of 6.0 to separate the strontium. The peak of the strontium elution then occurs at about 8 column volumes and that of barium at about 27 if elution with this eluant is continued (dotted curve, Fig. 1). The separated lanthanum, strontium, and barium were treated further as follows:

Ba^{139}–Ba^{140}.—After the separation of strontium only barium remains adsorbed on the resin. This was recovered by first thoroughly washing the eluant from the column with about 5 column volumes of 0.5 N hydrochloric acid and finally eluting the barium with 6 N acid (3) and collecting in a volumetric flask from which aliquots were taken for 4π counting. The end of the butyrate elution was taken as the time of the last La^{140}–Ba^{140} separation in establishing the absolute disintegration rate of Ba^{140} from the counting data. The decay of 84-minute Ba^{139} was followed over about six half-lives and that of the remaining Ba^{140}–La^{140} for a period of 2 weeks.

La^{141}.—The lanthanum fraction was adjusted to a pH of about 0.1. The lanthanum from this solution was then adsorbed on a second column of Dowex-50W resin. Activities of yttrium, which appear with the lanthanum from decay of the strontium isotopes

during elution from the first column, were eluted as previously along with newly grown Ce^{141}. In establishing the time of the last La^{141}–Ce^{141} separation account was taken of the growth of Ce^{141} during the elution, on the basis of a separation factor of 2.3 between lanthanum and cerium. The column was finally washed after the cerium elution, and the lanthanum collected in a volumetric flask using 6 N hydrochloric acid (3). The 77-minute La^{142} and 40-hour La^{140} were allowed to decay before La^{141} was determined by counting 32.5-day Ce^{141}. The decay was followed for 1 to 2 months.

Sr^{89} and Sr^{91}.—The 9.7-hour Sr^{91} was allowed to decay completely to 57.5-day Y^{91} in the original strontium fraction. About 100 μg. of yttrium carrier was added and the solution adjusted to a pH of 0.1. The strontium and yttrium were then adsorbed on the second column of Dowex-50W resin and yttrium eluted as previously. The 50.4-day Sr^{89} remaining on the resin was freed of organic eluant and collected in a volumetric flask using 6 N hydrochloric acid (3). The Y^{91} was freed from organic eluant by acidification, readsorption on another Dowex-50W column, washing, and final elution with 6 N hydrochloric acid. The Sr^{91} was determined by counting the 57.5-day Y^{91}. Small corrections to the counting data of Sr^{89} and Y^{91} were made for the presence of Sr^{90} and Y^{90}, assuming equal fission yields for the 27.7-year Sr^{90}. The decay of these nuclides was followed for about 60 days.

RESULTS AND DISCUSSION

The relative yields obtained in the experiments are collected in Table I. In principle, measurements could be made for all five nuclides studied in any one experiment. In practice, however, it was found more convenient to analyze for Ba^{139} separately from La^{141}. The average of six measurements of the yield of Sr^{89} was 0.751 relative to that of Ba^{140}, with a precision of 0.77%, and in several experiments the yields of La^{141} and Sr^{91} were measured relative to this value for Sr^{89}. In Table II the average values are presented, all calculated relative to a yield of 6.32% for Ba^{140} (10, 11, 17). The measurements made relative to Sr^{89} are included in these averages.

TABLE I

RELATIVE YIELDS IN THERMAL NEUTRON FISSION OF U^{235}

Experiment	Ba^{140}	Ba^{139}	La^{141}	Sr^{89}	Sr^{91}
1	1	1.03_8			
2	1	1.04_0		0.76_0	
3	1	1.03_8		0.75_0	
4	1	1.04_1		0.74_3	
5	1			0.74_6	0.89_8
6	1			0.75_6	0.90_3
7	1		1.00_8	0.75_2	0.91_2
8	1		1.00_0		
9	1		1.01_6		
10			1.33_2	1	1.23_2
11			1.32_7	1	1.18_8
12			1.29_8	1	1.19_6
13			1.31_1	1	1.19_9

The standard deviations associated with the yield measurements are also indicated in Table II. These are all less than 1.3% and comparable with the precision achieved in mass spectrometry. These errors are believed consistent with errors in counting, pipetting, timing, etc. The absolute yields quoted in Table II are of no greater accuracy, however, than ±3 to 5% associated with the yield of 6.32% for Ba^{140} (10, 17). Values

TABLE II

COMPARISON OF FISSION YIELDS

	Mass				
	140	139	141	89	91
% Yield	(6.32)*	6.57	6.30	4.74	5.71
Standard deviation		0.01$_5$	0.08	0.04	0.06
Data of Ref. 11	6.3	6.4		4.78	5.1
Data of Ref. 15	6.56				5.84
Data of Ref. 13	6.1		5.7		

Normalization yield (17).

of the fission yields quoted in the literature are also given in the table for comparison.

The yield of Ba^{139} is based on a value of 84 minutes for the half-life of this nuclide. A separate measurement of this half-life was made on Ba^{139} produced by neutron irradiation of enriched Ba^{138} (98 + % isotopic abundance). The half-life observed was 84.0 ± 0.2 minutes over about nine half-lives. The data for the Ba^{139}-yield measurements were all consistent with this value over five to six half-lives. The fission yield obtained, using this value, is about 2% higher than that found by Reed and Turkevich (11), who used a value of 85 minutes. The difference in yield values is, however, almost entirely due to the use of the different half-life in the calculations. The effect of a change in half-life on the calculated yield depends on the experimental conditions. A decrease in the value of the half-life will reduce the calculated yield, but this effect may be more than offset by an increase in yield arising from the extrapolation of the counting data to the end of the irradiation.

The best previous estimate of $5.7\pm0.5\%$ for the fission yield of Ce^{141} (2, 13) is based on a value of 6.1% for the yield of Ba^{140} and apparently on a value of 28 days for the half-life of Ce^{141}. If this yield measurement is simply increased appropriate to the presently accepted value of 32.5 days (4) for the half-life of Ce^{141}, and to correspond to 6.32% yield for Ba^{140}, then this yield of Ce^{141} becomes 6.85%. This value is greater than that found in this work for La^{141} by 8.7%, although the two results still agree within the quoted errors. Consideration of the available data (15) on independent fission yields along a mass chain indicates that the fission yield of Ce^{141} should be no more than 0.1% greater than that for La^{141}.

The 4.74% yield obtained in this work for Sr^{89} is in excellent agreement with that of 4.78% found by Reed and Turkevich (11), although these authors assumed a half-life of 53 days for Sr^{89}. The more recent half-life value of 50.4 days (6) is entirely consistent with our data and use of this value in the yield calculations apparently accounts for the small difference between these two measurements.

Two measurements of the mass 91 yield have recently been reported in the literature. The radiochemical yields of 5.1% (11, 12) and 5.2% (16) appear much too low when compared with the mass spectrometric value of 5.84% (15) obtained for Zr^{91} using isotope dilution techniques. The discrepancy could be attributed to a large independent yield for Y^{91}, though this was inconsistent with available information (12, 15). Recently Grummitt and Milton (5) have found that 2% of the Y^{91} yield is formed other than through 9.7-hour Sr^{91}. This result and the yield of 5.71% obtained in this work is in excellent agreement with that found mass spectrometrically (15).

REFERENCES

1. CHOPIN, G. R. and SILVA, R. J.   J. Inorg. Nuclear Chem. **3**, 153 (1956).
2. CORYELL, C. D. and SUGARMAN, N.   National Nuclear Energy Series. Div. IV. Vol. 9. McGraw-Hill Book Company, Inc., New York. 1951.
3. DIAMOND, R. M., STREET, K., and SEABORG, G. T.   U. S. Atomic Energy Comm. Rept., AECD–3517 (1951).
4. FREEDMAN, M. S. and ENGELKEMIER, D. W.   Phys. Rev. **79**, 897 (1950).
5. GRUMMITT, W. E. and MILTON, G. M.   J. Inorg. Nuclear Chem. (In press).
6. HERMANN, G.   Z. Elektrochem. **58**, 626 (1954).
7. HOLLANDER, J. M., PERLMAN, I., and SEABORG, G. T.   Revs. Mod. Phys. **25**, 469 (1953).
8. KRAUS, K. A. and NELSON, F.   International Conference on the Peaceful Uses of Atomic Energy. Vol. 7. United Nations, New York. 1956. p. 837.
9. Nuclear Data Cards, Nuclear Data Group, National Research Council, Washington, D.C.
10. PETRUSKA, J. A., THODE, H. G., and TOMLINSON, R. H.   Can. J. Phys. **33**, 693 (1955).
11. REED, G. W. and TURKEVICH, A.   Phys. Rev. **92**, 1473 (1953).
12. REED, G. W.   Phys. Rev. **98**, 1327 (1955).
13. SCHUMAN, R. P.   U. S. Atomic Energy Comm. Rept., CN–2929 (1945).
14. SMITH, H. L. and HOFFMAN, D. C.   J. Inorg. Nuclear Chem. **3**, 243 (1956).
15. STEINBERG, E. P. and GLENDENIN, L. E.   International Conference on the Peaceful Uses of Atomic Energy.   Vol. 7. United Nations, New York. 1956. p. 614.
16. HERRMANN, G. and STRASSMANN, F.   Z. Naturforsch. **11a**, 946 (1956).
17. YAFFE, L., THODE, H. G., MERRITT, W. F., HAWKINGS, R. C., BROWN, F., and BARTHOLOMEW, R. M.   Can. J. Chem. **32**, 1017 (1954).

CONDUCTIVITY OF AQUEOUS SOLUTIONS OF SOME PARAFFIN CHAIN SALTS[1]

E. D. GODDARD[2] AND G. C. BENSON

ABSTRACT

Specific conductivities of aqueous solutions of sodium dodecyl sulphate, sodium decyl sulphate, and sodium octyl sulphate were measured over concentration ranges about the respective CMCs and at temperatures from 10° to 55° C. Values of the increase in heat content associated with micelle formation are estimated from the temperature variation of the CMC and the relation of these results to the theory of micelle formation is considered.

INTRODUCTION

The electrical conductivity of a solution depends among other factors on the size and charge of the ionic species present. It is thus not surprising that in detergent systems, where micelle formation is possible, there is a fairly rapid change in the slope of the conductivity–concentration curve in the region of the critical micelle concentration (CMC). Measurement of the conductivity of such systems offers one of the best methods of determining the CMC. In this paper conductivity data for aqueous solutions of sodium dodecyl sulphate, sodium decyl sulphate, and sodium octyl sulphate in concentration ranges about the respective CMCs are presented for temperatures from 10° C. to 55° C. at intervals of 5° C.

EXPERIMENTAL

The a-c. conductivity bridge used for these measurements was built around a Leeds and Northrup Campbell-Shackelton shielded ratio box (1) which contained a Wagner earth connection. A Hewlett-Packard oscillator supplying an alternating voltage at a frequency of 1000 cycles per second was coupled to the bridge through a wave filter. The output of the bridge was amplified and applied to the vertical plates of a cathode ray oscilloscope which served to detect the balance point (9). The horizontal plates of this oscilloscope were connected through a phase shift circuit (10) to the filtered output of the bridge oscillator; thus it was possible to balance the resistive and capacitative components of the bridge separately.

The pyrex cell was of a design similar to that of Flockhart and Graham (3); the platinum electrodes 1 cm. in diameter and 4 cm. apart were given a light platinization. The total cell volume was 600 ml. but only 40 ml. of solution was needed to cover the electrodes adequately. A large oil bath controlled to ±0.005° C. was used to thermostat the cell at temperatures in the range 10° to 55° C. Absolute values of the temperatures were measured to 0.01° C. with a Leeds and Northrup resistance thermometer having a N.B.S. certificate. The cell constant was based on the specific conductivity of a 0.1D KCl solution at 25° C. as determined by Jones and Bradshaw (8). A periodic check of the cell constant was made during the course of the work. The temperature variation of the cell constant was computed with a formula (8) which allows for the linear expansion of the glass.

The sodium n-alkyl sulphates (C_{12}, C_{10}, and C_8) used in this work have been described

previously (6, 7). Conductivity water ($\kappa = 1.1 \times 10^{-6}$ mho cm.$^{-1}$ at 25° C.) was prepared from an alkaline permanganate solution in a pyrex glass still. Each concentration series was made up by progressive dilution in the cell. Steady readings were obtained approximately 20 minutes after each addition of water to the cell. The results of the conductivity measurements are indicated by the points in Figs. 1, 2, and 3. The concentration of the
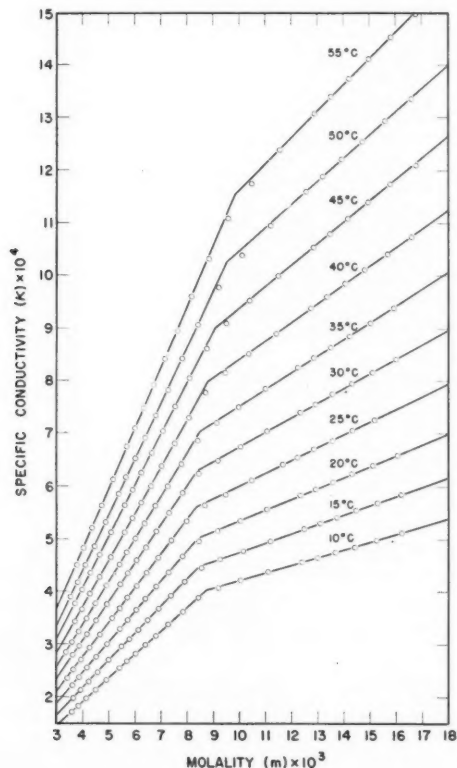

FIG. 1. The specific conductivity (κ in mho cm.$^{-1}$) of sodium dodecyl sulphate in aqueous solution plotted as a function of the molality for temperatures from 10° to 55° C.

solutions is stated in molality. Each of the curves is the result of a single series of dilutions. However in several cases the dilution runs were repeated and yielded points in very good agreement with those shown in the figures.

DISCUSSION

In considering the conductivity data of detergent systems there are two methods currently used to obtain the CMC: either the equivalent conductivity is plotted against the square root of the concentration, or the specific conductivity is plotted against the concentration. Both plots show a change of slope in the region of the CMC but there is generally a small difference (4) in the value of the CMC obtained by the two methods.

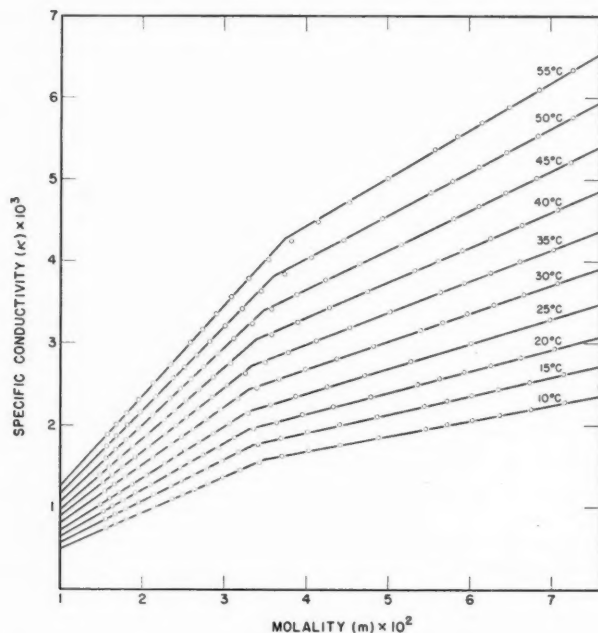Wright *et al.* (12) have pointed out that the equivalent conductivity loses some of its

FIG. 2. The specific conductivity (κ in mho cm.$^{-1}$) of sodium decyl sulphate in aqueous solution plotted as a function of the molality for temperatures from 10° to 55° C.

usual significance when micelles are present because it involves the effects of both micelles and single ions. They showed that in the case of the specific conductivity – concentration plot the points lay along two straight lines; the intersection was taken as the CMC. Concentration either as weight normality or as volume normality was used, depending on the availability of density data. A third possibility is to state the concentration as a molality. It is obvious that a straight line plot obtained in terms of one concentration scale can not in general yield a linear plot in terms of either of the other two concentration scales. However it appears in practice that for the concentration range of interest the specific conductivity data can be represented as a pair of straight lines to about the same approximation for all three methods of stating the concentration and that there is very little difference in the CMC values thus obtained. Complete density data are unavailable for the systems studied in the present work and it has proved convenient to express all the results as specific conductivity – molality plots.

The experimental data in Figs. 1 to 3 have been fitted with a pair of straight lines at each temperature and the point of intersection taken as the CMC. In all cases the experimental points indicate a smooth transition between the linear portions rather than the abrupt change in slope indicated by the lines as drawn. This rounding off is more pronounced at the higher temperatures. The lines below the CMC, when extrapolated to zero concentration, all give small positive intercepts indicating that the specific conductivity plot must really be curved and not linear between zero concentration and the CMC. In Table I values of the slope and of the intercept at zero concentration are given for the lines below and above the CMC at each temperature.
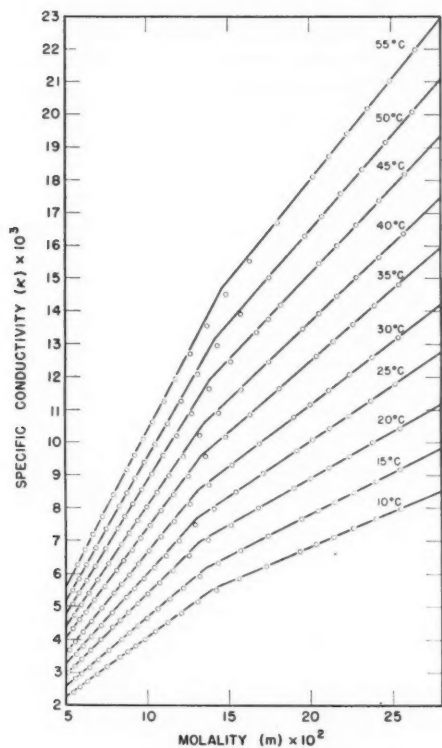
Fig. 3. The specific conductivity (κ in mho cm.$^{-1}$) of sodium octyl sulphate in aqueous solution plotted as a function of the molality for temperatures from 10° to 55° C.

TABLE I

COEFFICIENTS α AND β FOR THE LINES $\kappa = \alpha + \beta m$ DRAWN IN FIGS. 1–3

	Sodium alkyl sulphate											
	C_{12}				C_{10}				C_8			
	Below CMC		Above CMC		Below CMC		Above CMC		Below CMC		Above CMC	
° C.	$\alpha \times 10^4$	$\beta \times 10$	$\alpha \times 10^4$	$\beta \times 10$	$\alpha \times 10^3$	$\beta \times 10$	$\alpha \times 10^3$	$\beta \times 10$	$\alpha \times 10^3$	$\beta \times 10$	$\alpha \times 10^3$	$\beta \times 10$
10	0.09	0.449	2.76	0.146	0.05	0.440	0.92	0.190	0.44	0.363	2.60	0.211
15	0.09	0.517	2.99	0.176	0.07	0.502	1.01	0.226	0.47	0.420	2.78	0.251
20	0.12	0.580	3.30	0.205	0.08	0.566	1.10	0.262	0.55	0.483	3.21	0.284
25	0.12	0.655	3.60	0.241	0.07	0.636	1.18	0.302	0.51	0.548	3.22	0.340
30	0.13	0.732	3.97	0.277	0.09	0.710	1.31	0.342	0.63	0.602	3.53	0.382
35	0.12	0.811	4.35	0.317	0.09	0.788	1.44	0.386	0.80	0.656	3.78	0.434
40	0.16	0.884	4.87	0.354	0.10	0.866	1.58	0.432	0.76	0.725	4.18	0.474
45	0.19	0.969	5.30	0.408	0.12	0.940	1.71	0.484	0.66	0.814	4.65	0.525
50	0.18	1.052	6.07	0.440	0.14	1.016	1.90	0.532	0.84	0.864	5.00	0.574
55	0.24	1.141	6.64	0.499	0.15	1.100	2.11	0.582	0.90	0.940	5.61	0.618

The dependence of the CMC on temperature is illustrated in Fig. 4. In each of the three curves there is a minimum near 25° C. Similar plots have been obtained for lauryl sulphonic acid and potassium laurate by Brady and Huff (2) and for sodium dodecyl sulphate by Flockhart and Ubbelohde (4). The CMC values reported by the latter authors are lower than our results, the difference being about 10% at 50° C. and decreasing to a few per cent at 10° C.
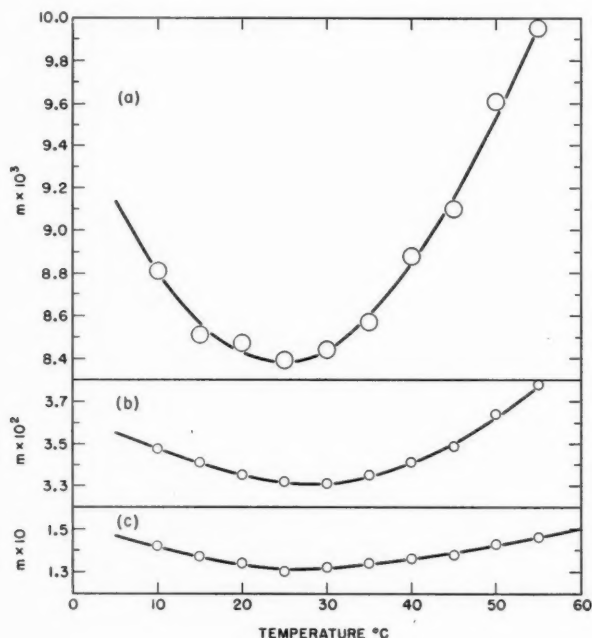

Fig. 4. Variation of the CMC with temperature. Curve (a) sodium dodecyl sulphate, (b) sodium decyl sulphate, and (c) sodium octyl sulphate.

The temperature variation of the CMC is of interest since Stainsby and Alexander (11) have suggested that it may be used to obtain the change in heat content ΔH_M associated with micelle formation by use of the formula

[1] $$\Delta H_M = -RT^2 d \ln(\text{CMC})/dT.$$

In this expression R is the gas constant and T the absolute temperature. Derivation of equation [1] involves the assumptions that the micelle can be treated as a separate phase with constant activity and that the activity coefficient of the single ions in solution is unity around the CMC. Values of ΔH_M have been calculated using this relation and are given in Table II. It may be argued that activity coefficients should be introduced for the decyl and octyl sulphates in view of the relatively high CMC of these compounds; we do not believe the reliability of the method warrants this. For comparison the ΔH_M values of sodium decyl and octyl sulphate estimated from direct calorimetric measurements (7) are included. Qualitatively, at least, there is agreement between these and the derived values in that at 25° they are small and positive. Values obtained by Flockhart

GODDARD AND BENSON: PARAFFIN CHAIN SALTS   991

TABLE II
ΔH_M (kcal./mole) CALCULATED FROM EQUATION [1]

Sodium alkyl sulphate	Temperature, °C.										
	5	10	15	20	25	30	35	40	45	50	55
C_{12}	0.8^*	1.0_9	0.7_1	0.4_0	-0.0_1 / 0.6^*	-0.5_5	-1.0_0	-1.1_7	-1.4_6 / -1.9^*	-1.7_2	-1.8_3
C_{10}		0.6_9	0.6_0	0.5_1	0.1_9 / 0.5†	-0.1_4	-0.5_8	-0.8_9	-1.2_4	-1.5_1	-1.7_9
C_8		1.1_2	0.9_6	0.7_1	0.2_0 / 0.8†	-0.2_8	-0.6_3	-0.7_9	-0.9_4	-1.0_2	-1.1_7

* *Values obtained by Flockhart and Ubbelohde (4).*
† *Values estimated from calorimetric measurements (7).*

and Ubbelohde (4) by a similar treatment of their results for sodium dodecyl sulphate are also included in Table I. Since the free energy change for the process of micelle formation is zero, values of the corresponding change in entropy ΔS_M may be obtained by dividing ΔH_M by the absolute temperature.

The existence of positive values for ΔH_M is at variance with most of the theories of micelle formation so far advanced. In these it has been assumed that aggregation is an energy effect resulting from the elimination or reduction of the hydrocarbon–water interface on micelle formation. Recently Goddard, Hoeve, and Benson (7) have suggested that although this picture is probably true at higher temperatures it does not hold at low temperatures. An explanation was made in terms of a water (so-called "iceberg") structure around the hydrocarbon chain of the single ions, as discussed by Frank and Evans (5). The hydrocarbon chain surrounded by the water structure represents a comparatively low energy state but the concomitant restriction of motion provides a driving force to aggregation, which is an entropy effect at lower temperatures. The CMC–temperature relationships observed in the present investigation are in qualitative agreement with this model.

REFERENCES

 1. BEHR, L. and WILLIAMS, A. J.   Proc. Inst. Radio Engrs. **20**, 969 (1932).
 2. BRADY, A. P. and HUFF, H.   J. Colloid Sci. **3**, 511 (1948).
 3. FLOCKHART, B. D. and GRAHAM, H.   J. Colloid Sci. **8**, 105 (1953).
 4. FLOCKHART, B. D. and UBBELOHDE, A. R.   J. Colloid Sci. **8**, 428 (1953).
 5. FRANK, H. S. and EVANS, M. W.   J. Chem. Phys. **13**, 507 (1945).
 6. GODDARD, E. D. and BENSON, G. C.   Trans. Faraday Soc. **52**, 409 (1956).
 7. GODDARD, E. D., HOEVE, C. A. J., and BENSON, G. C.   J. Phys. Chem. **61**, 593 (1957).
 8. JONES, G. and BRADSHAW, B. C.   J. Am. Chem. Soc. **55**, 1780 (1933).
 9. JONES, G., MYSELS, K. J., and JUDA, W.   J. Am. Chem. Soc. **62**, 2919 (1940).
10. LAMSON, H. W.   Rev. Sci. Instr. **9**, 272 (1938).
11. STAINSBY, G. and ALEXANDER, A. E.   Trans. Faraday Soc. **46**, 587 (1950).
12. WRIGHT, K. A., ABBOTT, A. D., SIVERTZ, V. and TARTAR, H. V.   J. Am. Chem. Soc. **61**, 549 (1939).

SELECTIVE SUBSTITUTION IN SUCROSE

II. THE SYNTHESIS OF 2,3,3',4,4'-PENTA-*O*-METHYL SUCROSE AND C4 TO C6 ACETYL MIGRATION IN SUCROSE[1]

G. G. McKEOWN[2] AND L. D. HAYWARD

ABSTRACT

Deacetylation of crystalline tri-*O*-trityl-penta-*O*-acetyl sucrose gave an amorphous tri-*O*-trityl sucrose derivative and methylation of this product followed by graded hydrolysis with acetic acid yielded a sirupy penta-*O*-methyl sucrose. Hydrolytic cleavage of the penta-*O*-methyl sucrose to nearly equal amounts of 2,3,4-tri-*O*-methyl-D-glucose and 3,4-di-*O*-methyl-D-fructose established the original positions of the *O*-trityl groups at the primary carbons in the sucrose molecule. It was therefore evident that acetyl migration from C_4 to C_6 in the glucose moiety had occurred during an earlier synthesis of 1',4,6'-tri-*O*-methyl sucrose from the tri-*O*-trityl-penta-*O*-acetyl sucrose. The probable conformation of the transition state in the acyl migration is discussed.

INTRODUCTION

The synthesis of 1',4,6'-tri-*O*-methyl sucrose from tri-*O*-trityl-penta-*O*-acetyl sucrose was described in Part I (14). The occurrence of an *O*-methyl group at C_4 of the glucose unit in the tri-*O*-methyl sucrose end product indicated either that C_4 of the glucose unit had been originally substituted by an *O*-trityl group in preference to C_6, or that the *O*-trityl substitution had been at C_6 and the *O*-acetyl group on C_4 had migrated to C_6 during the subsequent detritylation or methylation steps. The objective of the work described here was to establish the structure of the tri-*O*-trityl-penta-*O*-acetyl sucrose and thus provide a decision between the two possibilities. The structural proof is outlined in Fig. 1.
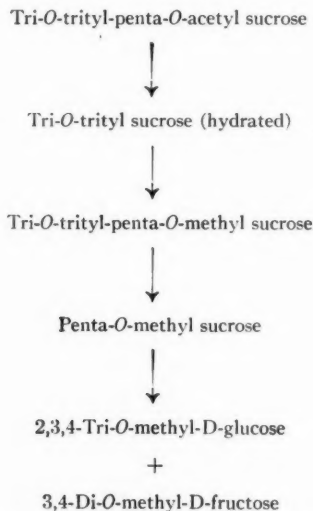
Tri-*O*-trityl-penta-*O*-acetyl sucrose

↓

Tri-*O*-trityl sucrose (hydrated)

↓

Tri-*O*-trityl-penta-*O*-methyl sucrose

↓

Penta-*O*-methyl sucrose

↓

2,3,4-Tri-*O*-methyl-D-glucose

+

3,4-Di-*O*-methyl-D-fructose

FIG. 1. Proof of the structure of the tri-*O*-trityl-penta-*O*-acetyl sucrose.

Our attempts to prepare tri-O-trityl sucrose by direct tritylation of sucrose yielded an intractable mixture (14); however, the pure compound was readily obtained by deacetylation of the crystalline tri-O-trityl-penta-O-acetyl sucrose. The product was a colorless glass, $[\alpha]_D^{22}$ +14.7° (c = 3.3 in chloroform), with a trityl content corresponding to that calculated for a tetrahydrate of tri-O-trityl sucrose. The powdered material reduced Fehling's solution only after acid hydrolysis, and acetylation gave back the original tri-O-trityl-penta-O-acetyl sucrose in 83% yield. Catalytic hydrogenation of the tri-O-trityl sucrose yielded only a trace of sucrose; catalyst poisoning as encountered in the attempted hydrogenolysis of the tri-O-trityl-penta-O-acetyl sucrose (14) appeared to halt the reaction at an intermediate stage.

Methylation of the hydrated tri-O-trityl sucrose by the Purdie method proceeded very slowly and 11 treatments were required to achieve a satisfactory degree of substitution. The course of the reaction was followed by detritylating and hydrolyzing a sample after each methylation and chromatographing the hydrolyzate on paper. The final product was a colorless glass, $[\alpha]_D^{17}$ +32.4° (c = 6.14 in chloroform), with trityl and methoxyl contents corresponding to a tri-O-trityl-penta-O-methyl sucrose.

The fully methylated tri-O-trityl sucrose was detritylated by graded hydrolysis in 98% acetic acid solution on the steam bath (14) and the course of the reaction was followed with a polarimeter. The specific rotation of the methylated tri-O-trityl sucrose in glacial acetic acid was approximately +50° and the assumption was made that the specific rotation of the corresponding penta-O-methyl sucrose would be in the range of +50° to +65° since sucrose, tri-O-methyl sucrose, and octa-O-methyl sucrose showed similar values (14). Taking into account the large change in molecular weight it was calculated that the apparent specific rotation of the acetic acid solution during the hydrolysis would decrease from about +50° to about +20° if detritylation were the predominant reaction. If hydrolysis of the glycosidic bond and mutarotation of the monosaccharides occurred concurrently and at a comparable rate, the optical rotation would decrease to zero, since the equilibrium specific rotations of the partially methylated D-glucose and D-fructose fragments were opposite in sign and nearly equal in magnitude (7, 9, 12, 13). Actually the observed apparent specific rotation decreased according to a second-order reaction rate curve from the initial value of +48.8° to +19.8° in 50 minutes; at this point, where the optimum yield of penta-O-methyl sucrose was expected, the reaction was interrupted by evaporation of the solvent under reduced pressure and below 50° C.

The sirupy detritylated product was separated from the triphenyl carbinol by extraction with water and was purified by chromatography on a cellulose column. The appropriate fractions from the column yielded 18.5% of the theoretical amount of pure penta-O-methyl sucrose as a colorless, viscous sirup, $[\alpha]_D^{23}$ +64.3° (c = 1.46 in water), which had the correct methoxyl content and reduced Fehling's solution only after acid hydrolysis. A sample of the sirup was hydrolyzed with 0.05 N sulphuric acid and the hydrolyzate was separated on a cellulose column into two chromatographically pure fractions which analyzed correctly for a tri-O-methyl hexose and a di-O-methyl hexose. The yields of the hexose derivatives isolated were 89% and 75% of the theoretical values respectively.

The sirupy tri-O-methyl hexose was identified as 2,3,4-tri-O-methyl-D-glucose on the following evidence: (a) the equilibrium specific rotation, $[\alpha]_D^{24}$ +70.6° (c = 3.26 in water), was in good agreement with previously reported values (7, 12); (b) paper chromatograms of the compound developed with two different solvents showed a single spot

identical in color and R_f value to that produced by an authentic sample of 2,3,4-tri-O-methyl-D-glucose; (c) treatment of the sugar derivative with aniline gave in good yield a crystalline product melting at 127–128° C. which showed no depression in melting point on admixture with an authentic sample of 2,3,4-tri-O-methyl-D-glucose anilide.*

The sirupy di-O-methyl hexose was identified as 3,4-di-O-methyl-D-fructose on the following evidence: (a) the specific rotation of our compound, $[\alpha]_D^{24}$ −58.5° (c = 2.0, equilibrium value in water), was in good agreement with previously reported values (9, 13); (b) a paper chromatogram of the compound showed a single spot of the color characteristic of a ketose and with R_{TG} value in agreement with the recorded value (8); (c) periodate oxidation of the sugar derivative consumed 1.8 moles of periodate and produced 1.53 moles of formaldehyde. Although the theoretical behavior of 3,4-di-O-methyl-D-fructose toward periodate required values of 2.0 and 2.0 moles respectively, this sugar derivative has been reported to give low yields of formaldehyde of the order of 1.5 moles (4) under the same conditions.

The isolation and identification of the partially substituted hexose units established the structure of the penta-O-methyl sucrose as the 2,3,3′,4,4′-penta-O-methyl derivative (Ia). The structures of the tri-O-trityl sucrose and the tri-O-trityl-penta-O-acetyl sucrose could then be designated as Ib and Ic respectively. The trityl groups therefore occupied the three primary hydroxyl groups of the sucrose molecule and it followed that the O-acetyl group at C_4 of the glucose moiety had actually migrated to C_6 during the synthesis of 1′,4,6′-tri-O-methyl sucrose (14).
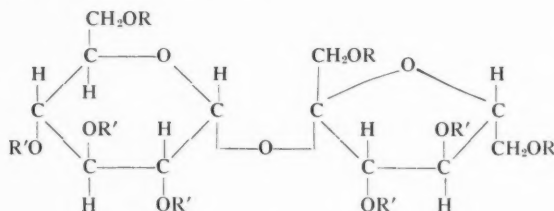

I

(a)   R = H, R′ = CH₃
(b)   R = C(C₆H₅)₃, R′ = H
(c)   R = C(C₆H₅)₃, R′ = COCH₃
(d)   R = H, R′ = COCH₃

The formation of cyclic ortho-acid ester has long been accepted as the intermediate step involved in acyl migration in polyols and aminoalcohols (5, 6). On this basis the migration of acetyl from C_4 to C_6 in the glucopyranose unit of the penta-O-acetyl sucrose (Id) involved a transition state in which a m-dioxane ring was fused to the pyranose ring at C_4 and C_5 (10). The well-established (15) preference for the trans-two chair conformation in such fused-ring systems suggested that the transition state had conformation II. This conformation of the glucose moiety was identical with that in crystalline sucrose as established by Beevers and co-workers (2, 3) from X-ray diffraction studies. The preference for the same conformation in weakly alkaline solutions of other poly-O-acyl-D-glucopyranose derivatives would be consistent with the facile C_4 to C_6 acyl migrations which have been reported (16). The assignment of the equatorial and axial positions on the m-dioxane ring to the methyl and hydroxyl groups of the orthoester could not be

*The authors wish to thank Dr. G. G. S. Dutton for a sample of 2,3,4-tri-O-methyl-D-glucose anilide.
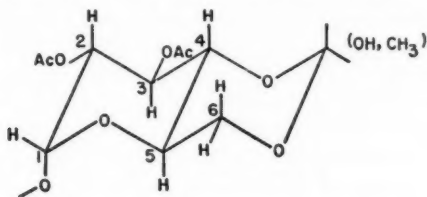
II

made from examination of the molecular models. The relative non-bonded interactions of axial methyl and hydroxyl substituents on cyclohexane rings have not been assessed (1).

EXPERIMENTAL

Paper chromatograms were prepared with the following solvent systems: (A) butanol: ethanol:water, 5:1:4; (B) methyl ethyl ketone:water azeotrope and p-anisidine spray reagent. Fructose derivatives, including sucrose, were distinguished from glucose derivatives by heating the developed and sprayed chromatograms for 1.5 minutes, which caused the preferential development of the yellow, U.V.-fluorescent ketose spots; heating for the usual 10 minutes caused the appearance of spots for both glucose and fructose derivatives (11). All melting points were corrected.

Tri-O-trityl Sucrose Tetrahydrate

To a solution of 10.0 g. of tri-O-trityl-penta-O-acetyl sucrose (14) in 25 ml. of anhydrous tetrahydrofuran were added 100 ml. of anhydrous methanol and 5 ml. of 0.1 N sodium methoxide solution. The solution was heated to reflux for 10 minutes, kept at room temperature overnight, and then evaporated to dryness under reduced pressure. The residue was taken up in ethyl acetate and washed with water; evaporation of the organic layer yielded a colorless glass (8.6 g., 103% yield calculated as anhydrous tri-O-trityl sucrose) which was ground to a fine white powder. The product softened at 125–130° C. and had $[\alpha]_D^{22}$ +14.7° (c = 3.3 in chloroform). Analysis: Calc. for $C_{69}H_{64}O_{11}$: trityl, 68.3% (tetrahydrate, 63.9%; pentahydrate, 63.0%); mol. wt. 1068. Found: trityl, 63.6, 63.5%; mol. wt. 950 (Rast). The compound was soluble in methanol and ethanol, insoluble in water and petroleum ether, and reduced Fehling's solution only after acid hydrolysis. When left standing for more than a year samples in various solvents failed to crystallize.

Acetylation of 71 mg. of the powdered glass with pyridine (2 ml.) and acetic anhydride (1 ml.) for 24 hours at room temperature and crystallization of the product from chloroform–methanol yielded 66 mg. (83%) of tri-O-trityl-penta-O-acetyl sucrose, m.p. 233–234° C., not depressed on admixture with an authentic specimen.

Methylation of Tri-O-trityl Sucrose

Tri-O-trityl sucrose tetrahydrate, 8.6 g., was dissolved in 50 ml. of methyl iodide and treated with 10 g. of silver oxide and 15 g. of Drierite at reflux temperature for 24 hours. The mixture was then filtered, the solids were washed with chloroform, and the combined filtrate and washings were evaporated to yield a colorless glass. The glass was methylated a second time and a sample of the colorless product was then hydrolyzed and detritylated by heating for 3 hours on the steam bath in aqueous acetic acid. A paper chromatogram of the hydrolyzate indicated it to be a complex mixture containing

D-fructose, mono-O-methyl-D-fructose, di-O-methyl-D-fructose, di-O-methyl-D-glucose, and tri-O-methyl-D-glucose. The spots (Solvent A) were respectively faint, yellow, R_f 0.13; distinct, yellow, R_f 0.28; distinct, yellow, R_f 0.51 (probably di-O-methyl-D-fructose and di-O-methyl-D-glucose); distinct, red-brown, R_f 0.74.

The glassy product was remethylated a further nine times by essentially the same procedure and a sample of the methylated material was hydrolyzed and examined on a paper chromatogram after each treatment. D-Fructose and di-O-methyl-D-glucose were absent after five methylations but a faint spot for mono-O-methyl-D-fructose persisted to the 10th methylation. The methoxyl content increased as follows: after seven methylations, 11.7%; after eight methylations, 12.6%; after nine methylations, 13.0%. The final product (11 methylations) was a colorless glass which was pulverized and dried *in vacuo*, $[\alpha]_D^{17}$ +32.4° (c = 6.14 in chloroform). Analysis: Calc. for $C_{74}H_{74}O_{11}$: trityl, 64.1%; OCH_3, 13.6%. Found: trityl, 63.9, 64.4%; OCH_3, 13.3, 13.4%.

Penta-O-methyl Sucrose

In a preliminary experiment 1 g. of methylated tri-O-trityl sucrose was dissolved in 25 ml. of glacial acetic acid, 1 ml. of water was added, and the solution was refluxed for 30 minutes, then evaporated under reduced pressure. The dried, partially crystalline residue was extracted with cold water and the filtered extract was evaporated to give a colorless sirup, 368 mg. (102% yield calculated as penta-O-methyl sucrose), $[\alpha]_D^{25}$ +28.3° (c = 7.36 in ethanol). Paper chromatography indicated that the sirup was a mixture of mono-O-methyl-D-fructose, 3,4,-di-O-methyl-D-fructose, 2,3,4-tri-O-methyl-D-glucose, tetra-O-methyl sucrose, and penta-O-methyl sucrose. The spots (Solvent A) were respectively faint, yellow, R_f 0.29 (R_{TG} 0.35); distinct, yellow, R_f 0.51 (R_{TG} 0.61); distinct, red-brown, R_f 0.71 (R_{TG} 0.85); faint, yellow, R_f 0.61 (R_{TG} 0.73); very distinct, yellow, R_f 0.77 (R_{TG} 0.93). The previously reported R_{TG} values for 2,3,4-tri-O-methyl-D-glucose and 3,4-di-O-methyl-D-fructose were 0.85 and 0.61 respectively in this solvent system (8). Heating a developed and sprayed chromatogram for 1.5 minutes produced only one ketose spot of R_f 0.75 (R_{TG} 0.91) which probably represented the penta-O-methyl sucrose and indicated its presence in high concentration.

Methylated tri-O-trityl sucrose, 2.28 g., was dissolved in 50 ml. of glacial acetic acid, 1 ml. of water was added, and the solution was heated on the steam bath under a reflux condenser. The apparent specific rotation of the solution, measured at room temperature, was +48.8°, +38°, +35°, +28.2°, +24.2°, +22.0°, and +19.8° after 0, 5, 10, 20, 30, 40, and 50 minutes respectively. The solution was then evaporated as rapidly as possible under reduced pressure and at a bath temperature below 50° C. and the partly crystalline residue was dried *in vacuo* over sodium hydroxide pellets. Extraction of the residue with cold water and evaporation of the solvent yielded a colorless sirup (700 mg., 85% calculated as penta-O-methyl sucrose), which was dissolved in 2 ml. of Solvent B and run onto a 50×2.6 cm. diam. column of cellulose. The chromatogram was developed with the same solvent and fractions of approximately 10 ml. were collected over 5-minute intervals and examined in the polarimeter and by paper chromatography. The bulk of the penta-O-methyl sucrose was found in four fractions which were combined, concentrated, and rechromatographed by the same procedure. Pure penta-O-methyl sucrose, 153 mg. (18.5% yield), was recovered from three fractions of the final eluate as a colorless viscous sirup, $[\alpha]_D^{23}$ +64.3° (c = 1.46 in water). Analysis: Calc. for $C_{17}H_{32}O_{11}$: OCH_3, 37.6%. Found: OCH_3, 37.7, 37.2%. The product reduced Fehling's solution only after acid hydrolysis.

Acid Hydrolysis of the Penta-O-methyl Sucrose

Penta-O-methyl sucrose, 146 mg., was dissolved in 10 ml. of 0.05 N sulphuric acid and the solution was heated on the steam bath for 2 hours. The hydrolyzate was neutralized with solid barium carbonate, filtered, and evaporated to dryness and the residue was extracted with acetone. The sirup recovered by evaporation of the acetone extract was chromatographed on a cellulose column with Solvent B to yield on evaporation of the appropriate fractions 70 mg. of a tri-O-methyl hexose and 55 mg. of a di-O-methyl hexose.

The tri-O-methyl hexose was a colorless, viscous sirup, $[\alpha]_D^{24}$ +70.6° (c = 3.26 in water, equilibrium value). Analysis: Calc. for $C_9H_{18}O_6$: OCH_3, 41.8%. Found: OCH_3, 41.1, 41.6%. Paper chromatograms of the compound revealed a single spot identical in color and R_f value to that obtained with authentic 2,3,4-tri-O-methyl-D-glucose using both Solvents A and B; red-brown spots were obtained with R_f values of 0.71 and 0.52 respectively. A sample of the tri-O-methyl hexose, 36 mg., was refluxed with 70 mg. of aniline and 2 ml. of absolute ethanol for 6 hours. The yellow sirup, 48 mg., was recovered by evaporation of the volatile components under reduced pressure, and crystallized in fine colorless needles upon seeding with 2,3,4-tri-O-methyl-D-glucose anilide. After three recrystallizations from ether – petroleum ether the derivative melted at 127–128° C. and the melting point was not depressed by admixture with an authentic specimen of 2,3,4-tri-O-methyl-D-glucose anilide.

The di-O-methyl hexose was a colorless, viscous liquid, $[\alpha]_D^{24}$ −58.5° (c = 2.0 in water, equilibrium value). Analysis: Calc. for $C_8H_{16}O_6$: OCH_3, 29.8%. Found: OCH_3, 29.5, 29.6%. A paper chromatogram of the compound prepared with Solvent A showed a single, bright yellow, U.V.-fluorescent spot of R_f 0.51 (R_{TG} 0.61). A 20.8 mg. sample of the compound was oxidized with 20 ml. of 0.02 M sodium metaperiodate at room temperature. The consumption of periodate after 6 hours was 1.5 moles; after 24 hours, 1.7 moles; after 48 hours, 1.8 moles. In 48 hours, 1.53 moles of formaldehyde was produced as determined by the formation of the dimedone complex which melted at 186–188° C.

ACKNOWLEDGMENT

REFERENCES

1. ANGYAL, S. J. and McHUGH, D. J. Chemistry & Industry, 1147 (1956).
2. BEEVERS, C. A. and COCHRAN, W. Proc. Roy. Soc. A, **190**, 257 (1947).
3. BEEVERS, C. A., McDONALD, T. R. R., ROBERTSON, J. H., and STERN, F. Acta Cryst. **5**, 689 (1952).
4. BELL, D. J., PALMER, A., and JONES, A. T. J. Chem. Soc. 1536 (1949).
5. CRAM, D. J. *In* Steric effects in organic chemistry. *Edited by* M. S. Newman. John Wiley & Sons, Inc., New York. 1956. p. 290 *et seq.*
6. DOERSCHUK, A. P. J. Am. Chem. Soc. **74**, 4202 (1952).
7. GREVILLE, G. D. and NORTHCOTE, D. H. J. Chem. Soc. 1945 (1952).
8. HIRST, E. L. and JONES, J. K. N. Discussions Faraday Soc. **7**, 268 (1949).
9. HIRST, E. L., MITCHELL, W. E. A., PERCIVAL, E. E., and PERCIVAL, E. G. V. J. Chem. Soc. 3170 (1953).
10. HIRST, E. L. and PEAT, S. Ann. Repts. Chem. Soc. **31**, 172 (1934).
11. HOUGH, L., JONES, J. K. N., and WADMAN, W. H. J. Chem. Soc. 1702 (1950).
12. IRVINE, J. C. and OLDHAM, J. W. H. J. Chem. Soc. **119**, 1744 (1921).
13. McDONALD, E. J. and JACKSON, R. F. J. Research Natl. Bur. Standards, **24**, 181 (1940).
14. McKEOWN, G. G., SERENIUS, R. S. E., and HAYWARD, L. D. Can. J. Chem. **35**, 28 (1957).
15. MILLS, J. A. *In* Advances in carbohydrate chemistry. Vol. 10. *Edited by* M. L. Wolfrom and R. S. Tipson. Academic Press, Inc., New York. 1955.
16. SUGIHARA, J. M. *In* Advances in carbohydrate chemistry. Vol. 8. *Edited by* C. S. Hudson and M. L. Wolfrom. Academic Press, Inc., New York. 1953.

THE ACTIVATION ENERGIES OF PHOTOCONDUCTION FOR SOME AROMATIC HYDROCARBONS[1]

J. KOMMANDEUR,[2] G. J. KORINEK,[2] AND W. G. SCHNEIDER

ABSTRACT

The variation of the photocurrent with temperature is found to obey the relation $i = i_0 e^{-E/RT}$ in naphthalene, stilbene, diphenyl, terphenyl, β-methylanthracene, anthracene, azulene, and pyrene. The activation energies have been measured and are found to increase in the above order. These activation energies show no apparent correlation with the corresponding activation energy of semiconduction, and it is suggested they are associated with the charge carrier transport process.

INTRODUCTION

In a series of papers from this laboratory (1, 2) an investigation of the photoconduction of anthracene has been reported. It was found that the temperature dependence of the photoconductivity follows the relation:

$$[1] \qquad i = i_0 e^{-E/RT} \qquad \text{where } E = 4.0 \text{ kcal.}$$

The magnitude of this value suggests that the temperature effect is not associated with the optical creation of charge-carriers but rather with the transport process of carrier migration. In order to obtain a better understanding of carrier migration in the photoconducting process, it was decided to investigate this property in a number of aromatic compounds which were found to exhibit photoconduction. The following compounds were studied: naphthalene, stilbene, diphenyl, terphenyl, β-methylanthracene, anthracene, azulene, pyrene. The photoconduction of some of these compounds has also recently been reported by Morris and Lyons (6).

EXPERIMENTAL

All substances used were purified by chromatography through alumina and subsequent recrystallization from petroleum ether. The purification was carried out in the dark.

In the case of anthracene, β-methylanthracene, azulene, and pyrene, sublimation flakes were used. These were grown in an atmosphere of CO_2, which has no influence on the photoconduction of anthracene (11). Reasonably large sublimation flakes of a thickness of 1–10 μ could be grown. Single crystals of naphthalene, diphenyl, and anthracene were kindly grown for us by Dr. F. R. Lipsett in a Bridgeman furnace (5), while single crystals of terphenyl, stilbene, and anthracene were obtained from the Harshaw Chemical Company. For anthracene the three types of crystals gave the same value of the activation energy.

Hanovia silver paste and aquadag electrodes in a surface arrangement were used (2) and gave identical results. For low temperature measurements silver paste is slightly more convenient to use because of its flexibility. Because of the large effects produced by oxygen and other gases on the photoconduction of anthracene employed as a surface cell (1, 11) it was considered very important to use single crystals rather than polycrystalline material, which is difficult to outgas. In the work reported here all measurements have

been made wherever possible on outgassed single crystals, in an inert atmosphere of hydrogen.

The d-c. measurements were carried out in a well-shielded glass cell with a silica window, which could be submerged in different low temperature baths (see Fig. 1). Measurements were taken at temperatures ranging from 210° K. to 300° K. The measurements could not be extended to liquid air temperatures because of cracks that developed in both crystal and contacts. At the start of each experiment the cell was evacuated and hydrogen, which does not affect the photocurrent, was admitted to the cell to facilitate heat exchange. Ample time was allowed for the system to reach thermal equilibrium.
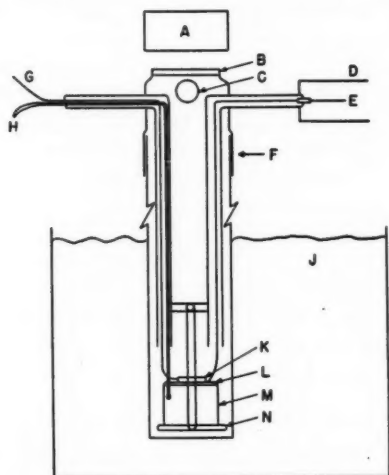
FIG. 1. Low temperature photoconductivity cell.
A—Mercury lamp	B—Silica window	C—Vacuum system connection
D—Shield	E—High impedance lead	F—Ground joint
G—Battery connection	H—Thermocouple	J—Bath
K—Crystal	L—Teflon disk	M—Copper block
N—Glass support		

The currents flowing through the crystals were in the range 10^{-8} to 10^{-15} amp. and were measured with a Keithley micromicroammeter which consisted of a vacuum tube electrometer and a set of shunt resistors of value up to 10^{12} ohms. The micromicroammeter was connected by a well-insulated lead to one electrode attached to the crystal, and the other electrode was connected to a 300 v. battery. The electric field between the electrodes of the crystal was 1000–1500 v./cm. The usual precautions were taken with insulation, screening, and the avoidance of vibration. In order to excite the photocurrent, the ultraviolet light source employed was a British Thomson Houston direct current 250 w. high pressure mercury lamp (type ME/D) operated from a stabilized (Nobatron) d-c. power source. A pyrex filter was used to cut out all light below 3200 Å to prevent photoemissive effects. For diphenyl and naphthalene, which have their spectral sensitivity at lower wavelengths, a filter cutting off at 2700 Å was employed.

RESULTS AND DISCUSSION

In all cases the results could be accurately represented by equation [1]. Fig. 2 shows the plot of log i values against $1/T$. Each line represents data of at least two independent
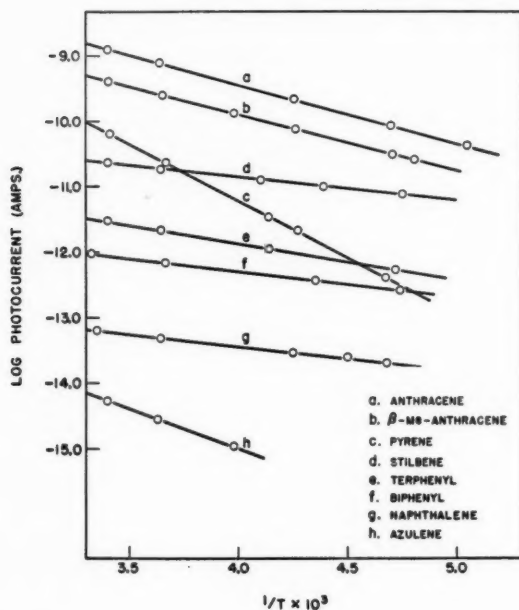
FIG. 2.

experiments on different crystals. The values of E (expressed in kcal.) evaluated from these plots are listed in Table I. They are arranged in increasing order of magnitude for the various compounds. Also shown in the table is a list of values for the activation energy for semiconductivity compiled from the literature. Considerable variation in the values reported by different authors is evident. The value quoted for the activation energy of the semiconductivity of azulene was measured by us. Because of a very low value for the dark current and other experimental difficulties, the accuracy is poor and the value should be taken as approximate.

Fig. 2 gives the order of the substances studied according to the magnitude of their photocurrent. This order is only qualitative because of different light absorption characteristics of the substances studied, different sizes of crystal and separation of electrodes. Nevertheless, the results are in fair agreement with the study of Lyons and Morris (6).

TABLE I

Compound	Activation energy	
	Photoconductivity	Semiconductivity
Naphthalene	1.8 ± 0.1	16.1 (10), 17.2 (9), 41.0 (9)
Stilbene	1.9 ± 0.1	21.1 (3)
Diphenyl	2.0 ± 0.1	
Terphenyl	2.4 ± 0.1	
β-Methylanthracene	3.9 ± 0.1	
Anthracene	4.1 ± 0.1	22.2 (8), 31.0 (4)
Azulene	5.6 ± 0.2	~ 23
Pyrene	8.1 ± 0.2	23.4 (8), 27.6 (4)

The order of substances according to the value of their photocurrent is as follows: anthracene > β-methylanthracene > pyrene > stilbene > terphenyl > biphenyl > naphthalene > azulene.

Except for azulene, the photoconduction activation energies increase with the size of the aromatic molecules. Thus a rough correlation can be made with certain electronic properties, e.g. molecular polarizability. Comparison of the photoconduction activation energies with available data for the corresponding activation energy for semiconduction (Table I, column 3) shows that there is no apparent correlation between the two. The majority of the activation energies for semiconduction seem to be in the range of 17–30 kcal. for different substances studied. These energies may well be composite and include both the energy of carrier formation and the activation energy of carrier migration. If the latter is of a much smaller order of magnitude individual differences for the different molecular crystals will be obscured in the over-all activation energy of semiconduction.

It is postulated that the activation energy could arise from the existence of shallow traps or small potential energy barriers hindering carrier transport in the crystal. One way such barriers could arise is by polarization of the molecules of the lattice by the charge carriers. A correlation with the molecular polarizability should then be expected. Since in general the polarizability of aromatic molecules is relatively high, a "reaction" field will be induced in the molecules in the immediate vicinity of the charged carrier. The latter is thus, in effect, weakly trapped, the trap depth being proportional to the measured activation energy of photoconduction (7). The anomalous position of azulene could perhaps be attributed to the polar nature of this non-alternant hydrocarbon.

REFERENCES

1. CHYNOWETH, A. G. and SCHNEIDER, W. G.   J. Chem. Phys. **22**, 1021 (1954).
2. COMPTON, D. M. J., SCHNEIDER, W. G., and WADDINGTON, T. C.   J. Chem. Phys. (In press).
3. DREHFEHL, G. and HENKEL, H. J.   Z. physik. Chem. **206**, 93 (1956).
4. INOKUCHI, H.   Bull. Chem. Soc. Japan, **29**, 131 (1956).
5. LIPSETT, F. R.   Can. J. Phys. **35**, 284 (1957).
6. LYONS, L. E. and MORRIS, G. C.   Proc. Phys. Soc. (London), B, **69**, 1162 (1956).
7. MOTT, N. F. and GURNEY, R. W.   Electronic processes in ionic crystals. Oxford University Press, London. 1950. p. 88.
8. NORTHRUP, D. C. and SIMPSON, O.   Proc. Roy. Soc. A, **234**, 124 (1956).
9. PICK, H. and WISSMAN, W.   Z. Physik, **138**, 436 (1954).
10. RIEHL, N. V.   Zhur. Fiz. Khim. **29**, 959 (1955).
11. SCHNEIDER, W. G. and WADDINGTON, T. C.   J. Chem. Phys. **25**, 358 (1956).

THE ULTRAVIOLET ABSORPTION SPECTRA OF THE FERRIC ION AND ITS FIRST HYDROLYSIS PRODUCT IN AQUEOUS SOLUTIONS[1]

R. C. TURNER AND KATHLEEN E. MILES

ABSTRACT

The absorption spectra of the ferric ion and its first hydrolysis product in an aqueous solution of perchloric acid was determined. The Fe^{3+} ion has two absorption bands, one with a maximum at 240 mμ and another which extends into the region below 200 mμ. The $FeOH^{2+}$ ion also has two absorption bands, the maxima of which occur at 300 mμ and 205 mμ. A figure shows the magnitude of the absorption of each of these ions from 200 to 350 mμ.

INTRODUCTION

The equilibrium constant for the formation of the first hydrolysis product of ferric ion in an aqueous solution has been determined in a number of laboratories (1, 2, 3, 4, 5, 6). Some of this work was done by means of ultraviolet absorption spectrophotometry so that there is a limited amount of information available concerning the absorption spectra of Fe^{3+} and $FeOH^{2+}$ in this region. The absorption band of Fe^{3+} apparently begins at about 320 mμ and has a maximum at 240 mμ. The absorption of $FeOH^{2+}$ is not as well known. Although it has one band with a maximum at about 300 mμ, there is evidence to indicate that it also absorbs at 240 mμ (3).

In work in this laboratory it was necessary to have the molar extinction coefficients of Fe^{3+} and $FeOH^{2+}$ in the ultraviolet region as well as the equilibrium constant, K_e, at relatively low ionic strengths. K_e is defined by the equation

[1] $$K_e = [FeOH^{2+}]H/[Fe^{3+}]$$

where H represents the hydrogen ion activity and the square brackets denote concentrations in moles per liter.

It has been indicated (4, 6) that with iron concentrations of the order of 10^{-4} molar and hydrogen ion concentrations greater than 10^{-3} molar only one hydrolysis reaction need be considered, i.e.,

$$Fe^{3+} + H_2O \rightleftharpoons FeOH^{2+} + H^+.$$

Consequently, K_e, as well as e_1 and e_2, the molar extinction coefficients of Fe^{3+} and $FeOH^{2+}$ respectively, can be calculated (4) at each wavelength by application of experimental results to the equation

[2] $$HE+K_eE = He_1+K_ee_2,$$

where E is the apparent molar extinction coefficient defined by

$$E = O.D./dFe_0,$$

where O.D. is the optical density at a particular wavelength, d is the length of the light path in cm., and Fe_0 is the total iron concentration in moles per liter.

EXPERIMENTAL

A stock solution of iron was prepared by dissolving solid $Fe(ClO_4)_3$ in a perchloric acid solution. The total iron concentration was determined by analysis.[2] Solutions of

the desired iron concentration were prepared by diluting aliquots of the stock solution with double-distilled water. The pH and the ionic strength were adjusted by the addition of $HClO_4$ and $NaClO_4$.

The diluted solutions were placed in a temperature-controlled water bath. The optical densities were determined within 4 hours of dilution. Preliminary work had shown that there was no measurable change in the optical densities during this time.

The optical densities were determined by means of a Beckman Model DU spectrophotometer equipped with a photomultiplier. The temperature of the cell compartment was controlled by pumping water from the bath through thermospacers supplied with the instrument. Matched fused silica cells, which afforded a light path of 1 cm., were employed.

A wavelength calibration of the instrument was made with a mercury arc lamp at the beginning of the work. During the experiments a periodic check was made with a standard K_2CrO_4 solution prepared by dissolving 0.0400 g. per liter of K_2CrO_4 in 0.05 N KOH.

The pH of the solutions was measured on a Cambridge meter graduated in 0.02 pH units.

RESULTS

Estimation of K_e

Since equation [2] has three unknowns, three values of E at each wavelength corresponding to three known values of H were required to eliminate e_1 and e_2 to permit solving for K_e. It was realized at the outset that small errors in the experimental values for E and H would cause large errors in a calculated K_e value. Consequently a large number of experiments were made so that a mean K_e value could be calculated in which the effect of these uncontrollable errors was minimized.

In one set of experiments two concentrations of iron, 1.50×10^{-4} molar and 2.00×10^{-4} molar, were used with an ionic strength of 0.01. At each iron concentration three different acidities, pH 2.08, 2.38, and 2.65, were used. Each experiment was carried out in duplicate. The optical densities were recorded at 5 mμ intervals from 200 to 350 mμ at 25° C. The three curves in Fig. 1, corresponding to the three levels of acidity, represent the averages of the results obtained. They have an isosbestic point at 272 mμ and another at 225 mμ.

A K_e value was calculated at each wavelength recorded from 235 to 310 mμ, excluding those near the isosbestic point at 272 mμ. There was no statistically significant difference in the K_e values between experiments or between the values on opposite sides of the isosbestic point. There was, however, a fairly wide variation among the individual values, as illustrated by the standard deviation shown in Table I. The mean value was 3.41×10^{-3} with a standard error of 0.21×10^{-3}.

As pointed out above, the Fe^{3+} absorption band starts at about 320 mμ. Therefore, at wavelengths greater than 320 mμ, e_1 in equation [2] could be put equal to zero and thus leave only two unknowns in the equation. The absorption was weaker in this region than at shorter wavelengths. Consequently a number of experiments were made with a range of total iron concentration from 1.50 to 6.00×10^{-4} molar. Only two hydrogen ion activities were required in each experiment because only two sets of results were necessary to solve for K_e. K_e values were calculated at each of the wavelengths recorded between 320 and 350 mμ. As before, there was no statistically significant difference between experiments or between wavelengths. Table I shows that the standard deviation was
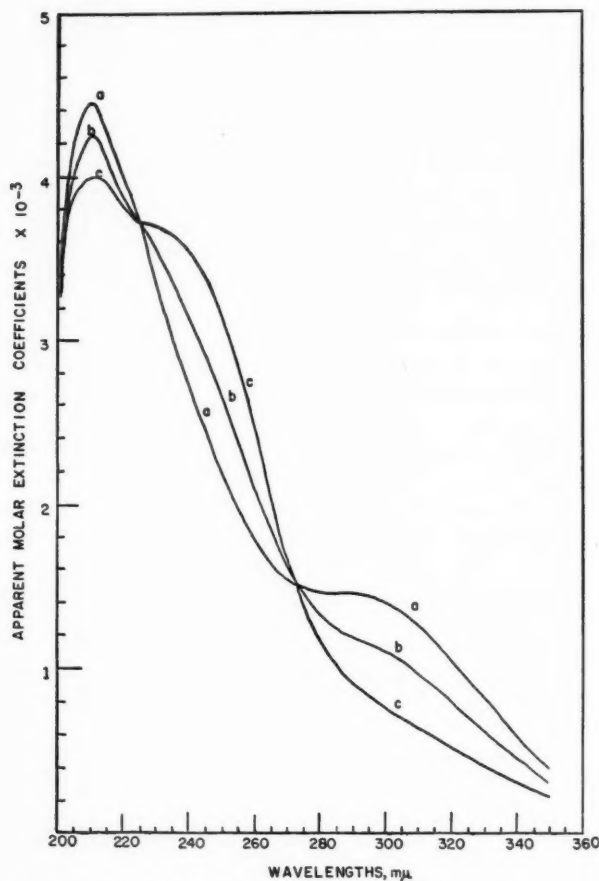
FIG. 1. Effect of hydrogen ion activity on the absorbance of dilute iron perchlorate solutions with an ionic strength of 0.01 at 25° C. Hydrogen ion activities: a, 2.24×10^{-3}; b, 4.17×10^{-3}; c, 8.41×10^{-2}.

TABLE I

STATISTICAL INFORMATION CONCERNING THE K_e VALUE CALCULATED AT 25° C. WITH SOLUTIONS OF 0.01 IONIC STRENGTH

Iron conc. $\times 10^4$, moles/l.	Wavelengths	No. of values	Standard deviation $\times 10^3$	Mean $\times 10^3$	Standard error of mean $\times 10^3$
1.50 and 2.00	235 to 310	42	1.41	3.41	0.21
1.50 to 6.00	320 to 350	120	0.86	3.40	0.08

smaller in these experiments than in the previous ones. The mean K_e value thus determined was 3.40×10^{-3} with a standard error of 0.08×10^{-3}.

Estimation of the Absorption Spectra of Fe^{3+} *and* $FeOH^{2+}$

With the K_e value of 3.40×10^{-3}, the e_1 and e_2 values were calculated at each of the wavelengths recorded from 220 to 350 mμ using equation [2]. For these calculations

the equation contained only the two unknowns, e_1 and e_2, but there was a characteristic value for each at every wavelength. The results from seven independent experiments were used and the means for each wavelength calculated. The results are presented in
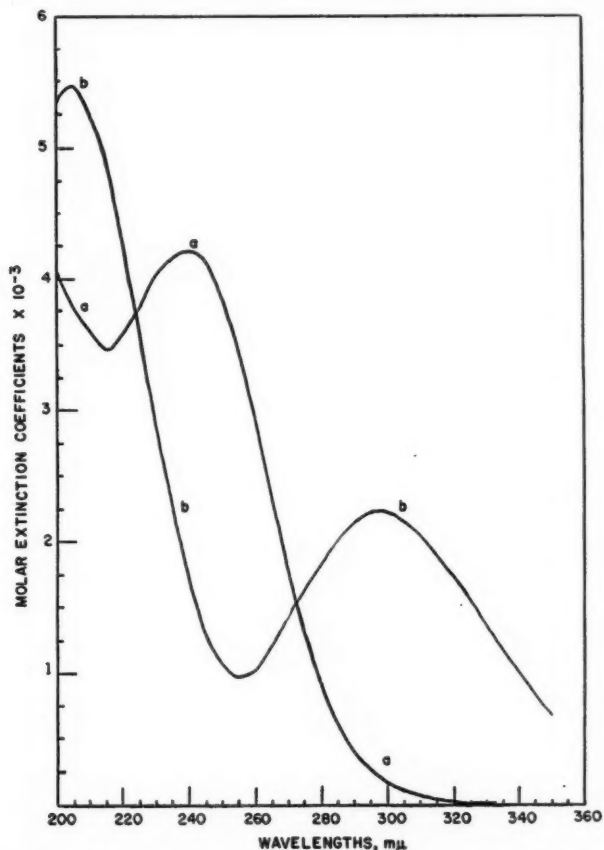

FIG. 2. The absorption spectra of the Fe^{3+} and $FeOH^{2+}$ ions. a, Fe^{3+}; b, $FeOH^{2+}$.

Fig. 2. From these curves it can be seen that Fe^{3+} has an absorption band starting at about 320 mμ with a maximum at 240 mμ. This agrees with published reports. The $FeOH^{2+}$ absorption band with a maximum near 300 mμ is fairly symmetrical. In addition, there is a second band for $FeOH^{2+}$ apparently starting somewhere near 260 mμ and increasing in height continuously to 220 mμ. The boundary of the Fe^{3+} band crosses that of one of the $FeOH^{2+}$ bands at 225 mμ and of the other at 272 mμ, which accounts for the two isosbestic points in Fig. 1.

The stray energy transmitted by the Beckman DU in the region between 220 mμ and 200 mμ was of such a magnitude as to make unreliable all the optical densities recorded below 220 mμ. In order to get experimental results which could be used to calculate the absorption of the two iron ions in this region, a Cary recording spectrophotometer

with a double monochromator[3] was used for some of the solutions. Recordings were made from 200 mμ to 300 mμ and the results of two of these experiments are shown in Fig. 3, together with the results obtained for the same solutions with the Beckman DU.
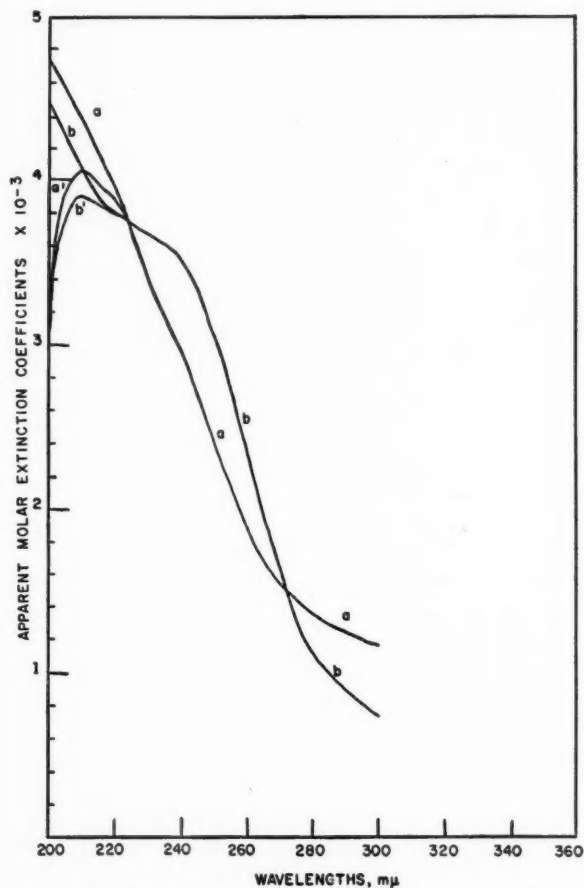

FIG. 3.   Absorbancy of dilute iron perchlorate solutions measured with a Beckman DU spectrophotometer and a Cary spectrophotometer.

a, pH 2.43, measured with a Cary instrument.   a', pH 2.43, measured with a Beckman instrument.
b, pH 2.08, measured with a Cary instrument.   b', pH 2.08, measured with a Beckman instrument.

From 300 mμ to 220 mμ the two instruments gave the same results but, as shown in the figure, the results from the Beckman instrument showed a maximum at about 210 mμ (see also the other figures) whereas in fact there was an increase in absorption to 200 mμ. The absorption of Fe^{3+} and $FeOH^{2+}$ between 200 mμ and 220 mμ shown in Fig. 2 was calculated from the results obtained with the Cary instrument. They showed a second absorption band for Fe^{3+}, only a small part of which was in the region above 200 mμ. The band for $FeOH^{2+}$ in this region has a maximum at 205 mμ.

[3]*Made available through the courtesy of the Division of Applied Biology, National Research Council, Ottawa.*

There was a possibility that, since the absorption bands were calculated on the basis of the assumptions involved in equation [2], the results were fortuitous, particularly since all the work was done at the same temperature and ionic strength. Experiments were therefore made at 15° and 35° C. with an ionic strength of 0.01, and at 25° C. at three different ionic strengths. The results of experiments in which the temperature was
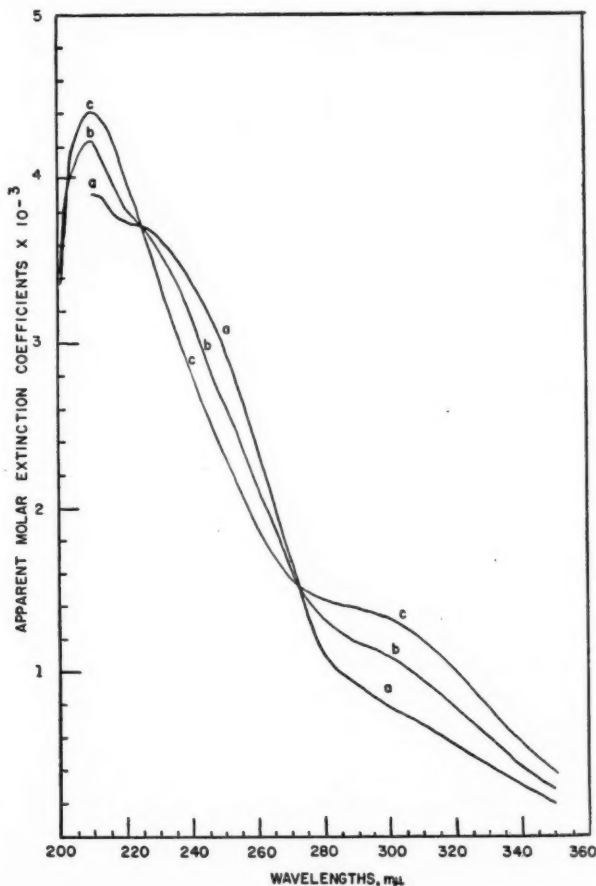

FIG. 4. Effect of temperature on dilute iron perchlorate solution with a hydrogen ion activity of 4.17×10^{-3} M. Temperatures at which the experiments were carried out: a, 15° C.; b, 25° C.; c, 35° C.

varied but the ionic strength, acidity, and total iron concentration were kept constant are presented in Fig. 4. They show that, although temperature had a marked effect on absorption, the two isosbestic points were identical with those in Fig. 1 where only the acidity was varied. From optical densities recorded at different ionic strengths and temperatures, K_c values were calculated at a number of wavelengths using the values for e_1 and e_2 in Fig. 2. The results presented in Table II show that the calculated values were fairly consistent regardless of wavelength for a given set of conditions. It seems

TABLE II

K_c VALUES CALCULATED FROM THE e_1 AND e_2 VALUES IN FIG. 2 FROM EXPERI-
MENTS CONDUCTED AT DIFFERENT IONIC STRENGTHS AND DIFFERENT
TEMPERATURES

Wavelength, mμ	T, ° C. = u^* =	$K_c \times 10^3$				
		35 0.01	15 0.01	25 0.01	25 0.004	25 0.02
240		5.0	1.9	3.4	3.9	3.2
245		5.2	1.9	3.5	3.9	3.3
250		5.2	2.0	3.5	3.9	3.2
255		5.1	2.0	3.4	3.9	3.3
260		5.0	2.0	3.5	3.9	3.2
265		5.0	2.0	3.5	4.0	3.2
285		5.2	2.0	3.4	3.9	3.2
290		5.2	1.9	3.4	3.8	3.1
295		5.3	1.9	3.4	3.9	3.2
300		5.3	1.9	3.4	3.8	3.2
305		5.3	1.9	3.4	3.9	3.2
310		5.3	1.9	3.4	3.9	3.2

*u designates ionic strength.

therefore that the absorption bands shown in Fig. 2 are not simply the result of forcing an assumption onto experimental results but are the legitimate bands for Fe^{3+} and $FeOH^{2+}$.

DISCUSSION

Hedstrom (1) using an electrochemical method and Mulay and Selwood (3) using magnetic susceptibilities showed that dimerization of $FeOH^{2+}$ occurs at sufficiently high iron concentrations. Their equilibrium constants for the formation of the dimer show that, with the concentrations used in the present investigation, dimerization is negligible. There is, however, a contradiction between the conclusions of Mulay and Selwood and those presented here with respect to the absorption of $FeOH^{2+}$ at 240 mμ. Whereas in the present work a molar extinction coefficient of 1730 was found for $FeOH^{2+}$ at 240 mμ, Mulay and Selwood reported that this value should be approximately 46,000.

Mulay and Selwood's results can, however, be interpreted in a way that is consistent with the results presented from this investigation. In this laboratory, a K_c value for a dilute iron solution, 3.0 molar to $NaClO_4$, having a measured pH of about 1.7 was determined to be 5×10^{-3}. This value and the e_1 and e_2 values from Fig. 1 were applied to the spectrophotometric data reported by Mulay and Selwood for a solution of similar composition, together with their K value for the formation of the dimer, to obtain an absorption curve for the dimer. This curve could not be considered quantitative but showed that the dimer absorbs in some respects similarly to the monomer, $FeOH^{2+}$. It has two absorption bands, one with a maximum at about 335 mμ and another which starts in the vicinity of 310 mμ and increases in height at least up to 240 mμ where it is considerably greater than that for Fe^{3+} for a given concentration of iron. The increased absorption at 240 mμ with decreasing acidities found by Mulay and Selwood may therefore be accounted for by the dimer formed, rather than by attributing a molar extinction coefficient of 46,000 to $FeOH^{2+}$ at this wavelength.

The K_c value of 5×10^{-3} for the formation of $FeOH^{2+}$ cannot be compared with that reported by Hedstrom (1). In Hedstrom's work the hydrogen ion concentration was used to calculate the equilibrium constant, whereas in this work the activity of the hydrogen

ion, calculated from a measured pH value, was used. Furthermore, a pH value obtained by inserting a saturated KCl bridge into a concentrated perchlorate solution must be in error from a liquid junction potential, aside from other considerations. It was for this reason that the K_e used in the experiments to estimate the absorption characteristics of the dimer from Mulay and Selwood's results was determined at a pH value which corresponded to that of their solution.

ACKNOWLEDGMENT

REFERENCES

1. HEDSTROM, B. O. A. Arkiv Kemi, **6**, 1 (1955).
2. MILBURN, R. M. and VOSBURG, W. C. J. Am. Chem. Soc. **77**, 1352 (1955).
3. MULAY, L. N. and SELWOOD, P. W. J. Am. Chem. Soc. **77**, 2693 (1955).
4. OLSON, A. R. and SIMONSON, T. R. J. Chem. Phys. **17**, 1322 (1949).
5. RABINOWITCH, E. and STOCKMAYER, W. H. J. Am. Chem. Soc. **64**, 335 (1942).
6. SIDDALL, J. H. and VOSBURG, W. C. J. Am. Chem. Soc. **73**, 4270 (1951).

CONSTITUTION OF AN ARABOGALACTAN FROM JACK PINE (PINUS BANKSIANA LAMB)[1]

C. T. Bishop

ABSTRACT

A water soluble arabogalactan isolated from jack pine was shown to have a molar ratio of arabinose to galactose of 1:13, and a number average degree of polymerization of 53 ± 3. Fractionation data and electrophoresis indicated that the arabogalactan was homogeneous. Hydrolysis of the methyl ether of the polysaccharide yielded 2,3,5-tri-O-methyl-L-arabinose (4 moles); 2,3,4,6-tetra-O-methyl-D-galactose (12–13 moles); 2,3,4-tri-O-methyl-D-galactose (19 moles); 2,6-di-O-methyl-D-galactose (1 mole); and 2,4-di-O-methyl-D-galactose (14 moles). Some features of the structure of the arabogalactan are discussed on the basis of these results.

Polysaccharides composed of galactose and arabinose units have been found in various species of larches (10, 20, 22, 32, 33), in black spruce (*Picea mariana*) (3), Southern yellow pine (*Pinus palustris*) (7), and Jeffrey pine (*Pinus jeffreyi*) (25). However, the only attempts to study structures in this class of polysaccharides have been made by White (28, 29, 30, 31) on the arabogalactan from *Larix occidentalis*, by Campbell *et al.* (4) on the E-galactan of *Larix decidua*, and by Wadman *et al.* (25) on the arabogalactan from *Pinus jeffreyi*. In all of these investigations there were differences of opinion as to whether the polysaccharide studied was one polysaccharide, of the arabogalactan or galactan class, or whether there was a mixture of a galactan with an arabogalactan or an araban. Thus Peterson *et al.* (21) found differences in the properties of fractions obtained by fractional precipitation of an arabogalactan and its derivatives from *Larix occidentalis*, indicating that the polysaccharide was heterogeneous. However, White (28, 29, 30, 31) interpreted his results, on an arabogalactan from the same source, as though the polysaccharide was homogeneous and reported no indications of heterogeneity. On the other hand, Campbell *et al.* (4) showed that the arabogalactan from *Larix decidua* was heterogeneous, being a mixture of galactan and arabogalactan or araban, and felt that White's results could also be interpreted on this basis. Wadman *et al.* (25) interpreted their results as indicating that the arabogalactan of *Pinus jeffreyi* was a single polysaccharide but did not exclude the possibility that it was a mixture of a galactan and an arabogalactan.

The present report describes the isolation and structural investigation of an arabogalactan from jack pine (*Pinus banksiana* Lamb). All the methods now available for testing heterogeneity in polysaccharides indicated that this material was not a mixture and the results of the structural studies are best interpreted on that basis. Therefore, it is highly probable that the arabogalactan from jack pine consists of arabinose and galactose units joined together, in the manner described below, in one polysaccharide.

The crude polysaccharide was removed from extractive-free jack pine wood by extraction with water at room temperature and was purified by fractional precipitation from water by ethanol (Table I).

This purification procedure yielded a polysaccharide material (Fractions 2 and 3) making up 67% of the crude polysaccharides and containing only arabinose and galactose units. The purified arabogalactan had a specific rotation of $[\alpha]_D^{23} +6°\pm2°$ and a molar ratio of arabinose to galactose of 1:13. This specific rotation is only slightly lower than

TABLE I

FRACTIONATION OF WATER-SOLUBLE POLYSACCHARIDES FROM JACK PINE

Fraction	Ethanol concentration (% by volume)	Weight (g.)	$[\alpha]_D^{23}$ (c, 1.0 in 2 N NaOH)	Component sugars
1	0.0	0.114	—	—
2	52.0	3.037	$+6°\pm2°$	Galactose, arabinose
3	60.0	0.318	$+10°\pm2°$	Galactose, arabinose
4	77.0	0.201	$+4°\pm2°$	Galactose, arabinose, glucose
5	80.0	0.259	$+15°\pm2°$	Galactose, arabinose, glucose, xylose (trace)
6	90.0	0.289	$+10°\pm2°$	Galactose, arabinose, glucose, xylose
7	95.0	0.133	$+8°\pm2°$	Galactose, arabinose, glucose, xylose, rhamnose
8	Not precipitated by 95% ethanol	0.260	—	—
		4.611 g. (92.2% recovery)		

those reported for arabogalactans of the larch family, $[\alpha]_D^{20}$ $+11°$ to $+15°$ (21), and of Jeffrey pine, $[\alpha]_D^{23}$ $+17°$ (25). However the molar ratio of component monosaccharides is at considerable variance with the corresponding ratios of 1:6 for arabogalactans from larch (21, 31, 32) and 4:5 for the arabogalactan from Jeffrey pine (25).

When the data in Table I was plotted graphically (26, 27) the fractionation curve
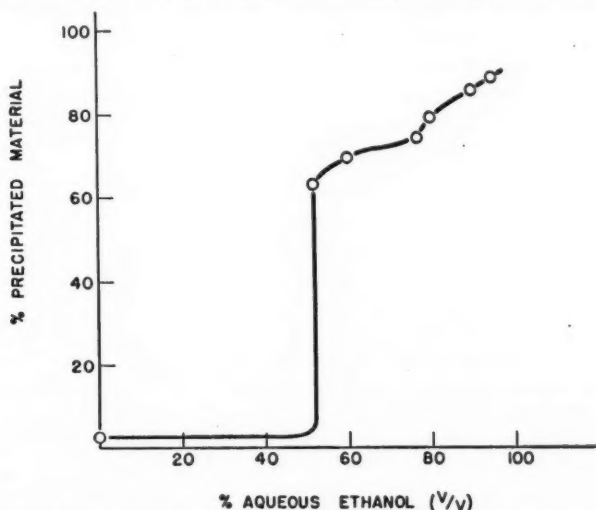

FIG. 1. Ethanol fractionation of water-soluble polysaccharide from jack pine.

shown in Fig. 1 was obtained. Such curves have proved useful as a test for homogeneity (26) or heterogeneity (27) of a polysaccharide. The shape of the curve in Fig. 1 indicated the presence of a single main component and this conclusion was substantiated by the electrophoretic pattern which showed only a single, sharp peak. No araban could be extracted from the polysaccharide by hot 75% or 65% ethanol (9).

Estimation of reducing end group in the arabogalactan gave a number average degree of polymerization of 53±3. Partial hydrolysis with dilute oxalic acid removed all of the arabinose units with very little concurrent release of galactose indicating that

arabinose was present in the furanoside form while most, if not all, of the galactose was in the pyranoside structure.

The arabogalactan was methylated and the methyl ether was hydrolyzed to give the methylated sugars listed in Table II all of which were characterized by the isolation of

TABLE II

SEPARATION OF HYDROLYSIS PRODUCTS FROM METHYLATED ARABOGALACTAN

| Fractions from Celite column	Compound	Yield (mg.)	Millimoles	$[\alpha]_D^{25}$ ($c = 1$–2% in water)
A (tubes 46–70)	2,3,5-Tri-O-methyl-L-arabinose	197	1.03	$\pm 0°$
B (tubes 71–110)	2,3,4,6-Tetra-O-methyl-D-galactose	760	3.22	$+109° \pm 2°$
C (tubes 111–129)	Impure 2,3,4-Tri-O-methyl-D-galactose	110	0.50	$+83° \pm 2°$
D (tubes 130–175)	2,3,4-Tri-O-methyl-D-galactose	994	4.5	$+110° \pm 2°$
E (tubes 185–214)	2,6-Di-O-methyl-D-galactose	47	0.23	$+80° \pm 2°$
F (tubes 215–310)	2,4-Di-O-methyl-D-galactose	703	3.38	$+86° \pm 2°$
			2811 (97% recovery)	

crystalline derivatives. These figures give the following approximate molar composition for the methylated arabogalactan:

2,3,5-tri-O-methyl-L-arabinose (4 moles),
2,3,4,6-tetra-O-methyl-D-galactose (12–13 moles),
2,3,4-tri-O-methyl-D-galactose (19 moles),
2,6-di-O-methyl-D-galactose (1 mole),
2,4-di-O-methyl-D-galactose (14 moles).

For purposes of this approximation the impure 2,3,4-tri-O-methyl-D-galactose fraction was considered only 50% pure, the impurities consisting of at least three minor components to which no structural significance was attached (see Experimental section).

The total number of moles (50–51) is in good agreement with the number average degree of polymerization (53±3) and the ratio of arabinose to galactose (4:46 or 47) is in reasonable agreement with the ratio of 1:13 found in the original polysaccharide.

On the basis of these results, certain features of the gross structure of the arabogalactan become clear. The following units must be present in the polysaccharide:
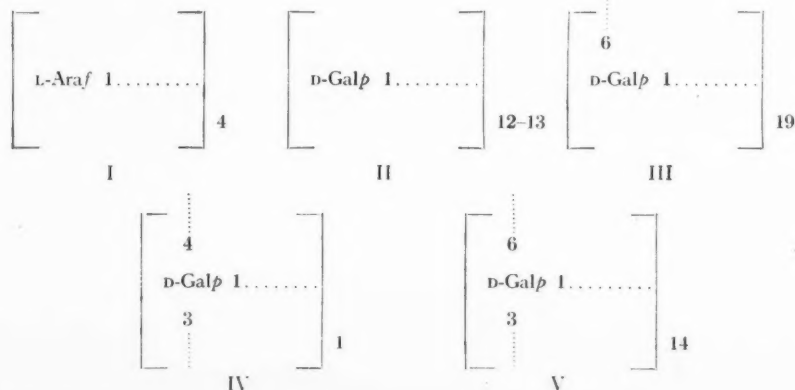
All of the arabinose was accounted for as non-reducing terminal units (I) and hence could not have arisen from an admixed araban. The large number of non-reducing terminal units, both of arabinose (I) and galactose (II), showed that the molecule had a highly branched structure, the branches occurring at positions in the galactose units as indicated by III, IV, and V. There are, of course, many ways in which these units could be joined in a polysaccharide and a unique structure cannot be deduced from the present information. However, if the unit which occurs most frequently (III) is taken as the main structural component then the arabogalactan can be visualized as a chain of $1 \rightarrow 6$ linked D-galactopyranose units terminated at the non-reducing end by an unsubstituted D-galactopyranose or L-arabofuranose residue. Through position 3 of some of the D-galactopyranose units in this chain, other $1 \rightarrow 6$ linked chains of D-galactopyranose units are attached, some of them being terminated by L-arabofuranose units. At one point in the molecule branching occurs through positions 3 and 4 of a D-galactopyranose residue instead of through 3 and 6. The number (15) of units forming branch points (IV and V) is in good agreement with the number (15–16) of non-reducing terminal units (I and II), not including the non-reducing unit which is regarded as terminating the main chain. The change in specific rotation from $[\alpha]_D^{25} -20°$ to $+50°$ when the methylated arabogalactan was hydrolyzed indicated that most of the glycosidic linkages were in the β-configuration. An arabogalactan such as that described should consume 1.3 moles of periodate per mole of anhydro-D-galactose with the formation of 0.61 moles of formic acid per mole anhydrogalactose. The actual values found (1.1 moles of periodate and 0.42 moles of formic acid) were of the right order but were numerically slightly lower than theoretical, possibly because the highly branched structure of the arabogalactan hindered the attack by periodate.

EXPERIMENTAL

Chromatographic separations were carried out using the following solvent systems (v/v ratios):

(A) pyridine:ethyl acetate:water—1:2:2 (14),
(B) ethyl acetate:acetic acid:water—3:1:3 (14),
(C) n-butanol:pyridine:water—10:3:3 (11),
(D) n-butanol:ethanol:water—40:11:19 (11),
(E) benzene:ethanol:water—169:47:15 (1),
(F) 2-butanone:water azeotrope (2).

Unsubstituted reducing sugars were detected on chromatograms by spraying first with silver nitrate in acetone then with alcoholic sodium hydroxide (24). Methylated sugars were located on the papers by p-anisidine hydrochloride spray reagent (11). Evaporations were done at 35° C. or less, melting points are corrected, and all rotations are equilibrium values unless stated otherwise.

Isolation of Polysaccharide

Bark-free logs of jack pine (*Pinus banksiana* Lamb) were planed and the planings were passed through a Wiley mill. The milled wood (4.83 kg., air-dried) was extracted exhaustively in a Soxhlet with ethanol:benzene (1:2 v/v) and then with ethanol. The extractive-free, air-dried wood (4.54 kg.) was extracted three times with water (100 ml./g.). The extractions were done successively and each one was carried out at room temperature (20–24° C.) with stirring, for 24 hours. The extraction mixture was filtered through linen cloth and the filtrate was passed through a Sharples centrifuge to remove

finely divided particles of residual wood. The centrifugate, evaporated to 1/20 of its original volume, gave a negative test (Fehling's) for reducing sugars and no sugars could be detected on heavily spotted chromatograms (solvent A). The concentrated aqueous extract was dialyzed against distilled water for 4 days. The solution of non-dialyzable material was then concentrated to $\frac{1}{4}$ its volume and freeze-dried to yield the crude, water-soluble polysaccharides as a light tan, spongy material (22.0 g., 0.49% of extractive-free wood) containing 2.3% ash and 0.6% nitrogen. A sample (50 mg.) of this crude product was heated with N hydrochloric acid (2 ml.) in a sealed tube at 97° C. for 6 hours. Paper chromatography (solvents A, B, and C) of this hydrolyzate revealed the presence of monosaccharides having the same mobilities as known samples of galactose, glucose, arabinose, xylose, and rhamnose run on the same paper strip. No uronic acids could be detected on the paper chromatograms or by electrophoresis of the hydrolyzate under conditions whereby uronic acids migrate and neutral sugars remain at the starting line (18).

Isolation of Arabogalactan

The crude polysaccharide (5.0 g.) was added to water (750 ml.) with stirring and a small amount of water-insoluble material (Fraction 1, 114 mg., 2.3%) was removed by centrifuging. The soluble polysaccharides were then fractionally precipitated from the clear, aqueous supernatant liquor by gradient addition of ethanol to the stirred solution. Ethanol concentration was increased by increments of 2% with fractions being removed successively as they appeared as distinct precipitates. Each fraction was washed once with aqueous ethanol of the same concentration that caused its precipitation and the washings were combined with the original mother liquor. The precipitates were then washed successively with absolute ethanol, ether, and petroleum ether before being dried at 0.02 mm. over anhydrous calcium chloride and paraffin. This procedure yielded Fractions 2–7 inclusive. Fraction 8 included all material that was not precipitated at an ethanol concentration of 95% and, together with Fraction 1, was not examined further. Specific rotations of the fractions were determined in 2 N sodium hydroxide because aqueous solutions, at the same concentrations, were too opaque to permit accurate readings. For qualitative determination of component sugars a sample (10 mg.) of each fraction was heated with N hydrochloric acid (1 ml.) in a sealed tube at 97° for 6 hours and the hydrolyzate was chromatographed on the same paper strip with known samples of monosaccharides. Solvents A, B, and C were used, solvent B being included to distinguish arabinose from mannose, these two sugars not being separated by the other solvent systems.

Fractionation data are summarized in Table I and the fractionation curve (26, 27) is shown in Fig. 1. These results suggested the presence of a single main component (67% of the crude polysaccharide) soluble in 51% ethanol but insoluble in 60% ethanol. The rest of the crude polysaccharides (17 g.) were fractionated in the same way, using pro-portionately larger volumes, to give further quantities of the same fractions. Quantitative estimation of component sugars (see below) showed that galactose and arabinose were present in the same amounts in Fractions 2 and 3. On the basis of this data, together with the specific rotations (Table I) and fractionation curve (Fig. 1), these two fractions were combined giving a total amount of 12.84 g. of purified arabogalactan on which all subsequent work was done. The arabogalactan, in 1% solution in 0.1 M borate, moved as a single, sharp peak on electrophoresis at 15 ma. in a Tiselius apparatus. Reducing end group estimation by hypoiodite using a phosphate buffer at pH 11.9 (5) gave a

number average degree of polymerization of 53 ± 3. Extraction of the arabogalactan with hot 75% and 65% aqueous ethanol removed only traces of material and left the arabinose content unchanged (9).

Quantitative Estimation of Component Sugars

Before combining Fractions 2 and 3, samples (20 mg.) of each were heated with N hydrochloric acid (2 ml.) in a sealed tube at 97° C. for 12 hours. The hydrolyzates were neutralized by Amberlite IR-45 resin and the component sugars were separated as bands on paper chromatograms (solvent A). The relative amounts of galactose and arabinose were then determined by measuring the area and intensity of their reaction with silver nitrate using a recording densitometer (Spinco) (17). Results of four checks on each hydrolyzate ($\pm2\%$ error) gave a molar ratio of galactose to arabinose of 13:1 for both fractions.

Partial Hydrolysis

The arabogalactan (20 mg.) was heated in a sealed tube with 0.025 N oxalic acid (2 ml.) at 97° C. for 5 hours. Monosaccharides in the hydrolyzate were estimated by quantitative paper chromatography as previously described and the molar ratio of galactose to arabinose was 1:13. Degraded polysaccharide material was precipitated from the hydrolyzate by adding 3 volumes of ethanol and was washed three times with methanol by centrifuging. The precipitate was dissolved in N hydrochloric acid (1 ml.) and the cold solution was examined by paper chromatography (solvent A). The methanol washings must have removed all monosaccharide hydrolysis products because none could be detected. The acidic solution was then heated in a sealed tube at 97° C. for 10 hours and was again chromatographed (solvent A). Galactose was the only sugar that could be detected. These results showed that arabinose was completely removed from the arabogalactan by partial hydrolysis with 0.025 N oxalic acid while the galactan portion of the polysaccharide was attacked to only a minor extent.

Periodate Oxidation

Duplicate samples (125.4 mg., 0.73 mm.) were dissolved in water (120 ml.) to which was added 30 ml. of periodate solution (6.9 g. of periodic acid in 120 ml. water, neutralized to methyl red indicator by sodium hydroxide). The solutions, together with two blanks, were placed in the dark at 30° C. At the intervals noted below, samples were removed for estimation of formic acid and periodate. Formic acid was determined on 20 ml. samples after destruction of excess periodate by 2,3-butanediol, by titrating the iodine liberated from potassium iodide with 0.01 N thiosulphate. Periodate was estimated on 10 ml. samples by the excess arsenite method (6, 8). The results, given in moles per mole anhydrogalactose unit were as follows:

Time (hours)	22	46	69	91
Formic acid production	0.375	0.387	0.398	0.415
Periodate consumption	0.835	1.06	1.13	1.08

Within the limits of experimental error the polysaccharide was found to have consumed 1.1 moles periodate per mole anhydrogalactose with liberation of 0.42 moles formic acid per mole anhydrogalactose.

The solutions of oxidized arabogalactan remaining after removal of samples for analysis were combined (total volume 60 ml.) and excess periodate was destroyed by 2,3-butanediol. This solution was then dialyzed through Visking casing against distilled

water for 3 days. Evaporation of the solution of non-dialyzable material yielded the periodate-oxidized arabogalactan which was then heated with N hydrochloric acid (2 ml.) in a sealed tube at 97° C. for 5 hours. Galactose, but no arabinose, was detected in the hydrolyzate by paper chromatography (solvent A).

Methylation

The arabogalactan (6.00 g.) in water (35 ml.) was methylated by the dropwise addition of 30% sodium hydroxide (160 ml.) and dimethyl sulphate (60 ml.). The reagents were added simultaneously at such rates that the solution was always alkaline. Complete addition of reagents required 4 hours after which the solution was stirred for 1 hour and another methylation was carried out in exactly the same way. After this second methylation the solution was stirred for 18 hours and another addition of reagents was made. The reaction mixture was again stirred for 18 hours and was then heated at 80–85° C. for $1\frac{1}{2}$ hours. Some solid material, probably methylated polysaccharide, separated at this point but was not collected. The mixture was cooled to 11° C. and brought to pH 7.0 by addition of glacial acetic acid at such a rate that the temperature never rose above 14° C. Water was added to the neutral mixture to dissolve all the salts and this solution was extracted 5 times with $\frac{1}{2}$ volumes of fresh chloroform. The chloroform extracts were dried over anhydrous sodium sulphate and evaporated to dryness yielding a glassy solid (4.50 g.) which showed a small, but definite, hydroxyl band at 3500–3600 cm.$^{-1}$ in its infrared spectrum. The partially methylated arabogalactan was taken up in methyl iodide (150 ml.) to which methanol (5 ml.) was added to promote solution. The solution was refluxed and methylation was carried out by addition of silver oxide (36 g.) in portions of 3.6 g. every $\frac{1}{2}$ hour. After the final addition the mixture was refluxed for 18 hours and silver salts were filtered off and washed successively with chloroform, methanol, and acetone. The combined washings and filtrate were evaporated to yield a glassy solid (4.30 g.) which still contained a definite hydroxyl band in its infrared spectrum. Two more methylations by the same procedure did not remove or reduce this hydroxyl absorption so the product was dissolved in tetrahydrofuran (200 ml.) and methylated by the dropwise addition of dimethyl sulphate (60 ml.) to the stirred solution to which solid sodium hydroxide (55 g.) had been added. Addition of dimethyl sulphate required 5 hours, after which the mixture was stirred at room temperature for 20 hours before being heated at 75° C. for 1 hour. Water was added in sufficient quantity to dissolve the sodium hydroxide and the solution was cooled to 10° C. in an ice bath. Glacial acetic acid was then added until the solution was neutral (pH 7.0), with the temperature always being kept below 14° C. The neutral solution was then extracted 5 times with $\frac{1}{2}$ volumes of fresh chloroform and the extracts were dried over anhydrous sodium sulphate. Evaporation of the chloroform left a light-brown, glassy solid (4.27 g.) having $[\alpha]_D^{25} = -20.0\pm1.5°$ ($c = 2.2\%$ in chloroform) and showing no hydroxyl band at 3500–3600 cm.$^{-1}$ in its infrared spectrum. Anal. Calc. for $(C_9H_{16}O_5)n$: OMe, 45.3%. Found: OMe, 43.8%.

Hydrolysis of Methylated Arabogalactan and Separation of Hydrolysis Products

The methylated arabogalactan (4.21 g.) was refluxed in 8% methanolic hydrogen chloride (150 ml.) for 13 hours. The methanolic solution was then evaporated in a glass dish by a stream of air from a fan and the sirupy residue was taken up in N hydrochloric acid (70 ml.) to form a turbid suspension. This mixture was heated on a boiling water bath for 12 hours and a small amount of insoluble material was removed by filtration. The acidic solution was neutralized by Amberlite IR-45 resin and the neutral hydro-

lyzate was evaporated to a sirup which was redissolved in 50% aqueous ethanol and stirred with a little charcoal. The charcoal was filtered off and the combined filtrate and washings were evaporated to dryness. The product was dried over anhydrous calcium chloride in a desiccator evacuated to 5 mm. pressure. The dark brown sirup (2.94 g.) had $[\alpha]_D^{25} = +50.2°\pm1.5°$ ($c = 2.5\%$ in methanol) and examination by paper chromatography (solvent D) indicated the presence of the following products with R_g values (movements relative to 2,3,4,6-tetra-O-methyl-D-glucose) given in parentheses: 2,3,5-tri-O-methyl arabinose (0.98); 2,3,4,6-tetra-O-methyl galactose (0.92); 2,3,4-tri-O-methyl galactose (0.76); and 2,4-di-O-methyl galactose (0.55).

The mixture of methylated sugars (2.9 g.) was resolved by partition chromatography on a column (5×50 cm.) of Celite using butanol, saturated with water, as the developing phase (16). A preliminary 150 ml. of eluate was run off and discarded before the column was mounted on an automatic fraction collector which separated the eluate into 13 ml. fractions by changing the receiver every 3 minutes. Every fifth fraction was examined by paper chromatography (solvent D) and fractions containing the same compound were combined, evaporated to dryness, taken up in water, filtered to remove finely divided Celite, and again evaporated in weighed flasks. Results of the separation are shown in Table II with the names of the compounds being based on their subsequent identification. Specific rotations are of the sirupy products obtained as just described without any further purification.

IDENTIFICATION OF COMPONENTS

2,3,5-Tri-O-methyl-L-arabinose

Fraction A was chromatographically identical with 2,3,5-tri-O-methyl-L-arabinose in solvents D, E, and F. Aqueous solutions of the sirupy product showed no optical activity. A portion (110 mg.) of the sirup, in water (3 ml.), was oxidized by bromine (0.5 ml.) for 50 hours. Bromine was removed by aeration and the solution was neutralized with silver carbonate. The filtrate from the insoluble silver salts was passed over Amberlite IR-120 resin and evaporated to yield sirupy 2,3,5-tri-O-methyl-L-arabonic acid. The acid was lactonized by distillation (bath temperature 125–140° C./0.02 mm.) and the lactone was dissolved in methanol saturated with ammonia at 0° C. This solution was stored at 5° C. for 24 hours and was then evaporated under diminished pressure in a desiccator. The amide crystallized; m.p. 132–134° C. raised to 134–136° C. by two recrystallizations from acetone – petroleum ether; $[\alpha]_D^{26} = +20°\pm4°$ ($c = 0.5\%$ in water). These physical constants are in agreement with those reported for 2,3,5-tri-O-methyl-L-arabonamide (12).

2,3,4,6-Tetra-O-methyl-D-galactose

Fraction B behaved the same chromatographically in solvents D, E, and F as an authentic sample of 2,3,4,6-tetra-O-methyl-D-galactose. A portion (64.5 mg.) of the sirup was refluxed with aniline (34.4 mg.) in ethanol (5 ml.) for 3 hours. The solution was evaporated in a desiccator leaving a crystalline residue that was recrystallized from ethanol to yield 48.2 mg. of 2,3,4,6-tetra-O-methyl-N-phenyl-D-galactosylamine (13), m.p. and mixed m.p. 196.5–198° C., $[\alpha]_D^{25} = -137°\pm1°$ ($c = 2\%$ in pyridine).

Impure 2,3,4-Tri-O-methyl-D-galactose

Fraction C contained mainly 2,3,4-tri-O-methyl-D-galactose (R_g 0.69 in solvent E, 0.51 in solvent F) and ran as a single diffuse spot on chromatograms in solvent D. However, chromatography in solvent F revealed the presence of two minor components

having R_g values of 0.68 and 0.84 and, in solvent E, three minor components with R_g values of 0.76, 0.84, and 0.94 were detected. On all chromatograms the spots caused by these compounds were small compared to the 2,3,4-tri-O-methyl-D-galactose spot, and the amounts of them were not sufficient to permit identification. The sirupy mixture (109 mg.) was refluxed with aniline (57 mg.) in ethanol (5 ml.) for 2 hours and the solution was evaporated in a desiccator leaving a crystalline residue. Recrystallization from ethanol yielded 41 mg. of 2,3,4-tri-O-methyl-N-phenyl-D-galactosylamine (19, 23) m.p. 163–166° C., raised to 166–168° C. by a further recrystallization; $[\alpha]_D^{26} = -68° \pm 3°$ $\rightarrow +42° \pm 3°$ in 5 hours ($c = 1.1\%$ in methanol). No other anilide could be isolated.

2,3,4-Tri-O-methyl-D-galactose

Fraction D was a sirup and was chromatographically homogeneous in solvents D, E, and F. A portion (88.5 mg.) of this fraction was refluxed with aniline (46 mg.) in ethanol (5 ml.) for 2 hours. Evaporation of the solution left a crystalline residue which was recrystallized from small volumes of ethanol to a constant melting point of 166–168° C. A mixed melting point with the 2,3,4-tri-O-methyl-N-phenyl-D-galactosylamine (19, 23) isolated from Fraction C was not depressed and the specific rotation was the same: $[\alpha]_D^{26} = -68° \pm 3° \rightarrow +42° \pm 3°$ in 5 hours ($c = 1\%$ in methanol).

Another sample (100 mg.) of Fraction D in water (5 ml.) was oxidized by bromine (0.5 ml.) for 66 hours. Bromine was removed by aeration, the solution was neutralized with silver carbonate, and insoluble silver salts were filtered off. Soluble silver in the filtrate was removed as the sulphide and the filtrate from this precipitate was evaporated to yield an acid which did not crystallize. The acid was lactonized by distillation at 150–165° C. (bath temperature) and 0.02 mm. and the distillate was dissolved in methanol saturated with ammonia at 0° C. The ammoniacal solution was stored at 5° C. for 24 hours and was then evaporated in a desiccator to yield a crystalline amide, m.p. 162–164° C. raised to 166–167° C. (constant) by recrystallizations from ethanol:petroleum ether. This melting point and the specific rotation, $[\alpha]_D^{26} = +35° \pm 3°$ ($c = 0.8\%$ in water) agree with reported values for 2,3,4-tri-O-methyl-D-galactonamide (23).

2,6-Di-O-methyl-D-galactose

Fraction E corresponded chromatographically to a di-O-methyl galactose but had a greater mobility than 2,4-di-O-methyl-D-galactose in solvents D, E, and F. Fraction E crystallized completely when recovered from its aqueous solution used for determining the specific rotation recorded in Table II. Recrystallization from acetone:petroleum ether gave the monohydrate of 2,6-di-O-methyl-β-D-galactose (15), m.p. 99–100° C., $[\alpha]_D^{29} = +61° \pm 2° \rightarrow +84° \pm 2°$ in 3 hours ($c = 1\%$ in water).

2,4-Di-O-methyl-D-galactose

Fraction F crystallized spontaneously and was chromatographically identical in solvents D, E, and F with 2,4-di-O-methyl-D-galactose. Recrystallization from acetone: ether:petroleum ether yielded 2,4-di-O-methyl-D-galactose monohydrate (23) m.p. 98–100° C. with sintering at 67–70° C., $[\alpha]_D^{26} = +119°$ (4 minutes) $\rightarrow +85° \pm 1°$ in 24 hours ($c = 2\%$ in water). The melting point was not depressed by admixture with an authentic sample. When a sample (116.8 mg.) of this compound was dried at 55° C. and 0.06 mm. over phosphoric anhydride for 16 hours the loss in weight (9.8 mg.) corresponded to 1.03 moles of water and the dried product had m.p. 103–104° C. (no sintering) and $[\alpha]_D^{26} = +125°$ (4 minutes) $\rightarrow +88° \pm 1$ in 24 hours ($c = 1.1\%$ in water). Analyses showed that the air-dried product was the monohydrate and that the vacuum-dried

compound was anhydrous 2,4-di-O-methyl-α-D-galactose. Anal. Calc. for $C_8H_{16}O_6 \cdot H_2O$: C, 42.48%; H, 8.02%. Found: C, 42.6%; H, 7.97%. Calc. for $C_8H_{16}O_6$: C, 46.15%; H, 7.75%. Found: C, 46.19%; H, 7.748%.

Fraction F (61 mg.) was refluxed with aniline (36.3 mg.) in ethanol (6 ml.) for 2 hours. The solution was evaporated in a desiccator and the crystalline residue was recrystallized from methanol giving 2,4-di-O-methyl-N-phenyl-D-galactosylamine (23); m.p. 218–221° C., $[\alpha]_D^{27} = -183°\pm5°$ ($c = 0.8\%$ in pyridine).

REFERENCES

1. ANDREWS, P., HOUGH, L., and JONES, J. K. N.   J. Chem. Soc. 2744 (1952).
2. BOGGS, L., CUENDET, L. S., EHRENTHAL, I., KOCH, R., and SMITH, F.   Nature, 166, 520 (1950).
3. BRAUNS, F. E.   Science, 102, 155 (1945).
4. CAMPBELL, W. G., HIRST, E. L., and JONES, J. K. N.   J. Chem. Soc. 774 (1948).
5. CHANDA, S. K., HIRST, E. L., JONES, J. K. N., and PERCIVAL, E. G. V.   J. Chem. Soc. 1289 (1950).
6. FLEURY, P. P. and LANGE, J.   J. pharm. chim. 17, 107 (1933).
7. FOREMAN, E. L. and ENGLIS, D. T.   Ind. Eng. Chem. 23, 415 (1931).
8. GRANGAARD, D. H., GLADDING, E. K., and PURVES, C. B.   Paper Trade J. 115, 41 (1942).
9. HIRST, E. L.   J. Chem. Soc. 70 (1942).
10. HIRST, E. L., JONES, J. K. N., and CAMPBELL, W. G.   Nature, 147, 25 (1941).
11. HOUGH, L., JONES, J. K. N., and WADMAN, W. H.   J. Chem. Soc. 1702 (1950).
12. HUMPHREYS, R. W., PRYDE, J., and WATERS, E. T.   J. Chem. Soc. 1298 (1931).
13. IRVINE, J. C. and McNICOLL, D.   J. Chem. Soc. 97, 1449 (1910).
14. JERMYN, M. A. and ISHERWOOD, F. A.   Biochem. J. 44, 402 (1949).
15. JONES, J. K. N.   J. Chem. Soc. 3141 (1949).
16. LEMIEUX, R. U., BISHOP, C. T., and PELLETIER, G. E.   Can. J. Chem. 34, 1365 (1956).
17. MARTIN, S. M.   Chemistry & Industry (In press).
18. MARTIN, S. M. and ADAMS, G. A.   Can. J. Microbiol. 2, 715 (1956).
19. McCREATH, D. and SMITH, F.   J. Chem. Soc. 387 (1939).
20. NIKITIN, N. I. and SOLOVIEV, I. A.   J. Appl. Chem. (U.S.S.R.) 8, 1016 (1935).
21. PETERSON, F. C., BARRY, A. J., UNKAUF, H., and WISE, L. E.   J. Am. Chem. Soc. 62, 2361 (1940).
22. SCHORGER, A. W. and SMITH, D. F.   Ind. Eng. Chem. 8, 494 (1916).
23. SMITH, F.   J. Chem. Soc. 1724 (1939).
24. TREVELYAN, W. E., PROCTER, D. P., and HARRISON, J. S.   Nature, 166, 444 (1950).
25. WADMAN, W. H., ANDERSON, A. B., and HASSID, W. Z.   J. Am. Chem. Soc. 76, 4097 (1954).
26. WHISTLER, R. L. and BeMILLER, J. N.   J. Am. Chem. Soc. 78, 1163 (1956).
27. WHISTLER, R. L. and KIRBY, K. W.   J. Am. Chem. Soc. 78, 1755 (1956).
28. WHITE, E. V.   J. Am. Chem. Soc. 63, 2871 (1941).
29. WHITE, E. V.   J. Am. Chem. Soc. 64, 302 (1942).
30. WHITE, E. V.   J. Am. Chem. Soc. 64, 1507 (1942).
31. WHITE, E. V.   J. Am. Chem. Soc. 64, 2838 (1942.)
32. WISE, L. E. and PETERSON, F. C.   Ind. Eng. Chem. 22, 362 (1930).
33. WISE, L. E. and UNKAUF, H. C.   Cellulosechemie, 14, 20 (1933).

KINETICS OF THE OXIDATION OF MERCURY(I) BY THALLIUM(III) IN AQUEOUS SOLUTION[1]

A. M. ARMSTRONG[2] AND J. HALPERN[3]

ABSTRACT

The kinetics of the oxidation of mercury(I) by thallium(III) in aqueous perchloric acid solution, i.e. $Hg(I)_2 + Tl(III) \rightarrow 2Hg(II) + Tl(I)$, have been examined. The rate law was found to be of the form $-d[Hg(I)_2]/dt = k_{exp}[Hg(I)_2][Tl(III)]/[Hg(II)]$ where k_{exp} is inversely dependent on the concentrations of H^+ and of ClO_4^-. The rate-determining step of the reaction appears to be a 'two-electron transfer' between a mercury atom, formed by the dismutation of Hg_2^{++}, and a hydrolyzed thallium ion, i.e. $Hg + TlOH^{++} \rightarrow Hg^{++} + Tl^+ + OH^-$. The rate constant, k, of this reaction is given by $k = 10^{16 \pm 2} \exp[-14000 \pm 3000/RT]$ liters mole^{-1} sec.$^{-1}$.

H^+ retards the reaction by opposing the hydrolysis of Tl^{+++}, while the effect of ClO_4^- appears to be due to its complexing with Hg_2^{++}. Cl^- and Br^- catalyze the reaction probably by complexing with Hg^{++}, thus displacing the Hg_2^{++} dismutation equilibrium, $Hg_2^{++} \rightleftharpoons Hg^{++} + Hg$, to the right and increasing the concentration of Hg atoms. The kinetics and mechanism of the Tl(I)–Tl(III) isotopic electron exchange reaction and of other electron transfer processes in solution are considered in the light of these observations.

INTRODUCTION

Among the considerations which led up to this investigation was the observation that, unlike most simple inorganic oxidation–reduction reactions, the oxidation of mercurous salts in aqueous solution by common inorganic oxidizing agents such as Ce(IV) and Cr(VI) proceeded very slowly. It seemed likely that this was in some way associated with the fact that the mercurous ion, Hg_2^{++}, is a dimeric species. One consequence of this is that its oxidation (i.e. to $2 Hg^{++}$) involves the over-all transfer of two electrons. The slow oxidation of mercury(I) by oxidants such as Ce(IV) might therefore be explained in terms of Shaffer's (26, 31) principle of 'equi-valence change' which states that, in general, oxidation–reduction reactions between one-electron donors and one-electron acceptors, or between two-electron donors and two-electron acceptors, will be rapid, while reactions between one-electron acceptors (or donors) and two-electron donors (or acceptors) will be slow. Accordingly it seemed of interest to examine the oxidation of mercury(I) by a two-electron oxidizing agent, and thallium(III), whose reactions with other reducing agents (23, 10, 2, 9) have been widely investigated from a related standpoint, was considered the logical choice for this purpose. The rate of oxidation of mercury(I) by thallium(III), while relatively rapid, proved to be measurable, and a kinetic study of the reaction is described in this paper. Some preliminary results, obtained in collaboration with Higginson, have been reported in an earlier note (1).

EXPERIMENTAL

Most of the experiments were made at 25° C., using perchloric acid solutions, maintained at constant ionic strength with sodium perchlorate, in order to minimize complications due to hydrolysis and complexing of the metal ions. However, as will be shown, it proved impossible to eliminate these effects entirely.

Baker and Adamson reagent grade perchloric acid (60%) was used; its chloride content was below the limit detectable with Ag^+ ($\approx 10^{-6} M$). Sodium perchlorate solutions were

prepared from perchloric acid and sodium bicarbonate which had been purified by repeated recrystallization. Mercuric perchlorate solutions were prepared from mercuric oxide which had been purified by repeated precipitation from perchloric acid with sodium hydroxide. The mercurous perchlorate was prepared by reducing this solution with triple-distilled mercury; the final solution was stored over a slight excess of mercury to prevent reoxidation. Thallous perchlorate solutions were prepared from reagent grade thallous nitrate, by repeated fuming with perchloric acid. Thallic perchlorate solutions were prepared by oxidizing the thallous perchlorate with sodium bromate, boiling off the excess bromine, adding sodium hydroxide to form thallic hydroxide which, after purification by repeated reprecipitation from perchlorate solutions, was dissolved in perchloric acid. Solutions of sodium chloride and sodium bromide were prepared from the reagent grade salts. The water used in the preparation of these solutions was purified by redistilling from alkaline permanganate in an all-glass still.

The solutions used in the kinetic experiments were prepared by mixing suitable aliquots of stock solutions of the various reagents, which had been prepared as described above, and standardized by recognized analytical procedures. All solutions were brought to the reaction temperature before mixing, and the final solution maintained at constant temperature during the reaction, by immersion in a water bath controlled to $\pm 0.03°$ C. The reaction was followed by withdrawing samples of the solution and analyzing for mercury(I) with a Beckman DK–2 recording spectrophotometer using the Hg_2^{++} absorption peak at 2365 Å (13). Corrections were applied for the small absorption of the other ions present.

RESULTS

The over-all stoichiometry of the reaction, which was found to proceed to completion, can be represented as

$$Hg(I)_2 + Tl(III) \rightarrow 2Hg(II) + Tl(I). \tag{1}$$
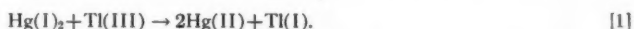
In this equation mercury(I) is represented as a dimeric species. Apart from this, the symbols used are intended to represent only the oxidation states of the various ions without reference to their state of complexing or hydrolysis.

Kinetics of the Reaction

Some typical rate plots, depicting the decrease in concentration of $Hg(I)_2$ with time, are shown in Fig. 1. One of the striking kinetic features of this reaction is the inhibitory influence of $Hg(II)$, while the other product $Tl(I)$ is without effect on the rate. Experimentally the rate law was found to be of the form

$$-d[Hg(I)_2]/dt = k_{exp} [Hg(I)_2][Tl(III)]/[Hg(II)], \tag{2}$$

which becomes, on integration,

$$\frac{[Hg(II)]_0 + 2[Hg(I)_2]_0}{[Tl(III)]_0 - [Hg(I)_2]_0} \log\frac{[Hg(I)_2]_0}{[Hg(I)_2]} - \frac{[Hg(II)]_0 + 2[Tl(III)]_0}{[Tl(III)]_0 - [Hg(I)_2]_0} \log\frac{[Tl(III)]_0}{[Tl(III)]} = \frac{k_{exp} t}{2.303} \tag{3}$$

where [ ]$_0$ denotes the initial total concentration of the designated species and [ ] the total concentration at time t.

In Fig. 2, the function (denoted as $F_{conc.}$) corresponding to the left-hand side of equation [3] is plotted against t, for all the experiments depicted in Fig. 1. In conformity with equation [3], all the points are seen to lie fairly close to a single straight line passing through the origin. While some scatter of the points is evident, a large number of experi-

ments at $3\ M$ $HClO_4$, in which the initial solution composition was varied over the range 10^{-5} to $5 \times 10^{-5}\ M$ $Hg(I)_2$, 10^{-5} to $10^{-3}\ M$ $Tl(III)$, 0 to $10^{-4}\ M$ $Hg(II)$, and 0 to $10^{-4}\ M$ $Tl(I)$, failed to reveal any systematic deviation from the proposed rate law. Values of the apparent rate constant, k_{exp}, were estimated from the slopes of linear rate plots such as those in Fig. 2, and were generally reproducible to $\pm 5\%$. The value of k_{exp} depended on the $HClO_4$ and $NaClO_4$ concentrations, and at high $NaClO_4$, the kinetic plots deviated slightly from linearity.
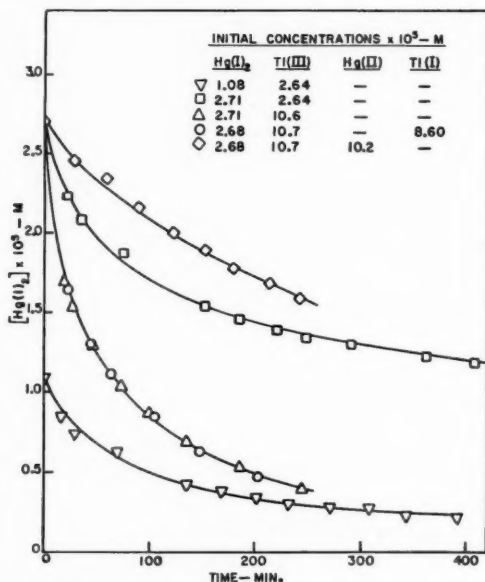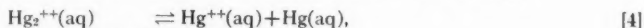

FIG. 1. Rate plots showing the oxidation of $Hg_2(ClO_4)_2$ by $Tl(ClO_4)_3$ at $25°$, $3\ M$ $HClO_4$.

To explain the inverse dependence of the rate on the $Hg(II)$ concentration it is proposed that the reaction proceeds through the following sequence of steps:

$$Hg_2{}^{++}(aq) \quad \rightleftharpoons Hg^{++}(aq)+Hg(aq), \qquad [4]$$
$$Hg(aq)+Tl(III) \rightarrow Hg(II)+Tl(I). \qquad [5]$$

The dismutation equilibrium (step 4), whose equilibrium constant is denoted as K_d, is assumed to be rapidly established and thus serves to determine the concentration of Hg atoms in solution, i.e.

$$[Hg] = K_d\,[Hg_2{}^{++}]/[Hg^{++}], \qquad [6]$$

while the subsequent reaction between Hg and Tl(III) is rate-determining. This leads to a rate law of the observed form.

The fact that $Hg_2{}^{++}$ undergoes dismutation in aqueous solution, and that this equilibrium is rapidly established has long been recognized. When reagents such as NH_3, CN^-, or Cl^-, which form stable mercuric complexes and thus decrease the concentration of free Hg^{++}, are added to a solution of a mercurous salt, they cause this equilibrium to be shifted to the right, leading ultimately to the formation of metallic mercury when the solubility of the latter in water (estimated to be about $10^{-7}\ M$ (21, 28)) is exceeded

(27). The value of K_d has recently been determined (5.5×10^{-9} M at 25°) by measuring the distribution of Hg atoms between aqueous solutions of mercurous nitrate and organic liquids, using radioactive tracer techniques (21). Evidence for the presence of Hg atoms in appreciable concentrations in aqueous solutions has also been obtained by spectroscopic observation of the 2537 Å absorption band of Hg in solution (24). Hg atoms have also been postulated as intermediates in at least two other reactions in aqueous solution, the rapid isotopic electron exchange between Hg^{++} and Hg_2^{++} (32) and the reduction of Hg^{++} by H_2 (15).
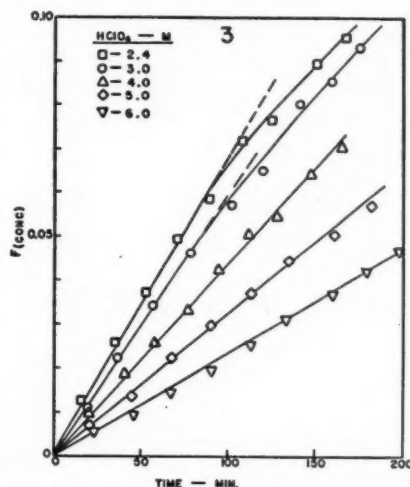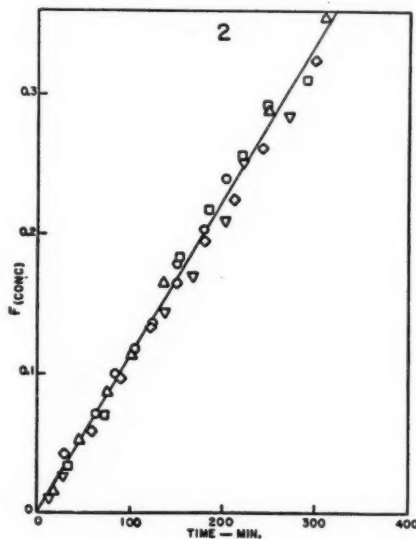

FIG. 2. Kinetic plots according to equation [3]. Symbols refer to same experiments as in Fig. 1.
FIG. 3. Kinetic plots showing effect of $HClO_4$ at 25°. Total perchlorate concentration held constant at 6 M with $NaClO_4$. Initial $Hg_2(ClO_4)_2$ and $Tl(ClO_4)_3$ concentrations, 2.64×10^{-5} and 5.65×10^{-5} M, respectively.

Effect of $HClO_4$

Increasing the concentration of $HClO_4$ between 2.4 and 6.0 M, while holding the total ionic strength (μ) constant at 6.0 with $NaClO_4$, was found to decrease the value of k_{exp} as shown in Fig. 3. The simplest interpretation of this effect is that the Tl(III) species which takes part in the rate-determining step (5) is not the Tl^{+++} ion but, as has been found (10, 2) for other reactions involving Tl(III), the first hydrolysis complex, $TlOH^{++}$. The concentration of this species is given by

$$[TlOH^{++}] = K_h[Tl(III)]/(K_h + [H^+]), \qquad [7]$$

where [Tl(III)] is the total thallium(III) concentration and K_h is the hydrolysis constant of Tl^{+++}, i.e. the equilibrium constant of the reaction

$$Tl^{+++} + H_2O \rightleftharpoons TlOH^{++} + H^+. \qquad [8]$$

Hydrolysis of Hg^{++} (11), Hg_2^{++} (8), and of Tl^+ (3) is negligible at the acidities used.

Unfortunately, there is currently some uncertainty and controversy concerning the

magnitude of K_h. The most widely accepted value, based on recent careful e.m.f. measurements of Biedermann (5), is 0.073 M (at $\mu = 3$) which would suggest that in the acidity range used here, most of the Tl(III) is unhydrolyzed (i.e. $K_h \ll [H^+]$) and hence equation [7] reduces to

$$[TlOH^{++}] = K_h[Tl(III)]/[H^+]. \qquad [9]$$

Thus, k_{exp} should vary inversely with $[H^+]$. The plot shown in Fig. 4 is considered to be in satisfactory accord with this, when account is taken of the experimental uncertainty of k_{exp} (particularly at low acidities when the kinetic plots (see Fig. 3) diverge from linearity) and of the fairly large 'medium' effect which could accompany substantial replacement of $NaClO_4$ by $HClO_4$ at the high total ionic strength used. (This is suggested by observations (13) that $HClO_4$ and $NaClO_4$ are not equivalent in their effects on the absorption spectrum of the mercurous ion.) Other interpretations of the effect of variation of the $HClO_4$–$NaClO_4$ ratio, in terms of hydrolysis of Tl^{+++}, were attempted but gave even less satisfactory accounts of the results. In particular, it was not possible to reconcile the observed behavior with much higher estimates (10) of K_h.
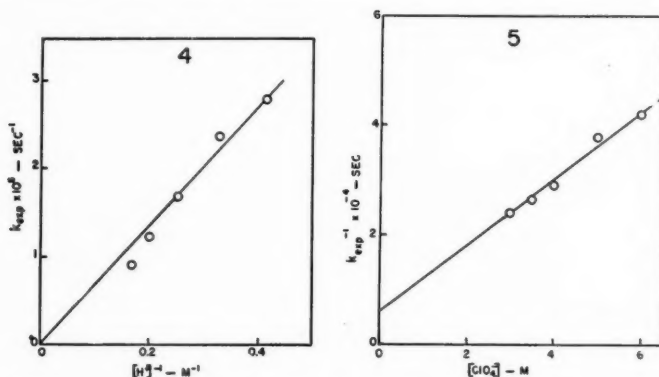

FIG. 4. Dependence of k_{exp} on the H^+ concentration at 25°, 6 M ClO_4^-.
FIG. 5. Dependence of k_{exp} on the concentrations of ClO_4^- at 25°, 3 M H^+.

No explanation can be offered for the deviation from linearity of the kinetic plots (see Fig. 3) for the experiments at low $HClO_4$ concentrations. This deviation was not observed at lower $NaClO_4$ concentrations (see Fig. 6) and may be due to an impurity (e.g. Cl^-) in the $NaClO_4$ which was added.

Effect of $NaClO_4$

Increasing the concentration of $NaClO_4$, at constant $HClO_4$ concentration, also resulted in a decrease in the rate as shown in Fig. 6. While it is possible that this may be, in part, the result of a variation in the ionic strength or medium properties, the effect is in the direction which would be expected to result from complexing* of Hg_2^{++} by ClO_4^-, i.e.

$$Hg_2^{++} + ClO_4^- \rightleftharpoons Hg_2ClO_4^+, \qquad [10]$$

*While it has become standard practice to use a perchlorate medium in studying reactions of metal ions, in order to minimize complexing, the assumption of the complete absence of complexing should be made with caution. A number of metal ions including Hg_2^{++} (12), Fe^{+++} (30), and Ce^{+++} (29) have now been shown to complex measurably with ClO_4^-, although in no case is the complexity constant very large. There is no evidence that either Hg^{++} or Tl^{+++} complexes appreciably with ClO_4^-.

the complexity constant, K_c, of $Hg_2ClO_4^+$ having recently been estimated (12) to be about 0.91 M^{-1}. This would decrease the concentration of free Hg_2^{++} in solution, i.e.

$$[Hg_2^{++}] = [Hg(I)_2]/(1+K_c[ClO_4^-]), \qquad\qquad [11]$$

and hence, according to equation [6] (since complexing of Hg^{++} by ClO_4^- is negligible (12)), the concentration of Hg atoms. Assuming the rate to be first order in Hg_2^{++}, it follows from equation [11] that a plot of k_{exp}^{-1} vs. $[ClO_4^-]$ should be linear and that the ratio of the slope and intercept of this plot should be equal to K_c. The plot shown in Fig. 5 (based on the kinetic results in Fig. 6) is in accord with this and gives a value of 1.0 M^{-1} for K_c, which is in excellent agreement with the value of 0.91 M^{-1} determined by Hietanen and Sillén (12) from e.m.f. measurements.
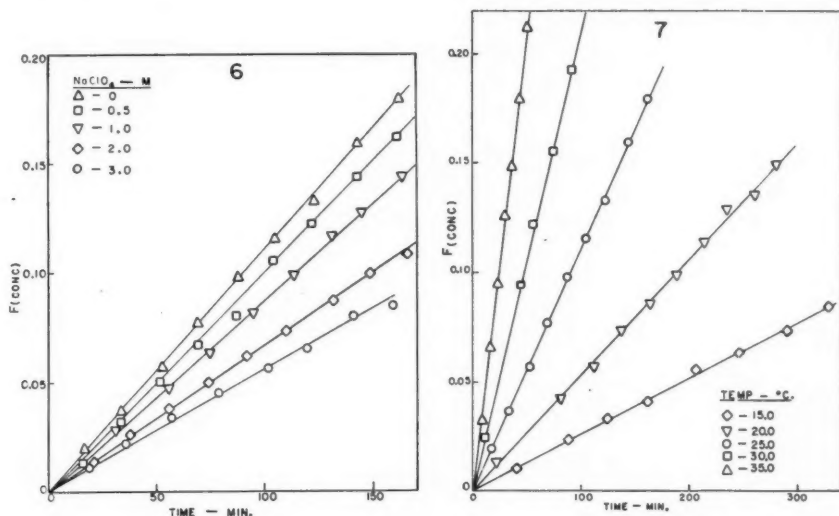

FIG. 6. Effect of $NaClO_4$ on the rate at 25°, 3 M $HClO_4$. Initial $Hg_2(ClO_4)_2$ and $Tl(ClO_4)_3$ concentrations 2.64×10^{-5} and 5.65×10^{-5} M, respectively.

FIG. 7. Kinetic plots for experiments at different temperatures, 3 M $HClO_4$. Initial $Hg_2(ClO_4)_2$ and $Tl(ClO_4)_3$ concentrations, 2.64×10^{-5} and 5.65×10^{-5} M, respectively.

Effect of Temperature

Rate plots obtained using solutions containing 3 M $HClO_4$, at various temperatures ranging from 15° to 35°, are shown in Fig. 7. The values of k_{exp}, determined from the slopes of these plots, ranged from 1×10^{-5} to 1.6×10^{-4} sec.$^{-1}$ and gave the Arrhenius plot shown in Fig. 8, whose slope corresponds to an apparent activation energy, E_{exp}, of 24.4 kcal./mole.

Effect of Chloride and Bromide

The addition of small amounts ($\approx 10^{-5}$ M) of NaCl to the solution was found to increase the rate of reaction, and to cause the kinetic plots to diverge slightly from linearity as shown in Figs. 9 and 10. Sodium bromide had a similar but somewhat greater effect as shown in Fig. 10.

An unequivocal interpretation of these effects is not possible. Both Tl^{+++} and Hg^{++}
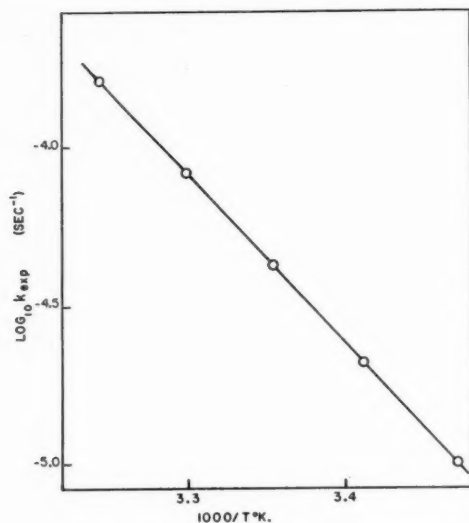
FIG. 8. Arrhenius plot showing the temperature dependence of k_{exp} at 3 M HClO$_4$.
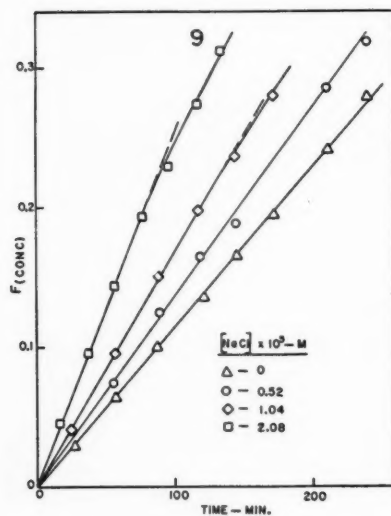

FIG. 9. Effect of NaCl on the reaction at 25°, 3 M HClO$_4$. Initial Hg$_2$(ClO$_4$)$_2$ and Tl(ClO$_4$)$_3$ concentrations, 2.64×10^{-5} and 3.67×10^{-5} M, respectively.
FIG. 10. Dependence of k_{exp} at 25°, 3 M HClO$_4$, 2.64×10^{-5} M Hg$_2$(ClO$_4$)$_2$, and 3.67×10^{-5} M Tl(ClO$_4$)$_3$ on the concentration of NaCl or NaBr.
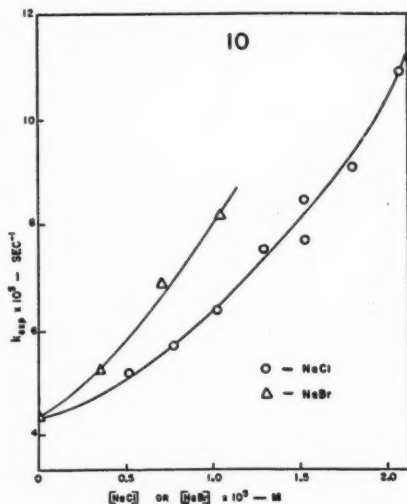
are strongly complexed by Cl$^-$ and Br$^-$ (22, 17, 4). Complexing of Hg^{++} would be expected to increase the rate by shifting the Hg$_2$$^{++}$ dismutation equilibrium (equation 4) to the right, thus increasing the concentration of Hg atoms. This is offset by the decrease in the TlOH^{++} concentration resulting from complexing of Tl^{+++}; the relative

magnitude of these two effects is determined by the relative magnitudes of the complexity constants of the mercuric and thallic halide complexes. In addition, it is possible that the thallic halide complexes, $TlCl^{++}$ and $TlBr^{++}$, like $TlOH^{++}$, react with Hg atoms and thus contribute to the over-all rate. The complexity constants which have been dete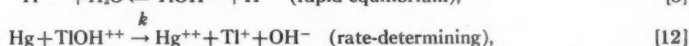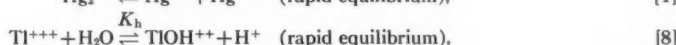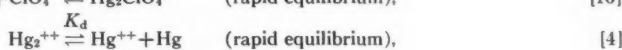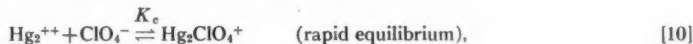rmined (17, 4) for $HgCl^+$ and $HgBr^+$ (5.4×10^6 and 1.1×10^9 M^{-1} respectively, both at 25° and $\mu = 0.5$) are sufficiently larger than those (22) for $TlCl^{++}$ and $TlBr^{++}$ (1.8×10^6 and 7.9×10^8 M^{-1} respectively, both at 25° and $\mu = 1.2$) to account for the observed increase in rate, in terms of the first of the above effects, i.e. the enhanced dismutation of Hg_2^{++}, suggesting that $TlCl^{++}$ and $TlBr^{++}$ do not contribute appreciably to the reaction with Hg. Unfortunately, relatively small errors in the above values could invalidate this conclusion. However, in view of the relatively small increase in rate which was observed, even when as much as half the Tl(III) was present as $TlCl^{++}$ or $TlBr^{++}$, it is possible to conclude that the reactivity of these complexes, while possibly greater than that of Tl^{+++}, must be very much smaller than that of $TlOH^{++}$. This is consistent with observations that other reactions of Tl(III), such as the Tl(I)–Tl(III) isotopic electron exchange (23, 10) and the oxidation of Fe(II) by Tl(III) (2, 7), are catalyzed by OH^- but inhibited by Cl^-.

Complexing of Hg^{++} and Tl^{+++} by Cl^- or Br^- could also give rise to deviations from the simple rate law represented by equation [2] and thus account for the fact that some of the kinetic plots in Fig. 9 diverge slightly from linearity.

DISCUSSION

The kinetic results in perchlorate solutions have been shown to be consistent with a reaction mechanism involving the following combination of steps:

$$Hg_2^{++} + ClO_4^- \overset{K_c}{\rightleftharpoons} Hg_2ClO_4^+ \qquad \text{(rapid equilibrium)}, \qquad [10]$$

$$Hg_2^{++} \overset{K_d}{\rightleftharpoons} Hg^{++} + Hg \qquad \text{(rapid equilibrium)}, \qquad [4]$$

$$Tl^{+++} + H_2O \overset{K_h}{\rightleftharpoons} TlOH^{++} + H^+ \quad \text{(rapid equilibrium)}, \qquad [8]$$

$$Hg + TlOH^{++} \overset{k}{\rightarrow} Hg^{++} + Tl^+ + OH^- \quad \text{(rate-determining)}, \qquad [12]$$

$$H^+ + OH^- \rightleftharpoons H_2O \qquad \text{(rapid equilibrium)}, \qquad [13]$$

where k is the true rate constant (i.e. that of the rate-determining step) of the reaction, and the other constants have been previously defined.

The rate of the reaction is thus given by

$$-d[Hg(I)_2]/dt = k[Hg][TlOH^{++}], \qquad [14]$$

which becomes on combination with equations [6], [9], and [11]

$$\frac{-d[Hg(I)_2]}{dt} = \frac{k\,K_d\,K_h}{(1 + K_c[ClO_4^-])[H^+]} \cdot \frac{[Hg(I)_2][Tl(III)]}{[Hg(II)]} . \qquad [15]$$

Comparison of equations [2] and [15] shows that

$$k_{exp} = k\,K_d\,K_h / \{(1 + K_c[ClO_4^-])[H^+]\}. \qquad [16]$$

The value of k_{exp} at 25°, 3 M H^+, and 3 M ClO_4^- is 4.2×10^{-5} sec.$^{-1}$. Substituting $K_c = 0.91$ M^{-1} (12), $K_d = 5.5 \times 10^{-9}$ M (22), and $K_h = 0.073$ M (5) in equation [16], the value of k is found to be 1×10^6 liters mole^{-1} sec.$^{-1}$.

Equation [16] also leads to the following expression for the apparent activation energy of the reaction:

$$E_{exp} \approx E + \Delta H_d + \Delta H_h - \Delta H_e, \qquad [17]$$

where E is the true activation energy (i.e. of step 12) and ΔH_d, ΔH_h, and ΔH_e are the enthalpies of reactions [4], [8], and [10], respectively. ΔH_d has been estimated (32) at +10.6 kcal./mole, and ΔH_h (20) at about −0.5 kcal./mole. ΔH_e has not been determined, but with $\Delta F_e° = 0$ (12) it is likely that ΔH_e (as well as $\Delta S_e°$) is close to zero. Using these values and the measured E_{exp} of 24.4 kcal./mole, E is estimated to be about 14±3 kcal./mole, the large uncertainty being due principally to the uncertainty in ΔH_h.

The above values lead to the following Arrhenius expression for k:

$$k = 10^{16 \pm 2} \exp[-14000 \pm 3000 / RT] \text{ liters mole}^{-1} \text{ sec.}^{-1}. \qquad [18]$$

The frequency factor in this expression, which corresponds to an entropy of activation of +13±10 cal.mole⁻¹ deg.⁻¹, is unexpectedly high for a bimolecular reaction. This may be due to the fact that the combination of a doubly charged cation, $TlOH^{++}$, with a large neutral atom, Hg, to form the activated complex is accompanied by a considerable 'spreading-out' of the charge and hence by a decrease in the 'electrostriction' of the surrounding solvent molecules (6). In this respect the activation process resembles the reaction

$$Hg(aq) + Hg^{++}(aq) \rightarrow Hg_2^{++}(aq) \qquad [19]$$

for which $\Delta S°$ (about +2 cal. mole⁻¹ deg.⁻¹, based on data given above) is also positive, although not as large as the apparent entropy of activation.

It is of interest to compare the rate-determining step of this reaction (step 12) with the reaction

$$Tl^+ + \overset{*}{T}lOH^{++} \rightarrow Tl^{+++} + \overset{*}{T}l^+ + OH^-, \qquad [20]$$

which has been proposed as the rate-determining step of the Tl(I)–Tl(III) isotopic electron exchange. This comparison is particularly significant since the corresponding species in the two reactions, Tl^+ and Hg, are isoelectronic, differing only in the fact that the former is charged and the latter neutral. This appears to be the first time that it has been possible to make this type of comparison and, indeed, the first time that the kinetics of a simple 'electron-transfer' reaction† in solution involving an uncharged monatomic species have been examined. From the results it should be possible to derive some direct information about the dependence of the rate of electron-transfer reactions on the charges of the reacting species.

Estimates of the rate constant of reaction [20] at 25° range between 2.5×10^{-5} and 3.3×10^{-4} liters mole⁻¹ sec.⁻¹ (23, 10, 25), i.e. 10^9 to 10^{10} times smaller than that for the reaction between $TlOH^{++}$ and Hg. The activation energies of the two reactions are of the same order (23, 10), the large rate difference thus being attributable to a difference in the entropies of activation. This difference, although unexpectedly large, is in the expected direction, since unlike the reaction between Hg and $TlOH^{++}$ for which, as shown

---

†*Following conventional usage the term 'electron-transfer' reaction is employed in this paper to designate a reaction in which the over-all stoichiometry can be described in terms of a net transfer of electrons between reactants. Whether the mechanism actually involves electron transfer in this sense, or, alternatively, the transfer of H or O atoms or of OH radicals etc., remains an open and somewhat controversial question (33, 14, 19). At the present time, the evidence on this point for most electron-transfer reactions, including the one considered here, does not appear to be conclusive.*

above, the entropy of activation is apparently positive, the reaction between Tl^+ and $TlOH^{++}$, like most reactions between ions of the same sign, should have a large negative entropy of activation because of the greater electrostriction of the solvent around the activated complex (6, 16). The fact that the Hg atom is undoubtedly larger than the isoelectronic, but positively charged, Tl^+ ion may also contribute to its higher rate of reaction with $TlOH^{++}$.

It has often been suggested that the major contribution to the activation barrier in electron transfer reactions between metal ions arises from the electrostatic repulsion which accompanies the mutual approach of the reacting species, and that the catalytic influence which small negative ions such as OH^-, Cl^- etc. generally exert in such reactions reflects their ability to lower this electrostatic repulsion (33). The observations that the activation energies for the reaction of $TlOH^{++}$ with Tl^+ and with Hg are similar, and that the catalytic role of OH^- is evidenced also in the latter reaction, despite the fact that one of the reacting species, i.e. Hg, is uncharged, do not lend support to this view. It seems more likely that the barrier to electron transfer is related to the reorganization of the solvent surrounding the reacting species during the activation process (33, 19, 18). It is possible that the presence of polarizable negative ions such as OH^- facilitates this reorganization or, alternatively, that the reactions can occur by an atom or group transfer mechanism which directly involves these ions (19).

It is of interest to note that although the direct reaction between Hg_2^{++} and $TlOH^{++}$, i.e.

$$Hg_2^{++} + TlOH^{++} \rightarrow 2Hg^{++} + OH^- + Tl^+,\qquad [21]$$
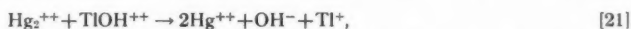
like that between Hg and $TlOH^{++}$ (equation 12) appears formally as a simple two-electron transfer, the kinetics suggest that the contribution from this path is negligible even when the concentration of Hg_2^{++} ions is 10^5 times as great as that of Hg atoms. From this it can be concluded that the rate constant for this reaction at 25° is less than 1 liter mole^{-1} sec.$^{-1}$, i.e. at least 10^6 times smaller than that for the reaction between Hg and $TlOH^{++}$. The reason for this may be the much more negative entropy of activation which, as indicated earlier, would be expected for a reaction between two ions of like sign, or it may reflect a Franck-Condon barrier to electron transfer (33) resulting from the dimeric configuration of Hg_2^{++}.

Finally, in view of the considerations which led up to this investigation, it seems appropriate to note that the 'two-equivalent' oxidation–reduction process, corresponding to the over-all stoichiometry of the reaction, whether it occurs by electron- or group-transfer, appears to be accomplished in a single step, i.e. that represented by equation [12]. There is no evidence that the rate-determining reaction between Hg and $TlOH^{++}$ involves successive 'one-equivalent' oxidation steps in which Hg(I) (monomeric) and Tl(II) are formed as unstable intermediates and, indeed, the high rate constant for the reaction makes this appear very unlikely. Thus, a mechanism of this type would not provide a favorable path for the oxidation of $Hg(I)_2$ by a one-electron oxidizing agent and the observation that such reactions are very slow is therefore not surprising. An investigation of the kinetics of the oxidation of $Hg(I)_2$ by Ce(IV) and other oxidants is now in progress.

REFERENCES

1. ARMSTRONG, A. M., HALPERN, J., and HIGGINSON, W. C. E.   J. Phys. Chem. **60**, 1661 (1956).
2. ASHURST, K. G. and HIGGINSON, W. C. E.   J. Chem. Soc. 3044 (1953).
3. BELL, R. P. and PANCKHURST, M. H.   Rec. trav. chim. **75**, 726 (1956).
4. BETHGE, P. O., JONEVALL-WESTOO, I., and SILLÉN, L. G.   Acta Chem. Scand. **2**, 828 (1948).

5. BIEDERMANN, G.   Arkiv Kemi, **5**, 441 (1953).
6. BURRIS, C. T. and LAIDLER, K. J.   Trans. Faraday Soc. **51**, 1497 (1955).
7. DUKE, F. R. and BORNONG, B.   J. Phys. Chem. **60**, 1015 (1956).
8. FORSLING, W., HIETANEN, S., and SILLÉN, L. G.   Acta Chem. Scand. **6**, 901 (1952).
9. HALVORSON, H. N. and HALPERN, J.   J. Am. Chem. Soc. **78**, 5562 (1956).
10. HARBOTTLE, G. and DODSON, R. W.   J. Am. Chem. Soc. **73**, 2442 (1951).
11. HIETANEN, S. and SILLÉN, L. G.   Acta Chem. Scand. **6**, 747 (1952).
12. HIETANEN, S. and SILLÉN, L. G.   Arkiv Kemi, **10**, 103 (1956).
13. HIGGINSON, W. C. E.   J. Chem. Soc. 1438 (1951).
14. Kinetics and mechanism of inorganic reactions in solution.   The Chemical Society, London. 1954.
15. KORINEK, J. G. and HALPERN, J.   J. Phys. Chem. **60**, 285 (1956). Can. J. Chem. **34**, 1372 (1956).
16. LAIDLER, K. J.   Discussions Faraday Soc. **22**, 88 (1956).
17. LINDGREN, B., JONSSON, A., and SILLÉN, L. G.   Acta Chem. Scand. **1**, 461 (1947).
18. MARCUS, R. A.   J. Chem. Phys. **24**, 966 (1955).
19. MARCUS, R. A.   J. Chem. Phys. **26**, 867 (1956).
20. MATTOCK, G.   Acta Chem. Scand. **8**, 777 (1954).
21. MOSER, H. C. and VOIGT, A. F.   J. Am. Chem. Soc. **79**, 1837 (1957).
22. PESCHANSKI, D. and VALLADOS-DUBOIS, S.   Bull. soc. chim. France, 1170 (1956).
23. PRESTWOOD, R. J. and WAHL, A. C.   J. Am. Chem. Soc. **71**, 3137 (1949).
24. REICHARDT, H. and BONHOEFFER, K. F.   Z. Elektrochem. **36**, 753 (1930). Z. Physik, **67**, 780 (1931).
25. ROSSOTTI, F. J. C.   J. Inorg. Nuclear Chem. **1**, 159 (1955).
26. SHAFFER, P. A.   J. Am. Chem. Soc. **55**, 2169 (1933).
27. SIDGWICK, N. V.   The chemical elements and their compounds. Vol. I. Oxford University Press,
    London. 1950. pp. 285–292.
28. STOCK, A.   Z. anorg. Chem. **217**, 241 (1934).
29. SUTCLIFFE, L. H. and WEBER, J. R.   Trans. Faraday Soc. **52**, 1225 (1956).
30. SYKES, K. W.   *In* Kinetics and mechanism of inorganic reactions in solution. The Chemical Society,
    London. 1954. p. 64.
31. WESTHEIMER, F. H.   *In* The mechanism of enzyme action. *Edited by* W. D. McElroy and B. Glass.
    Johns Hopkins Press, Baltimore, Md. 1954. p. 321.
32. WOLFGANG, R. L. and DODSON, R. W.   J. Phys. Chem. **56**, 872 (1952).
33. ZWOLINSKI, B. J., MARCUS, R. J., and EYRING, H.   Chem. Revs. **55**, 157 (1955).

N-ACYLATED AMINO ACID IMINO CHLORIDES AND A QUALITATIVE STUDY OF RING CLOSURE AMONG N-ACYLAMINO ACID CHLORIDES[1]

Edward Ronwin[2,3]

ABSTRACT

Products have been isolated from the treatment of N-acylaminoacetonitriles with dry hydrogen chloride which are either the open-chain imino acid chlorides or the dissociated salt forms. These compound types have often been postulated as reaction intermediates but never isolated with an unsubstituted nitrogen atom. In the unsubstituted condition they are analogous to *regular* or oxygen acid chlorides.

Several N-acylamino acids were treated with PCl_5 and the reaction solutions were subjected to infrared spectral analyses. The results indicate that the open-chain acid chloride, rather than the azlactone salt, is the predominant product obtained with the compounds used in this investigation.

N-Acylated Amino Acid Imino Chlorides

This work is an outgrowth of attempts to prepare substrates which comply with the specificity requirements of beef pancreatic carboxypeptidase, but which contain imino ether or amidine linkages at the susceptible link.

Efforts to synthesize the hippuryl imino ether derivatives of *dl*-mandelic and *dl*-malic acids by the Pinner (6, 7) method were unfruitful. Treatment of hippurylnitrile and *dl*-mandelic acid in chloroform with dry HCl gave a product which may be hippuric iminoazlactone.HCl (I), or hippuryl imino chloride (II). The same product was obtained when *dl*-mandelic acid was omitted.
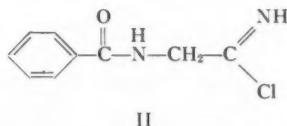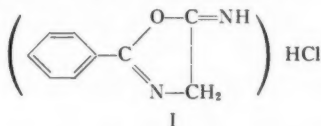
The compound yielded a positive chloride ion test, decomposed sharply at 122°, was readily soluble in concentrated nitric acid, and gave a somewhat acidic solution in water. Analyses for N and Cl were compatible with either structure I or II.

These facts, in themselves, do not permit a definite formula assignment. In the hope of resolving the structure problem, infrared spectral analysis was employed. In addition, *p*-nitrohippurylnitrile and *p*-toluenesulphonylaminoacetonitrile were prepared for a comparison of their behavior. The latter compound could not be synthesized by the Schotten-Baumann method but was obtained by acylation of the nitrile in anhydrous ethyl acetate in the presence of sodium bicarbonate. Upon HCl treatment, these compounds yielded materials having similar properties to those of the hippurylnitrile–HCl compound. All HCl addition compounds are exceedingly hygroscopic and difficult to handle.

The infrared spectra for the nitriles and their HCl reaction products are presented in Fig. 1. The spectrum for N-*p*-toluenesulphonylaminoacetonitrile (Curve A) shows a sulphonyl peak at 8.58μ (part of another peak whose identity is uncertain). Upon treatment with HCl (Curve B), the sulphonyl band remains; however, a new peak appears at 6.06μ. Since the sulphonyl band is unchanged, it is unlikely that this group

WAVE NUMBERS IN CM⁻¹

FIG. 1. Infrared spectra of N-acylated aminoacetonitriles and their HCl-treated products. Baird Associates, Model B, infrared spectrophotometer, sodium chloride prism. All run as Nujol mulls.

has been involved in ring closure. Therefore, the new strong band at 6.06 μ is ascribable to the appearance of a C=NH grouping in the molecule which points to the structure of the compound as either an open-chain imino acid chloride (IIIA) (N-p-toluenesulphonyl-glycyl imino chloride) or the dissociated relative, IVA. The data do not allow a choice between the two formulas nor do they exclude an equilibrium between them.

III
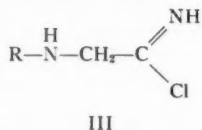
R = A—p-Toluenesulphonyl
B—p-Nitrobenzoyl
C—Benzoyl

IV
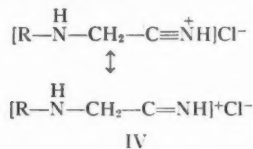
The existence of imino acid chlorides as acylating intermediates in such reactions as the Hoesch ketone synthesis (3), the Stephan aldehyde synthesis (3), the Pinner imino ether and amidine synthesis (6, 7, 8, 9), and the Walther and Grossmann amidine synthesis (11) has been often postulated. While earlier workers have reported the preparation of imino chlorides in which the nitrogen was substituted (6), this is believed to be the first report of the isolation of non-N-substituted imino acid chlorides and supports the proposed mechanisms of the above-mentioned reactions.

The curve for p-nitrohippurylnitrile (Curve C) shows a peak at 6.06 μ due to the amide grouping. The HCl-treated derivative has two peaks (Curve D) in the vicinity, one at 6.06 μ ascribable to the unchanged amide (hence, no ring closure took place) and the other at 5.98 μ due to the formation of a C=NH grouping which points to structure IIIB or IVB for this compound. The spectral picture for hippurylnitrile and its HCl-treated compound (Curves E and F) is much the same as for the other two nitriles and indicates that the HCl addition compound possesses either formula IIIC or IVC.

Qualitative Study of Ring Closure among N-Acylamino Acids

The infrared absorption spectra for several N-acylated amino acids were ascertained. The acids were treated with PCl_5 and samples of the reaction mixture were taken for infrared analysis. The spectral curves are presented in Fig. 2. Controls eliminated the effects observed as due to anything but reaction between the N-acylamino acid and PCl_5.

Group assignments to the various bands is based on the data compilation of Randall *et al.* (10) and by comparison with the band assignments of Carter and Hinman (1) for the free carboxyl group of benzoyl-p-methoxyphenyl-L-alanine (5.82 μ), the carbonyl of its azlactone ring (5.48 μ), and the carbonyl of the azlactone ring of the azlactone.HBr salt (5.35 μ).

N-p-Toluenesulphonylglycine (Curve A) shows a free carboxyl absorption at 5.78 μ and a sulphonyl absorption at 8.58 μ. After treatment with PCl_5 (Curve B), the sulphonyl group remains unchanged and the open-chain acid chloride carbonyl absorption appears at 5.53 μ. This result agrees well with Carter and Hinman's (1), who reported an acid chloride carbonyl band at 5.51 μ for N-p-toluenesulphonyl-p-methoxyphenyl-L-alanyl chloride. Curve C for N-carbobenzoxy-DL-valine and the product resulting from its PCl_5 treatment (Curve D) are typical of the carbobenzoxylated derivatives. The free carboxyl absorption shifts to that of an open-chain acid chloride carbonyl at 5.63 μ. The small but broad and distinct band at 5.42 μ may be due to the N-carboxy derivative or to the closed ring azlactone. The curves for N-carbobenzoxy-DL-leucine (Curves E and F) show almost identical values; those for N-carbobenzoxyglycine (Curves G and H) have bands shifted to slightly shorter wave lengths. These results are in accord with Carter and Hinman's conclusion that N-carbobenzoxy-p-methoxyphenyl-L-alanine yields the open-chain acid chloride which they drew as a result of the reactivity shown by their product. If the bands in the vicinity of 5.40 μ are not due to an N-carboxy derivative, then it would indicate that the reaction in this series is not wholly in one direction, but that some quantity of closed ring azlactone forms, which eluded Carter and Hinman since they isolated only the major product.

These authors noted that their acid chloride "could not be kept for more than a few hours at room temperatures before it passed to the N-carboxy anhydride". The reaction mixtures in this work were maintained at 0° for 24 hours before subjection to infrared analyses. From the shapes of the curves it would seem that the life of the N-carbobenzoxy amino acid chlorides is considerably extended at lower temperatures.

WAVE NUMBERS IN CM^{-1}

WAVE LENGTH IN MICRONS

PER CENT TRANSMITTANCE

Fig. 2 (A to L).

WAVE NUMBERS IN CM⁻¹

PER CENT TRANSMITTANCE

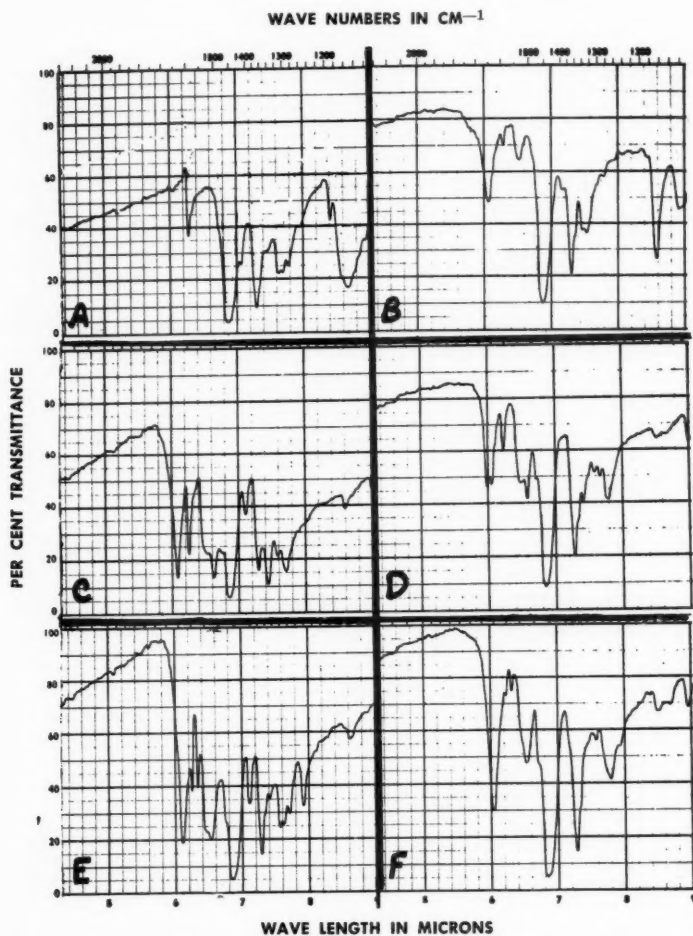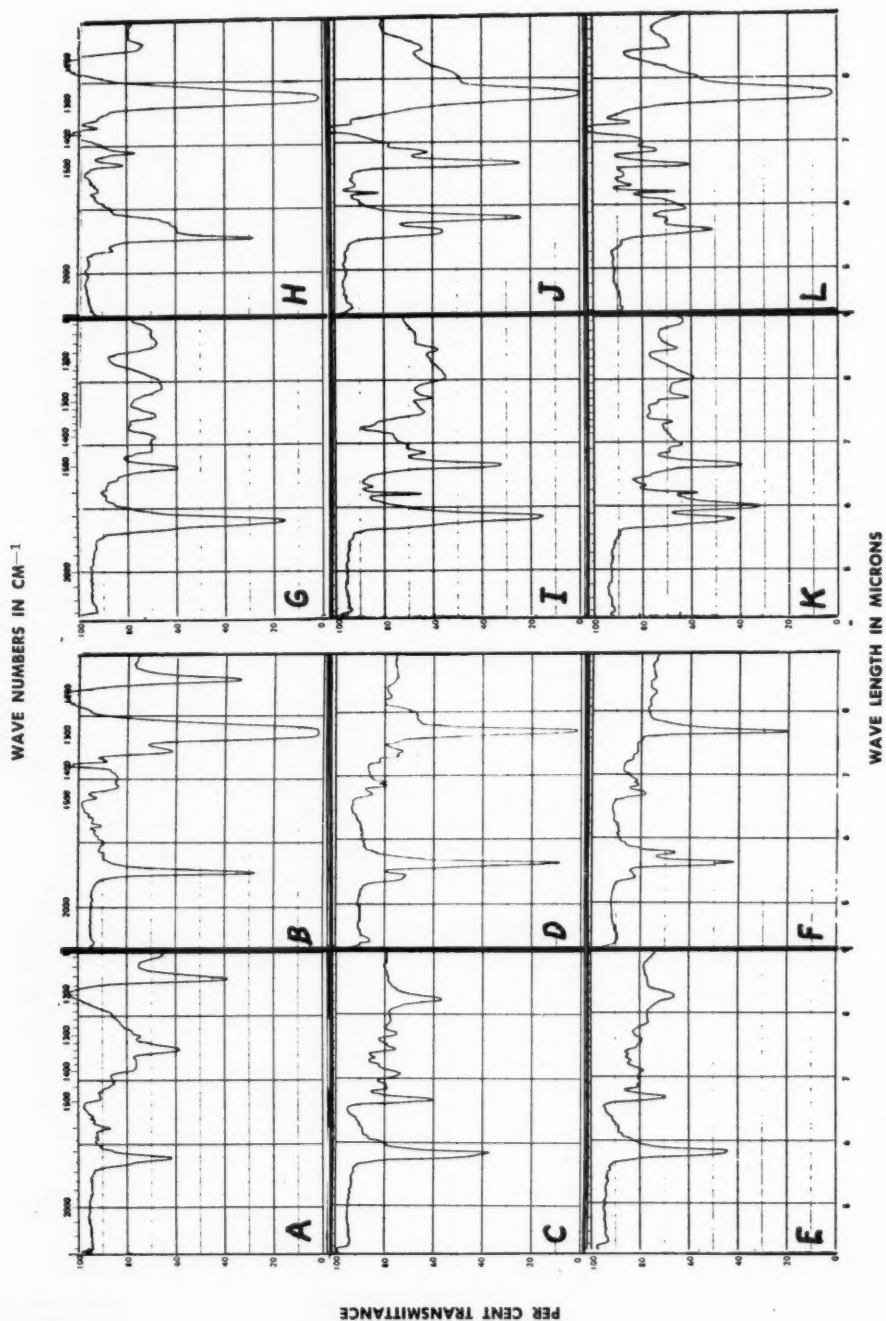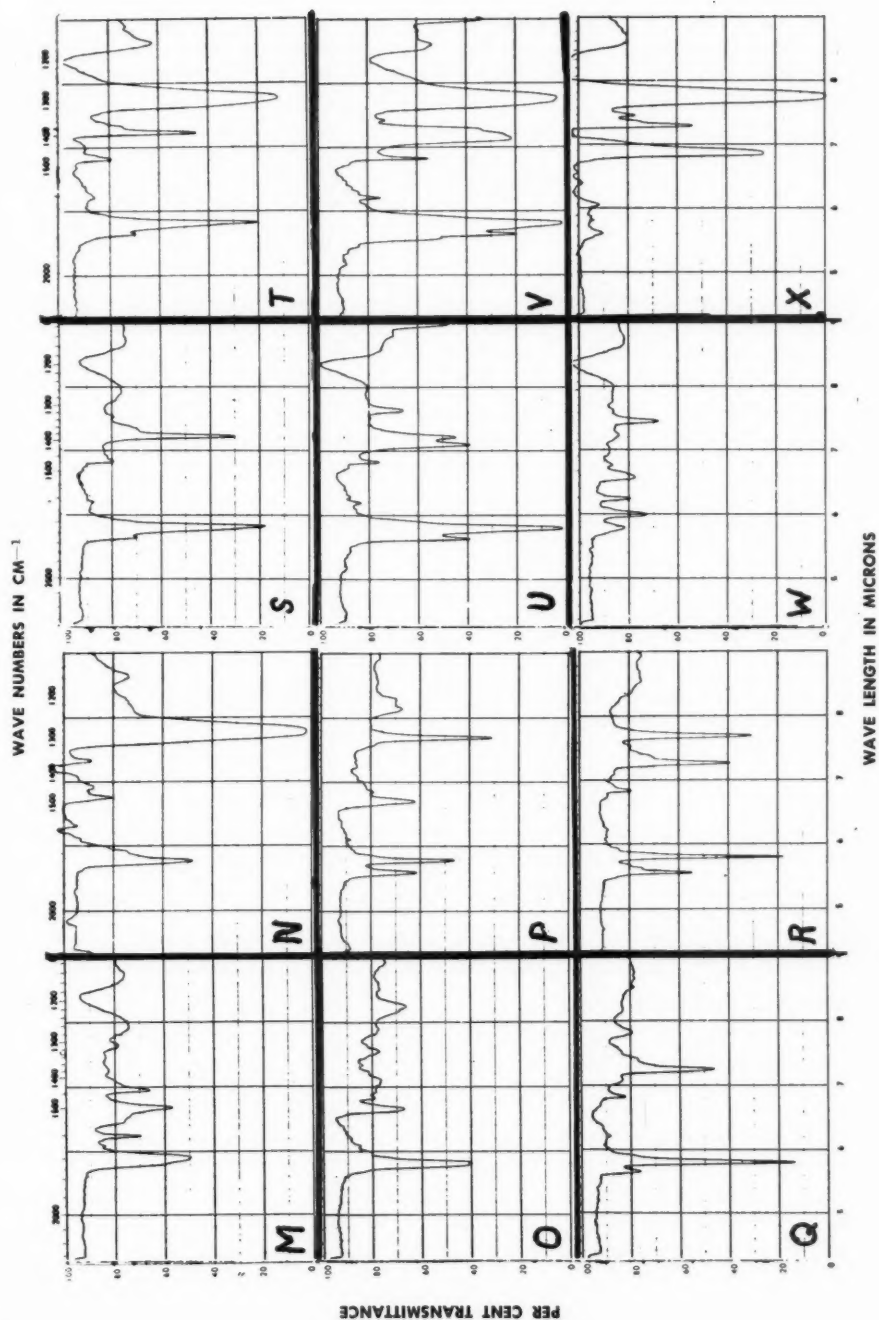WAVE LENGTH IN MICRONS

Fig. 2 (M to X).

Fig 2. Infrared spectra of N-acylated amino acids and their PCl₅-treated product mixtures. Baird Associates, Model B, infrared spectrophotometer, sodium chloride prism, 0.4 mm. cell path length.
Saturated solutions in: CHCl₃—A, B, G, H, I, J, K, L, M, N, S, T, U, V, W, X.   CCl₄—C, D, E, F, O, P, Q, R.

The curve for N-carbobutoxy-*p*-methoxyphenyl-L-alanine (Curve I) shows free carboxyl absorption at 5.84 μ and that for N-acetyl-*p*-methoxyphenyl-L-alanine (Curve K) at 5.80 μ; both results agree well with the absorption value for this group in the benzoyl derivative (1). Upon treatment with PCl_5, the new major bands for both compounds appear at 5.60 μ (Curves J and L). These shifts are similar to the open-chain acid chlorides discussed in the preceding paragraphs and are decidedly less than anticipated for azlactone formation (1, 2). In the case of the carbobutoxy compound, there does not appear to be any indication of N-carboxy anhydride or azlactone formation as is found with the carbobenzoxy derivatives. The small, but definite, band at 5.35 μ for the acetyl derivative may be indicative of azlactone salt formation (no N-carboxy anhydride can form in this case).

N-Carboallyloxyglycine (Curve M) has a free carboxyl absorption at 5.90 μ. After treatment with PCl_5 (Curve N), the carbonyl absorption shifted to 5.76 μ, indicative of acid chloride formation. On the other hand, the free carboxyl absorption for N-carbo-allyoxy-DL-leucine (Curve O) occurred at 5.81 μ and its acid chloride carbonyl absorption peak was found at 5.59 μ (Curve P). The curve of neither PCl_5-treated compound bears any indication of a closed ring carbonyl group. The free acid band accompanying the leucine acid chloride indicates that an incomplete conversion or partial hydrolysis of the product had occurred.

The reaction for all three phthaloyl derivatives with PCl_5 was incomplete (Curves Q to V). The COOH band occurs at 5.80 μ accompanied by the phthalimide carbonyl absorption at about 5.67 μ. After PCl_5 treatment the acid chloride carbonyl absorption is observed in the vicinity of 5.55 μ.

The curve for N-*p*-nitrobenzoylglycine (Curve W) is weak. This was primarily due to the insolubility of the compound and its PCl_5 reaction product in chloroform. Nevertheless, its free carboxyl absorbs at 5.78 μ. Reaction with PCl_5 shifts the carbonyl band to 5.60 μ as for the other acid chlorides (Curve X).

Randall *et al.* (10) assigned a frequency of 5.2 to 5.4 μ for the acid halide carbonyl on the basis of three compounds (acetyl chloride and bromide, and phenacetyl chloride). However, the carbonyl band of benzoyl chloride comes at 5.61 μ, which variation was attributed to the conjugated quality of this carbonyl group. The average value for the acid chloride found here is 5.60 μ. This suggests that the α-carbon of N-acylated amino acid halides (or polypeptides or proteins) is involved in a bond of multiple character, possibly with the α-nitrogen atom.

EXPERIMENTAL

Hippurylnitrile and p-Nitrohippurylnitrile

These compounds were obtained by the procedure of Klages and Haack (4). A 35% yield was realized for hippurylnitrile, m.p. 144° (lit. 144°). *p*-Nitrohippurylnitrile was made in 45% yield, m.p. 144° (lit. 145°).

N-p-Toluenesulphonylaminoacetonitrile

p-Toluenesulphonyl chloride (9.4 g., 0.05 M.), the sulphate salt of aminoacetonitrile (7.7 g., 0.05 M.), and sodium bicarbonate (15.0 g., 0.17 M.) were mixed with 100 ml. of anhydrous ethyl acetate and refluxed for 1½ hours (heating beyond this point caused extensive decomposition). After being refluxed, the mixture was filtered and the filtrate was treated with hexane. A white precipitate formed, which, however, carried along a contaminant. It was found that the contaminant could be removed by dilution preci-

pitation from acetone with hexane. In this way three pure fractions weighing a total of 1.95 g. (19%), m.p. 136° (corr.), were obtained. The compound is soluble in acetone, ethanol, and ethyl acetate, but is insoluble in ether, hexane, chloroform, and water. Anal. Calc. for $C_9H_{10}N_2O_2S$: N, 13.4. Found: N, 13.6.

General Procedure for the Reaction between the Nitriles and HCl

The nitrile (1 to 10 g.) was suspended in dry, redistilled chloroform (20 to 200 ml.) and the suspension was cooled in an ice bath. Then dry HCl gas was passed in for about 30 minutes. The nitriles dissolved almost completely within 10 minutes after the start of the gassing operation. For the cases of hippurylnitrile and the nitrated derivative, the product began to precipitate after 15 to 20 minutes of gassing. No precipitate was observed in the case of p-toluenesulphonylaminoacetonitrile. At the end of the gassing period, the solvent was removed in vacuo.

Hippuryl Imino Chloride

The compound was obtained as white needles which melted with gaseous decomposition at 122° (corr.). It is highly reactive with water and quickly becomes sticky in air, but appears to be indefinitely stable when stored in vacuo. Anal. Calc. for $C_9H_9ClN_2O$: N, 14.3; Cl, 18.1. Found: N, 14.2; Cl, 17.9.

p-Nitrohippuryl Imino Chloride

This material appeared as white needles melting at 216–218° (corr.) with decomposition to a black liquid. Its properties are similar to hippuryl imino chloride. Anal. Calc. for $C_9H_8ClN_3O_3$: N, 17.4; Cl, 14.7. Found: N, 17.2; Cl, 14.3.

N-p-Toluenesulphonylglycylimino Chloride

This compound formed as white crystals which melted with gaseous decomposition at 110–112° (corr.). Its properties are similar to hippuryl imino chloride. Anal. Calc. for $C_9H_{11}ClN_2O_2S$: Cl, 14.4. Found: Cl, 13.6.

The water solutions of all these compounds yield positive chloride ion tests.

N-p-Toluenesulphonylglycine

This acylamino acid was prepared by the method of McChesney and Swann (5) in 37% yield, m.p. 147° (lit. 147°).

N-Carbobutoxy-p-methoxyphenyl-L-alanine

p-Methoxyphenyl-L-alanine (9.8 g., 0.05 M.) was dissolved in 50 ml. of 2 N NaOH. Butyl chloroformate (Pittsburgh Glass Co.) (6.8 g., 6.8 ml., 0.05 M.) was dissolved in 100 ml. of ethyl ether and added to the amino acid solution. The resulting mixture was shaken at room temperature for 1½ hours in a tightly stoppered flask. After the shaking period, the ether layer was separated and discarded. The water layer was acidified to Congo red with 4 N HCl. This precipitated a white oil. After a night in the refrigerator, the oil crystallized. It was filtered off and air-dried. The product was recrystallized from 1:1 ethanol:water. It first appears as an oil, which after scratching becomes crystalline. Pure material (14.8 g., 100%) was obtained, m.p. 84° (corr.), $[\alpha]_D^{25°}$ +30.4° (59.1 mg. in 3 ml. of 95% ethanol). Anal. Calc. for $C_{15}H_{21}NO_5$: N, 4.8. Found: N, 4.9.

Other N-Acylamino Acids

These derivatives were all present in pure form in this laboratory. Before use the melting points of these compounds were checked and found to compare favorably with those previously established in this laboratory or reported in the literature.

General Procedure for the Reaction between the Acylamino Acids and PCl$_5$

From 1 to 2 mg. of the acylamino acid was dissolved or suspended in a few milliliters of dry chloroform and approximately 2 to 3 mg. of PCl$_5$ was added. The test tube was tightly stoppered and left in the refrigerator for 24 hours. A sample of the chloroform solution was subjected to infrared analysis.

ACKNOWLEDGMENT

REFERENCES

1. CARTER, H. E. and HINMAN, J. W.   J. Biol. Chem. **178**, 403 (1949).
2. CLARKE, H. T., JOHNSON, J. R., and ROBINSON, R. The chemistry of penicillin. Princeton Univ. Press, Princeton, N.J. 1949. p. 387.
3. FUSON, R. C.   Advanced organic chemistry. John Wiley & Sons, Inc., New York, N.Y. 1950.
4. KLAGES, A. and HAACK, O.   Ber. **36**, 1646 (1903).
5. MCCHESNEY, E. W. and SWANN, W. K., Jr.   J. Am. Chem. Soc. **59**, 1116 (1937).
6. McELVAIN, S. M. and STEVENS, C. L.   J. Am. Chem. Soc. **69**, 2667 (1947).
7. PINNER, A.   Ber. **16**, 352 (1883).
8. PINNER, A.   Ber. **16**, 1643 (1883).
9. PINNER, A.   Ber. **17**, 179 (1884).
10. RANDALL, H. M., FOWLER, R. G., FUSON, N., and DANGL, J. R.   Infrared determinations of organic structures.   D. Van Nostrand Co., Inc., New York, N.Y. 1949.
11. WALTHER, R. VON and GROSSMANN, A.   J. prakt. Chem. (II), **78**, 478 (1908).

OCCURRENCE OF
2,7-DIHYDROXY-4-ISOPROPYL-2,4,6-CYCLOHEPTATRIEN-1-ONE
(7-HYDROXY-4-ISOPROPYLTROPOLONE) IN WESTERN RED CEDAR
(THUJA PLICATA DONN.)[1]

J. A. F. Gardner, G. M. Barton, and H. MacLean

ABSTRACT

The tropolones of western red cedar were collected as the green copper chelates deposited on copper–bronze screen exposed to the vapor from the heated wood in commercial kilns. Decomposition of the chelates with hydrogen sulphide yielded a new tropolone as well as the expected thujaplicins. Its infrared and ultraviolet absorption together with hydrogenation and oxidation reactions established it to be 2,7-dihydroxy-4-isopropyl-2,4,6-cycloheptatrien-1-one. Synthesis was achieved by persulphate oxidation of γ-thujaplicin. The natural substance is identical with the 7-hydroxyhinokitiol obtained by Nozoe from the diazonium salt of 7-amino-hinokitiol and on the basis of color reactions and R_f appears to be the unknown "enol" previously noted by Zavarin and Anderson in paper chromatography of tropolone fractions of western red cedar and incense cedar. The concentration in the wood, determined by quantitative paper chromatography, ranged from 0.01 to 0.08%.

The generic name tropolone, originally suggested by Dewar (7), has come into general use for 2-hydroxy-2,4,6-cycloheptatrien-1-one and its derivatives which possess special characteristic properties due to the 1,2 arrangement of the carbonyl and hydroxyl groups on an unsaturated seven-membered carbon ring. The literature on the chemistry of these substances has been reviewed recently by Pauson (20) and also by Nozoe (15). In naming derivatives, the carbonyl is taken to occupy position 1 and the hydroxyl position 2. Because tropolones are considered to possess a highly mobile tautomeric system the formulae Ia and Ib are considered to represent a single substance. For such derivatives, the name has been based on the formula Ia, which gives the lowest number for the position of the substituent, in this case 3 instead of 7. However, in the special case where the substituent X is another hydroxyl group, this convention is not altogether satisfactory.

In a symmetrical arrangement of the two hydroxyls about the carbonyl, as in formula II based on I(b), the effect of the neighboring carbonyl will be shared by two equal hydroxyl groups instead of one, and special characteristics assignable to this arrangement would be evident in contrast to that based on I(a). Thus in the case of II use of the 7 terminology rather than the 3 may be more accurately descriptive of the observed properties of the substance and may, therefore, be preferable. Accordingly, in this paper, which describes the isolation, characterization, and synthesis of a naturally occurring hydroxy tropolone, the 3 and 7 positions are differentiated for purposes of nomenclature.

Western red cedar heartwood (*Thuja plicata* Donn.) has been shown to be a rich source of the simplest naturally-occurring tropolones, the isomeric 3-, 4-, and 5-isopropyltropolones, III, IV, and V, known as α-, β-, and γ-thujaplicin respectively (2, 8). Although as much as 1.2% by weight of these potent natural preservatives occurs in the outer butt heartwood of mature trees (14), the preparation of research samples in the laboratory by steam distillation of the wood is tedious and expensive. The volatile oil must be recovered from a relatively large volume of aqueous distillate and consists of a mixture of the desired thujaplicins with thujic acid and its methyl ester (4).
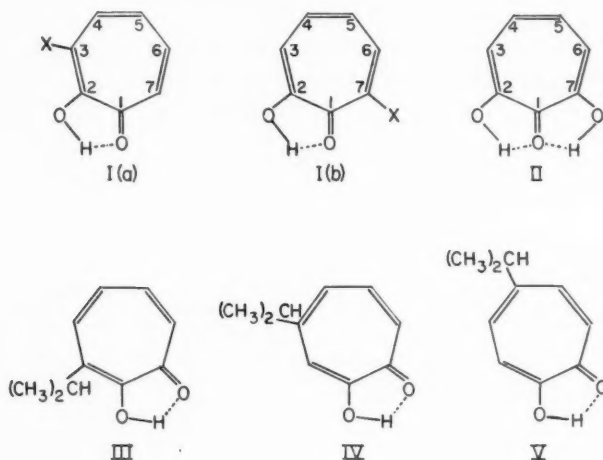
In a search for a simple inexpensive method of preparing large samples of the β and γ isomers, advantage was taken of the ability of the thujaplicins to combine directly with copper. At the temperature used in commercial kilns while drying cedar lumber, 75° to 95° C., a small proportion of the oil of the wood is volatilized and the thujaplicins therein coat any exposed copper with a stable water-insoluble green chelate compound. Thujic acid and its methyl ester, which are also present in the vapor, do not react with copper metal. Accordingly, sheets of copper–bronze screening were installed in the free spaces of commercial kilns being used for drying cedar lumber. After five weeks' exposure, the green deposit which had formed on the screens was washed off with chloroform and the solution concentrated. Decomposition of the copper chelates with hydrogen sulphide yielded an oily mixture of the thujaplicins. This procedure proved to be a convenient and inexpensive method of obtaining research samples of thujaplicin concentrates.

Vacuum distillation of the thujaplicin mixture gave a crystalline high boiling fraction which was not the expected γ-thujaplicin nor either of the lower boiling α and β isomers. After recrystallization from hexane or ethanol, the light-yellow crystals melted at 57.5–58° C. The thujaplicins, α, β, and γ, are colorless, have melting points of 34° C., 51–52° C., and 79–80° C. respectively, and cannot readily be recrystallized from ethanol because of very high solubility in that solvent.

The new substance in chloroform solution gave a red color in the organic layer when treated with aqueous ferric salt solutions and a green color with copper acetate solutions. These color reactions are characteristic of the thujaplicins and other tropolones (20). However, the colors obtained in both cases contained more yellow than those from thujaplicins. Furthermore, the red ferric color was stable to excess ferric ion and no green color was formed in the aqueous layer as is the case with the thujaplicins.

The substance was optically inactive, highly refractive (n_D^{70} 1.6170), distillable with steam, very soluble in organic solvents, and only slightly soluble in water.

Tests for nitrogen, halogen, methoxyl, and carbonyl content were negative. The Folin-Denis test for phenols and the coupling reaction with diazotized p-toluidine were positive. Analytical values for carbon and hydrogen content coincided with the theoretical for the molecular formula $C_{10}H_{12}O_3$, which requires a molecular weight of 180.2. Molecular weight determination by the Rast method gave results ranging from 178 to 224. However,

isothermal distillation in acetone and freezing point depression in benzene gave values of 189 to 190.

Methylation with diazomethane gave a distillable oil (n_D^{22} 1.5828) which analyzed for methoxyl content as a dimethyl ether, $C_{10}H_{10}O(OCH_3)_2$. The crystalline copper chelate analyzed correctly as the monocopper derivative, $C_{10}H_{10}O_3Cu$. The infrared absorption spectra of both these derivatives exhibited no bands assignable to hydroxyl groups.

All of the above properties were in accord with the new substance being a tropolone and, moreover, the molecular weight and analytical and methylation data indicated it to be a thujaplicin containing one additional hydroxyl group.
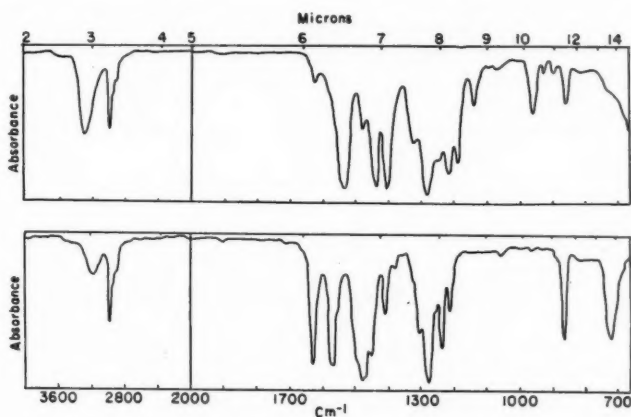

FIG. 1. Infrared spectrum of 2,7-dihydroxy-4-isopropyl-2,4,6-cycloheptatrien-1-one (upper) and 2 hydroxy-5-isopropyl-2,4,6-cycloheptatrien-1-one (lower).

Four different positions for an additional hydroxyl are available in α-thujaplicin (III), namely 4, 5, 6, and 7, and also in β-thujaplicin (IV), 3, 5, 6, and 7. However the product of substitution in the 3 position of β-thujaplicin would be equivalent to that of substitution in the 7 position of α-thujaplicin. Also in the symmetrical γ isomer (V) only the 3 and 4 positions are different and, of these, the product of substitution in the 3 positions would be equivalent to that of substitution in the 7 position in the β isomer. Thus a total of eight possible isomers were to be considered.

The infrared absorption spectrum, compared with that of γ-thujaplicin in Fig. 1, also indicated a substituted thujaplicin structure and was useful in indicating the position of the additional hydroxyl group. The bands in the spectrum of thujaplicin at 1265, 1440, 1468, 1558, 1618, and 3165 cm.$^{-1}$ have been considered by several investigators (3, 11, 12, 22) to be characteristic of the tropolone nucleus. The spectrum of the new substance shows bands at or near these frequencies, namely 1270, 1429, 1467, 1524–1530, 1613, and 3260 cm.$^{-1}$. The sharp band at 2950 cm.$^{-1}$ in the γ-thujaplicin spectrum has been ascribed to C—H stretching on the ring and the inflections at 2930 cm.$^{-1}$ and 2870 cm.$^{-1}$ to the isopropyl group. A similar band at 2955 cm.$^{-1}$ with inflections at 2930 cm.$^{-1}$ and 2870 cm.$^{-1}$ occurs in the spectrum of the new substance.

The broad absorption band of medium intensity at 3160 cm.$^{-1}$ in the case of γ-thujaplicin and at or near there in the case of other simple tropolones has been assigned to the hydroxyl group. The displacement from the free hydroxyl frequency of 3600 cm.$^{-1}$ has

been attributed to rather strong intramolecular hydrogen bonding. In the new compound, the strong broad band at 3260 cm.$^{-1}$ indicates weaker hydrogen bonding, almost weak enough to be assigned to intermolecular polymeric association bonds. However, as this band does not disappear in dilute solutions in carbon tetrachloride and no dimeric or free hydroxyl bands appear in the 3450–3600 cm.$^{-1}$ region, intermolecular polymeric association bonds are ruled out since only intramolecular hydrogen bonds are independent of the concentration (5).

The presence of only one strong hydroxyl band moderately displaced in the spectrum suggested symmetrical placement of the two hydroxyl groups in the molecule about the carbonyl. This arrangement would account for weaker hydrogen bonding than in a simple tropolone since the influence of the carbonyl would be shared between two hydroxyls instead of one. Of the possible isomers only two would have this arrangement, the 7-hydroxy derivative (VI) of α-thujaplicin and the 7-hydroxy derivative (VII) o
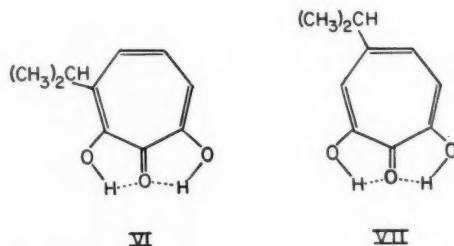
β-thujaplicin. Of these, the latter was more attractive because of the more nearly symmetrical placement of the isopropyl group in relation to the hydroxyls. In the former, the adjacent position of the isopropyl group would be expected to influence one of the hydroxyls, giving rise to two bands in the spectrum.

The band due to the C=O bond occurs in the 1610–1630 cm.$^{-1}$ region in tropolones, the large shift from normal frequencies being assigned to conjugation, ring strain, and to some extent intramolecular hydrogen bonding (11, 12). The band in this region in the spectrum of the new compound (1613 cm.$^{-1}$) is much less intense than the corresponding band for γ-thujaplicin (1618 cm.$^{-1}$). A non-symmetrical placement of the additional hydroxyl groups about the carbonyl, as in the 4, 5, or 6 position, would correspond to normal substituted tropolone structure and in dilute solution should give normal intensity in the 1610–1630 cm.$^{-1}$ region.

In investigating the hydroxylation of tropolone, Nozoe et al. (17) obtained the 5-hydroxyl derivative and small yields of the 3-hydroxyl (or 7-hydroxyl) derivative by alkaline persulphate oxidation. However, with α- and β-thujaplicin only the 5-hydroxyl derivatives were obtained (17). However, previously, in examining the diazo reactions of 7-aminohinokitiol (hinokitiol = β-thujaplicin) Nozoe, Kitahara, and Doi (16) obtained a crystalline product, m.p. 44–58° C., which was separated by fractional crystallization into three modifications melting at 59–60° C., 51–52° C., and 45–46° C. respectively. These analyzed correctly as the hydroxyl derivative and were believed by the authors to be tautomers of 7-hydroxyhinokitiol. No derivatives were described but in a later publication the ultraviolet absorption spectrum determined in iso-octane was given (18). The spectrum of the new substance from cedar in the same solvent (Fig. 2) appeared to be identical, exhibiting the same marked fine structure and enhanced intensity in the
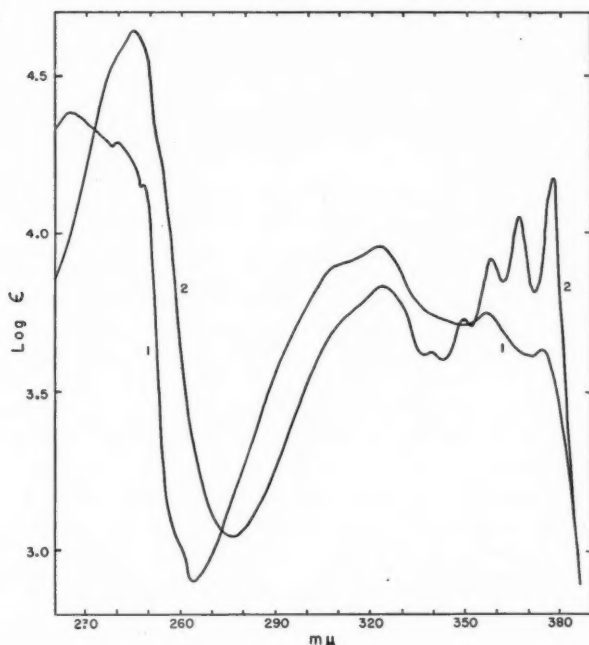
Fig. 2. Ultraviolet spectrum of 2-hydroxy-5-isopropyl-2,4,6-cycloheptatrien-1-one (Curve 1) and 2,7-dihydroxy-4-isopropyl-2,4,6-cycloheptatrien-1-one (Curve 2) in 2,2,4-trimethylpentane (iso-octane).

long wave region. Similar fine structure and enhanced intensity in this range compared with that of tropolone have also been observed for 3-hydroxy tropolone (2,7-dihydroxy-2,4,6-cycloheptatrien-1-one) (10, 18).

The structure 2,7-dihydroxy-4-isopropyl-2,4,6-cycloheptatrien-1-one (7-hydroxy-4-isopropyltropolone) (VII), favored for the new tropolone over the other seven possible isomers by the spectral data, was proved by a degradative experiment and synthesis (Fig. 3). Hydrogenation over Adams' catalyst used the theoretical 4 moles of hydrogen, yielding a crystalline product which analyzed correctly as the triol, $C_{10}H_{20}O_3$ (VIII). This product on oxidation consumed 2 moles of periodate and produced 1 mole of formic acid, in agreement with theory. The cleavage product from this oxidation was not isolated but was oxidized with alkaline permanganate to β-isopropyl adipic acid, identical with a synthetic sample. These results proved the vicinal arrangement of the three oxygens on the ring and fixed the relative position of the isopropyl group.

Of the three possible tautomeric structures which may be written to satisfy the vicinal arrangement of the carbonyl and two hydroxyl groups, the infrared absorption spectrum, as pointed out above, clearly indicates the symmetrical arrangement, i.e. a hydroxyl on each side of the carbonyl.

In the hydroxylation of simple phenols by treatment with alkaline persulphate solutions, satisfactory yields of the ortho isomer are obtained only when the para position is already substituted. Similarly in the case of tropolone, the product is a mixture of the 5- and 7(or 3)-hydroxy derivatives in which the former predominates. Blocking of the 5 position in tropolone with an isopropyl group as in γ-thujaplicin (corresponding to the
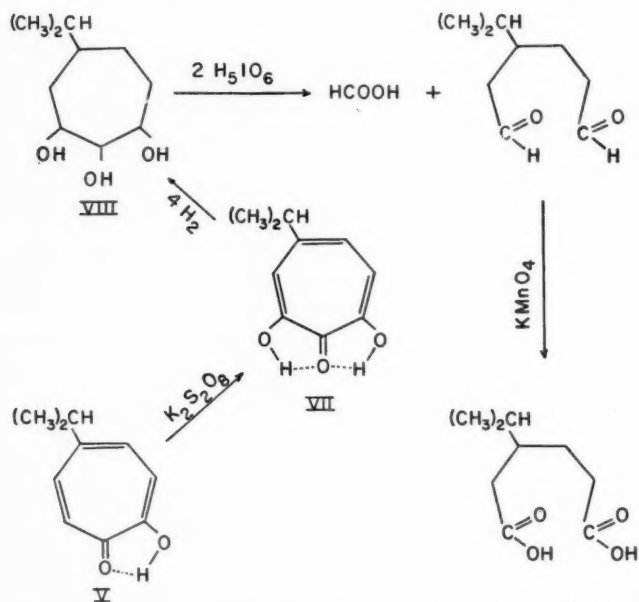
FIG. 3. Proof of structure of 2,7-dihydroxy-4-isopropyl-2,4,6-cycloheptatrien-1-one.

para position in phenol) should lead to hydroxylation only in the equivalent 3 and 7 positions (corresponding to ortho) and yield one isomer, the desired 2,7-dihydroxy-4-isopropyl-2,4,6-cycloheptatrien-1-one (VII). On this theory, the oxidation of γ-thujaplicin by alkaline persulphate was investigated. The product obtained in 28% yield was identical with the natural substance.

The possibility was examined that 7-hydroxy-4-isopropyltropolone (VII) did not occur in the cedar but had been generated from the thujaplicins by a copper catalyzed oxidation during the isolation procedure. Samples of steam volatile oil prepared from the wood in all glass apparatus were examined by the paper chromatographic technique for tropolones developed by Zavarin and Anderson (24). 7-Hydroxy-4-isopropyltropolone proved to be present in all samples tested. Furthermore it exhibited the same R_f and violet color reactions on paper as the unknown "enol" first noted by Zavarin and Anderson on paper chromatograms of the tropolone fraction of western red cedar and also incense cedar (*Libocedrus decurrens* Torr.).

The content of 7-hydroxy-4-isopropyltropolone in cedar was determined by quantitative paper chromatography of the steam volatile oil obtained by exhaustive steam distillation of the finely ground wood. The results for four samples of cedar heartwood are compared in Table I with the thujaplicin content determined by a colorimetric method (13).

In the richest sample, which also contained the highest thujaplicin content, the content of 7-hydroxy-4-isopropyltropolone was less than 0.1% of the wood and approximately one-tenth of the thujaplicin content. This low content and the relatively low order of toxicity to fungi compared with thujaplicin found in toxicity tests (21) indicate that 7-hydroxy-4-isopropyltropolone is a minor influence on cedar wood durability.

The high proportion (50%) of 7-hydroxy-4-isopropyltropolone in the tropolone fraction

TABLE I

CONTENT OF 7-HYDROXY-4-ISOPROPYLTROPOLONE AND
THUJAPLICINS IN WESTERN RED CEDAR HEARTWOOD
(results in percentage of moisture-free wood)

7-Hydroxy-4-isopropyltropolone	Thujaplicins
0.01	0.026
0.01	0.16
0.05	0.44
0.08	0.78

obtained by use of the copper–bronze screen technique in spite of its relatively low concentration in the volatile oil may be due to its greater reactivity with copper as compared with the thujaplicins.

The extent of interference of 7-hydroxy-4-isopropyltropolone in the previously reported analytical method for thujaplicins in cedar wood (13) was determined by control tests. Owing to unfavorable solubility in the solvents prescribed and relatively poor color response, it was found that concentrations of up to 0.05% in the wood did not interfere.

Recently, the occurrence of another natural tropolone, chamaecin, in the essential oil of Formosan hinoki (*Chamaecyparis Taiwanensis* Masamune et Suzuki) has been reported (23). The authors suggested that chamaecin is an ether of 7-hydroxy-4-isopropyltropolone (7-hydroxyhinokitiol) based on analytical values and its rearrangement by alkali fusion to 2-hydroxy-4-isopropyl benzoic acid.

After completion of this paper a sample of pure 7-hydroxyhinokitiol, m.p. 57–58° C., synthesized from 7-aminohinokitiol by Nozoe *et al.* (16), became available together with its infrared absorption spectrum.* A mixed m.p. with 7-hydroxy-4-isopropyltropolone from western red cedar showed no depression and the infrared absorption spectra and R_f characteristics were identical.

EXPERIMENTAL

Evaporations were carried out under reduced pressure at 40° C. Melting points were determined on a Fisher-Johns melting point apparatus and are uncorrected. Carbon and hydrogen microanalyses were done by Clark Microanalytical Laboratory, Urbana, Illinois, and W. Manser, Herrliberg, Switzerland. Infrared absorption spectra were determined on a Perkin-Elmer Model 21 spectrophotometer at the British Columbia Research Council. Ultraviolet absorption spectra were determined with a Beckman DU spectrophotometer.

Isolation of 7-Hydroxy-4-isopropyltropolone (VII)

Copper–bronze screen (18 mesh) was stretched over wooden frames in the free space of a commercial kiln being used for drying high grade western red cedar lumber at temperatures between 75° and 95° C. After 5 weeks of exposure, the screen which had become light green in color was removed from the kiln and washed with chloroform. The resultant green chloroform solution was filtered through hyflo supercel and concentrated. Removal of solvent left the crude crystalline copper derivatives of the tropolones (2.4 g. per sq. ft. of screen).

The copper derivatives were decomposed by saturating a chloroform solution with hydrogen sulphide and removing the precipitated copper sulphide by filtration. Solvent

Private communication from Tetsuo Nozoe, Chemical Institute, Tôhoku University, Sendai, Japan, March 27, 1957.

removal left a mixture of tropolones as an oil which was distilled through a simple widmer (bath temp. 140–180° C./0.5 mm.). Yield from copper derivatives, 84%. The product distilling in the 150–180° C. range was light yellow in color and crystallized spontaneously.

Trituration with cold hexane, filtration, and recrystallization from hexane gave light yellow crystals, m.p. 54–55° C. Recrystallization from hexane, ethanol, or ethanol–water raised the melting point to 57.5–58° C., n_D^{70} 1.6170. Fractional crystallization of the lower boiling fractions gave additional material. A total of 62 g. was obtained from 122.5 g. of distilled tropolone mixture. Calc. for $C_{10}H_{12}O_3$: C, 66.65; H, 6.71; mol. wt. 180.2. Found: C, 66.67; H, 6.46; mol. wt. 190 by freezing point depression in benzene, 189 by isothermal distillation in acetone (6). For the infrared absorption spectrum in carbon tetrachloride see Fig. 1 and the ultraviolet absorption spectrum in iso-octane see Fig. 2.

Copper Chelate of 7-Hydroxy-4-isopropyltropolone (VII)

This was prepared in quantitative yield by shaking chloroform solutions of VII with 5% aqueous copper acetate solutions, washing with bicarbonate solution and water, and removing the solvent. Green needles, recrystallized from chloroform or chloroform–ethanol, m.p. 237–238° C. Calc. for $C_{10}H_{10}O_3Cu$: C, 49.69; H, 4.17; Cu, 26.29. Found: C, 49.66; H, 4.21; Cu, 26.34. $\nu_{max}^{CCl_4}$ in cm.$^{-1}$: no hydroxyl band, *2985*, 1621, *1525*, *1500*, *1423*, *1326*, *1305*, 1250, *1212*, 1185, 940, 900, 873, 838, 692.*

Dimethyl Ether of 7-Hydroxy-4-isopropyltropolone (VII)

Prepared by treatment with excess diazomethane in ether solution. The crude ether obtained after removal of the solvent was distilled in a Späth tube (bath temp., 50–155° C. at 0.5 mm.) to yield a yellow oil, n_D^{22} 1.5828. Calc. for $C_{10}H_{10}O(OCH_3)_2$: OCH$_3$, 29.7. Found: OCH$_3$, 29.4. $\nu_{max}^{CCl_4}$ in cm.$^{-1}$: no hydroxyl band, *2985*, *1630*, *1590*, 1505, *1469*, 1438, 1400, 1368, 1342, 1315, *1250*, *1238*, 1192, *1158*, *1132*, 1062, 991, 845.

Hydrogenation of 7-Hydroxy-4-isopropyltropolone (VII) to the Triol (VIII)

A solution of 7-hydroxy-4-isopropyltropolone (0.497 g.) in ethanol (75 ml.) was hydrogenated at atmospheric pressure in all glass apparatus using Adams' catalyst (0.2 g.). The absorption of hydrogen ceased in 20 minutes, the theoretical volume for absorption of 4 moles having been consumed. The residue (0.494 g.) crystallized after the removal of catalyst and solvent, m.p. 111–114° C. Recrystallization from ethyl acetate gave colorless needles, m.p. 112–113° C. Anal. Calc. for $C_{10}H_{20}O_3$: C, 63.79; H, 10.71. Found: C, 63.75; H, 10.76.

Periodate Oxidation of the Triol (VIII)

The octahydro derivative (0.1095 g.) was dissolved in water, 0.1M sodium meta-periodate solution (25 ml.) added, and the total volume adjusted to 100 ml. with water. The solution was kept at room temperature in the dark for 4 hours before analysis. Periodate consumption was determined on an aliquot (5 ml.) by the usual arsenite method (9). Simultaneously formic acid production was determined on a similar aliquot using the iodometric method (1). Blank determinations were conducted in each case. Found: periodate consumption, 2.07 moles; formic acid formed, 0.995 moles.

Oxidation of Periodate Cleavage Product to β-Isopropyl Adipic Acid

The above periodate oxidation solution (70 ml.), remaining after withdrawal of the aliquots for analysis, was extracted with diethyl ether. After removal of the solvent, the residual oil was dissolved in water, the solution made alkaline with sodium bicarbonate,

Frequencies of peaks of high intensity are printed in italics.

and dilute potassium permanganate solution added dropwise until a pink color persisted. The mixture was filtered, acidified, and the excess permanganate decomposed with sodium bisulphite before extraction with diethyl ether. The ether solution was extracted with 5% sodium bicarbonate solution, the bicarbonate solution acidified, and the acid re-extracted into diethyl ether. Evaporation of the solvent gave colorless crystals (0.04 g.), m.p. 78–80° C. Recrystallization raised the melting point to 80–80.5° C. A mixed melting point with β-isopropyl adipic acid, m.p. 79–80° C., prepared by permanganate oxidation of 4-isopropylcyclohexanol (19), showed no depression.

Persulphate Oxidation of γ-Thujaplicin (V) to 7-Hydroxy-4-isopropyltropolone (VII)

γ-Thujaplicin (0.5 g.) was dissolved in 10% potassium hydroxide solution (5.7 ml.) and the solution stirred in an ice bath for 2 hours while potassium persulphate (0.99 g.) in water solution (20 ml.) was added through a dropping funnel. The solution turned from a yellow to brown color and some tar was deposited. After the mixture had been kept overnight at 15° C., it was acidified to pH 4 and extracted with ether (2×5 ml.). The extracted solution was then acidified to pH 2, heated 1 hour on the steam bath, adjusted to pH 4, and again extracted with ether (2×10 ml.). The solution was washed with water and dried over sodium sulphate before removal of the solvent to leave light yellow crystals (0.03 g.), m.p. after recrystallization from ethanol–water, 57–58° C. The substance had the same R_f and color reactions as 7-hydroxy-4-isopropyltropolone isolated from cedar wood and a mixed melting point showed no depression.

The ether extract obtained in the first extraction at pH 4 was extracted with 3 N sodium hydroxide solution (2×3 ml.) and the alkaline extract cooled to 0° C. The sodium salt (0.17 g.) of γ-thujaplicin crystallized out and was collected on a stainless steel filter. The filtrate was acidified and extracted with ether. Removal of the solvent left an oil (0.136 g.) which by paper chromatographic analysis contained γ-thujaplicin (0.09 g.) and additional 7-hydroxy-4-isopropyltropolone (0.046 g.). Yield based on γ-thujaplicin consumed, 28%.

Paper Chromatography

The qualitative technique of Zavarin and Anderson (24) using paper impregnated with phosphoric acid was employed. Toluene was used as developing solvent. For quantitative determinations, the appropriate areas of the paper were excised and eluted with isopropyl alcohol. By comparing the absorbance of the eluted solutions at 375 mμ with those prepared in exactly similar manner from standard solutions of reference samples, the concentrations of the various tropolones in the solutions examined were calculated.

ACKNOWLEDGMENTS

REFERENCES

1. ABDEL-AKHER, M. and SMITH, F. J. Am. Chem. Soc. **73**, 994 (1951).
2. ANDERSON, A. B. and GRIPENBERG, J. Acta Chem. Scand. **2**, 644 (1948).
3. AULIN-ERDTMAN, G. and THEORELL, H. Acta Chem. Scand. **4**, 1490 (1950).
4. BARTON, G. M. and GARDNER, J. A. F. Pulp Paper Can. **55** (10), 132 (1954).
5. BELLAMY, L. J. The infra-red spectra of complex molecules. Methuen & Co., London. 1954. p. 89.
6. CHILDS, C. E. Anal. Chem. **26**, 1963 (1954).
7. DEWAR, M. J. S. Nature, **155**, 50 (1945).
8. ERDTMAN, H. and GRIPENBERG, J. Acta Chem. Scand. **2**, 625 (1948).
9. FLEURY, P. and LANGE, J. J. pharm. chim. (8), **17**, 107 (1933).
0. JOHNS, R. B., JOHNSON, A. W., and TISLER, M. J. Chem. Soc. 4605 (1954).

11. KOCH, H. P. J. Chem. Soc. 512 (1951).
12. KURATANI, K., TSUBOI, M., and SHIMANOUCHI, T. Bull. Chem. Soc. Japan, 25, 250 (1952).
13. MACLEAN, H. and GARDNER, J. A. F. Anal. Chem. 28, 509 (1956).
14. MACLEAN, H. and GARDNER, J. A. F. Forest Prod. J. 6, 510 (1956).
15. NOZOE, T. Progress in the chemistry of organic natural products. Vol. XIII. Springer-Verlag, Vienna.
    1956. p. 234.
16. NOZOE, T., KITAHARA, Y., and DOI, K. Proc. Japan Acad. 27, 282 (1951).
17. NOZOE, T., SETO, S., ITO, S., SATO, M., and KATANO, T. Proc. Japan Acad. 28, 488 (1952).
18. NOZOE, T., SETO, S., ITO, S., SATO, M., and KATANO, T. Sci. Repts. Tôhoku Univ. First Ser., 37,
    191 (1953).
19. OVERBERGER, C. G., FISCHMAN, A., ROBERTS, C. W., AROND, L. H., and LAL, J. J. Am. Chem. Soc.
    73, 2540 (1951).
20. PAUSON, P. L. Chem. Revs. 55, 9 (1955).
21. ROFF, J. W. and WHITTAKER, E. I. Forest Products Laboratory, Vancouver, British Columbia.
    Unpublished results.
22. SCOTT, G. P. and TARBELL, D. S. J. Am. Chem. Soc. 72, 240 (1950).
23. YAU-TANG LIN, KUNG-TSUNG WANG, and CHEN-LOUNG CHEN. Bull. Chinese Assoc. Advance. Sci.
    (3), 6, 13 (1956).
24. ZAVARIN, E. and ANDERSON, A. B. J. Org. Chem. 21, 332 (1956).

LIGHT ABSORPTION STUDIES

PART VIII. THE SECONDARY BAND OF ACETOPHENONES AND BENZOIC ACIDS IN ULTRAVIOLET SPECTRA[1]

W. F. Forbes, W. A. Mueller,[2] Audrey S. Ralph, and J. F. Templeton

ABSTRACT

The absorption spectra of some acetophenones and benzoic acids have been measured in different solvents in the region 220–400 mμ. The two major bands are compared and it is found that steric interactions which considerably alter the high-intensity band have less and somewhat different effects on the secondary band. Solvent effects and the changes observed on substitution indicate that the weaker band (C-band) is essentially of similar character to the high intensity primary band (B-band). A unifying hypothesis to account for the observed changes is presented.

INTRODUCTION

In previous parts of this series (12, 13, 16) and elsewhere (5 and references cited therein), steric effects in the B-band of the acetophenone series were classified into three types. Generally it was found that the location of maximal absorption of this band depended primarily on the steric and mesomeric (resonance) effects of the substituents (cf. 16, 18). The present investigation is intended to examine the secondary band in this region, and to present a consistent explanation in terms of electrical and steric effects for the changes observed in this band.

The secondary band will be referred to as the C-band, and the main absorption band as the B-band, following the nomenclature adopted by Moser and Kohlenberg (26). This alphabetical order assigns the letters A, B, and C to the bands as they are normally found proceeding from about 200 mμ to longer wavelength. Other designations have been proposed for this C-band, which has also been referred to as the B-band (3) to indicate its association with "benzene". This latter designation receives support since the symmetry assignment of the excited state is most probably B_{2u} (cf. 2). Alternatively the band has been described as the secondary band (10), because the band is of much smaller intensity and therefore in a sense "secondary". The approximate wavelength and intensity ranges of the bands are as follows: The C-band normally lies in the wavelength range $\lambda = 270$–360 mμ with ϵ values between about 250 and 6000, whereas the B-band occurs around $\lambda = 200$–320 mμ with ϵ values in the range 6000–20,000.

THE C-BAND IN ULTRAVIOLET ABSORPTION SPECTRA

Monosubstituted Benzenes

It is well known that the C-band of the compounds listed in Table I has been ascribed to transitions involving the benzene ring, since similar bands are found in phenols, anilines, and in a large number of other benzenoid compounds, as well as in benzene itself. In most cases the intensity of absorption of the C-band is considerably smaller than the intensity of the B-band. For benzene the C-band is located at approximately 260 mμ ($\epsilon = 250$). For monosubstituted benzene derivatives, both B- and C-bands are displaced to longer wavelengths and often maintain, regardless of the degree of displacement, a relatively regular wavelength relationship. (Doub and Vandenbelt (10) report

TABLE I

ABSORPTION SPECTRA OF SUBSTITUTED ACETOPHENONES AND BENZOIC ACIDS

Wavelengths and intensities of the B- and C-bands (values in italics represent inflections in this and subsequent tables)

Substituent	Acetophenones								Benzoic acids							
	Absolute or 95% ethanol				Cyclohexane or ether				Absolute or 95% ethanol				Cyclohexane or ether			
	B-band		C-band		B-band		C-band		B-band		C-band		B-band		C-band	
	λ_{max} mμ	ϵ_{max}	λ_{max} mμ	ϵ_{max}	λ_{max} mμ	ϵ_{max}	λ_{max} mμ	ϵ_{max}	λ_{max} mμ	ϵ_{max}	λ_{max} mμ	ϵ_{max}	λ_{max} mμ	ϵ_{max}	λ_{max} mμ	ϵ_{max}
None	240	12,500[1]	276	1000[1]	237–238	12,500	277	900	227	11,000[2]	271 / 279	760[4] / 550	230	13,000[7]	275 / 280	750[4] / 760
(Toluene)																
o-Methyl-	242	8500[1]	283	1250[1]	207	9500	260	300	207 / 228	9300 / 5000[2]	260 / 279	300 / 725[3]				
m-Methyl-	244–245	11,200	285 / 291	1300 / 1200	241–242 / 246	11,300 / 9850	ca. 277 / 283 / 293	975 / 1200 / 1000	232	9000[2]	279	1000[3]				
p-Methyl-	252	15,000[1]	278	850[1]	247	15,000	273 / 286	900 / 600	236	14,000[2]	—	—	238	13,000[7]	266 / 279	760 / 550
2,6-Dimethyl-	251 / 256	5600[3] / 5200	281 / 290	890[3] / 740					—	—[3]	270	725[3]				
(Fluorobenzene)																
o-Fluoro-	236	10,000	280	1550	233	9500	279	1600	204	6200[4]	254	900[4]	225–226	10,500	276 / ca. 284	2000 / 1600
m-Fluoro-	236	10,500	281 / 289	1700 / 1250	235	10,500	280 / 290	1700 / 1250	223	9500[2]	273 / 280	1020 / 1900	228	11,000[7]	277	1900 / 1700
p-Fluoro-	242	11,500	—	—	240	12,000	266	850	225	10,000[3]	274 / 281	1700 / 1400	230	12,600[7]	263 / 269	650 / 400
(Chlorobenzene)																
o-Chloro-	238	5500	281	750	235	5700	280 / 286 / 295	650 / 1100 / 900	228	11,000[2]	262 / 268	500 / 300	237	15,000[4]	280	1000[4]
m-Chloro-	240	10,000	286	1050	239	10,000	272 / 284	900 / 500	210 / 229	7500[4] / 5000[2]	257 / 278	170[4] / 760[3]				
p-Chloro-	249	16,000	286	660	249	17,000			230	8500[2]	284	950[3]			275	730[4]
2,6-Dichloro-									234	15,000[2]	—	—				
(Bromobenzene)																
o-Bromo-	234–236	4900	282	780	234–236	4900	282	700	210 / 224	8600[4] / 6600[2]	264 / 274	440[3] / 500			282	1050[4]
m-Bromo-	240	9500	287 / ca. 293	1050 / 960	240 / ca. 245–246	10,000 / 8000	ca. 282 / 287 / 296	900 / 1100 / 950	225	8500[2]	261 / 262 / 282	200[4] / 560[3] / 760			284	1100[4]
p-Bromo-	253	16,000	286	900	253	19,500	286	600	238.5	16,000[2]	280	830[3]	212	16,100[4]	270	800[4]
2,6-Dibromo-									—	—	262 / 272	930[3] / 870				

TABLE I (cont'd)

TABLE I (*concluded*)

ABSORPTION SPECTRA OF SUBSTITUTED ACETOPHENONES AND BENZOIC ACIDS

Wavelengths and intensities of the B- and C-bands (values in italics represent inflections in this and subsequent tables)

Substituent	Acetophenones								Benzoic acids							
	Absolute or 95% ethanol				Cyclohexane or ether				Absolute or 95% ethanol				Cyclohexane or ether			
	B-band		C-band		B-band		C-band		B-band		C-band		B-band		C-band	
	λmax mμ	εmax	λmax mμ	εmax	λmax mμ	εmax	λmax mμ	εmax	λmax mμ	εmax	λmax mμ	εmax	λmax mμ	εmax	λmax mμ	εmax
(Iodobenzene)																
o-Iodo-	224	24,500			224	24,500			226	13,000[4]	256	800[4]	ca.232; ca.240; ca.247	8600; 7000; 4600	286	1600
m-Iodo-	250	7100	295	1040	246; 250	6800; 6000	292	1050	233	7000[2]	285	1450	233	9800	283; 291	1000; 900
p-Iodo-	262	16,000	—	—	263	19,500	300	930	217; 251–252	26,000; 18,000[2]	284; 290	950; 900	251–252	18,500	ca.283	1350
(Phenol)																
o-Hydroxy-					210	6000	263; 269; 276	1400; 2200; 2100	218.5	6000	271	1900	237–238	8000[7]	307	4400[4]
m-Hydroxy-					251	9700[4]	327	3800[4]	236	7500[7]	307	3700[3]	235–236	6500[7]	296	2900[4]
p-Hydroxy-					246	8900[4]	306	2900[4]	234–235; 253–254	6000[7]; 15,000[7]	301	2200[3]	251	15,000[7]	—	—[4]
2,6-Dihydroxy-					267	19,100	—	—	250	6300[4]	277; 311	1950[3]; 3500	—	—	—	—
(Anisole)																
o-Methoxy-					220	7500	270; 276	2100; 2100	219	7000	270; 277	1700; 1500				
m-Methoxy-					246	8000[4]	306	2600[4]	230	6000[3]	291	2700[3]	234	7000[4]	291	3500[4]
p-Methoxy-					246	8500[4]	304	2800[4]	230	7000[3]	293	2450[3]	251	18,300[3]	295	2500[4]
2,6-Dimethoxy-					266	18,000[4]	—	—	249	14,000[3]	282	1850[3]	—	—	—	—[4]
(Aniline)																
o-Amino-	254	5600	359	4350	233–234; 252	8500; 5500	286; 347	1800; 4350	234–236; 247	8000; 6500	284–285; 332	1600; 4500	252	7400[4]	333	5200[4]
m-Amino-	231	23,000	338	1900	226; 246	26,500; 9000	320	2500	ca.241	7000	319	2100	244	7800[4]	320	2800[4]
p-Amino-	316	20,000	—	—	285	19,000	—	—	288	19,000	—	—	277	20,600[4]	—	—[4]
(Nitrobenzene)																
o-Nitro-	257	6000	—	—	252	9000	ca.285	1600	257–258; ca.260	8000; 3500	—	—	—	—	ca.278	1350
m-Nitro-	226; ca.260	22,500; 6600	ca.300	800	224; 254	23,000; 7000	288; 298	1100; 750	255	7500	—	—	250–251	7000	ca.278; ca.296	1100; 600
p-Nitro-	261	14,000	ca.298; ca.312	2200; 1200	258	14,000	292; 308	2000; 1000	258	12,000	ca.294	2500	255	13,000	ca.294	2000

[1]Ref. 12. [2]Ref. 19. [3]Ref. 26. [4]Ref. 9. [5]Ref. 5. [6]Ref. 8. [7]This band is concentration dependent (17).

the spectra of 13 monosubstituted benzene derivatives where the ratio of the maximal wavelengths $\lambda_{C\text{-band}}/\lambda_{B\text{-band}}$ is consistently 1.23 ± 0.05.) Exceptions are nitrobenzene, and to a lesser degree acetophenone and benzaldehyde, where the wavelength ratios are different.

Displacements to longer wavelength are generally accompanied by increased absorption intensities in both bands, but the absorption increments in the C-band show only slight similarities to the absorption increments observed in the B-band on bathochromic displacement. The main differences are: first, NH_2-, OH-, and OMe-groups produce more marked intensity increments in the C-band than in the B-band; next, intensity changes for three of the mono-halogen-substituted benzenes are in the reverse order ((28), Bowden and Braude (2) for solution spectra report an order $F \gg Br > Cl$) to wavelength shifts and intensity changes in the B-bands (18). This apparent dependence of intensities in the C-band on inductive effects for some monosubstituted benzenes has received a theoretical interpretation from molecular orbital theory calculations (28).

A number of points arising out of these observations may be noted. In the first place, the molecular orbital treatment as described by Matsen and co-workers (28), while providing a semiquantitative interpretation of the intensities of monosubstituted benzenes, does not readily lend itself to the interpretation of more complex derivatives (cf. also the "Theoretical Considerations" below). Secondly, the possible significance of inductive effects in the C-band suggests examination of para-disubstituted compounds, where any inductive interaction of the two substituents on each other would be small in comparison with similar effects in the ortho position. Further, the "anomalous" nature of some of the spectra of iodine-substituted compounds may be noted (see Table I for the C-band of iodobenzene and p-iodobenzoic acid, and cf. previous paragraph). This may be because of steric factors (cf. 18), and requires further elucidation.

Para-disubstituted Benzenes

The data for the C-band of para-disubstituted compounds suggest a different type of interaction from that observed in the B-band. Since the C-bands of many para-disubstituted compounds often resemble one of the parent compounds, or are intermediate with respect to both the monosubstituted parent compounds, this indicates that both inductive and mesomeric interactions are frequently small (cf. for example, in Table I the C-band of the following groups of compounds: p-chloroacetophenone and acetophenone; p-fluoroacetophenone, acetophenone, and fluorobenzene; p-chlorobenzoic acid and benzoic acid). Exceptions arise (cf. for example phenol (Table I) and p-cresol (21)), where the introduction of a para-substitutent gives rise to approximately equal bathochromic shifts and absorption increments in both B- and C-bands; these will be referred to again later.

We may also note that this, generally different, interaction in the two bands of para-disubstituted compounds is of some practical importance. For example, it accounts for the observation that the C-band in para-isomers is frequently obscured by the considerably displaced and intensified B-band. In this way, the band in the 320–360 mμ region for aminoacetophenones and aminobenzoic acids may be assumed to be a C-band because this band is covered in the para-isomers. Therefore no great displacement to longer wavelength nor absorption increase has occurred as would be expected if the absorption were to be associated with a B-band.

Meta- and Ortho-disubstituted Benzenes

In meta-disubstituted compounds, we note that the C-band only occasionally resembles

the C-band of one of the monosubstituted analogues; more frequently there is some evidence for interaction particularly for the hydroxy, methoxy, and amino derivatives of the compounds studied (see Table I for the C-bands of the corresponding acetophenones and benzoic acids). This interaction sometimes becomes increasingly important for the C-band of ortho-disubstituted derivatives. Generally, however, using the meta-disubstituted isomer as the reference compound, the interaction in ortho-isomers may be divided into at least two types; compounds in which a hypsochromic shift and loss of absorption intensity is observed (for example, *o*-chloroacetophenone), and compounds for which a distinct bathochromic shift with enhanced absorption intensity is observed (for example, *o*-hydroxyacetophenone).

At this point, the choice of reference compound used for comparing "ortho-effects" may be briefly discussed. For the B-band it was shown (13) that the para-isomer is usually the most satisfactory reference compound. For the C-band, by contrast, the para-isomer is unsuitable as a reference compound because para- and ortho-isomers, even in the absence of steric effects, do not give rise to similar C-bands. Further, the para-isomer would make an unsatisfactory reference compound, since there the C-band is often submerged by the displaced B-band (see above). Hence the choice for a suitable reference band lies between the C-band of the meta-isomer and the C-band of one of the monosubstituted parent compounds, and both will be used in the discussion. Neither of them is entirely satisfactory; the meta-isomer has the advantage that frequently there is a resemblance between the bands of ortho- and meta-isomers. The monosubstituted parent compound may be of value since there are indications that for the B-band (cf. 17) the spectrum of the monosubstituted compound often resembles that of both the ortho- and meta-disubstituted compounds.

Returning now to the main theme, it is evident from Table I that ortho-effects in the C-band differ from the ortho-effects as observed in B-bands. Thus, the C-bands in the ortho-substituted compounds listed in Table I are well defined, even if both ortho-positions are occupied. The C-bands are also normally displaced towards the visible compared to the monosubstituted compounds, and this bathochromic shift is in the order $NH_2 >$ OH > OMe > Br > Cl (compared to the meta-disubstituted isomer, as has been noted above, either a hypsochromic or bathochromic shift is observed). This order is the same as the order of bathochromic shifts in the B-band for para-substituted acetophenones or benzoic acids, and may be related to the ability of the substituents to release unshared electrons. Further, the C-band apparently never completely disappears in ortho-disubstituted benzoic acids, and this indicates that conjugation between the benzene ring and the carboxyl group still takes place; actually for some of the disubstituted compounds (for example, 2,6-dibromobenzoic acid) the C-band is enhanced with respect to both the unsubstituted and the ortho-substituted compound.

STERIC EFFECTS AND AN INTERPRETATION OF THE CHANGES OBSERVED IN THE C-BAND ON SUBSTITUTION

Previous explanations concerning steric effects in the C-band vary. Moser and Kohlenberg (26), for example, state that steric interactions between the carboxyl group and another atom or group in ortho-substituted benzoic acids apparently have no effect upon this band. Cram and Cranz (8) have also discussed this band and conclude that the C-band is particularly sensitive to transitions associated with ortho-resonance forms.

Our hypothesis of why steric inhibition of resonance has a marked effect upon the

B-band but apparently none or quite a different effect on the C-band is based on the following assumptions:

(i) The electronic excitation leading to the C-band involves transitions which require more energy at the energetically most favorable interplanar angle of the ground state than at interplanar angles which are slightly different.

(ii) This ground state attains an energy minimum at an interplanar angle of about 90°, because there may then be a secondary maximum of interaction between the π-electrons of the benzene ring and some of the p- or π-electrons of a substituent. These assumptions are illustrated in Fig. 1.
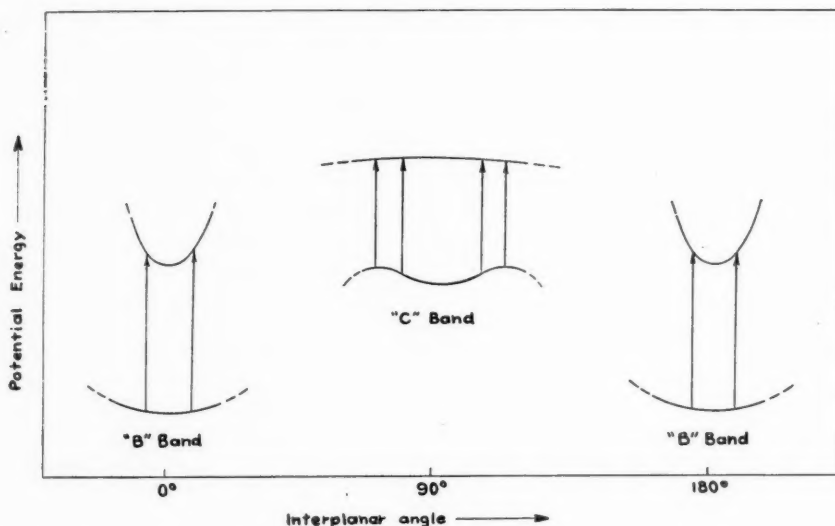
FIG. 1. Schematic representation of the energy of electronic states in benzenoid compounds (steric interactions between substituents are assumed small) as a function of twist about the C-nuclear bond. The vertical arrows represent the transitions leading to the B- and C-bands respectively.

Examining the data in the light of the hypothesis it may first be noted that in contrast to the B-band, the C-band is comparatively insensitive to smaller steric effects. An example of this is provided by ortho-methyl derivatives, such as o-methylacetophenone, where the intensity of the B-band is approximately halved while the C-band shows no such change (see Table I). Intensity losses of this type in the B-band have been ascribed to the excited state—because of a different energy relationship with respect to interplanar angles—no longer participating in some of the transitions which lead to the observed absorption intensity of a planar reference compound (cf. 14, 16). Consequently in the C-band, since the energy relation of the electronic excited state with respect to changes in interplanar angles is assumed to be different, no such restriction is observed.

Next, in the example cited (o-methylacetophenone), there will, however, be a change in the C-band, since as transitions leading to a B-band become less probable because of the increased angle of twist in the ground state, this same increased angle of twist will make transitions leading to the C-band more probable (see Fig. 1). Hence a slight bathochromic shift accompanied by increased absorption intensity is frequently observed

(cf. Table I for the C-bands of ortho-substituted compounds). This effect is considerably enhanced in compounds like 4-acetylhydrindacene (λ_{max} 308 mμ, $\epsilon = 3000$ (12)), where both planar forms are subject to steric interaction.

The hypothesis also accounts for the observation that even in considerably hindered compounds where the interplanar angle is quite large (cf. 14, 15), the C-band still absorbs with appreciable intensity (see Table I for the C-bands of ortho-disubstituted compounds). If we assume that conjugation is still possible in the ground state, although transitions leading to the B-band no longer occur, transitions leading to the C-band would be expected to occur. This follows, since only the B-band is particularly sensitive to steric interactions on account of the normally greater sensitivity to steric hindrance in the electronic excited state. But the assumption that conjugation is still possible in the ground state, even in the presence of steric inhibition of resonance, is reasonable and also receives support from the carbonyl stretching frequencies of hindered acetophenones (16). Thus, conjugation may be assumed to occur in the ground state even if steric hindrance is appreciable. However, the molecule will also absorb as two distinct entities, since some of the conjugation no longer occurs. Hence, as steric hindrance between vicinal atoms increases, the absorption intensity of the C-band—and other physical data which are a measure of conjugation between two chromophores in a molecule—will eventually decrease. Next, it may be noted that for OH-, OMe-, and NH$_2$-substituents, in the C-band, a pronounced bathochromic shift is observed, accompanied by increased absorption intensity (see Table I). For this observation the hypothesis again provides an answer, since OH-, OMe-, and NH$_2$-substituents all contain unshared electrons. This may be assumed to give rise to interaction which is less direction-dependent than the π–π interaction of acetophenones. Therefore a larger bathochromic shift accompanied by increased absorption intensity is observed in the C-band of anilines and similar compounds. The increased intensity of absorption is particularly marked (see Table I) and can be explained by the reduced energy difference between the ground state of molecules in positions which give rise to B- and C-bands respectively; in this way the ratios of the absorption intensities in the C- and B-bands are affected. This is illustrated in Fig. 2.

This effect, i.e. the large intensity increase because of an amino or similar substituent, is characteristic of the C-band, and therefore may also be used in the assignment of absorption bands. An example of this is provided by the long wavelength band of ortho-bridged diphenyls (see Table 3 of a discussion (4) dealing with diphenyls), where it may be noted that the introduction of ortho-methoxy groups considerably increases the intensity of the band; this suggests that the long wavelength band is a C-band. This different effect of a methoxy-group on B- and C-bands in the ortho and para positions has already been noted by Burawoy and co-workers (7), but these authors propose a different explanation for the B- and C-bands.

More generally, the effect of mesomeric interaction may be deduced in a similar manner, namely by considering distribution curves of the type shown in Fig. 2. In this way, if the operation of the mesomeric effect is confined principally to one plane, a large mesomeric effect will, by maintaining a large percentage of molecules in the near-planar or planar conformation, reduce the percentage of molecules subtending a large interplanar angle. Since a large interplanar angle aids absorption leading to the C-band, *a large mesomeric effect will normally give rise to a low intensity C-band and vice versa*. This generalization is well illustrated by a number of compounds. For example, nitrobenzenes on account of the large mesomeric effect of the nitro group exhibit only a weak C-band, which is

often submerged (cf. also 17). Another example is the order of the observed intensities in halogen-substituted benzenes which can also be rationalized from the above generalization; if the mesomeric effect decreases, as in fluoro-substituted benzenes, the intensity of the C-band increases, and thus the order of intensities *apparently* corresponds to the inductive effect. An exception is provided by the intensities of the C-bands of *p*-halogen benzoic acids, but since these C-bands occur mostly as inflections and since the B- and C-band maxima are situated fairly close to each other, the data cannot be considered too reliable in providing exact C-band intensities.
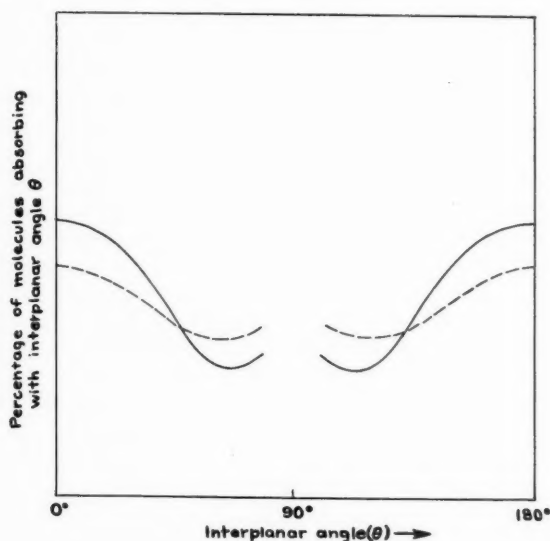
FIG. 2. Schematic representation of distribution curves for benzenoid molecules contributing to the observed absorption. Curve 1 (———), in the absence of amino or similar substituent. Curve 2 (– – – –), with amino or similar substituent.

The difficulty of finding a suitable reference compound for the study of the ortho-effect in the C-band can also now be better appreciated. For para-disubstituted benzenes there is normally maximum resonance interaction and hence the C-band is weak. In meta-isomers mesomeric interaction is secondary and this accounts for the generally more pronounced C-band. In ortho-isomers steric interaction frequently destroys most of the mesomeric interaction by increasing the angle of twist, and consequently interaction may again be secondary and thus the meta- and ortho-isomers may resemble each other. However, this similarity between ortho- and meta-isomers is not general, because steric inhibition of resonance in neutral solution is seldom complete, and because other effects such as hydrogen bonding frequently play a part (17). The effect of the ortho-substituent in the C-band is therefore perhaps best estimated by using the absorption of the mono-substituted parent compound and then allowing for both the mesomeric and the steric interaction of the second substituent. As in the B-bands, the absorption of the C-bands may usually be correlated by considering only mesomeric and steric effects. The bands differ in that for the C-band, the mesomeric effect will normally weaken and steric

effects strengthen this band (by decreasing mesomeric interaction *and* by increasing the mean interplanar angle), whereas for the B-band mesomeric interaction reinforces the band while steric effects weaken it (12, 13, 18, 19).

The hypothesis also explains why quite generally for pairs of compounds differences in intensity ratios between the two bands are often more marked than differences in wavelength ratios. This follows because absorption intensities are frequently more sensitive to steric interactions (cf. 13).

Solvent Effects

The effect of substituents has indicated (see above) that the transitions leading to the B-band and C-band are essentially similar. Thus, for example, the over-all electro-negativity of a substituent will normally cause similar changes in both bands, which suggests that both excited states possess a related electronic distribution. Confirmatory evidence should be forthcoming from a study of solvent effects since these have been shown to be characteristic for other bands (6). With this in mind, the B- and C-bands have been determined in different solvents, firstly in ethanol and cyclohexane (see Table I), then in dioxane–water mixtures (17), and finally in concentrated sulphuric acid (see Table II).

Changing the solvent from ethanol or 95% aqueous ethanol to cyclohexane or ether generally reinforces the C-band, and thus assists in defining the band. For example, in some para-substituted benzoic acids it is necessary to determine the spectra in hydro-carbon solvents, before the C-band may be identified (cf. Table I). More important, examination of the B- and C-bands for acetophenones shows that, in agreement with Burawoy *et al.* (7, and references cited therein), both B- and C-bands are usually displaced to longer wavelength on increasing the dielectric constant of the solvent (cf. 30, and the changes observed in Table I on changing the solvent from cyclohexane to ethanol).

It should be noted, however, (cf. Experimental, Table I, and (17)), that there are a number of exceptions to this general rule. Thus, values are sometimes dependent on the concentration of the solution (17). Also, values for benzoic acids are anomalous, although fairly uniformly so for both B- and C-bands (17). Since these exceptional changes raise a number of additional points and can be more satisfactorily examined by considering dioxane–water mixtures, this particular aspect of the discussion will be deferred for the present.

Addition of sulphuric acid to this type of compound generally displaces both bands to longer wavelength. The absorption spectra of some B- and C-bands in concentrated sulphuric acid are shown in Table II (cf. 6).

It is seen that the bathochromic shift due to the ortho-substituent in the C-bands for sulphuric acid solution spectra again supports the general hypothesis as does the over-all similarity of the changes observed in both bands on increasing the proton availability of the solvent (see Table II).

Theoretical Considerations

The C-band has been assumed to correspond to the 255 mμ ($A_{1g} \rightarrow B_{2u}$) transition in benzene (30). These assignments are supported by calculation of the expected absorption intensities. However, observed substitution effects (cf. 2, 27, 28) do not completely support these assignments.

If calculations are extended to more complicated molecules (cf. 20, 28, 29) we find that good agreement between the calculated and observed intensity is only seldom obtained. According to our hypothesis, for example, it is unnecessary to invoke the

TABLE II

VARIATION OF ABSORPTION SPECTRA WITH ACIDITY

Compound	B-band				C-band			
	In ethanol		In H$_2$SO$_4$		In ethanol		In H$_2$SO$_4$	
	λ_{max}, mμ	ϵ_{max}	λ_{max}, mμ	ϵ_{max}	λ_{max}, mμ	ϵ_{max}	λ_{max}, mμ	ϵ_{max}
Acetophenone	240	12,500[1]	293	20,000	276	1000[1]	ca. 325	2500
o-Methylacetophenone	242	8500[1]	293	14,000	283	1250[1]	354	1600
m-Methylacetophenone	244–245	11,200[1]	300	21,000	{ 285 291	1300[1] 1200	349–350	2000
p-Methylacetophenone	252	15,000[1]	309	24,500	278	850[1]	ca. 350	2000
Benzaldehyde	242	14,000[2]	293	21,000	{ 280 289	1400[2] 1200	ca. 335	2000
o-Methylbenzaldehyde	251	13,000[2]	295	17,000	291	1700[2]	364	2000
p-Methylbenzaldehyde	251	15,000[2]	310	23,000	279	1200[2]	—	—
Benzoic acid	227	11,000[1]	260	15,500	{ 271 279	760[1] 550	294	2000
o-Methylbenzoic acid	228	5000[1]	264	16,000	279	725[1]	312	2700
m-Methylbenzoic acid	232	9000[1]	265	16,400	279	1000[1]	310	2200
p-Methylbenzoic acid	236	14,000[1]	275	21,100	—	—[1]	—	—
p-Nitroacetophenone[3]	262	14,000	286	21,500	ca. 310	1600	ca. 340	3200
Nitrobenzene	257–258	8000	287.5	8600	—	—	ca. 302	7200

[1]Table I.
[2]In n-hexane or cyclohexane (5).
[3]Ref. 30.

inductive effect in order to account for the C-band of halogen-substituted benzenoid compounds (cf. 28*); further, the occasional similarity in the frequency and intensity of absorption of ortho- and meta-substituted compounds for the C-band, which has received a quantum mechanical interpretation by Förster (20), is only of limited value in correlating the C-bands for the compounds discussed in this paper. It may be that these calculations are correct for the ground states—and hence might incidentally be expected to hold for the B-bands also—but that the superimposed effect of the electronic excited states so alters the spectrum that any original ortho–meta similarity is often hidden (cf. previous sections, and References 11, 13, 16, 18, 19, 26). A similar comment would apply to the intensity ratios proposed by Sklar (29).

EXPERIMENTAL

The ultraviolet absorption spectra were determined with quartz cells of 1 cm. path length using a Unicam SP500 spectrophotometer. For each compound at least two independent sets of observations were made. Some of the spectra have already been described in previous parts of this series.

The physical constants of the purified compounds not previously reported in this series are listed in Table III.

m-Methylacetophenone was prepared by the method of Birch et al. (1).

m-Bromo-, m-iodo-, and m-hydroxy-acetophenones were obtained by diazotization of m-aminoacetophenone, followed by the standard Sandmeyer procedure. The halogen compounds were purified by vacuum distillation, while the hydroxy compound crystallized from aqueous ethanol.

o-Hydroxy- and p-hydroxy-acetophenones were prepared by means of a Fries

*A referee of this paper has kindly drawn our attention to a recent communication (25), which is also relevant to the effect of inductive-type interactions on the C-band.

TABLE III

PHYSICAL CONSTANTS OF ACETOPHENONES

Acetophenone	Melting point, or boiling point and refractive index	Yield	Reported value of physical constants
m-Methyl-	B.p. 65–71°, 3 mm., n_D^{22} 1.5170	57%	B.p. 109°, 12 mm., n_D^{15} 1.533 (22)
m-Bromo-	B.p. 72°, 3 mm., n_D^{22} 1.5756	25%	B.p. 131–132°, 17 mm., n_D^{20} 1.5755 (24)
m-Iodo-	$n_D^{23.5}$ 1.6228	40%	B.p. 117°, 4 mm., n_D^{20} 1.6220 (23)
o-Hydroxy-	B.p. 72°, 4 mm., n_D^{21} 1.5590	30%	B.p. 96°, 10 mm., n_D^{21} 1.558 (22)
m-Hydroxy-	M.p. 95–96°	50%	M.p. 96° (22)
p-Hydroxy-	M.p. 104°	26%	M.p. 109° (22)

rearrangement of phenyl acetate, using aluminum chloride. The ortho-compound was purified by vacuum distillation, while the para-isomer crystallized from ethanol.

C.P. Reagent sulphuric acid (C.I.L., 95.5% min.) was used in the determination of the acid spectra.

ACKNOWLEDGMENTS

REFERENCES

1. BIRCH, S. F., DEAN, R. A., FIDLER, F. A., and LOWRY, R. A. J. Am. Chem. Soc. 71, 1362 (1949).
2. BOWDEN, K. and BRAUDE, E. A. J. Chem. Soc. 1068 (1952).
3. BRAUDE, E. A. Ann. Repts. Chem. Soc. 42, 105 (1945).
4. BRAUDE, E. A. and FORBES, W. F. J. Chem. Soc. 3776 (1955).
5. BRAUDE, E. A. and SONDHEIMER, F. J. Chem. Soc. 3754 (1955).
6. BURAWOY, A. Discussions Faraday Soc. 9, 70 (1950).
7. BURAWOY, A., CAIS, M., CHAMBERLAIN, J. T., LIVERSEDGE, F., and THOMPSON, A. R. J. Chem. Soc. 3721 (1955).
8. CRAM, D. J. and CRANZ, F. W. J. Am. Chem. Soc. 72, 595 (1950).
9. DANNENBERG, H. Z. Naturforsch. 4b, 327 (1949).
10. DOUB, L. and VANDENBELT, J. M. J. Am. Chem. Soc. 69, 2714 (1947).
11. DOUB, L. and VANDENBELT, J. M. J. Am. Chem. Soc. 71, 2414 (1949).
12. FORBES, W. F. and MUELLER, W. A. Can. J. Chem. 33, 1145 (1955).
13. FORBES, W. F. and MUELLER, W. A. Can. J. Chem. 34, 1340 (1956).
14. FORBES, W. F. and MUELLER, W. A. Can. J. Chem. 34, 1347 (1956).
15. FORBES, W. F. and MUELLER, W. A. Can. J. Chem. 34, 1542 (1956).
16. FORBES, W. F. and MUELLER, W. A. Can. J. Chem. 35, 488 (1957).
17. FORBES, W. F., MUELLER, W. A., RALPH, A. S., and TEMPLETON, J. F. Unpublished information.
18. FORBES, W. F. and RALPH, A. S. Can. J. Chem. 34, 1447 (1956).
19. FORBES, W. F. and SHERATTE, M. B. Can. J. Chem. 33, 1829 (1955).
20. FÖRSTER, T. Z. Naturforsch. 2a, 149 (1947).
21. FRIEDEL, R. A. and ORCHIN, M. Ultraviolet spectra of organic compounds. John Wiley and Sons, Inc., New York. 1951.
22. HEILBRON, Sir I. and BUNBURY, H. M. Dictionary of organic compounds. Eyre and Spottiswoode, Ltd., London. 1946.
23. LEONARD, N. J. and BOYD, S. N., Jr. J. Org. Chem. 11, 405 (1946).
24. MARVEL, C. S., ALLEN, R. E., and OVERBERGER, G. G. J. Am. Chem. Soc. 68, 1089 (1946).
25. MOFFITT, W. J. Chem. Phys. 22, 320 (1954).
26. MOSER, C. M. and KOHLENBERG, A. I. J. Chem. Soc. 804 (1951).
27. ROBERTSON, W. W. and MATSEN, F. A. J. Am. Chem. Soc. 72, 5248 (1950).
28. ROBERTSON, W. W. and MATSEN, F. A. J. Am. Chem. Soc. 72, 5252 (1950).
29. SKLAR, A. L. J. Chem. Phys. 10, 135 (1942).
30. TANAKA, J., NAGAKURA, S., and KOBAYASHI, M. J. Chem. Phys. 24, 311 (1956).

THE ANALYSIS OF NUCLEAR MAGNETIC RESONANCE SPECTRA

II. TWO PAIRS OF TWO EQUIVALENT NUCLEI[1]

J. A. POPLE,[2] W. G. SCHNEIDER, AND H. J. BERNSTEIN

ABSTRACT

This paper deals with the analysis of the nuclear magnetic resonance spectrum of two pairs of two equivalent nuclei (of spin $\frac{1}{2}$) whose relative chemical shift is of the same order as the spin-coupling constants of the system (A_2B_2 in the notation of Part I). The complete matrix is set up and correlated with the results of McConnell, McLean, and Reilly (4) for the corresponding theory with large chemical shifts.

The proton resonance spectrum of naphthalene is reported and is analyzed as an A_2B_2 system on the hypothesis that spin couplings between protons on different rings are negligible. A complete analysis of the spectrum of o-dichlorobenzene, which represents a further example of an A_2B_2 system, is also given. The spectrum of 1-chloro-2-bromoethane at room temperature is also analyzed as an A_2B_2 system.

1. INTRODUCTION

This series of papers is concerned with problems of spectral analysis in nuclear magnetic resonance experiments on molecules which contain non-equivalent nuclei of the same species, the relative chemical shift being of the same order as the splittings due to spin coupling. In Part I (3) the theory of some standard groups of two and three nuclei was considered and used to analyze the observed proton resonance spectra of certain compounds. The present paper contains the corresponding theory for four nuclei (of spin $\frac{1}{2}$) which can be divided into two equivalent pairs. According to the notation of Part I, this would be referred to as a group A_2B_2, if the relative chemical shift between A and B nuclei is of the same order of magnitude as the various spin-coupling constants involved. If the chemical shift is large, on the other hand, or if the nuclei are of different species, the spectral lines will split into two distinct sets and we shall have a grouping of the type A_2X_2. The theory of A_2X_2 has been discussed in some detail by McConnell, McLean, and Reilly (4), who have applied it to the analysis of proton and fluorine resonance spectra in 1,1-difluoroethylene. The analysis of the present paper is therefore a generalization of this and the notation will be chosen so that some of their results can be obtained as a particular case by proceeding to the appropriate limit.

2. GENERAL THEORY OF A_2B_2

If H_0 is the applied magnetic field external to the specimen, the local fields at nuclei A and B can be written

[2.1]
$$H_A = H_0(1-\sigma_A),$$
$$H_B = H_0(1-\sigma_B),$$

where σ_A and σ_B are screening constants whose difference is a measure of the relative chemical shift. We shall suppose that $\sigma_B > \sigma_A$ so that the B-nuclei are more screened. Consequently, if the experiment is performed by varying the external field to obtain resonance at a given frequency, the B-signal will appear 'at higher field' than A.

In general there will be four different spin-coupling constants as shown in Fig. 1. It is convenient to define new quantities:

[2.2]
$$K = J_A + J_B, \quad L = J - J',$$
$$M = J_A - J_B, \quad N = J + J'.$$

We start by setting up a complete set of basic functions, all stationary state wave functions being expressible as linear combinations of them. Using α and β for the two possible spin states of a single nucleus, we use the set given in Table I, following McConnell, McLean, and Reilly (4). The symbols s and a are used for symmetric and antisymmetric under the operation of reflection in the plane of symmetry, and the suffix indicates the corresponding total spin component in the direction of the applied
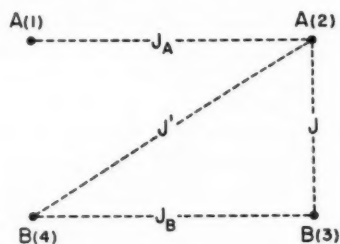
FIG. 1.

field. The next step is then to evaluate the complete matrix of the spin Hamiltonian using the rules given in Part I. These are also listed in Table I. There are no non-zero off-diagonal elements between functions of different symmetry, or between functions of different spin, so the problem of diagonalization is reduced to that of a number of smaller matrices, the largest being of fourth order. The actual wave functions are appropriate linear combinations of the basic functions, but they may be labelled in a corresponding manner. Thus we shall write $1s_1'$ for the stationary state wave function which reduces to the basic function $1s_1$ as the off-diagonal elements tend to zero.

Transitions will only occur between states of the same symmetry whose total spin components differ by ± 1. This leads to a total of 20 symmetric transitions and 8 antisymmetric. These may be further classified as A, B, or combination transitions according to their behavior in the limit $J, J' \to 0$ when wave functions and basic functions coincide.

TABLE I

BASIC FUNCTIONS AND COMPLETE MATRIX OF HAMILTONIAN H FOR A_2B_2

Function*	A	B	Diagonal matrix elements†	Off-diagonal matrix elements
s_2	$\alpha\alpha$	$\alpha\alpha$	$\eta H_0(2-\sigma_A-\sigma_B)+\frac{1}{2}N$	
$1s_1$	$2^{-\frac{1}{2}}(\alpha\beta+\beta\alpha)$	$\alpha\alpha$	$\eta H_0(1-\sigma_B)$	$(1s_1|\mathscr{H}|2s_1)=\frac{1}{2}N$
$2s_1$	$\alpha\alpha$	$2^{-\frac{1}{2}}(\alpha\beta+\beta\alpha)$	$\eta H_0(1-\sigma_A)$	
$1s_0$	$\beta\beta$	$\alpha\alpha$	$\eta H_0(\sigma_A-\sigma_B)-\frac{1}{2}N$	$(1s_0|\mathscr{H}|2s_0)=0,\quad (2s_0|\mathscr{H}|3s_0)=\frac{1}{2}L$
$2s_0$	$\alpha\alpha$	$\beta\beta$	$\eta H_0(-\sigma_A+\sigma_B)-\frac{1}{2}N$	$(1s_0|\mathscr{H}|3s_0)=\frac{1}{2}L,\quad (2s_0|\mathscr{H}|4s_0)=\frac{1}{2}N$
$3s_0$	$2^{-\frac{1}{2}}(\alpha\beta-\beta\alpha)$	$2^{-\frac{1}{2}}(\alpha\beta-\beta\alpha)$	$-K$	$(1s_0|\mathscr{H}|4s_0)=\frac{1}{2}N,\ (3s_0|\mathscr{H}|4s_0)=-\frac{1}{2}L$
$4s_0$	$2^{-\frac{1}{2}}(\alpha\beta+\beta\alpha)$	$2^{-\frac{1}{2}}(\alpha\beta+\beta\alpha)$	0	
$1s_{-1}$	$2^{-\frac{1}{2}}(\alpha\beta+\beta\alpha)$	$\beta\beta$	$\eta H_0(-1+\sigma_B)$	$(1s_{-1}|\mathscr{H}|2s_{-1})=\frac{1}{2}N$
$2s_{-1}$	$\beta\beta$	$2^{-\frac{1}{2}}(\alpha\beta+\beta\alpha)$	$\eta H_0(-1+\sigma_A)$	
s_{-2}	$\beta\beta$	$\beta\beta$	$\eta H_0(-2+\sigma_A+\sigma_B)+\frac{1}{2}N$	
$1a_1$	$2^{-\frac{1}{2}}(\alpha\beta-\beta\alpha)$	$\alpha\alpha$	$\eta H_0(1-\sigma_B)-\frac{1}{2}(K+M)$	$(1a_1|\mathscr{H}|2a_1)=-\frac{1}{2}L$
$2a_1$	$\alpha\alpha$	$2^{-\frac{1}{2}}(\alpha\beta-\beta\alpha)$	$\eta H_0(1-\sigma_A)-\frac{1}{2}(K-M)$	
$1a_0$	$2^{-\frac{1}{2}}(\alpha\beta+\beta\alpha)$	$2^{-\frac{1}{2}}(\alpha\beta-\beta\alpha)$	$-\frac{1}{2}(K-M)$	$(1a_0|\mathscr{H}|2a_0)=-\frac{1}{2}L$
$2a_0$	$2^{-\frac{1}{2}}(\alpha\beta-\beta\alpha)$	$2^{-\frac{1}{2}}(\alpha\beta+\beta\alpha)$	$-\frac{1}{2}(K+M)$	
$1a_{-1}$	$2^{-\frac{1}{2}}(\alpha\beta-\beta\alpha)$	$\beta\beta$	$\eta H_0(-1+\sigma_B)-\frac{1}{2}(K+M)$	$(1a_{-1}|\mathscr{H}|2a_{-1})=-\frac{1}{2}L$
$2a_{-1}$	$\beta\beta$	$2^{-\frac{1}{2}}(\alpha\beta-\beta\alpha)$	$\eta H_0(-1+\sigma_A)-\frac{1}{2}(K-M)$	

*A serial notation is used. Thus $\alpha\alpha\beta\beta$ means $\alpha(1)\ \alpha(2)\ \beta(3)\ \beta(4)$, the numbering being as in Fig. 1.
†For convenience, $\frac{1}{4}K$ is subtracted from all diagonal matrix elements. This makes no difference to calculated transition energies. $2\pi\eta$ is the gyromagnetic ratio for the nuclei.

Thus the transition $1s_1' \rightarrow s_2'$, for example, corresponds, in the limit, to changing the spin of an A-nucleus and is referred to as an A-transition. On the other hand, $1s_{-1}' \rightarrow 1s_0'$ in the limit involves changing the spin of three nuclei and is a combination transition. Combination transitions are forbidden in this limiting case, but may appear with small intensities when the wave functions become mixed. We shall not consider them in the analysis, however, as they are unlikely to be observed in practice. There are four combination transitions, which leaves a total of 24 transitions to be considered. Detailed inspection of Table I also shows that the set of A-lines is always a mirror image of the B-lines about the central position $\eta H_0\{1 - \frac{1}{2}(\sigma_A + \sigma_B)\}$. We need therefore only examine theoretical expressions for the energy of the 12 A-transitions.

Of these 12, six will involve states of type s_0, the energies of which require the solution of a fourth order secular equation. Explicit expressions can be obtained for the energies and wave functions of all the second order secular equations, however. It is convenient to define angles ϕ, $\psi_\pm$, θ_s, and θ_a by

[2.3]
$$\begin{aligned}
\cos 2\phi &: \sin 2\phi : 1 = \eta H_0\delta &&: N : \{(\eta H_0\delta)^2 + N^2\}^{\frac{1}{2}} \\
\cos 2\theta_s &: \sin 2\theta_s : 1 = K &&: L : (K^2 + L^2)^{\frac{1}{2}} \\
\cos 2\theta_a &: \sin 2\theta_a : 1 = M &&: L : (M^2 + L^2)^{\frac{1}{2}} \\
\cos 2\psi_\pm &: \sin 2\psi_\pm : 1 = \eta H_0\delta \pm M &&: L : \{(\eta H_0\delta \pm M)^2 + L^2\}^{\frac{1}{2}}
\end{aligned}$$

where we have written δ for the relative chemical shift

[2.4]
$$\delta = \sigma_B - \sigma_A.$$

Then explicit energy expressions and wave functions for some of the stationary states are as given in Table II. Using these, we get the energies for six transitions listed in Table III.

TABLE II

EXPLICIT ENERGY EXPRESSIONS AND WAVE FUNCTIONS FOR A_2B_2

	Energy	Wave function
$1s_1'$	$\eta H_0\{1 - \frac{1}{2}(\sigma_A + \sigma_B)\} - \frac{1}{2}\{(\eta H_0\delta)^2 + N^2\}^{\frac{1}{2}}$	$(1s_1) \cos\phi - (2s_1) \sin\phi$
$2s_1'$	$\eta H_0\{1 - \frac{1}{2}(\sigma_A + \sigma_B)\} + \frac{1}{2}\{(\eta H_0\delta)^2 + N^2\}^{\frac{1}{2}}$	$(1s_1) \sin\phi + (2s_1) \cos\phi$
$1s'_{-1}$	$-\eta H_0\{1 - \frac{1}{2}(\sigma_A + \sigma_B)\} + \frac{1}{2}\{(\eta H_0\delta)^2 + N^2\}^{\frac{1}{2}}$	$(1s_{-1}) \cos\phi + (2s_{-1}) \sin\phi$
$2s'_{-1}$	$-\eta H_0\{1 - \frac{1}{2}(\sigma_A + \sigma_B)\} - \frac{1}{2}\{(\eta H_0\delta)^2 + N^2\}^{\frac{1}{2}}$	$-(1s_{-1}) \sin\phi + (2s_{-1}) \cos\phi$
$1a_1'$	$\eta H_0\{1 - \frac{1}{2}(\sigma_A + \sigma_B)\} - \frac{1}{2}K - \frac{1}{2}\{(\eta H_0\delta + M)^2 + L^2\}^{\frac{1}{2}}$	$(1a_1) \cos\psi_+ + (2a_1) \sin\psi_+$
$2a_1'$	$\eta H_0\{1 - \frac{1}{2}(\sigma_A + \sigma_B)\} - \frac{1}{2}K + \frac{1}{2}\{(\eta H_0\delta + M)^2 + L^2\}^{\frac{1}{2}}$	$-(1a_1) \sin\psi_+ + (2a_1) \cos\psi_+$
$1a_0'$	$-\frac{1}{2}K + \frac{1}{2}(M^2 + L^2)^{\frac{1}{2}}$	$(1a_0) \cos\theta_a - (2a_0) \sin\theta_a$
$2a_0'$	$-\frac{1}{2}K - \frac{1}{2}(M^2 + L^2)^{\frac{1}{2}}$	$(1a_0) \sin\theta_a + (2a_0) \cos\theta_a$
$1a'_{-1}$	$-\eta H_0\{1 - \frac{1}{2}(\sigma_A + \sigma_B)\} - \frac{1}{2}K + \frac{1}{2}\{(\eta H_0\delta - M)^2 + L^2\}^{\frac{1}{2}}$	$(1a_{-1}) \cos\psi_- - (2a_{-1}) \sin\psi_-$
$2a'_{-1}$	$-\eta H_0\{1 - \frac{1}{2}(\sigma_A + \sigma_B)\} - \frac{1}{2}K - \frac{1}{2}\{(\eta H_0\delta - M)^2 + L^2\}^{\frac{1}{2}}$	$(1a_{-1}) \sin\psi_- + (2a_{-1}) \cos\psi_-$

If we now proceed to the limit A_2X_2, when the relative chemical shift is large, the fourth order secular equation breaks up, for the functions $1s_0$ and $2s_0$ become effectively stationary state wave functions. Explicit expressions for all energy levels and intensities can then be obtained. These were originally derived by McConnell, McLean, and Reilly (4) and are also included in Table III.

3. PRACTICAL METHODS OF ANALYSIS

As the complete spectrum for A_2B_2 depends in a rather complicated way on the relative chemical shift and spin-coupling constants, it is no longer possible to give such a direct deductive method of analysis as was possible for the simpler groups dealt with

TABLE III

ENERGIES AND INTENSITIES OF A-TRANSITIONS

Transition	A_2B_2 Energy relative to $\eta H_0\{1-\tfrac{1}{2}(\sigma_A+\sigma_B)\}$	Intensity	A_2X_2 Energy relative to $\eta H_0(1-\sigma_A)$	Intensity
1. $1s_1' \rightarrow s_2$	$\tfrac{1}{2}N+\tfrac{1}{2}\{(\eta H_0\delta)^2+N^2\}^{\frac{1}{2}}$	$1-\sin 2\phi$	$\tfrac{1}{2}N$	1
2. $1s_0' \rightarrow 1s_1'$			$\tfrac{1}{2}N$	1
3. $s_{-2} \rightarrow 1s'_{-1}$	$-\tfrac{1}{2}N+\tfrac{1}{2}\{(\eta H_0\delta)^2+N^2\}^{\frac{1}{2}}$	$1+\sin 2\phi$	$-\tfrac{1}{2}N$	1
4. $1s'_{-1} \rightarrow 2s_0'$			$-\tfrac{1}{2}N$	1
5. $3s_0' \rightarrow 2s_1'$			$\tfrac{1}{2}K+\tfrac{1}{2}(K^2+L^2)^{\frac{1}{2}}$	$\sin^2\theta_s$
6. $2s'_{-1} \rightarrow 4s_0'$			$-\tfrac{1}{2}K+\tfrac{1}{2}(K^2+L^2)^{\frac{1}{2}}$	$\cos^2\theta_s$
7. $4s_0' \rightarrow 2s_1'$			$\tfrac{1}{2}K-\tfrac{1}{2}(K^2+L^2)^{\frac{1}{2}}$	$\cos^2\theta_s$
8. $2s'_{-1} \rightarrow 3s_0'$			$-\tfrac{1}{2}K-\tfrac{1}{2}(K^2+L^2)^{\frac{1}{2}}$	$\sin^2\theta_s$
9. $2a_0' \rightarrow 2a_1'$	$\tfrac{1}{2}\{(\eta H_0\delta+M)^2+L^2\}^{\frac{1}{2}}+\tfrac{1}{2}(M^2+L^2)^{\frac{1}{2}}$	$\sin^2(\theta_a-\psi_+)$	$\tfrac{1}{2}M+\tfrac{1}{2}(M^2+L^2)^{\frac{1}{2}}$	$\sin^2\theta_a$
10. $2a'_{-1} \rightarrow 1a_0'$	$\tfrac{1}{2}\{(\eta H_0\delta-M)^2+L^2\}^{\frac{1}{2}}+\tfrac{1}{2}(M^2+L^2)^{\frac{1}{2}}$	$\cos^2(\theta_a+\psi_-)$	$-\tfrac{1}{2}M+\tfrac{1}{2}(M^2+L^2)^{\frac{1}{2}}$	$\cos^2\theta_a$
11. $1a_0' \rightarrow 2a_1'$	$\tfrac{1}{2}\{(\eta H_0\delta+M)^2+L^2\}^{\frac{1}{2}}-\tfrac{1}{2}(M^2+L^2)^{\frac{1}{2}}$	$\cos^2(\theta_a-\psi_+)$	$\tfrac{1}{2}M-\tfrac{1}{2}(M^2+L^2)^{\frac{1}{2}}$	$\cos^2\theta_a$
12. $2a'_{-1} \rightarrow 2a_0'$	$\tfrac{1}{2}\{(\eta H_0\delta-M)^2+L^2\}^{\frac{1}{2}}-\tfrac{1}{2}(M^2+L^2)^{\frac{1}{2}}$	$\sin^2(\theta_a+\psi_-)$	$-\tfrac{1}{2}M-\tfrac{1}{2}(M^2+L^2)^{\frac{1}{2}}$	$\sin^2\theta_a$

in Part I. However, there are certain general classes of A_2B_2 spectra which are likely to be found in similar forms in a variety of molecules. To develop methods for making a detailed assignment, it is helpful to consider first of all the general type of spectrum to be expected if the chemical shift is large (that is if the grouping is A_2X_2). Then the modification of line positions can be traced in detail as the chemical shift is reduced continuously. A knowledge of this behavior may then make it possible to make an assignment for individual lines in an experimental A_2B_2 spectrum. Once an assignment is decided on, the various parameters can be adjusted until the best fit is obtained and certain internal checks carried out.

The simplest A_2B_2 spectrum occurs if the two A–B coupling constants are equal ($J = J'$). If the chemical shift is large (A_2X_2 limit), the spectrum will consist of two triplets (intensity ratios 1–2–1), the separation between the components of each triplet being equal to the coupling constant, J. When we proceed to the intermediate A_2B_2 case, the shape of the spectrum is only a function of the ratio $J/\eta H_0(\sigma_B-\sigma_A)$ and is completely independent of the spin-coupling constants J_A and J_B. (This is similar to the general AB_2 spectrum (3), the shape of which depended only on a single parameter.) This result follows from the details of the matrix given in Table I. Since $L = 0$ (i.e. $J = J'$), the basic function $3s_0$ does not mix with any others, and the energies of all allowed symmetric transitions only involve N. Also there is no mixing in the anti-symmetrical part of the matrix and the corresponding allowed transitions are independent of *all* coupling constants.

The number of allowed A-transitions is now reduced to eight, two of them (10 and 11 in Table III) being always degenerate. The complete spectrum is still symmetrical about the mid-point, of course. Numerical values of the A-transition energies are given for a range of values of the ratio $J/\eta H_0(\sigma_B-\sigma_A)$ in Table IV. The numbering of transitions is as in Table III and energies are measured relative to the center of the spectrum in units of $\eta H_0(\sigma_B-\sigma_A)$. The form of a typical half-spectrum is given in Fig. 2, together with a correlation between the lines and the triplet of the A_2X_2 limit. It is useful to note that the position of the degenerate pair (10, 11) gives directly the chemical shift of the A-nuclei.

An example of this type of spectrum has been obtained for β-propiolactone which was interpreted satisfactorily by Anderson (1) using perturbation methods, on the basis of $J/\eta H_0(\sigma_B-\sigma_A) = 0.265$.

TABLE IV

ENERGIES OF A-TRANSITIONS WITH TWO EQUAL A–B COUPLING CONSTANTS
(RELATIVE TO CENTER OF BAND)

$J/\eta H_0(\sigma_B - \sigma_A)$	Transition (see Table III)						
	4	3	10, 11	6	7	2	1
0.1	0.401	0.410	0.500	0.508	0.512	0.599	0.610
0.2	0.309	0.339	0.500	0.524	0.554	0.694	0.739
0.3	0.233	0.283	0.500	0.535	0.631	0.785	0.883
0.4	0.176	0.240	0.500	0.536	0.744	0.872	1.040
0.5	0.134	0.207	0.500	0.528	0.886	0.955	1.207
0.75	0.077	0.151	0.500	0.482	1.320	1.158	1.651
1.00	0.052	0.118	0.500	0.429	1.807	1.363	2.118

Although exact equality of the two A–B coupling constants may be rare, the spectra tabulated in Table IV and illustrated in Fig. 2 may sometimes be useful as a guide to the analysis of more complex systems which approximate to this in some way. For example, we may note that mixing of $3s_0$ with the other states may also fail to occur if $K(= J_A + J_B)$ is sufficiently large. (That is because mixing can be neglected either if
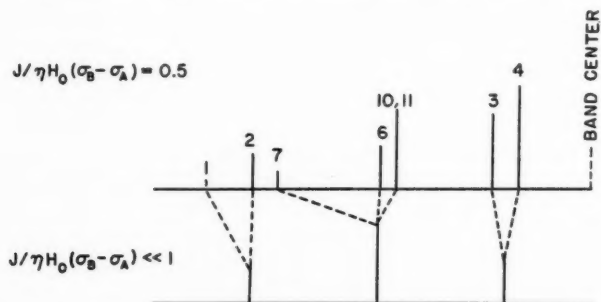
FIG. 2. Correlation of the A-transitions of the A_2X_2 triplet in the limit $J/\eta H_0(\sigma_B - \sigma_A) \ll 1$, with the A_2B_2 spectrum for $J/\eta H_0(\sigma_B - \sigma_A) = 0.5$ when $J = J'$.

off-diagonal elements are sufficiently small or if the difference between diagonal elements is sufficiently large.) For such a system (even though $J \neq J'$) the *symmetrical* transitions (that is 1, 2, 3, 4, 6, and 7) will be given as in Table IV. Lines 5 and 8 will still be effectively forbidden. *Antisymmetrical* transitions, however, are independent of K and these may have a more complex structure. In section 6 we shall show that the proton spectrum of bromochloroethane can be analyzed in this manner.

Another important class of A_2B_2 spectra consists of those from four nuclei arranged so that one of the pairs (B_2 say) is more closely coupled than the other.

Such groups often occur if the two B-nuclei are relatively close and each A-nucleus is close to one B-nucleus. An example would be an ortho-disubstituted benzene

$$A \langle \overset{B \quad B}{\underset{R \quad R}{\hexagon}} \rangle A$$
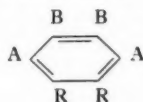
where the substituent R has a nucleus with zero moment bonded to the benzene ring. The general form of such a spectrum will be dominated by the chemical shift and the spin-coupling constants J and J_B (Fig. 1). We shall examine its behavior under conditions

$$J \gg J' > 0,$$

$$J_B \gg J_A > 0.$$

It is appropriate for protons (5) to take all spin-coupling constants to be positive.

We begin by considering the A-spectrum in the limit A_2X_2, which is easily constructed from Table III and is illustrated in Fig. 3 (note that $M = J_A - J_B$ is negative). It consists
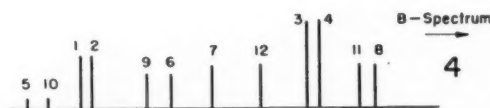
FIG. 3. Typical A-spectrum for A_2X_2 with $J \gg J' > 0$, and $J_B \gg J_A > 0$.
FIG. 4. The A-spectrum in A_2B_2 with $J \gg J' > 0$, and $J_B \gg J_A > 0$.

of a symmetrical arrangement of 10 lines, two of them degenerate pairs and the four outermost lines being rather weak. If $J_A = 0$, so that $K = -M$, the pairs (5, 10), (9, 6), (7, 12), and (11, 8) become degenerate. The B-spectrum, which is to the right of the figure, will be identical. An example of such a spectrum (in which the nuclei are of different species) is that of 1,1-difluoroethylene which was examined by McConnell, McLean, and Reilly (4). As the $A-B$ chemical shift decreases, this spectrum becomes modified in a characteristic manner. The part of the A-spectrum on the right (Fig. 4), that is the part closest to the B-spectrum, becomes more intense at the expense of the left-hand part (cf. Figs. 3 and 4). The signals 5 and 10 may become so weak as to be practically unobservable. The two degenerate pairs (1, 2) and (3, 4) become split slightly and there is a tendency for the separation of both the inner pairs (9, 6 and 7, 12) to be increased. The pair (7, 12) in fact is widened most. The A-spectrum in the intermediate case then appears as in Fig. 4. The outermost right-hand pair (11, 8) may cross the corresponding B-lines, but this will not occur with the strong pair (3, 4). In the practical analysis of a spectrum of this type the pairs (1, 2) and (3, 4) are usually easily recognized. Lines 1 and 3 can immediately be used (Table III) to find the chemical shift and the parameter $N(= J+J')$. The positions of the inner lines can then be used to obtain values for the other combinations of spin-coupling constants. In the next two

sections we shall analyze the proton spectra of naphthalene and o-dichlorobenzene as examples of this type.

4. THE PROTON RESONANCE SPECTRUM OF NAPHTHALENE

Naphthalene is not strictly an example of A_2B_2, but it may be considered to be approximately so if we make the hypothesis that spin-couplings between protons in different rings may be neglected. We shall label the two α-protons A and the β-protons B. Since we have assumed $\sigma_B > \sigma_A$ throughout this paper, this presupposes that the α-protons are the 'less shielded' (this is discussed further below).

The spectrum of naphthalene measured* in dioxane solution is shown in Fig. 5.
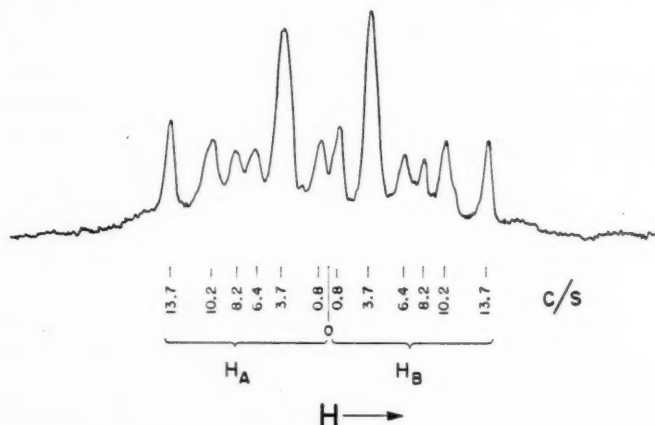
FIG. 5. Complete proton resonance spectrum of naphthalene at 40 Mc./second.

The spectrum is completely symmetrical within the limits of experimental error and consists of 12 lines, some of which appear to be doublets. The mean positions of the lines (in c./second) relative to the center are also given. If we suppose the spin-coupling constants between protons attached to neighboring carbon atoms are the most important, the spectrum should be of the general type discussed in the previous section and it is indeed found to be similar to that illustrated in Fig. 3. If, to begin with, we assume the spin-coupling constants to be positive, we may make an assignment on this basis. The strongest line at 3.75 c./sec. is then supposed to be an unresolved doublet of lines 3 and 4 and the innermost A-line to be another doublet (8, 11). The outermost observable line (at 13.7 c./sec.) is not weak as in Fig. 3 so that it is assigned to the pair (1, 2). There should be four lines in the region between (1, 2) and (3, 4) but only three are observed. However, that at 10.2 c./sec. does show some sign of being a doublet so the assignment is completed as illustrated in Fig. 6.

We next proceed to find numerical values for the basic parameters from this assignment and look for internal checks to support it. This is most conveniently done using the

*The spectra described in the present work were measured with a field-stabilized Varian High Resolution Spectrometer operating at a fixed frequency of 40 Mc./second. Signal separations were measured by the side-band technique in the usual manner. The spectra were measured using a spinning sample tube (5 mm. O.D.). Sweep rates were approximately 0.2 parts per million/minute.

explicit formulae for the transition energies of lines 1, 3, 10, 11, and 12 given in Table III. Thus, immediately

$$N = E_1 - E_3 = 9.95 \text{ c./second (assuming all } J\text{'s are positive (5)),}$$

$$\{(\eta H_0 \delta)^2 + N^2\}^{\frac{1}{2}} = E_1 + E_3 = 17.45 \text{ c./second,}$$
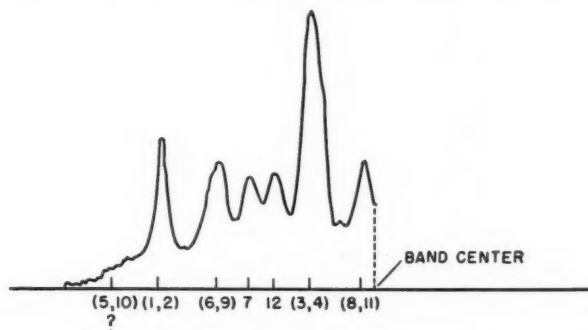
FIG. 6. Assignment of the A-lines in the naphthalene spectrum.

whence

$$\eta H_0 \delta = 14.34 \text{ c./second.}$$

Also,

$$(M^2 + L^2)^{\frac{1}{2}} = E_9 - E_{11} = 9.4 \text{ c./second}$$

and

$$\{(\eta H_0 \delta + M)^2 + L^2\}^{\frac{1}{2}} = E_9 + E_{11} = 11.0 \text{ c./second,}$$

from which

$$L = 7.21 \text{ (assuming } J > J') \text{ and } M = -6.03 \text{ c./second.}$$

One check can now be made by calculating the position of line 12 from these parameters. This is found to be at 6.1 c./second to be compared with 6.45 c./second for the line we have assigned as 12.

To get a complete set of constants we also need to find K; this cannot be done in any very direct manner. In fact, the whole spectrum is rather insensitive to the value of K, so we shall make the assumption that $K = -M$. This corresponds to $J_A = 0$, which is reasonable since the A-protons are far apart. The complete set of basic parameters is then as shown in Fig. 7.

As a final test of this interpretation of the spectrum, we may use these parameters to calculate a complete set of 12 A-lines and compare with experiment (Table V). The transitions 2, 4, 5, 6, 7, and 8 were calculated following the numerical solution of the fourth order secular equation involving S_0 states (See Table I). One immediate check is the position of line 7 which is calculated to be 0.7 c./second below that observed. This represents the limit of consistency obtained with these parameters. However, the general features are in very satisfactory agreement with observation. Thus the splitting between lines 7 and 12 is predicted to be considerably larger than that between the components of any other doublet, so that it is reasonable that this should be the only pair completely resolved. The outermost lines are predicted to be weak, but they are predicted to lie at a point where there is just a slight indication of absorption. The general features of the

TABLE V

COMPARISON OF CALCULATED AND OBSERVED PROTON SPECTRA OF NAPHTHALENE

Line	Energy relative to center of band (cycles/second)		Relative intensity	
	Calc.	Obs.	Calc.	Obs.*
11	0.8 ⎫	0.8	0.52 ⎫	1.1
8	1.6 ⎭		0.45 ⎭	
4	3.2 ⎫	3.7	1.87 ⎫	2.8
3	3.7 ⎭		1.57 ⎭	
12	6.1	6.4	0.93	0.9
7	7.5	8.2	0.62	0.6
6	9.9 ⎫	10.2	0.53 ⎫	1.3
9	10.2 ⎭		0.49 ⎭	
2	13.2 ⎫	13.7	0.46 ⎫	1.1
1	13.7 ⎭		0.43 ⎭	
10	15.5	—	0.07	
5	15.8	—	0.07	

Normalized to same total intensity as calculated values.

intensity distribution are reproduced fairly satisfactorily, the chief discrepancy being that the strongest pair is predicted to be rather stronger than actually observed. This may well be due to the difficulty in obtaining accurate intensities by integrating under the peaks.

This analysis is all based on the assumption that $\sigma_B > \sigma_A$ and that the spin-coupling constants are positive. Neither of these signs are, in fact, determined by the spectrum. If $\sigma_B < \sigma_A$, the same expressions could have been deduced by some relabelling. However, an experimental confirmation of the positions of the α- and β-proton signals at low and high field respectively (i.e. $\sigma_B > \sigma_A$) was obtained by measuring the spectrum of naphthalene monodeuterated in the β-position.* This assignment is consistent with that based on the theory of the chemical shift in aromatic hydrocarbons proposed elsewhere by the present authors (2). It is interesting that the new value of the chemical shift is substantially greater than that reported in (2) using unstabilized equipment, and is in better agreement with the theory developed in that paper.

The signs of all the spin-coupling constants can be reversed without altering the calculated spectrum apart from relabelling. It is hardly likely that J and J_B will have different signs, and the result $|N| > |L|$ implies that J and J' have the same sign. Therefore it seems probable that the only indeterminacy in the results of Fig. 7 is a possibility of changing the sign of all three spin-coupling constants simultaneously. One point about the spin-coupling constants which is worthy of comment concerns the relative values of J and J_B. The coupling between neighboring α- and β-protons is larger than that between the two β-protons.

5. THE PROTON RESONANCE SPECTRUM OF o-DICHLOROBENZENE

o-Dichlorobenzene is another good example of the general class of A_2B_2 groups discussed at the end of Section 3. (The coupling of the chlorine nuclei with the protons is not observed owing to the quadrupole relaxation of the halogen nucleus.) Its spectrum is illustrated in Fig. 9.

This spectrum is symmetrical (apart from some drift in the base line). Consequently there is no direct means of deciding which parts of the spectrum belong to the two types

We are indebted to Dr. L. C. Leitch for preparing this compound.

of proton. For notational convenience we shall assume that $\sigma_B > \sigma_A$ as for naphthalene (that is, the protons next to the chlorine positions have lower screening constants). This is purely arbitrary, however, and we really determine only $|\sigma_B - \sigma_A|$.

In the A-part of the spectrum (the left-hand side of Fig. 8) the resolvable signals are marked a–h. There is also an indication of slight absorption at j. To assign these signals to the various A-transitions, we compare with Fig. 4. This suggests immediately that
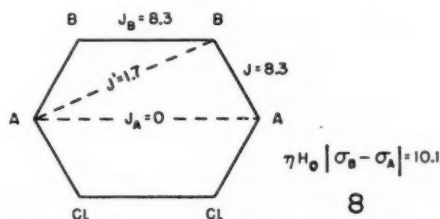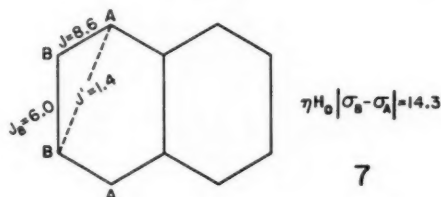
Fig. 7. Chemical shift and spin-coupling constants in naphthalene in c./second.
Fig. 8. Chemical shift and spin-coupling constants for o-dichlorobenzene in c./second.

h and g correspond to transitions 1 and 2 and the principal signal c to transitions 3 and 4. From the positions of lines 1 and 3, values of $\eta H_0(\sigma_B - \sigma_A)$ and $N = J + J'$ follow immediately. This gives

$$\eta H_0(\sigma_B - \sigma_A) = 10.1 \text{ c./second,}$$

$$N = 10.0 \text{ c./second.}$$

In the intermediate region, the three signals d, e, and f have to be assigned to the four lines 12, 7, 6, and 9. Since the separation between 12 and 7 is larger than that between 6 and 9, a reasonable interpretation is that 6 and 7 overlap at e. This is also suggested by the relative intensities of d, e, and f. The signals at f and d are then assigned to transitions 9 and 12 respectively. This gives enough information to obtain the remaining parameters K, L, and M with some trial and error fitting. Within the limits of error of this calculation, K and M turn out to be equal, so that there does not appear to be any coupling constant between the two A-nuclei (that is directly across the benzene ring). The final set of spin-coupling constants is illustrated in Fig. 8 assuming $J > J'$ and $J_B > J_A$.

The complete set of calculated energies using these parameters is given in Table VI. This shows that the innermost transitions 11 and 8 are actually in the right-hand part of the spectrum, so the signal marked a and a signal overlapped by c in Fig. 9 in fact belong to the B-spectrum. Finally, the two outermost signals 5 and 10 correspond to the weak absorption at j.

6. THE PROTON RESONANCE SPECTRUM OF 1,2-CHLOROBROMOETHANE

The molecule 1,2-chlorobromoethane (CH_2Cl—CH_2Br) is expected to lead to a rather different type of A_2B_2 spectrum since there is now no reason to suppose that J_B is large compared with J_A or vice versa. The spectrum observed at room temperature is illustrated in Fig. 10.
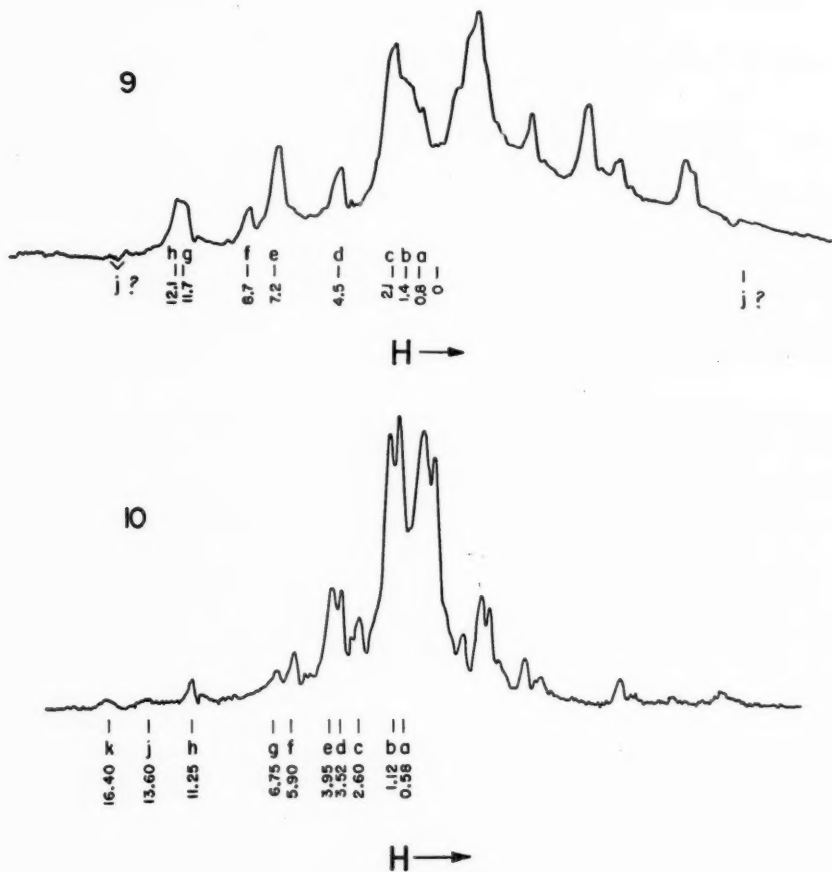
Fig. 9. Complete proton resonance spectrum of liquid *o*-dichlorobenzene at 40 Mc./second. Energies are given in c./second measured from the band center.

Fig. 10. Complete proton resonance spectrum of chlorobromoethane (liquid) at 40 Mc./second. Energies are given in c./second measured from the band center.

It is well known that molecules of this type may exist in either of two isomeric forms. One possibility is that the two halogen atoms may be *trans* relative to the C—C bond and the alternative is that they are *gauche* or skew. Now, if the molecule were in one of the two *gauche* forms for a sufficiently long period, it would give a spectrum of four non-equivalent nuclei (type *ABCD*). In fact, the observed spectrum is completely symmetrical from which we may deduce that the molecule is either in the *trans* form, or

TABLE VI

CALCULATED AND OBSERVED A-LINES IN o-DICHLOROBENZENE SPECTRUM
(cycles/second)

Transition	Calculated energy	Observed energy	
11	− 1.9	− 2.1	(c')
8	− 1.0	− 0.8	(a')
4	+ 1.5	+ 1.4	(b)
3	+ 2.1	+ 2.1	(c)
12	+ 4.5	+ 4.5	(d)
7	+ 7.2	+ 7.2	(e)
6	+ 7.0		
9	+ 8.7	+ 8.7	(f)
2	+11.6	+11.7	(g)
1	+12.1	+12.1	(h)
10	+15.1	15.0	$(j?)$
5	+15.2		

is rotating from one configuration to another sufficiently rapidly for it to be necessary to replace the coupling constants by averaged values. The latter is probably the correct interpretation. It should be noted, however, that even if the molecule is rotating about the central bond, the average spin-coupling constants between one of the A-protons and the two B-protons are not necessarily equal (i.e. $J \neq J'$ in Fig. 1). The fact that the observed spectrum contains at least 20 lines confirms this, since for the case where $J = J'$ there would be only 14 separate lines as described in Section 3.

We begin the detailed assignment with the preliminary hypothesis that the coupling constants between protons attached to the same carbon atom will be greater than those between protons attached to different carbon atoms. This implies that the constant K ($= J_A + J_B$) is large and this in turn suggests (see Section 3) that the symmetrical transitions 1, 2, 3, 4, 6, and 7 should be as in Table IV. The outermost signal at k is therefore assigned to transition 1 and signal b to transition 3. From the explicit expressions for the energies of these transitions (Table III) we get estimates for the parameters $N = J + J'$ and $\eta H_0(\sigma_B - \sigma_A)$. (Once again we arbitrarily assume $\sigma_B > \sigma_A$, there being no direct way of distinguishing which protons give signals at higher field.)

Although K is large, the difference $M = J_A - J_B$ may be small and the antisymmetric transitions 9, 10, 11, and 12 may be all distinct. The energy expressions given in Table III show that they should consist of two equally spaced pairs. These are most satisfactorily assigned to signals g, f, e, and c, leading to immediate values for M and for L ($= J - J'$). It is then possible to calculate the positions of the remaining lines and it is found that signals a, d, h, and j correspond to transitions 4, 6, 2, and 7 within experimental error. In this way the positions of 10 lines are all given in terms of four constants, providing a good internal check on the assignment.

Values for the chemical shift and spin-coupling constants are

$\eta H_0(\sigma_B - \sigma_A) = \quad 8.9$ c./second,

$N = J + J' = \quad 15.2$ c./second (assuming all J's are positive (5)),

$L = J - J' = \pm 3.1$ c./second,

$M = J_A - J_B = \pm 1.0$ c./second.

The signs of L and M are indeterminate. The value of K ($= J_A + J_B$) cannot be determined. It must be large enough to prevent any significant mixing of the basic function

$3s_0$ with other functions. If this were not so, the agreement with experiment would disappear. In this way, we estimate that $K > 20$ c./second. The calculated positions of the lines using the above parameters and assuming K large are given in Table VII and compared with experiment. The calculated relative intensities correspond satisfactorily with those shown in the observed spectrum* (Fig. 10).

TABLE VII

CALCULATED AND OBSERVED A-LINES IN CHLOROBROMOETHANE SPECTRUM

Transition	Energy (c./second)		Calculated relative intensity
	Calc.	Obs.	
4	0.57	0.58 (a)	2.75
3	1.21	1.12 (b)	1.86
12	2.61	2.60 (c)	0.53
11	3.55	3.52 (d)	0.79
6	4.10	3.95 (e)	0.81
10	5.88	5.90 (f)	0.47
9	6.81	6.75 (g)	0.21
2	11.06	11.25 (h)	0.32
7	13.52	13.60 (j)	0.11
1	16.41	16.40 (k)	0.14

REFERENCES

1. ANDERSON, W. A. Phys. Rev. 102, 151 (1956).
2. BERNSTEIN, H. J., POPLE, J. A., and SCHNEIDER, W. G. Proc. Roy. Soc. A, 236, 515 (1956).
3. BERNSTEIN, H. J., POPLE, J. A., and SCHNEIDER, W. G. Can. J. Chem. 35, 65 (1957).
4. McCONNELL, H. M., McLEAN, A. D., and REILLY, C. A. J. Chem. Phys. 23, 1152 (1955).
5. McCONNELL, H. M. J. Chem. Phys. 24, 460 (1956).

*Only very approximate intensity measurements can be made in a spectrum where the signals are partially overlapped owing to incomplete resolution. For this reason, they are not included in Table VII.

COMPARISON OF EFFECTIVE IONIC RADII IN SOLUTION

William J. Canady

Couture and Laidler (5) have devised an empirical equation relating the partial molal volumes of ions to the ionic radii. They found that for a given value of the charge the volumes vary linearly with the cube of the ionic crystal radii. They also noted that in order to obtain a good fit for the ions investigated it was necessary to multiply the experimental crystal radius r by the factor 1.25. This evidence indicates that the effective radius of an ion in solution is larger than that in the crystal. It is also possible to calculate the effective ionic radii of some spherical ions, by means of simple electrostatic theory, from their solubilities in pure solvents. This has been done, and the effective radii thus obtained have been compared with the values derived from partial molal volumes.

Brönsted (4) has considered the differential free energy in a saturated solution. At saturation, the algebraic sum of the changes of thermal, electrical, and chemical energy was set equal to zero. Chemical forces of the van der Waals type were ignored for the purposes of a first approximation. If only the thermal and charge effects are considered, the molar solubilities can be expressed in terms of the Born equation (3). The expression is

$$-d \ln N = (e^2/2\bar{r}kT)d(1/D)$$

where $\bar{r}$ is the mean effective ionic radius, D is the dielectric constant of the solvent, e is the charge on the electron, and N the mole fraction of salt dissolved at saturation. It can be seen that a plot of $-\ln N$ against $1/D$ should give a reasonably straight line of slope $e^2/2\bar{r}kT$, provided that the saturated solutions formed are not too concentrated, which would bring about ionic interaction, and that solvents of reasonably high dielectric constant are used to avoid significant contributions from ion pair formation.

The Born–Brönsted treatment has been applied to ionization processes with considerable success by Wynne-Jones (10), but it was necessary to relate the ionization constants to a standard acid in order to avoid solvation of the proton, and also to keep to pure solvents of varying dielectric constant rather than to use mixtures. The main difficulty in applying the Born treatment to solvent mixtures is probably due to segregation or sorting of the solvent molecules by the ions. Solubility data for salts in various pure solvents are sparse, but some results are available. In Fig. 1 the negative log of N has been plotted against $1/D$ for some spherical ions which would be expected to fit the Born model. Solubilities of the sodium and potassium halides were calculated from the data of Larson and Hunt (8); solubilities being measured in water, methanol, ethanol, 1-propanol, 1-butanol, 2-propanol, 2-me-1-propanol, 1-pentanol, and 2-butanol. The values for ammonium bromide were obtained from the solubility in methanol, ethanol, and propanol as determined by Bedwell (1). The fact that most of the salts are very soluble in water makes ionic association probable; therefore the values in water have not been used. In the work of Larson and Hunt, a reasonably good fit to a straight line was obtained in all organic solvents except 1-pentanol. Since this solvent is approaching aliphatic character, it was felt that ion-pairing was probably taking place, and the results in 1-pentanol were also omitted. Sodium and potassium iodides are extremely soluble in all

solvents, and because of their unusual character do not give reasonable radii. This is probably due to ionic association in all of the solvents. The radii calculated from the solubility data together with the crystal radii and the factor relating them are shown in Table I. The slopes were evaluated by the method of least squares. The factor obtained
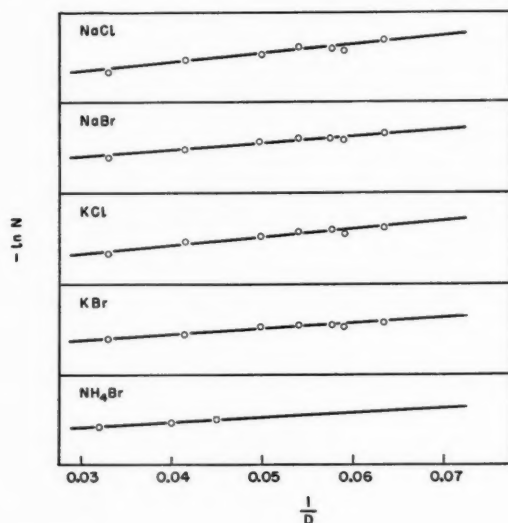

FIG. 1.

TABLE I

COMPARISON OF EFFECTIVE RADII CALCULATED FROM ELECTROSTATIC THEORY
WITH EXPERIMENTAL CRYSTAL RADII

Salt	$2\bar{r}$ cryst., Å	$2\bar{r}$ calc., Å	Factor
NaCl	2.54	2.68	1.06
NaBr	2.61	3.49	1.34
KBr	3.17	3.42	1.08
KCl	3.07	3.34	1.09
NH₄Br	3.38	4.48	1.33
(CH₃)₄NI	—	—	1.28
			Mean 1.20

by Bjerrum and Jozefowicz (2) for tetraethyl ammonium iodide is also included. The crystal radii are those of Goldschmitt (6) with the exception of the ammonium ion for which the value of Pauling (9) was used.

The mean factor calculated from the solubility data by electrostatic theory is 1.20 as compared to the value of 1.25 obtained by Couture and Laidler from partial molal volumes. It would appear that since the agreement between the two methods is quite startling, the ionic radii are actually greater in solution than in the crystal. This would seem reasonable since distortion of electronic orbitals in the crystalline state could account for such an observation. The view that, within limits, the Born model is reasonably good is further substantiated by the fact that Laidler (7) found that ionic entropies exhibit a dependence on the square of the valence as predicted by the Born equation.

ACKNOWLEDGMENT

The author wishes to thank Dr. K. J. Laidler for his kind interest and comments on this paper.

1. BEDWELL, M. E.   Trans. Faraday Soc. **39**, 205 (1943).
2. BJERRUM, N. and JOZEFOWICZ, E.   Z. physik. Chem. **159**, 194 (1932).
3. BORN, M.   Z. Physik, **1**, 45 (1920).
4. BRÖNSTED, J. N.   Chemistry at the Centenary Meeting British Assoc. Adv. Sci. (1931), p. 39.
5. COUTURE, A. M. and LAIDLER, K. J.   Can. J. Chem. **34**, 1209 (1956).
6. GOLDSCHMITT, V. M.   Skrifter Norske Videnskaps-Akad. Oslo, I, Mat. Naturv. Kl. (1926).
7. LAIDLER, K. J.   Can. J. Chem. **34**, 1107 (1956).
8. LARSON, R. G. and HUNT, H.   J. Phys. Chem. **43**, 417 (1939).
9. PAULING, L.   The nature of the chemical bond. Cornell University Press, Ithaca, New York. 1939.
10. WYNNE-JONES, W. F. K.   Proc. Roy. Soc. A, **140**, 440 (1933).

THE CRYSTAL AND MOLECULAR STRUCTURE OF ANNOTININE BROMOHYDRIN[1]

MARIA PRZYBYLSKA AND LÉO MARION

Annotinine bromohydrin, $C_{16}H_{22}O_3NBr$, crystallizes in the orthorhombic system, space group $P2_12_12_1$, with constants $a = 11.89$, $b = 13.40$, and $c = 9.68$ Å. There are four molecules per unit cell.

The coordinates of the bromine atom, derived from two-dimensional Patterson syntheses, are $x = 0.779$, $y = 0.262$, and $z = 0.011$. These values refer to the origin given by the International Tables.

The determination of the structure by the two-dimensional heavy-atom method was rendered difficult by the position of the bromine atom close to $y = \frac{1}{4}$ and $z = 0$, as many structure factors to which its contribution was very small had to be omitted.

Three-dimensional data were therefore collected from Weissenberg films. The intensities of about 2000 reflections were estimated and the number of observed reflections amounted to 87% of those theoretically possible. The values of $|F|^2_{hkl}$ were sharpened and multiplied by a modification function and a three-dimensional Patterson synthesis was computed for 15,000 points.

'Vector Convergence Method' (1) of interpretation was applied and with the help of Fourier projections it was possible to locate 10 atoms of the molecule. A second, differently modified, three-dimensional Patterson function was then evaluated. It was used to construct another 'Vector Convergence Distribution', which was much more complex owing to enhanced resolution. Since the coordinates of the bromine atom for the 'Vector Convergence Distribution' were assumed to be $y = 0.25$ and $z = 0$, two different sets of mirror planes of symmetry were introduced at $y = \frac{1}{4}, \frac{3}{4}$ and $z = 0, \frac{1}{2}$ and four convergence peaks were obtained for each atom of the molecule. The examination of the second 'Vector Convergence Distribution' gave five additional atoms and the remaining ones were derived from F_0 and (F_0-F_c) projections along the three axes of the unit cell. The structure factors for these projections were calculated using the contribution of the 15 carbon atoms in addition to that of the bromine atom.

[1]Issued as N.R.C. No. 4440.

No chemical assumptions were made in deriving the skeleton of the molecule, but chemical evidence (2, 3, 4) was used in distinguishing the oxygen and nitrogen atoms from carbon atoms. It was found, however, that the positions of these atoms were in good agreement with the $(F_0 - F_c)$ syntheses and a decrease in discrepancy between the observed and calculated structure factors resulted when the corresponding oxygen and nitrogen f values were used instead of those of carbon.

The structure of annotinine bromohydrin is represented by the schematic drawing and by the photograph of the molecular model.
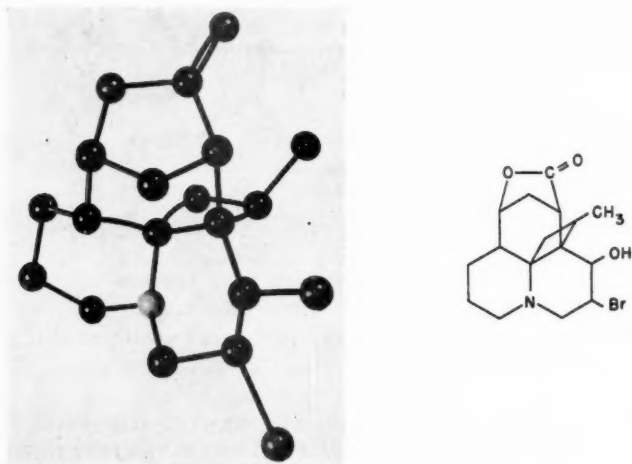
FIG. 1. The molecular model of
annotinine bromohydrin.

It is interesting that in the molecule the carbon atom of the methyl group is directed towards the carbonyl oxygen and to keep these atoms at a distance equal to the sum of their van der Waals radii, some of the bond angles deviate considerably from the value of 109.5°, thus decreasing the stability of the molecule.

The bromine atom was found to be *trans* with respect to the hydroxyl group and this is in agreement with the chemical evidence.

The structure recently proposed for annotinine by Martin-Smith, Greenhalgh, and Marion (5) is, therefore, in error, although it may represent one of the intermediate transformation products, and the latest formula published by Wiesner (6) is the correct one.

The refinement of the parameters is still in progress and the reliability index, $R = \sum ||F_0| - |F_c|| \div \sum |F_0|$, is at present about 0.21 for each of the $\{0kl\}$, $\{h0l\}$, and $\{hk0\}$ zones.

A detailed account of this work will be published later in a different journal.

We are greatly indebted to Dr. F. R. Ahmed for programming and computing structure factors, a three-dimensional Patterson syntheses, and most of the F_0 and $(F_0 - F_c)$ two-dimensional syntheses using the electronic digital computer FERUT. Grateful acknowledgment is made to Dr. W. H .Barnes for his continued interest in this determination and to Dr. M. Martin-Smith for preparing authenticated crystals. Thanks are also due

to Miss W. Paisley for her assistance with the computational work and to Mr. C. N. Hellyer for calculating some of the structure factors with I.B.M. equipment.

1. ROBERTSON, J. H. Acta Cryst. **4**, 63 (1951).
2. MacLEAN, D. B. and PRIME, H. C. Can. J. Chem. **31**, 543 (1953).
3. MEIER, H. L., MEISTER, P. D., and MARION, L. Can. J. Chem. **32**, 268 (1954).
4. HENDERSON, D. R., STONNER, F. W., VALENTA, Z., and WIESNER, K. Chemistry & Industry, 544 (1954).
5. MARTIN-SMITH, M., GREENHALGH, R., and MARION, L. Can. J. Chem. **35**, 409 (1957).
6. WIESNER, K., AYER, W. A., FOWLER, L. R., and VALENTA, Z. Chemistry & Industry, 564 (1957).

CANADIAN JOURNAL OF CHEMISTRY

Notes to Contributors

Manuscripts

(i) *General.* Manuscripts, in English or French, should be typewritten, double spaced, on paper $8\frac{1}{2} \times 11$ in. **The original and one copy are to be submitted.** Tables and captions for the figures should be placed at the end of the manuscript. Every sheet of the manuscript should be numbered.

Style, arrangement, spelling, and abbreviations should conform to the usage of this journal. Names of all simple compounds, rather than their formulas, should be used in the text. Greek letters or unusual signs should be written plainly or explained by marginal notes. Superscripts and subscripts must be legible and carefully placed.

Manuscripts and illustrations should be carefully checked before they are submitted. Authors will be charged for unnecessary deviations from the usual format and for changes made in the proof that are considered excessive or unnecessary.

(ii) *Abstract.* An abstract of not more than about 200 words, indicating the scope of the work and the principal findings, is required, except in Notes.

(iii) *References.* References should be listed **alphabetically by authors' names,** numbered, and typed after the text. The form of the citations should be that used in this journal; in references to papers in periodicals, titles should not be given and only initial page numbers are required. The names of periodicals should be abbreviated in the form given in the most recent *List of Periodicals Abstracted by Chemical Abstracts.* All citations should be checked with the original articles and each one referred to in the text by the key number.

(iv) *Tables.* Tables should be numbered in roman numerals and each table referred to in the text. Titles should always be given but should be brief; column headings should be brief and descriptive matter in the tables confined to a minimum. Vertical rules should be used only when they are essential. Numerous small tables should be avoided.

Illustrations

(i) *General.* All figures (including each figure of the plates) should be numbered consecutively from 1 up, in arabic numerals, and each figure referred to in the text. The author's name, title of the paper, and figure number should be written in the lower left corner of the sheets on which the illustrations appear. Captions should not be written on the illustrations (see Manuscripts (i)).

(ii) *Line Drawings.* Drawings should be carefully made with India ink on white drawing paper, blue tracing linen, or co-ordinate paper ruled in blue only; any co-ordinate lines that are to appear in the reproduction should be ruled in black ink. Paper ruled in green, yellow, or red should not be used unless it is desired to have all the co-ordinate lines show. All lines should be of sufficient thickness to reproduce well. Decimal points, periods, and stippled dots should be solid black circles large enough to be reduced if necessary. Letters and numerals should be neatly made, preferably with a stencil (do NOT use typewriting), and be of such size that the smallest lettering will be not less than 1 mm. high when reproduced in a cut of suitable size.

Many drawings are made too large; originals should not be more than 2 or 3 times the size of the desired reproduction. In large drawings or groups of drawings the ratio of height to width should conform to that of a journal page but the height should be adjusted to make allowance for the caption.

The original drawings and one set of clear copies (e.g. small photographs) are to be submitted.

(iii) *Photographs.* Prints should be made on glossy paper, with strong contrasts. They should be trimmed so that essential features only are shown and mounted carefully, with rubber cement, on white cardboard with no space or only a very small space (less than 1 mm.) between them. In mounting, full use of the space available should be made (to reduce the number of cuts required) and the ratio of height to width should approximate that of a journal page ($5\frac{1}{2} \times 7\frac{3}{4}$ in.); however, allowance must be made for the captions. Photographs or groups of photographs should not be more than 2 or 3 times the size of the desired reproduction.

Photographs are to be submitted in duplicate; if they are to be reproduced in groups one set should be mounted, the duplicate set unmounted.

Reprints

A total of 50 reprints of each paper, without covers, are supplied free. Additional reprints, with or without covers, may be purchased.

Charges for reprints are based on the number of printed pages, which may be calculated approximately by multiplying by 0.5 the number of manuscript pages (double-spaced typewritten sheets, $8\frac{1}{2} \times 11$ in.) and including the space occupied by illustrations. An additional charge is made for illustrations that appear as coated inserts. The cost per page is given on the reprint requisition which accompanies the galley.

Any reprints required in addition to those requested on the author's reprint requisition form must be ordered officially as soon as the paper has been accepted for publication.

Contents